A Study of Controlled Auto Ignition (CAI) Combustion in Internal Combustion Engines

By

Nebojša Milovanović

Submitted in partial fulfilment of the requirements for the
degree of Doctor of Philosophy
at
Loughborough University
Loughborough, Leicestershire
October 2003

Table of Contents

List of Tables

List of Figures

Abstract

Controlled Auto Ignition (CAI) combustion is a new combustion principle in internal combustion engines which has in recent years attracted increased attention. In CAI combustion, which combines features of spark ignition (SI) and compression ignition (CI) principles, air/fuel mixture is premixed, as in SI combustion and auto-ignited by piston compression as in CI combustion. Ignition is provided in multiple points, and thus the charge gives a simultaneous energy release. This results in uniform and simultaneous auto-ignition and chemical reaction throughout the whole charge without flame propagation. CAI combustion is controlled by the chemical kinetics of air/fuel mixture with no influence of turbulence.

The CAI engine offers benefits in comparison to spark ignited and compression ignited engines in higher efficiency due to elimination of throttling losses at part and idle loads. There is a possibility to use high compression ratios since it is not knock limited, and in significant lower NO_x emission ($\approx 90\%$) and particle matter emission ($\approx 50\%$), due to much lower combustion temperature and elimination of fuel rich zones.

However, there are several disadvantages of the CAI engine that limits its practical application, such as high level of hydrocarbon and carbon monoxide emissions, high peak pressures, high rates of heat release, reduced power per displacement and difficulties in starting and controlling the engine.

Controlling the operation over a wide range of loads and speeds is probably the major difficulty facing CAI engines. Controlling is actually two-components as it consists of auto-ignition phasing and controlling the rates of heat release. As CAI combustion is controlled by chemical kinetics of air/fuel mixture, the auto-ignition timing and heat release rate are determined by the charge properties such as temperature,

composition and pressure. Therefore, changes in engine operational parameters or in types of fuel, results in changing of the charge properties. Hence, the auto-ignition timing and the rate of heat release.

The Thesis investigates a controlled auto-ignition (CAI) combustion in internal combustion engines suitable for transport applications. The CAI engine environment is simulated by using a single-zone, homogeneous reactor model with a time variable volume according to the slider-crank relationship. The model uses detailed chemical kinetics and distributed heat transfer losses according to Woschini's correlation [1].

The fundamentals of chemical kinetics, and their relationship with combustion related problems are presented. The phenomenology and principles of auto-ignition process itself and its characteristics in CAI combustion are explained. The simulation model for representing CAI engine environment is established and calibrated with respect to the experimental data. The influences of fuel composition on the auto-ignition timing and the rate of heat release in a CAI engine are investigated. The effects of engine parameters on CAI combustion in different engine concepts fuelled with various fuels are analysed. The effects of internal gas recirculation (IEGR) in controlling the auto-ignition timing and the heat release rate in a CAI engine fuelled with different fuels are investigated. The effects of variable valve timings strategy on gas exchange process in CAI engine fuelled with commercial gasoline (95RON) are analysed.

Key Words: CAI, HCCI, PCCI, Chemical Kinetics, Auto-ignition, Heat Release Rate, Fuel Composition, Engine Parameters, Internal Exhaust Gas Recirculation, IEGR, Gas Exchange Process, Variable Valve Timings, Commercial Gasoline, N-heptane, Iso-octane, Ethanol, Methane, Dimethyl ether, Bio-diesel fuel, RON.

Acknowledgements

Here I am, at last, in the last page of my thesis and it seems that the lights at the end of tunnel can be seen. It has been scientific marathon in discovering the new knowledge through sometimes dark much less times illuminated tunnel. Despite the difficulties and problems to keep the *'right'* roads all the way through research, it has been pleasure working and learning from many nice people with whom I have been surrounded.

It is know completed and I would like to acknowledge the financial support from Lotus Engineering Ltd, UK. I would like to thank my supervisor Dr Rui Chen for his contribution and guidance in running the marathon and escaping many of the *'wrong'* roads. I would like to thank family Kalawsky, Christine, Roy, Anna and Katryna, for looking after me and being my second family in The Holt. There are many other friends who helped me by listened to my ups and downs along the way in *EHB, 641, Swans, Moomba, Amirul, Lufbra gym* ...

I would especially like to thank my parents for their endless love and support. At the end, any personal success needs support from another special and beloved person. I would like to thank Ivana for her part in everything.

Nomenclature

List of Symbols

A	Pre-exponential factor in rate constant expression (-)
A	Area (m^2)
a	Crank radius (m)
B	Bore (m)
c	Specific heat capacity (Jkg^{-1}K^{-1})
c_p	Specific heat capacity at constant pressure (Jkg^{-1}K^{-1})
c_p	Specific heat capacity at constant volume (Jkg^{-1}K^{-1})
D	Diameter (m)
E	Activation energy (Jmol^{-1})
exp	2.71828
H	Enthalpy (J)
h	Specific enthalpy (Jkg^{-1})
h	Heat transfer coefficient (W/m^{2}K)
K	Equilibrium constant (-)
k	Rate constant (-)
k_f	Forward rate constant (-)
k_r	Reverse rate constant (-)
L	Stroke (m)
l	Connecting rod length (m)

M	Molar mass (kgmol^{-1})
$\bar{M}$	Mean molar mass (kgmol^{-1})
m	Mass (kg)
$\dot{m}$	Mass flow rate (kgs^{-1})
n	Mole quantity (mol)
Nu	Nusselt number (-)
p	Pressure (Pa)
Pr	Prandtl number (-)
Q	Heat (J)
q	Specific heat (Jkg^{-1})
q	Process progress variable (-)
R	Specific gas constant (Jkg^{-1}K^{-1})
$\tilde{R}$	Universal gas constant (8.314 Jmol^{-1}K^{-1})
Re	Reynolds number (-)
S	Surface area (m^2)
$\bar{S}_p$	Mean piston speed (ms^{-1})
T	Temperature (K)
T_a	Temperature (^{0}C)
t	Time (s)
U	Internal energy (J)
u	Specific internal energy (Jkg^{-1})
V	Volume (m^3)
v	Specific volume (m^{3}kg^{-1})
Y	Mass fraction (-)
y	Mole fraction (-)

Greek Letters

β	Temperature exponent in rate constant expression (-)
γ	Ration of principal heat capacities (c_p/c_v)
θ	Crank angle (^{0})
λ	Equivalence air to fuel ratio(-)
λ	Gas conductivity ($\text{WK}^{-1}\text{m}^{-1}$)
μ	Gas viscosity ($\text{kgm}^{-1}\text{s}^{-1}$)
ν	Reaction rate (-)
π	3.14592...
ϖ	Rotational speed of crankshaft (rads^{-1})
ρ	Density (kgm^{-3})
τ	Dimensionless time (-)
$\tau_{1/2}$	Half time (s)
υ	Stoichiometric coefficient (-)
ϕ	Equivalence fuel to air ratio (-)
Ω	Rotation of crank angle (-)
$\dot{\omega}$	Molar production rate (mol s^{-1})

List of Abbreviations

ABDC	After bottom dead centre
$ABDC_{comp}$	After bottom dead centre compression
ATDC	After top dead centre
$ATDC_{exh}$	After top dead centre gas exchange process
AVT	Active valve train
BDC	Bottom dead centre
$BBDC_{exh}$	Before bottom dead centre gas exchange process
CA	Crank angle
CF	Cool flame
CR	Compression ratio
EEGR	External exhaust gas recirculation
EVC	Exhaust valve closure
EVO	Exhaust valve open
FVVT	Fully variable valve train
HRR	Heat release rate
IEGR	Internal exhaust gas recirculation
IMEP	Indicated mean effective pressure
IVC	Inlet valve closure
IVO	Inlet valve open
MI	Main ignition
PCP	Peak cylinder pressure
PM	Particulate matter
RON	Research octane number
SAI	Start of auto-ignition
TDC	Top dead centre

Publications

2003

1. Chen, R., Turner, J., Milovanovic, N. and Blundell. D., *Thermal Effect of Internal Gas Recirculation on Controlled Auto Ignition*, SAE Paper 2003-01-0750, SAE World Congress, Detroit, USA, March 2003.

2002

1. Chen, R., Milovanovic, N., Law., D. and Turner, J., *A Computational Study on The Effect of Exhaust Gas Recirculation on Auto-Ignition Timing of HCCI Engine Fuelled with N-heptane, Iso-octane, Ethanol and Methane*, Proceeding from 17th Internal Combustion Engine Symposium, Tokyo, Japan, October 2002, Paper no: 20026074, pp. 351-355.

2. Milovanovic, N., Chen, R., Law, D. and Turner, J., *Homogeneous Charge Compression Ignition Combustion and Fuel Composition*, Proceedings from 17th Internal Combustion Engine Symposium, Tokyo, Japan, October 2002, Paper no: 20026075, pp. 361-365.

3. Milovanovic, N., Chen, R., Law., D. and Turner, J., *Modelling of Homogeneous Charge Compression Ignition Combustion with Diesel Type Fuels: N-heptane, Dimethyl Ether, Methyl Butanate and Methyl Formate*, Proceeding from 17th Internal Combustion Engine Symposium, Tokyo, Japan, October 2002, Paper no: 20026077, pp. 365-369.

4. Chen, R., Milovanovic, N., and Law., D., *A Computational Study on the Ignition Timing of HCCI Combustion in IC Engine Fuelled with Methane*, Proceedings from 2002 Spring Technical Meeting of The Combustion Institute, Canadian Section, Windsor, Canada, May 2002, Paper no: 51, pp.158-163.

2001

1. Chen, R. and Milovanovic, N., *A Computational Study Into the Effect of Exhaust Gas Recycling on Homogeneous Charge Compression Ignition Combustion in Internal Combustion Engines Fuelled With Methane*, International Journal of Thermal Science, accepted for publication, October 2001. Published Vol.41, pp 805-813, 2002.

2. Milovanovic, N. and Chen, R., *Modelling of the Engine Operating Condition Effects on the HCCI Combustion of Methane*, "Current Research in Combustion", Conference Organised by Institute of Physics - Combustion Physics Group, Advantica Research Center, Loughborough, UK, September 2001.

3. Milovanovic, N. and Chen, R., *A Review of Experimental and Simulation Studies on Controlled Auto-Ignition Combustion*, SAE Paper 2001-01-1890, SAE Spring Fuel, Lubricant Conference and Exhibition, Orlando, FL, USA, May 2001.

Chapter 1

Introduction

The purpose of the internal combustion engine is to produce mechanical energy from the chemical energy contained in fuel and to use as it a source of motive power. Since the spark ignition (SI) and the compression ignition (CI) engine strategies were first introduced in transport applications at the end of 19th Century, they have achieved a great success, and now they are in use in almost 400 million vehicles worldwide, with estimation that in year 2025 the figure is expected to reach 700 million. It is becoming very important to ensure that combustion process in internal engines is performed in the most efficient manner regarding need to minimise waste of energy, to avoid unnecessary emissions and to reduce adverse effects on the environment, which may arise through pollutant emissions. In parallel with this, the new Emissions Regulation Standards for Transport Application engines imposed worldwide is to take effect in coming years. For example EURO 4, Tier II, ULEV, is required to meet very strict norms for levels of carbon oxide, hydrocarbons, NO_x and particulate matter (Refer to Appendix A).

To meet proposed stringent emission levels, without deteriorating engine efficiency, new exhaust gas treatment technologies have to be designed. However, another approach proposed by Onishi et al [2] and later Opennheim [3], based on the idea *'rather to prevent the cause than to cure the consequence'*, focused research work in

a different direction in order to change the whole process of the internal combustion engines by *replacing diffusion depending combustion in CI engine and turbulence depending combustion in SI engine, with homogeneous and simultaneous combustion strategy*, which has the potential to be more efficient and environmental friendly.

In recent years this idea has attracted a great deal of research work worldwide. The work presented in this Thesis represents the author's contribution to a greater understanding and implementations of this new combustion principle in internal combustion engines.

1.1 Highlights of Controlled Auto-Ignition Combustion

Controlled Auto Ignition (CAI) combustion is a new combustion principle in internal combustion engines among the well-known compression-ignition (CI) and spark-ignited (SI) principles. CAI combustion is a process where air and fuel are premixed and then auto-ignited by compression from a piston. During the compression process, some parts of mixture will have different heat capacities due to local inhomogeneities, and therefore the hottest parts of mixture will ignite first. As a result the ignition is provided on multiple points. The released energy further compresses and increases temperature in the rest of the charge, which ignites after a short time delay. In that way, the charge gives a simultaneous energy release, resulting in uniform and simultaneous auto-ignition and chemical reaction throughout the whole charge without flame propagation.

Therefore, it can be said that CAI combustion is dominated by the chemical kinetics of the air/fuel mixture with no requirements for turbulence and mixing. There is no large-scale flame propagation, since combustion starts at many points, at the same time. Thus, the entire mixture also burns close to homogenous condition simultaneously.

An engine with CAI combustion can provide efficiencies as high as the compression

ignition (CI) engine, but unlike CI engines produces very low emissions of NO_x and particulate matter (PM) [2, 4, 5, 6, 7]. A CAI engine operates on the principle of having a diluted, premixed charge that reacts and burns volumetrically through the cylinder as it is compressed by the piston. In the same way, CAI incorporates the best features of both spark ignition (SI) and compression ignition (CI) process. In Figure 1.1 these three different processes are shown. The charge in a CAI (HCCI) engine is well mixed, as in a SI engine, but ignited with compression from the piston. In that way the fuel rich area that occurs in the CI engine, is eliminated, and PM emission is minimised. Compression ignition of charge, together with no throttling losses, leads to the high efficiency. In comparison to SI and CI engines the combustion in the CAI engine occurs simultaneously throughout the volume rather than in a flame front. This important attribute of CAI allows combustion to occur at much lower temperatures, and therefore significantly reduces the NO_x emission.

CAI combustion is a widely recongised name, together with Homogeneous Charge Compression Ignition (HCCI) combustion and Premixed Charge Compression Ignition (PCCI combustion. However, the followings names are also in use:

1. **For two-stroke engines:**

    - *ATAC* (Active Thermo-Atmosphere Combustion) [2, 9, 10, 11],

    - *AR* (Activated Radicals) combustion [12, 13],

    - *IAPAC*(Compressed Air Assisted Fuel Injection Process)[14],

    - *TS* (Toyota-Soken) combustion [4].

2. **For four-stroke engines:**

    - *CIHC* (Compression Ignited Homogeneous Charge) combustion [5] and

    - *UNIBUS* (Diesel Combustion Under Uniform Higher-dispersed Mixture Formation) [15].

The name *CAI* combustion is used more in Europe, *HCCI* combustion is used more in USA and *PCCI* combustion more in Japan.

CIDI   HCCI   SIDI

High Pressure Fuel Injection

Low Pressure Fuel Injection, No Ignition System

Spark Ignition with Moderate Pressure Fuel Injection

Intake   Exhaust   Intake   Exhaust   Intake   Exhaust
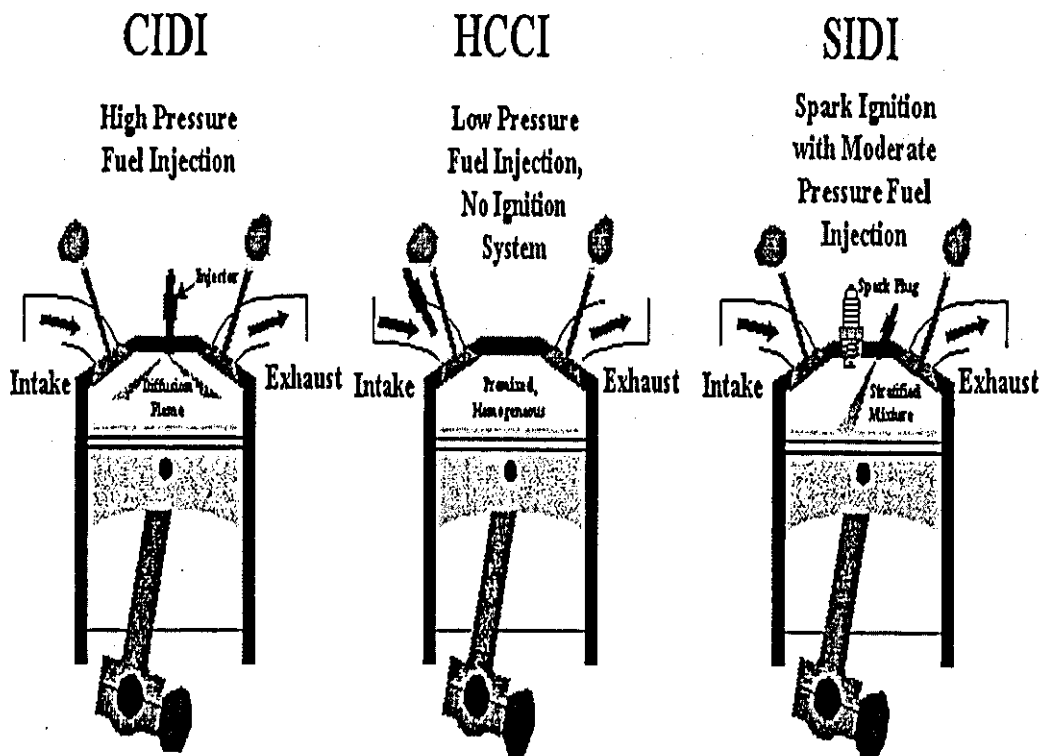
Figure 1.1: Three different combustion strategies in internal combustion engines, CI, CAI and SI [8].

1.2 Advantages of CAI combustion

The advantages of CAI are numerous and depend on the combustion system to which it is compared.

1. *In comparison to the SI gasoline engine*

   o The CAI engine is more efficient, approaching the efficiency of the CI engine. Improved efficiency is a result of the followings:

   a) *Elimination of Throttling Losses.* The CAI engine offers the possibility for unthrottled idle and part load operations. Hence, a reduction in pumping losses.

b) *Possibility to use High Compression Ratios.* Higher compression ratios might be used for higher octane fuels since they are not associated with problems regarding knock, as in the SI engine.

c) *Shorter Combustion Duration.* The shorter combustion duration is the consequence of the non-existence of the flame propagation across the cylinder. Instead, the whole mixture burns simultaneously throughout the cylinder volume. This results in shorter combustion duration.

○ The CAI engine has lower NO_x emission than the SI engine, due to the much lower combustion temperature. Even though the three-way catalysts technology provides satisfactory reduction in NO_x emission for the SI engine, it cannot achieve the level obtained from the CAI engine without any catalyst [16].

2. *In comparison to the CI engine*

- The CAI engine has significantly lower emissions of NO_x and PM. This is a results of the homogeneous (premixed) air and fuel mixture and low combustion temperature. With premixed air-fuel mixture, fuel rich zones that are characteristic of the direct injection CI process, are avoided. The charge, which can be used in a CAI engine might be diluted to very lean by using exhaust gas recirculation (EGR) or stratification or a combination of these [17, 18, 19]. As there is no need for flame propagation to combust the rest of un-burned mixture after the start of ignition, the employed mixture can be significantly diluted in comparison to one in the SI or the CI engine. Combustion is induced throughout the charge by compression heating due to the piston motion, and it will occur in almost any air/fuel/egr mixture once the ignition temperature is reached.

As a homogenous combustion the CAI combustion gives simultaneous energy release of the whole charge. CAI requires a decentralised initiation of the ignition in contrast to SI and CI where it is done by spark plug and fuel

injection, respectively. As the ignition represents partial chemical activation initiating a serial consumption of the charge, decentralised activation by compression heating provides every element of charge with sufficient activation energy to reach the level of energy release. In that way decentralised initiation of the ignition has the advantage to extend combustion limit towards leaner fuel-air mixture. This allows that the very lean mixture in a CAI engine can be ignited and completely consumed. The ignition temperature is in the range of 800 to 1100 K, depending on the type of fuel [20]. The low heating value of very lean mixture lowers the peak temperature of combustion below the temperature of NO_x formation (1800K). In contrast, in typical CI engines minimum flame temperatures are 1900 and 2100 K, high enough to make unacceptable level of NO_x emissions [21].

- Additionally, the combustion duration in a CAI engine is much shorter than in a CI engine since it is not limited by the rate of air/fuel mixing. This shorter combustion duration gives the CAI engine an efficiency advantage.

- The potential benefit of CAI engine might be lower cost than CI engine because it would likely use lower pressure fuel injection equipment [16].

3. *In comparison to both engines - SI and CI.*

  * Another advantage of the CAI engine is its *fuel-flexibility*. Since CAI combustion is not constrained by knock as in SI combustion, a wide range of fuels can be used [22].

  * The results of experiments prove that under optimised conditions CAI combustion can be very repeatable, resulting in a smoother operation [23, 24]. There are small cycle-to-cycle variations, due to the fact that ignition takes place at many points simultaneously. Consequently, the

whole mixture burns close to homogeneous at the same time, and there-
fore unstable flame propagation is avoided.

* The CAI engine might be suitable for use in internal combustion(IC)-
  engine/electric motors or fuel cell hybrid vehicles. In these hybrids, en-
  gines can be optimised for operation over a limited range of speeds and
  loads, and thus eliminate many of the control difficulties normally asso-
  ciated with CAI. The result being a highly fuel-efficient vehicle.

* The CAI combustion is applicable to both automotive and heavy truck
  engines. It could be easily scaled to virtually every size class of trans-
  portation engines from small motorcycle engines to large ship engines.
  CAI is also applicable to piston engines used outside the transportation
  sector such as those for electrical power generation, pipeline pumping and
  heavy duty equipment.

1.3 Challenges of CAI Combustion

CAI combustion is achieved by controlling the temperature, composition and pres-
sure of the air-fuel mixture so that it auto-ignites near top dead centre (TDC) as it
is compressed by the piston. This mode of ignition is fundamentally different and
more demanding than using direct control mechanisms such as in the SI and CI
engines. In the SI engine the ignition and further flame propagation is controlled by
the sparking timing of the spark-plug, while in the CI engine it is controlled by the
amount of injected fuel and duration of injection. Although the CAI combustion has
been known for twenty years, it is only with the recent implementation of electronic
engine controls that CAI combustion has begun to be considered for the applica-
tion in commercial two stroke and four stroke engines. Even with these advanced
control systems, there are several technical barriers that have to be overcome before
the CAI engine will be applicable for a wide range of vehicles and a high-volume
production. In the following text the most important challenges for developing the

practical CAI engine for transport applications are described. Potential solutions for these challenges, based on previous experimental and numerical research, together with their effectiveness are discussed in Chapter 2.

1. **Controlling Ignition Timing and Heat Release Rate Over a Range of Speeds and Loads.** Controlling the operation of a CAI engine over a wide range of speeds and loads is probably the major difficulty facing CAI engines. CAI ignition is determined by the charge temperature, composition and pressure. The influence of pressure is minor in comparison to influences of temperature and composition. Changing the power output (load) of a CAI engine requires a change in the fuelling rate and therefore in the charge composition. As a result, the charge temperature has to be adjusted to maintain proper ignition timing and further combustion process.

   Similarly, changing the engine speed, changes the amount of time for the auto-ignition chemistry to occur relative to the piston motion. To compensate for this, the charge temperature has to be re-adjusted. In the rapid transient mode, during engine accelerations and de-accelerations, compensation for load and speed effect becomes very demanding.

2. **Expanding the Operating Range.** Although the CAI engines have been operated well at low and medium loads, problems occur at high loads. Combustion process (heat release rate) becomes very fast and intense, causing unacceptable levels of engine noise, potential engine damage and unacceptable levels of NO_x emission. There is a need to develop a method to slow down the heat release rate at high load operation to prevent engine noise and high levels of NO_x emission. Due to the problems with high load operation, some CAI concepts combine traditional SI and CI combustion with CAI combustion [12, 25]. In these concepts the operation is to switch either to SI or CI mode where CAI operating conditions are causing problems. This dual mode operation provides the benefits of CAI over a part of the driving cycle but adds

complexity by switching the engine between operating modes.

3. **Problems with Cold Start of the CAI engine.** In order to 'cold start' a CAI engine the problems of achieving auto-ignition temperature have to be overcome. At cold start, the compressed gas temperature in a CAI engine will be reduced because the charge will not receive preheating from the intake manifold. Moreover, the compressed charge will be rapidly cooled by intensive heat transfer to cold cylinder walls. Without the existence of some compensating mechanism, the low compressed charge temperature could lead to a misfire (with the result that the CAI engine will not fire).

4. **Hydrocarbon and Carbon Monoxide Emissions.** The CAI engine has very low NO_x and PM emissions, but relatively high emissions of hydrocarbons (HC) and carbon monoxide (CO). Excessive HC and CO emissions are particularly noticeable at low loads. In order to successfully control these emissions it is likely that new exhaust emission control devices are required. Catalyst technology for HC and CO removal is well understood and has been standard equipment for many years. However, the lower exhaust temperatures from CAI engine might increase catalyst light-off time and decrease average effectiveness.

   As a result, meeting future emission standards for HC and CO emissions will likely require further development of oxidation catalysts for low temperature exhaust streams. On the other hand, HC and CO emission control devices are simpler, more durable, and less dependent on rare, expensive precious metals than are the NO_x and PM emission control devices. Therefore, simultaneous chemical oxidation of HC and CO (in a CAI engine) is much easier than simultaneous chemical reduction of NO_x and oxidation of PM (in the CI engine).

1.4   Fundamental Understanding of CAI Combustion

Over the last few years, a consensus of opinion has developed about the nature of CAI combustion. It is now generally agreed that CAI combustion is dominated by local chemical kinetic reaction rates, with no requirement for flame propagation [2]. This notion has been supported by spectroscopic data indicating that the order of radical formation in CAI combustion corresponds to auto-ignition rather than flame propagation [26, 27, 28]. During the compression process auto-ignition is provided at multiple points in the air/fuel charge, consuming fuel and releasing the energy. Therefore, the charge gives a simultaneous energy release, resulting in uniform and simultaneous auto-ignition and chemical reaction throughout the whole charge without flame propagation. The appearance of radicals that lead to formation of exothermal ignition centres is sequential at multiple charge locations. The released energy from the former sequence further compresses, and increases the temperature of the part of the charge in the next sequence. This ignites after a short time delay. This results in combustion which consists of many simultaneous auto-ignition sequences that take place one after another. Therefore, the charge gives a parallel energy release resulting in almost homogeneous combustion without flame propagation.

Moreover recent analytical developments support the theory that CAI combustion is composed from *sequences of simultaneous auto-ignition* dominated by chemical kinetics of the employed air-fuel mixture [20, 29, 30]. If a fairly homogeneous mixture exists at the time of combustion, then turbulence has little or no direct effect on CAI combustion. However, it is highly likely that turbulence will have indirect effect by altering the temperature distribution and the boundary layer thickness inside the cylinder [31, 32, 33]. Small temperature differences inside the cylinder have a significant effect on combustion due to the sensitivity of chemical kinetics to temperature [34, 35]. As a result, heat transfer and mixing are important in formation of the charge properties prior to ignition. However, they play a secondary

role during the CAI combustion process itself, because CAI combustion is very rapid [23, 30].

1.5   Objectives and Aims

The overall objective of this work is to investigate controlled auto-ignition (CAI) combustion in internal combustion engines suitable for transport applications. The work is targeted to understand:

* The principles of CAI combustion,

* The influence of:

    - fuel composition,

    - engine parameters,

    - internal exhaust gas recirculation and

    - variable valve timing strategy

on the auto-ignition timing and the rates of heat release in a CAI engine.

The aims of the research are:

• To critically review experimental and modelling work on CAI combustion in engines for transport applications-Chapter 2.

• To present fundamentals of chemical kinetics, and its relations with combustion related problems-Chapter 3.

• To present phenomenology and principles of auto-ignition process with its characteristics in CAI combustion-Chapter 4.

• To establish and validate model for simulation of a CAI engine-Chapter 5.

• To investigate the influences of fuel composition on the auto-ignition timing and the rate of heat release in a CAI engine by numerical modelling -Chapter 6.

- To analyse the effects of engine parameters on CAI combustion in different engine concepts fuelled with various types of fuel by numerical modelling-Chapter 7.

- To investigate the effects of internal exhaust gas recirculation (IEGR) on controlling of the auto-ignition timing and the rate of heat release in a CAI engine fuelled with different types of fuel by numerical modelling -Chapter 8.

- To analyse the effects of variable valve timings on gas exchange process in CAI engine fuelled with commercial gasoline (95RON)by experimental and modelling approaches -Chapter 9.

- To draw conclusions and suggest areas where there is potential to conduct further research-Chapter 10.

Chapter 2

Literature Survey

CAI combustion phenomena was identified as a distinct combustion phenomena in the late 70's [2, 4]. In the 80's and early 90's there was not too much interest in CAI combustion and few experimental works, mainly for two-stroke engines, had been carried out. However, interest in CAI combustion was dramatically increased in the late 90's, with the imposition of new stringent emissions legislation, and with the advent of electronic sensors and controls that made CAI engines potentially a practical reality.

With the increasing interest, experimental work was the dominant method of investigation of CAI combustion and only few simulation studies were performed. However, the number of simulation studies rapidly increased from the year 2001.

This survey will be focused on the experimental work performed to date and numerical analysis of CAI combustion in 2 and 4-stroke engines. A critical review of some experimental projects focusing on different methods of obtaining stable CAI combustion will be presented first. This will include a discussion regarding their effectiveness and contribution to the CAI combustion control. After that, a critical review of numerical analysis of CAI combustion, which includes a discussion about different types of models, their accuracy and demand for computational time, will be presented. In the summary, recommendations for future experimental and numerical work will be given.

2.1 Recent Developments in Controlling CAI engines

Over the past two decades a number of technologies have been developed to initiate CAI combustion in both 2 and 4-stroke engines using various fuels, but none of them could maintain adequate combustion over the whole engine operation range [36, 37, 38]. The main two problems currently limiting the commercial application of CAI, as mentioned earlier in Chapter 1, are: *(i) successful control of combustion and (ii) emissions of HC and CO over wide engine loads-speeds range.*

Combustion control is the biggest challenge as CAI combustion is mostly controlled by its chemical kinetics, which enables the use of direct controlling methods as in SI and CI engines. Other methods, namely *indirect methods* which have the potential to control the combustion will be discussed in further text. These methods can be generally divided into two categories:

- *Modification of engine operational and design parameters* such as, variable compression ratio, variable valve timing, supercharging, and using different concepts of fuel injection.

- *Modification of air-fuel mixture properties* by varying intake temperature, changing the air-fuel ratio, using the exhaust gas recirculation (EGR) technique, application of some additives (promoters and inhibitors of ignition) and fuel modification (blending or pre-conditioning).

2.1.1 Modification of Engine Operational and Design Parameters

The general purpose of engine operational and design parameter modification is to achieve and to stabilize CAI combustion during various engine operating conditions (various loads and speeds). These can be accomplished by influencing the charge properties, such as temperature, composition and pressure. Effectiveness of different engine operational and design parameters modifications will be discussed.

2.1.1.1 Variable Compression Ratio - VCR

CAI combustion is strongly affected by the compression ratio (CR) of the engine. A higher compression ratio increases the charge temperature and therefore advances the start of ignition of the CAI combustion [22, 24, 39]. In addition, higher compression and thus expansion ratios contribute to higher indicated thermal efficiency. Therefore, a VCR engine has the potential to achieve satisfactory operation in CAI mode over a wide range of conditions, because the compression ratio can be adjusted as the operating conditions change. Changes occur very quickly in vehicle applications, hence a fast control system that has ability to modify the CR in relatively short time (a few fractions of second) is necessary. Several options have been studies to obtain VCR engines:

i) One option is to mount a plunger in the cylinder head whose position can be varied to change the CR [22],

ii) Another option is to use an opposed-piston engine design with variable phase shifting between the two crankshafts to change CR [40],

iii) SAAB has recently announced the development of another method based on a hinged, tilting cylinder arrangement [41].

Whilst any of these three systems or some other mechanism might succeed, only the variable-valve plunger system has been demonstrated in a CAI engine [22]. For these tests the plunger was controlled by a hydraulic system allowing its position to be varied during engine operation. The data show that the VCR system is capable of controlling CAI auto-ignition timing to maintain optimal combustion phasing, across a very wide range of intake temperatures, and fuel types of different research octane number [22]. The transient operation and variations in speed and load were not reported, but the results suggest that a VCR system with a sufficiently fast response time has the ability to control a CAI engine. However, a VCR would add some cost and complexity to the engine.

2.1.1.2 Variable Valve Timing - VVT

VVT can be used to change the amount, composition and pressure of trapped exhaust gases. By varying the amount of trapped exhaust gases, the temperature and mixture of the new fresh charge can be adjusted. Increasing the charge temperature in this manner can be used to initiate CAI combustion, even with relatively low geometric compression ratios or under cold engine conditions [42, 43]. Changing the trapped charge compression ratio, i.e. the amount of compression after the exhaust gases are trapped, can be done by changing the intake valve closure (IVC) event. In addition, altering the charge composition with partial mixing of exhaust gasses could benefit auto-ignition timing and heat release rate control as will be discussed in Chapter 9. In that way, VVT cannot only achieve a similar effect on CAI combustion as VCR, but also can affect the temperature and pressure of the engine charge.

VVT can be implemented in an engine with mechanical [44], magnetic or electro-hydraulic valve actuators [42]. Like VCR, a VVT system would add significant cost and complexity to the engine.

2.1.1.3 Supercharging

A CAI engine usually runs on a lean air-fuel mixture in order to prevent high peak cylinder pressure and to slow down high release rate. This has the consequence that the engine power output is very low (10% of total available engine's output) and it practically limits using CAI combustion in very lean modes.

One way to increase the power which the engine can deliver is to use supercharging. The maximum power that an engine can deliver is limited by the amount of fuel that can be burned efficiently inside the engine cylinder. This is further limited by the amount of air that is introduced into the cylinder in each cycle. If the inducted air is compressed to a higher density than ambient, prior to entry into the cylinder, the maximum power an engine of fixed dimensions can deliver will be increased [21].

This is the primary purpose of supercharging.

Application of supercharging in CAI combustion will increase the power that the engine can deliver and extend the operation range of air-fuel ratio. Different fuels have been tested with various compression ratios and boost pressures. Results obtained show that supercharging (up to 2 bar boost pressure) increases attainable IMEP, broadens air-fuel ratio range, but the inlet temperature needs additional adjustment [24]. However, supercharging resulted in high pressure values inside the cylinder ($\approx$ 250 bar for 2 bar boost pressure), which might be a limiting factor regarding the mechanical strength of the engine.

2.1.1.4 Fuel Injection Strategy

Different fuel injection strategies have different effects on temperature history and charge composition, prior to the start of a compression stroke, and therefore on CAI ignition timing and combustion phasing. For diesel fuel types, port injection and direct injection strategies have been investigated, while for gasoline fuel only a direct injection strategy has been studied.

1. **Diesel Fuels.**

   - *Port fuel injection*, or fumigation of heavy fuels during CAI combustion, results in high HC and CO emissions and an increase in fuel consumption, due to a poor vaporization process and wall interaction within the combustion chamber [45, 46, 47, 48, 49].

   - *Direct in-cylinder fuel injection* offers better results for heavy and light diesel fuels than port fuel injection. Two strategies have been experimentally investigated; early [50] and late fuel injection [51].

     i) In *Early in-cylinder* injection a portion or all of the necessary fuel is injected early during the compression stroke. The vaporization process of directly injected fuel draws heat from the initial CAI combustion during the early stage of the compression stroke, and thus reduces

its heat release rate. Therefore, the temperature-time history of the mixture is affected significantly by the vaporization process that limits the control of the CAI combustion. Experimental results obtained with early injection of diesel fuel from Takeda et al [50], show good results in emission reduction, but fuel wall impingent causes a problem when heavy fuels were injecting into the low-density charge.

ii) *Late in-cylinder injection* is a new approach applied in "homogenous" diesel CAI combustion developed by Nissan [51]. During low load, fuel was injected around TDC and the ignition delay was managed by EGR, reduction in CR and severe swirl. As a result, combustion begins well after the end of injection and the combustion jet that usually appears in the conventional CI engine is eliminated. However, this method suffers from a short ignition delay and if EGR, reduction in CR and swirl are not employed, the ignition delay cannot be controlled properly, which limits the application of this method.

2. **Gasoline Fuel.** Recently, some experimental investigations of gasoline direct injection in an engine running in CAI mode has been carried out [17, 18, 19]. The target of these experiments was to analyse the effect of different injection timings, durations, swirls and levels of stratification on the controlling of combustion and emissions of NO_x, HC and CO when the engine was operated in relatively lean regimes λ [1] from 2.5 to 5 [17, 18] and λ from 3.3 to 5 [19].

Results suggest than injection timing and duration are strongly connected with engine load.

At a very low engine load ($\lambda = 5$), heterogeneous (stratified) air-fuel charge, created by late injection timing, gave better combustion phasing, higher efficiency, lower HC, CO emissions and slightly higher NO_x emissions in comparison to a homogeneous air-fuel charge. A homogeneous charge, created by

---

[1] λ represents equivalence air to fuel ratio, i.e. is equal to actual air to fuel ratio divided by the stoichiometric air to fuel ratio.

early injection timing, resulted in a very low combustion efficiency and high emissions of HC and CO, due to late combustion phasing and thus incomplete combustion. On the other hand, when the engine was running at the higher engine load ($\lambda \approx 3.5$), a homogeneous charge resulted in a higher combustion efficiency and lower emissions than a heterogeneous one [17, 18, 19].

In general, stratification of the air/fuel charge, obtained by different injection timings and durations, shows potential to maintain combustion phasing over relatively wide engine loads and speed. However, fuel stratification is not adequate for controlling the combustion phasing and emissions at higher loads due to unacceptable levels of noise and NO_x emission.

The use of swirl has shown some potential in reducing the level of HC and CO emissions at very low engine loads ($\lambda \approx 5$) [19]. This might be the result of improved mixing of air and fuel during the direct injection process but additional investigations are needed.

2.1.2 Modifications of Fuel-Air Mixture Properties

The purpose of these modifications is to influence the chemical reactivity of the intake charge by changing its thermo-chemical properties, thus influencing control of the CAI combustion.

2.1.2.1 Intake temperature

One popular method for generating CAI combustion and influencing the ignition timing is adjusting the intake air temperature [22, 23, 24, 52, 53]. Additional equipment, such as heat exchangers have been used to heat the intake air. A higher intake temperature advances the start of ignition and reduces the peak pressure but the range over which CAI can be controlled is limited. Also, the engine volumetric and thermal efficiency are reduced due to the fact that ignition is advanced into the compression stroke which causes significant negative work on the piston. Moreover, the use of additional equipment for heating the intake air adds complexity and

additional cost to this concept.

2.1.2.2   Air-Fuel Ratio

Changing the air-fuel ratio affects the ignition timing and heat release rate [23, 24, 52]. A decrease in the air-fuel ratio (enriching the mixture) causes a decrease in the ratio of mixture specific heats (γ), and thus reduces the amount of available compression heating for the charge. Consequently, a rich mixture has to be compressed more than a lean one in order to reach the auto-ignition temperature, hence auto-ignition timing is delayed.

In the case of fuel with two stage-ignition behaviour, the overall ignition time is affected by the fuel-air ratio through competition between the amount of compression heating due to changes in (γ) and the strength of the first stage of ignition.

2.1.2.3   Exhaust Gas Recirculation -EGR

One way to control the engine charge temperature, mixture and pressure is the use of the exhaust gas recirculation (EGR) process. EGR can be mixed with a fresh air-fuel mixture before its induction into the engine cylinder (in intake manifold) - *external EGR* [24, 52] or trapped and mixed with induced fresh air-fuel charge inside the cylinder - *internal EGR* [42, 43, 54, 55]. The main purpose of the EGR trapping is to increase the charge temperature to the value necessary for ignition in a short time period. The EGR must be trapped inside the cylinder prior to the compression stroke and this is achieved by adjusting the exhaust valve timing. Variable valve timings were explained earlier in the text in Section 2.1.1.2.

In the case of the *external EGR technique* the addition and mixing of EGR with the air-fuel charge is carried out at the intake manifold. Therefore, the added EGR has a lower temperature than the trapped EGR, and it slows down the rate of chemical reactions and thus delays the ignition time, reduces the heat release rate and lowers the peak cylinder pressure. Christensen, et al [23] performed a series of experimental studies by introducing EGR into the inlet manifold. The reported results revealed

that stable CAI combustion could be achieved by using up to 57 % of EGR with iso-octane as a fuel, 62 % with ethanol and 48 % with natural gas. The compression ratio was 18:1, IMEP $\approx$ 5 bar and the inlet temperatures were $\approx$ 110, 120 and 150 ^{0}C for iso-octane, ethanol and natural gas, respectively. When diesel fuel was used, stable CAI combustion was achieved in a certain load range with a higher air-fuel mixture intake temperature (175-240 ^{0}C) and lower compression (8:1) ratio with up to 50% of EGR [56].

2.1.2.4 Additives

As will be presented later in the text (Chapter 4), the main auto-ignition occurred approximately at the same temperature independently of the type of fuel. Nevertheless, variations in any engine parameters or air-fuel mixture properties that would advance heat release rate early in the auto-ignition history, and thus brought reactive engine charge earlier to main auto-ignition temperature would advance ignition and vice versa [20]. Some chemical components have the ability to inhibit or promote the rate of heat release early in the auto-ignition process, and thus can be used as additives to the air-fuel mixture.

Dimethyl-ether (DME) has a low Octane number (high Cetane number) and high heat release rate, and in mixing with some fuels, contributes to better stability of CAI combustion. Results of tests carried on a Cooperate Fuels Research (CFR) engine [57] indicated that adding DME in methane (15 % by volume) contributes to better auto-ignition of methane by promoting the heat release rate of the first stage of ignition. Neat methane has a very modest rate of heat release at the first stage of ignition, and this causes difficulty in achieving conditions for auto-ignition in an engine cycle, compared to other fuels. Reported results also suggest that some further adjustment of intake temperature and air-fuel ratio according to engine load range are necessary for achieving successful control of CAI and improving the engine efficiency.

An attempt at using water for controlling ignition timing and heat release rate of the

CAI combustion has been carried out by Christensen et al [52]. The results showed that injected water delays the start of ignition and slows down the combustion rate, but only in a narrow load range. On the other hand, emissions of unburned HC and CO increased, which indicated that the combustion became incomplete.

2.1.2.5 Fuel Modifications

Fuel behavior is influenced by its composition, molecule size and structure. Therefore, fuel pre-conditioning or blending can make some fuels more favorable for CAI combustion and also make controlling process more achievable. By separating a premium fuel with a standard 95 octane number (ON) into vapor and liquid fractions, Lavy et al [44] showed that the fractions formed have different octane numbers. The vapour phase has 90ON, while the liquid phase 95ON. The fraction with the lower octane number is more suitable for CAI combustion due to its better auto-ignition characteristic.

Results obtained by Iida et al [58] suggest that DME-air mixture gives a higher heat release rate, lower emissions and stable CAI combustion over wider air-fuel ratio than n-butane-air mixture. Blending DME with methane gives an even broader controllable range and lower emission especially at light load [59].

However, sometimes fuel blending can limit the operational range of the CAI combustion. Results from experiments carried out with blended fuel (19% of hexadecane and 81% of heptane) [39], show that the suitable air-fuel ratio range for the CAI combustion narrows significantly with the compression ratio increasing. This trend was much lower when diesel fuel was used [56]. In this case fuel blending has not been properly chosen, so the final target of obtaining a wider operating range has not been achieved. Choosing proper fuel pre-conditioning or blending must be done very carefully and must consider all engine parameters, otherwise it can bring more problems than benefits [39, 56, 57, 59].

2.1.3 Summary of the Review of Experimental Works on CAI Combustion

From the afore-mentioned studies it is evident that the control of the CAI combustion engine has been achieved only in a limited load range, for lean air-fuel mixture and large amounts of EGR. As the air-fuel mixture becomes richer, the combustion stability vanishes, knock phenomena appear and the emissions benefits disappear [23, 24, 39, 52, 56].

2.2 Modelling Work on CAI Combustion

There are far fewer numerical analyses of CAI combustion, which have been reported in the literature than experimental studies. Numerical analyses can be divided into several categories, depending on their assumptions of in-cylinder and general engine process phenomena:

- Fluid dynamics

- Chemical kinetics

- Combined fluid dynamics and chemical kinetics

- Other approaches.

In this section a discussion of these approaches will be carried out, together with the critical analysis of their benefits and deficiencies.

2.2.1 Fluid Dynamics Approach

The **fluid dynamics approach** is based on using fluid mechanics codes, like KIVA, with relatively simplified chemical kinetics models [60, 61, 62, 63, 64]. These models are mainly focus on mixing and diffusion phenomena where turbulence plays an important role and chemical kinetics secondary role. This results that these models are limited in accuracy due to simplified chemical kinetics, that do not give satisfactory

prediction of CAI combustion (values of cylinder pressure, auto-ignition timing, heat release rate, etc.) under all possible operating conditions. The use of fluid mechanics codes is very important in operating conditions where the charge is not homogeneous (operations with DI in CI engines), and fuel mixing and evaporation processes might have a considerable effect on the combustion [65].

2.2.2 Chemical Kinetics Approach

The **chemical kinetics approach** for analysing the CAI combustion is based on the use of detailed chemical kinetics codes [66, 67]. These codes include complete chemical kinetics, i.e. all sequences of the steps that reactions go through in proceeding from reactants to products.

One of the methods is based on using a zero-dimensional *single-zone model*, which assumes the cylinder as a volume with uniform composition and thermodynamic properties. These assumptions are applicable to the CAI engine, where mixing is not a controlling factor [2, 20, 68]. A A single-zone analysis can predict the start of auto-ignition (auto-ignition timing) with good accuracy, if the conditions at the beginning of the compression stroke are known, but it suffers from over-prediction of peak cylinder pressure and NO_x emission, under-prediction of the burn duration and less accurate prediction of unburned HC and CO [69, 70].

Impacts of CR, engine speed, air-fuel ratio and EGR on the ignition timing of the CAI combustion of primary reference fuels n-heptane and iso-octane have been analysed in [71]. In this analysis the single-zone model was used for the cylinder environment together with the assumption of adiabatic compression and expansion. The results obtained suggest that the onset of ignition was affected by the operating conditions. Iso-octane allows higher CR than n-heptane and thus provides the potential for high efficiency. Engine operating conditions have a reduced effect upon ignition timing for iso-octane than n-heptane.

A single-zone model with heat transfer sub-model, based on Woschini's correlation [1], was used for the simulation of methane CAI combustion and for the analysis of

impacts of CR and residual gas trapping on ignition timing, duration of combustion and emissions of HC and CO in [69, 70]. The heat transfer sub-model employed ignores spatial variations in the cylinder, treating heat loss as a distributed heat transfer rate proportional to the temperature difference between the average gas temperature and a time averaged wall temperature. The results obtained indicate that an acceptable region of controlled CAI combustion (efficiency above 50% and NOx emission below 100pm) is achieved for the low fuel-air ratios (ϕ up to 0.5) and CR up to 18:1 with supercharging (boost pressure 3 atmosphere). In addition, the model indicates that residual gas trapping and air-fuel ratio can be effective methods.

The model used in [69, 70] has a heat transfer sub-model whilst the model used in [71] assumes adiabatic compression and expansion (without heat transfer). Therefore, over-prediction of peak cylinder pressure, NOx emission and under-prediction of burn duration are less in comparison to the adiabatic case. Both models, in [71] and [69, 70], suffer from an oversimplification of the real conditions within the cylinder. The boundary layer, which contains a significant mass of the charge is likely to be at a lower temperature than the bulk gas around the TDC. The fuels inside the boundary layer and crevices can only be burnt during the very late stage of combustion when their temperature rises to the required levels, and their combustion extends over the entire heat release process. By assuming unified temperature throughout the entire combustion chamber, the estimated combustion duration and heat release process was reduced, therefore, peak cylinder pressure, and pressure rise rate were overestimated. Additionally, CO and HC emissions could not be predicted accurately due to the fact that they relate to crevices and wall boundaries [20]. However, prediction of the ignition timing and NO emission, that depends on the peak temperature of the bulk gases inside cylinder, were estimated with good agreement with the experimental data obtained in [24].

In order to overcome deficiencies of the single-zone model and to take into account

the influence of the boundary layer and crevices, Easley et al [72] used a multi-zone modelling approach. The cylinder was divided into six zones: three adiabatic core zones, one outer core zone, a boundary layer and crevices. The mass exchange between the outer zone, boundary layer and crevices was considered, while the mass in the core zones was assumed to be constant. The model gives a better prediction of heat release rate and peak cylinder pressure than the single zone model, since temperature and mass distribution are taken into account. However, the multi-zone model cannot accurately predict the HC and CO emissions, as the mixing between the cold boundary gases and hot bulk gasses was not considered.

Ogink et al [73] applied a similar approach as Easely et al [72], but the cylinder was divided into ten zones and mixing between the core zones and boundary layer was included. Although these improvements lead to a better prediction of HC and CO emissions, the model still cannot predict these emissions accurately. A possible reason for this can be due to the use of reduced chemical kinetics scheme (in-house), which failed to predict accurately the HC and CO emissions compared to a detailed kinetics scheme. Additional adjustment and validation of the reduced mechanism is needed.

For multi-zone modelling the computational time (CPU time) is a few orders of magnitude higher than that needed for single-zone modelling.

2.2.3 Combined Fluid Dynamics and Chemical Kinetics Approach

A combined fluid dynamics and chemical kinetics approach is used in order to overcome the inability of a single-zone model to model the temperature gradient, mass distribution and thermal boundary layers within the air-fuel mixture. The combined approach uses a fluid dynamics code to model temperature and mass distribution within the air-fuel mixture, and a detailed chemical kinetic code to model ignition and further combustion processes. The entire cylinder charge is divided into several zones, each of which has a different temperature and mass distribution. The fluid dynamics code is used to calculate the pressure and temperature in each

of the zones, from the beginning of the compression stroke (point of intake valve closing-IVC) to the transition point (several crank angle degrees before TDC) [29]. After that, until the end of expansion stroke, the detailed chemical kinetics code is used.

This approach demands a significant amount of CPU time for running each set of data. The order of the run time varies from a several days for relatively simple hydrocarbon fuel such as methane, to several weeks for a higher hydrocarbon fuel like iso-octane [16, 29, 30]. In order to reduce the run time, a segregated modelling approach [16, 30] and reduced chemical kinetics have been employed [74].

In comparison to sequential multi-zone modelling, where all zones are solved simultaneously during a given time interval, in the segregated approach each zone is solved separately. This reduces the run time of a ten zone problem by an order of magnitude [16].

A reduced chemical mechanism was applied together with a segregated approach to reduce the run time for combined fluid dynamics and chemical kinetics multi-zone modelling of higher hydrocarbon fuels [74]. The run time was reduced by factor of 20 for the 10 zone problem, compared to the run time for the detailed chemical kinetics. However, the emission of HC and CO was not accurately predicted with reduced mechanism.

Kong et al [31] used a combined multi-dimensional CFD code (Kiva-3V [60]) with a detailed chemical kinetics code (Chemkin [67]) for modelling direct injection CAI engine fuelled with natural gas. The effect of turbulence was taken into account by modifying the reaction rates, to incorporate the effects of both chemical kinetics and turbulent mixing through the characteristic timescale. The turbulent time scale was defined as the eddy break-up time, whereas the kinetics timescale was estimated as the time needed for a species to reach the equilibrium state under perfectly mixed conditions. The results show that turbulence has a strong effect on ignition timing in the case of direct fuel injection as evaporation and mixing processes play important roles in the preparation of the air-fuel mixture. It was also found that radicals from

EGR have an influence on the ignition timing and heat release rate.

Recently, Hong et al [75] proposed an improved, but more computationally demanding model to simultaneously account for effects of detailed chemistry and mixing on ignition delay, under directed injection stratified charge conditions. The model is comprised of a combination of the laminar flame approach, used during the induction time, and a modified Eddy Dissipation Concept (EDC), used subsequently. The EDC is used to predict the reaction rate based on the interaction between chemical and mixing rates. A transition model was also developed to predict local ignition and transition phenomena between the chemistry-only and chemistry-mixing regimes based on branched chain explosion and thermal explosion. Although this has a strong physico-chemical basis, fully coupled CFD and detailed chemistry models were accompanied with significant computational requirements, which has so far constrained their routine use for parametric studies.

2.2.4 Other Approaches

In **other approaches** for numerical modelling of a CAI combustion, two different attempts were made:

- Partially stirred reactor model for the cylinder environment

- Full cycle simulation model.

In the **partially stirred reactor model**, a probability density function (PDF) was used to introduce a certain degree of inhomogeneity for the mixture temperature and composition [76, 77]. This model is based on a stochastic approach, which includes the effects of turbulent mixing and diffusion together with detailed chemical kinetics. A CAI engine fuelled with natural gas was simulated. This model considers the existence of a boundary layer and an air-fuel mixture in the crevices, that are significantly cooler than bulk gases. The prediction of ignition, combustion duration, cylinder peak pressure and HC and CO emissions was in good agreement with the

experimental results carried out in [24]. The major advantage of such an approach is the possibility of modelling incomplete combustion, which is a consequence of the mixing of cold and hot regions of gas. The CPU time for running a single set of data is considerably shorter than for the case of multi-dimensional CFD modelling involving detailed chemical kinetics, but much longer than using only a single-zone detailed chemical kinetics approach. Moreover, the integration of a partially stirred reactor model with detailed chemical kinetics can be sometimes very troublesome, and needs additional adjustments and extra run time.

The **full cycle simulation model** was recently applied [78, 79, 80], in order to account for the influence of gas exchange process on air-fuel mixture preparation during exhaust and induction strokes.

Ogink et al [78] incorporated a single-zone model into the AVL BOOST engine cycle simulation code. In that way the simulation of compression and expansion were carried out by using a single-zone model with detailed chemical kinetics, whilst the exhaust and induction stroke were simulated by the 1-D gas dynamic AVL BOOST code. The major advantage of this approach is that the initial values of the charge properties and EGR fraction at the start of compression (IVC point) no longer have to be specified. Instead, they can be automatically calculated by the code.

Cantore et al [79] used a similar approach, where a partially stirred reactor (PaPSR) based PDF code [76] was connected by an interface with the GT-Power 1-D fluid dynamics code. An interface was developed in order to exchange information between these two codes.

Both integrated codes [78, 79], give a good prediction of ignition timing, but suffer from a slight overprediction of the heat release rate and peak cylinder pressure. Furthermore, HC and CO emissions could not be correctly predicted. These problems were associated with a single-zone model approach and the fact that mixing between zones and layer was not considered.

Fiveland et al [80] proposed a physically-based quasi dimensional model for full cycle simulation. The model considers a multi-zone approach, and the cylinder was divided into three zones: an adiabatic core, thermal boundary layer of varying thickness and crevices zone of variable volume throughout the cycle. A detailed chemical kinetics model could have been incorporated, but it was preferred to run the model with reduced kinetics, due to the considerably shorter CPU time. The simulation was able to predict well the ignition timing and NO_x emission but slightly unpredicted the cylinder peak pressure and heat release rate. The emission of HC was overpredicted, while the CO emission was unpredicted.

2.3   Summary of the Modelling Work on CAI combustion

The summary of the analysis of different numerical approaches for the modelling of CAI combustion is as follows:

- The use of a fluid dynamics approach is limited in accuracy due to simplified chemical kinetics that do not give satisfactory results under all possible operating conditions.

- The insensitivity of CAI combustion to turbulence makes it possible to use a chemical kinetics approach for analysis of CAI combustion. The use of detailed chemical kinetics gives very good results in prediction of the auto-ignition timing, heat release rate, peak cylinder pressure and NO_x emissions. However HC and CO emission were often poorly predicted. There were generally two basic chemical kinetics approaches: single-zone and multi-zone modelling. A *single-zone model* offers good accuracy in the prediction of ignition timing and NO_x emission, but suffers from a slight overprediction of heat release rate and peak cylinder pressure. All these problems were improved by using the *multi-zone model*, but run time was increased by several orders of magnitude. The average run time for single-zone model, for running one set of data, was

around one hour for a higher hydrocarbon fuel, whereas in the case of ten-zone modelling it increased to around several days. Problems with the prediction of HC and CO emissions could not be solved by a using multi-zone model, because mixing effects with the boundary layer, which mainly depends on turbulence, were not taken into account.

- Much more complex models, which incorporated CFD and detailed chemistry, were used to resolve the problems of accurate modelling of HC and CO emissions. These models considered the turbulence effect together with the effect of chemical kinetics on auto-ignition, combustion and emission formation processes. Ignition timing, heat release rate, peak cylinder pressure and NO_x emission were predicted to the same accuracy as in the case of using only chemical kinetics modelling without turbulence. This is more evidence, besides the other experimentally derived evidence [2, 26, 27, 28], that CAI combustion is a process dominated by chemical kinetics without the influence of turbulence. Emissions of HC and CO were predicted with greater accuracy in comparison with using only a chemical kinetics approach. It was concluded that these emissions were mainly dependent on interaction between crevices, boundary layers and the core zone. This interaction influences the mixing processes, which in turn determines temperature, mass distribution and available oxygen and thus the processes of HC and CO formation. However, the simultaneous use of CFD and detailed chemical kinetics was accompanied by a significant increase in run time (up to several weeks for higher hydrocarbon fuels). This implies that either reduced chemistry or a less dense mesh have to be used, which will affect accuracy. Due to the excessive computational requirements this method is not suitable for routine use for parametric studies or as a design tool.

- The coupling of a detailed chemical kinetics code with a 1-D engine cycle simulation code is a relatively new and interesting approach. This approach combines a detailed chemical kinetics scheme for the modelling of compression

and exhaust strokes, and an engine cycle simulation code for modelling the influence of gas exchange process on the air-fuel mixture formation during the exhaust and induction strokes. The benefit from this approach is the ability to automatically calculate the charge properties, such as temperature, composition and pressure at the the start of compression process (IVC point). This is very valuable, since the auto-ignition and subsequent combustion is determined by the charge properties at the IVC point. It is likely, that this combined modelling can be used in the future as a tool to analyze engine behaviour under various operating conditions, and to asses the proper engine control strategies. However, validation and adjusting of this coupled code is still in the investigation phase and additional improvements have to be done before these approaches can be used as a accurate engine design tool.

From the above-discussioned simulation studies it emerges that the use of a single-zone model seems to be very convenient for parametric studies of CAI combustion. It offers good accuracy in the prediction of the auto-ignition timing, heat release rate, peak cylinder pressure and NO_x versus run time.

Chapter 3

Combustion Phenomena and Chemical Kinetics

How many times we have heard the question, *"What actually is combustion?"*. The answer to this question is neither simple nor straightforward. The shortest answer would be that the combustion is a self-sustained chemical reaction.

Combustion phenomena arises from an interaction of chemical and physical processes. The heat release originates in chemical reactions, but its exploitation in combustion involves heat transport process and fluid motion. Therefore, in order to the interpret combustion process, physics, fluid mechanics and mathematics have to be applied [34, 81].

Combustion provided early man with his first practical source of energy. It gave him warmth and light, it extended the range of foodstuffs which he could digest, and it enabled him to modify metals. Throughout the world today combustion still provides more than 95% of the energy consumed and, despite the continuing search for alternative energy sources, it is very likely that combustion will remain important for a very considerable time to come. The use of combustion fuels remains especially attractive for the foreseeable future, for example in transport applications [34].

It is very important to ensure that combustion processes are performed in the most efficient manner. The most important ones are the need to minimise waste of energy, to avoid unnecessary emissions of carbon dioxide as one of the contributors to

the 'greenhouse effect', and to minimise adverse effects on the environment which may arise through pollutant emissions. Reserves of fossil fuels are also running out in varying extents, so that fuels themselves are becoming less accessible, and more expensive to recover. Therefore, the study of combustion processes becomes an important area of scientific work, and it will remain so having regard to the requirements of society and the demands of national and international legislation which control the environmental impact [34]

This chapter is organised so that principles of combustion phenomena and chemical kinetics will be presented first. Reaction rate and its dependence of concentrations, temperature and pressure will be explained next, followed by thermo-molecular reactions and elements of chain reaction mechanism. At the end of the Chapter the use of chemical kinetics for combustion related problems will be discussed.

3.1 Overview of Combustion Phenomena

Combustion begins in chemistry with a self-supported, exothermic reaction. The physical processes involved are principally those which pertain to transport material and energy. The conduction of heat, the diffusion of chemical species and the bulk flow of gas may all develop from the release of chemical energy in an exothermic reaction, as a consequence of the thermal and concentration gradients that exist in the reaction zone. Interaction of all these various processes leads to the phenomenon called *combustion*. Other effects such as light emission, depend on specific chemical processes which may have only a negligible influence on the combustion.

The chemical reaction usually involves two components. One component is *fuel* and the other is *oxidant* (air). Each component plays its part in the reaction. The simple case for combustion to take place is when the gaseous, premixed components, are introduced into a container, maintained at uniformly controlled temperature. If the vessel is hot enough, measurable exothermic oxidation of the fuel will occur. If the heat produced by the reaction is transported sufficiently rapidly to the container

walls by conduction and convection, a steady reaction is maintained. This balance of the heat release and loss rates, such that reaction proceeds smoothly to completion, is usually referred to as *'slow reaction' or 'slow oxidation'*. Even though there is no absolute criterion of reaction rate alone from which one can conclude *'how slow is slow?'* [34].

Above a certain temperature in the container, the rate of energy release from the chemical reaction may exceed the rate at which it can be transported to the vessel walls by the various heat transfer processes. Consequently, the temperature in the container then increases, the rate of reaction increases and then the rate of heat release increases. This acceleration of reaction rate leads to a further increase in temperature and the combined effect leads to an *'explosion'*. The term *explosion* refers to the violent increase in pressure which must accompany rapid self-acceleration of reaction, usually ending physically by its damaging consequences [34].

This type of explosion is driven solely by the rate of energy release through thermal feedback. The state of self-acceleration is termed *ignition* and the phenomenon described here is called a *thermal ignition* or *thermal explosion*. Thermal ignition is discussed in Chapter 4. The afore-mentioned description illustrates how an interaction between the *physics* (i.e. heat transport processes) and the *chemistry* (determined here in solely by the rate of heat release and how it is affected by the temperature) governs whether or not the explosion will occur. The underlaying properties that make such an event possible are the reaction rates normally increase exponentially with temperature, whereas the heat transfer often depends almost linearly on temperature [34].

In a propagating combustion wave, called a *'deflagration'* or *'flame'*, reaction is initiated by a spark or other stimulus. Reaction is then induced in the layer of reactant mixture ahead of the flame front by two possible mechanisms, by heat conduction or by diffusion of reactive species from the hot burned gas or reaction zone behind the flame front. Therefore, the thermal and chemical reaction properties of the combustion system may still drive the reaction but now there is a spatial

structure, and both the heat and mass transport processes have to be taken into account.

If the premixed reactants are forced to flow towards the flame front, and their velocity is equal to the rate of which the flame would propagate into stagnant gas, i.e. the burning velocity, the flame itself would come to a standstill. This is put into practice in combustion applications that involve burners, the design of the appliance being aimed at holding the flame in one position and render it stable towards small disturbances.

An alternative to the *premixed flame* is the *diffusion flame* in which the separate stream of fuel and oxidant are brought together and reaction takes place at their interface. The candle flame is one example. The supply of air to the reaction zone is sustained by the convection currents set up by the flame itself. This flow also provides cooling to the sides of the cup of the melted fuels.

The velocities of premixed flames are limited by transport processes. For example, heat conduction and species diffusion. The velocities cannot exceed the speed of sound in the reactant gas. However, it is often found that a propagating combustion wave undergoes a transition to a quite different type of wave, a *detonation wave*, which travels at the velocity much higher than the speed of sound. In this type of wave the chemical reaction is initiated by a supersonic compression, or *shock wave*, travelling through the reactants. The chemical energy that is released in the hot, compressed gas, behind shock front, provides the driving force for the shock wave. In this case, it is necessary to consider the chemistry of the system, only to the extent that it provides a source of energy at a rate which is governed by the prevailing temperature, pressure and reactant concentrations [34].

3.2   Combustion Principles and Applications

The combustion phenomena described so far are not restricted to gaseous media. Most occur in liquids and solids, and in dispersions of one phase within another

(droplets mists or dust clouds). Combustion can also occur at the interface between bulk phases, and is termed as *heterogeneous combustion.*

It can be noted in Section 3.1 that there are three broad subject areas within combustion [34]:

1. Chemical kinetics and spontaneous processes in an essentially homogeneous reactant mixture.

2. Flame propagation.

3. Detonation or shock.

This classification is arguable and it may be also subdivide or extend the scope of each to more than one area.

The most important characteristic of combustion is its self-sustaining nature. Heat and free radicals originate in the chemistry itself, whereas the physical processes, heat and mass transport in particular, enable these sources to be used to promote (to sustain) the reaction without any other external agency being applied [34].

The energy released in combustion may be turned directly into mechanical energy and used as a source of motive power, as in spark ignition engines, diesel engines or gas turbines, or it may be used indirectly to generate mechanical energy, as in the case when steam is generated to drive the turbines in an electricity power station. Combustion processes are also involved in heating applications, ranging from domestic gas, oil or solid-fuel central heating units to large industrial furnaces. In all of these applications the oxidant is atmospheric air, which may impose constraints on efficiency and which may contribute to pollutant emissions. The efficiency of combustion processes may be enhanced by raising the pressure above atmospheric, as in turbo-charging of spark ignition or diesel engines.

In specialist applications, especially where extremely high energy liberation and also high density of the fuel are essential, the oxidant may not be air or oxygen. Also, it cannot be in gaseous phase or it can even be molecularly separated from the fuel

[34]. The class of substances that fall within these categories are *high explosives* for commercial or military uses, or *low-order explosives* that are used for armament and rocketry. In high explosives the maximum amount of energy is liberated in a minimum time, as is characteristic of detonations. Further explanations about these interesting areas will be beyond the scope of this work, and will not be performed.

3.3 Chemical Kinetics

Chemical kinetics is the study of the rate and mechanisms of chemical change. Its function is first to determine the rates at which chemical reactions take place in different circumstances and secondly to arrive at an understanding of the relevant facts about reactions. The latter endeavor necessarily entails the study of reaction mechanisms. At the most macroscopic level this involves elucidating the intermediate steps by which many reactions proceed to the final products. Also, at the most microscopic level it includes considering the events that occur during individual molecular collisions [81].

In short, *chemical kinetics* is the study of the rates of chemical reactions as well as the study of the sequences of the steps that reactions go through in proceeding from reactants to products. The steps of a chemical reaction are collectively called the *reaction mechanism* or *chemical kinetic mechanism*.

While all combustion processes depend on the total amount of energy released by chemical reaction, not all depend on rate of reaction, provided that it exceeds some minimum value. Thus the overall behaviour in detonation waves, diffusion flames, burning droplets are virtually independent of *chemical kinetics*. On the other hand, premixed flames, fire and the internal combustion engine are sensitive to the *chemical kinetics* involved. The fundamentals or reaction kinetics will be discussed in this section.

3.3.1 Reaction rate, Kinetic Rate Laws and Reaction Orders

The quantitative behaviour of a chemical reaction is described by a *rate law* which specifies the rate of change in the concentration of chemical species. It is represented in terms of the product of concentration and a rate constant (or rate coefficient) which is independent on concentration but usually not on temperature. For the reaction represented by the following stoichiometric equation:

$$v_A A + v_B B + \ldots = v_P P + v_Q Q + \ldots \tag{3.1}$$

the rate law with respect to these four components takes the form

$$\frac{-1}{v_A}\frac{d[A]}{dt} = \frac{-1}{v_B}\frac{d[B]}{dt} = \frac{-1}{v_P}\frac{d[P]}{dt} = \frac{-1}{v_Q}\frac{d[Q]}{dt} = k[A]^a[B]^b \tag{3.2}$$

where k is the *rate constant* or *rate coefficient* of reaction. The powers a and b are known as the *orders of reaction* with respect to the concentrations of the reactants A and B, respectively, and the *overall order* is given by *(a+b)*. The individual orders of reaction quantify the dependence of the reaction rate on the species concentrations. The terms on the left-hand side of Equation (3.2) rationalise the reaction rate in terms of changes of any of the molecular reactants or product concentrations through respective stoichiometric coefficient. By the convention [34, 35, 81] the rate of change of concentration is regarded positive, and thus the negative stoichiometric coefficients representing the reactant consumption. The square brackets denote either a molecular or a molar concentration of a species, and thus the reaction rate is expressed as molecules (or moles) per unit volume per unit time [34].

Frequently the some species may be in excess. In this case their concentration do not change noticeably. If, for instance, $[A]$, $[B]$, ... remain nearly constant during the reaction, an effective rate coefficient can be generated from the rate coefficient and a nearly constant concentration of the species in excess. By using $k_{new} = k[A]^a[B]^b\ldots$, a simplified version of (Equation 3.2) can be obtained

$$\frac{d[A]}{dt} = -k_{new}[A]^a \tag{3.3}$$

For the *first order* reaction (a=1) integration of (Equation 3.3) yield the first time order behaviour

$$\ln \frac{[A]_t}{[A]_0} = -k_{new}(t - t_o) \tag{3.4}$$

where $[A]_0$ and $[A]_t$ denote the concentrations of species A at time t_0 and t, respectively.

Accordingly, the *second order* reaction behavior (a=2) leads to

$$\frac{1}{[A]_t} - \frac{1}{[A]_0} = k_{new}(t - t_o) \tag{3.5}$$

Finally, for the *third order* reactions (a=3)the temporal behaviour is expressed with

$$\frac{1}{[A]_t^2} - \frac{1}{[A]_0^2} = 2k_{exp}(t - t_o) \tag{3.6}$$

If the time behaviour is measured, the reaction order can be determined. Logarithmic plots of the concentrations versus time for the *first order* reaction, shown in Figure 3.1 (Diagram (a)), lead to linear dependencies with the slope $-k_{new}$ and plots of $1/[A]_t$ versus the time. For the *second order* reaction, shown in Figure 3.1 (Diagram (b)), the dependence is also linear but with slope k_{new} [35].
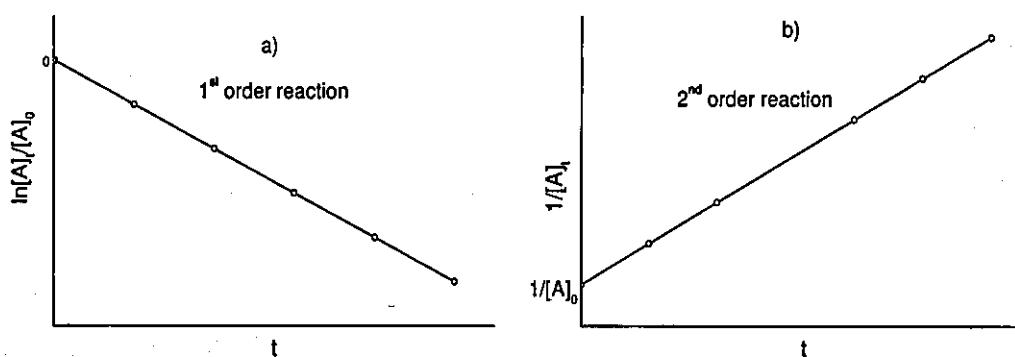
Figure 3.1: Time behaviour of concentrations (a) for the first order reaction and (b) for second order reaction [35].

Factors that affect the *reaction rate* are:

- Concentrations of the reactants

- Temperature

- Pressure at which reactions occur.

3.3.2 The Dependence of Reaction Rate on Concentration

Before the start of the discussion the difference between a rate expression which represents an *overall reaction* (often referred as a *global reaction*), and an *elementary step* have to be made. The latter represents one of the components of the mechanism that makes up overall reaction. For example, the process

$$H + O_2 \rightarrow OH + O \tag{3.7}$$
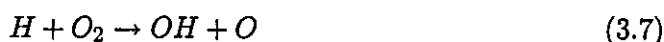
is an elementary step in which hydrogen atom collides with an oxygen molecule and three atoms rearrange to give a hydroxyl radical and an oxygen atom [34]. In this case, the rate law may be derived directly from this concept of the molecular interaction. Doubling the concentration of oxygen molecules in the system would double the frequency of collisions of H atoms with them, and hence the rate of conversion to product species. Thus *bimolecular interaction* must have a linear dependence on $[O_2]$, i.e. be the first order with respect to it. The *molecularity* of a reaction describes the number of molecules involved in the reactive event. On the basis of a similar argument with respect to the H atoms, the rate law for Equation (3.7) is expressed as

$$\frac{-d[H]}{dt} = \frac{-d[O_2]}{dt} = \frac{d[O]}{dt} = \frac{d[OH]}{dt} = k[H][O_2] \tag{3.8}$$

That is, the rate law is the *first order* with respect to each of the reactants and *second order overall*. The reaction rate of an elementary reaction is never dependent on a product concentration. The forward and reverse rate constant of an elementary reaction, k_f and k_r, are related through the expression $k_f/k_r = K_c$, where K_c is the equilibrium constant defined in terms of reactant and product concentrations.

Most combustion processes take place by a series of elementary steps, as part of a chain reaction. Thus, an overall equation which represents the stoichiometry of the

reaction does not necessarily reflect the detailed events as the species react, nor does it give information about the concentration dependences in the appropriate rate law. For example, the overall stoichiometry of

$$2H_2 + O_2 = 2H_2O \qquad (3.9)$$

may be represented by a global rate law like

$$\frac{-1}{2}\frac{d[H_2]}{dt} = \frac{-d[O_2]}{dt} = \frac{-1}{2}\frac{d[H_2O]}{dt} = k[H_2]^{1.5}[O_2]^{0.7} \qquad (3.10)$$

but this cannot be regarded to represent two hydrogen molecules colliding with a single oxygen molecule to form water [34]. The global process consists of complex sequence of elementary steps, so a global rate law is needed to represent it. The global rate law is an empirical representation of the dependence of reaction rate on concentration which applies over a very specified range of conditions. In some cases it can happen that the detailed reaction mechanism is not completely understood, or that its complexity makes it unsuitable for incorporation into a computer model, and then a global expression has to be used. For a global reaction the order must be established by experiment. The fractional reaction order, as measured, should provide information that reaction mechanism is a complex composite of elementary reactions.

However, solutions of a global reaction sometimes can be a very tedious and a time-consuming task. The formation of water (Equation 3.9), can be described by many elementary reactions [35].

The concept of using elementary reactions has one advantage, the reaction order of elementary reaction is always constant (in particular independent of time and experimental conditions) and can be determined easily. The important thing about elementary reaction, which has to be looked at, is molecularity of the reaction. Three possible values of the *reaction molecularity* are observed:

1. *Unimolecular* reactions describe the re-arrangement or dissociation of a molecule

$$A \rightarrow products \qquad (3.11)$$

and they have a *first order* rate law (*first order kinetics*). If the initial concentration is doubled, the reaction rate is also doubled.

2. *Bimolecular* reactions are the reaction type which takes place most frequently [35]. They proceed according to the reaction equations

$$A + B \rightarrow products \quad \text{or} \quad A + A \rightarrow products \quad (3.12)$$
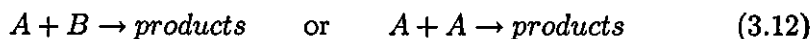
Bimolecular reactions always have a *second order* rate law. Doubling the concentration of each reactant quadruples the reaction rate.

3. *Trimolecular* reactions are usually recombination reactions. They obey a *third order* rate law

$$A + B + C \quad \rightarrow \quad products \quad \text{or} \quad (3.13)$$
$$A + A + B \quad \rightarrow \quad products \quad \text{or}$$
$$A + A + A \quad \rightarrow \quad products$$
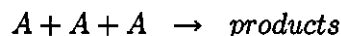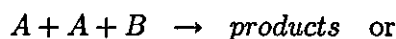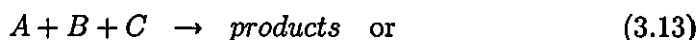
In general the molecularity equals the order of elementary reactions and thus, the rate laws can be easily derived. If the equation of an elementary reaction r is given by

$$\sum_{s=1}^{S} \nu_{rs}^r A_s \longrightarrow \sum_{s=1}^{S} \nu_{rs}^p A_s \quad (3.14)$$

then the rate law for the formation of species i in reaction r is given by the expression

$$(\frac{\partial C_i}{\partial t})_{chem,r} = k_r (\nu_{ri}^p - \nu_{ri}^r) \prod_{s=1}^{S} C_s^{\nu_{rs}^r} \quad (3.15)$$

Here ν_{ri}^r and ν_{ri}^p denote stoichiometric coefficients of reactants and products respectively and C_s concentrations of the S different species-s.

The units of the rate constants are governed by the overall reaction order (be it a global representation or an elementary reaction), since the units on the right-hand side must equate to those on the left-hand side. Thus a first-order rate constant has the dimensions of time $[time]^{-1}$, whereas a second-order rate constant has units

[concentration]$^{-1}$ [time]$^{-1}$. In combustion reactions, the units of time are almost always seconds, whereas convenient concentration units may be molecules cm^{-3}, mol cm^{-3}, mol dm^{-3} or mol m^{-3}.

A useful parameter that gives some concept of the time scale on which the chemistry takes place, especially with respect to frst order reactions, is the *half-life* of the reaction ($\tau_{1/2}$). This represents the time for 50 % of the reactant to be consumed, and is given by $\ln 2/k$. For a second or higher order reactions, the corresponding parameter is derived under pseudo first order conditions, that is by subsuming certain reactant concentrations into the rate constant [34].

3.3.3 The Dependence of Reaction Rate on Temperature

The temperature dependence of a reaction is incorporated in the rate constant, and is expressed in Arrhenius form, as

$$k = A \exp^{(\frac{-E}{RT})} \tag{3.16}$$

The parameters A and E are independent of temperature in this representation. Although they are derived experimentally, these terms have clear identities even in quite simple interpretation of reaction rate theory. Therefore, A is termed the *frequency factor* with respect to first order reactions, since it may be identified with the rate at which chemical bonds can rearrange in a molecule and relates to a vibrational frequency (10^{13}s^{-1}). In other circumstances, A is called a pre-exponential term and explains some relationship to collision frequencies between the interacting species in elementary reactions [34]. The units of A also stand for k. For bimolecular reactions A corresponds to a product of collision rate and probability of reaction. This collision rate is an upper limit for the reaction rate. The kinetic theory gases yields values for A in the range from 10^{13} to 10^{14} cm^{3}mol^{-1}s^{-1}.

E represents the *activation energy* of the reaction. It may be regarded as an energy barrier which has to be overcome during the reaction. The maximum value of E corresponds to the bond energies in the molecule (in dissociation reactions, for

example E is approximately equal to the bond energy of the split bond), but it can also be much smaller (or even zero), if new bonds are formed simultaneously with the breaking of the old bonds. The *activation energy* has the units $Jmol^{-1}$ or $kJmol^{-1}$. The quotient $(E/R)/K$ represents a temperature coefficient, which testifies to its experimental origin as a quantitative measure of the way in which rate constant varies with temperature [34]. The coefficient E/R is often quoted in rate data, rather than the activation energy.

The two-parameters representation of the temperature dependence (Equation 3.16) is satisfactory for most reactions, especially over limited temperature ranges, and is confirmed by the linearity of the relationship

$$\ln k = \ln A - \frac{E}{RT} \tag{3.17}$$

in the classical Arrhenius plot $\ln k$ versus $(1/T)$. However, in some applications in combustion the rate constant has to be represented over considerable wide temperature range (for instance 500-2500 K). Where experimental measurements are available it might be found that the two parameters representation (Equation 3.16) is inadequate, and that three-parameters representation has to be used

$$k = A'T^n \exp^{\left(\frac{-E}{RT}\right)} \tag{3.18}$$

where n is a number of order unity. The products $A'T^n$ now has the units of the rate constant.

3.3.4 Pressure Dependence of Rate Coefficients

The apparent pressure dependence of rate coefficients, in some dissociation (unimolecular) and recombination (trimolecular) reactions, is an indication that these reactions are actually not elementary. They do, in fact, represent a sequence of reactions. In the simplest case, the pressure dependence can be explained by using the Lindemann model [82]. According to this model, a unimolecular decomposition is only possible if the energy in the molecule is sufficient to break the bond. Therefore,

it is necessary that before the decomposition reaction takes place, energy is added to the molecule by collision with other molecules M. For example, for the excitation of molecular vibrations, then the excited molecule may decompose into the products, or it can deactivate through collision,

$$A + M \quad \rightarrow \quad A' + M \quad \text{(activation, with } k_a)$$

$$A' + M \quad \rightarrow \quad A + M \quad \text{(deactivation, with } k_{-a})$$

$$A' \quad \rightarrow \quad P_{products} \quad \text{(unimolecular reaction, with } k_u) \qquad (3.19)$$
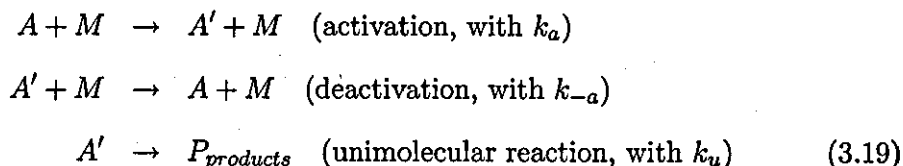
According to (Equation 3.3), the rate equations for this case are given by

$$\frac{d[P]}{dt} \quad = \quad k_u[A'] \quad \text{and}$$

$$\frac{d[A']}{dt} \quad = \quad k_a[A][M] - k_{-a}[A'][M] - k_u[A'] \qquad (3.20)$$

Assuming that the concentration of the reactive intermediate A' is in a quasi-steady state,

$$\frac{d[A']}{dt} \approx 0 \qquad (3.21)$$

then from Equation (3.20) concentration of the activated species $[A']$ and the formation of the products P are obtained

$$[A'] \quad = \quad \frac{k_a[A][M]}{k_{-a}[M] + k_u}$$

$$\frac{d[P]}{dt} \quad = \quad \frac{k_u k_a[A][M]}{k_{-a}[M] + k_u} \qquad (3.22)$$

Two extremes can be distinguished: (i) the reaction that take place at very low pressure and (ii) the reaction that occur at very high pressure.

In the *low pressure range*, the chaperone molecule (third body) M is very small. With $k_{-a}[M] \ll k_u$ it can be obtained a second-order rate law

$$\frac{d[P]}{dt} = k_a[A][M] \qquad (3.23)$$

Thus, the reaction rate is proportional to the concentrations of species A and the third body M, as a consequence of the slow activation, which is the rate limiting factor at low pressure [35].

In the *high pressure rate*, the third body M has a large concentration and together with $k_{-a}[M] \gg k_u$, it can obtain a first-order rate law

$$\frac{d[P]}{dt} = \frac{k_u k_a [A]}{k_{-a}} \tag{3.24}$$

Here, the reaction rate does not depend on the concentration of the third body, since at high pressure, collisions occur very often, and thus decomposition of the activated molecule A' is the rate-limiting factor, instead of the activation step.

The Lindemann mechanism [82] illustrates the fact that the reaction orders of complex, non-elementary reactions, depends on the chosen conditions. However, the mechanism itself is a simplified model. More accurate results for the pressure dependence of unimolecular reactions can be obtained from the theory of unimolecular reactions [83, 84, 85]. This theory takes into account that not only activated species can be defined, but also a large number of activated molecules with different levels of activation.

3.3.5 Thermo-molecular Reactions and Elements of Chain Reaction Mechanism

The thermo-molecular reaction

$$H + O_2 + M \rightarrow HO_2 + M \tag{3.25}$$

obeys third-order kinetics in certain conditions

$$\nu = k[H][O_2][M] \tag{3.26}$$

The symbol M is used to denote any molecule present in the system and its function is to remove some of the energy released by the formation of the new chemical bond, and thus to prevent the product from immediately re-dissociation. M is termed a *third body* or *chaperon* molecule. The rate constant has dimensions of [concentration]$^{-2}$ [time]$^{-1}$ in this case. Third-order reactions often have rates which fall slightly with increasing temperature, which means that the measured activation

energy is slightly negative. This has no obvious physical meaning, and signifies that the mechanism of the overall process is not properly represented as a single *three-body* interaction. Unlike unimolecular reactions, the rate constants for termolecular reaction show a pressure dependence, they become second order at a high pressure limit [34].

The probability of termolecular reactions is so low that these reactions might be expected to be unimportant. However, since they provide virtually the only route for the homogeneous removal of reactive intermediates in gaseous combustion, and they are responsible for the liberation of a consider amount of energy, they are very important. Such reactions tend to predominate in the post-flame region which follows the main reaction zone of a flame. Termolecular recombination reactions, such as

$$H + OH + M \rightarrow H_2O + M \quad \Delta H_{298}^{\ominus} = -468 \text{kJmol}^{-1} \qquad (3.27)$$

or

$$C + O + M \rightarrow CO_2 + M \quad \Delta H_{298}^{\ominus} = -532 \text{kJmol}^{-1} \qquad (3.28)$$
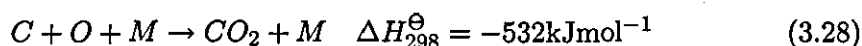
fall in this category.

Combustion reactions normally involve a complex mechanism, or sequence of elementary steps. The mechanism involves chain reactions, in which an active species (usually a free radical or an atom) reacts with a stable molecule to give a product molecule and another active species which can propagate the chain. Thus, in the reaction between hydrogen and chlorine [86], the chain is propagated by the cycle

$$Cl + H_2 \rightarrow HCl + H \qquad (3.29)$$

$$H + Cl_2 \rightarrow HCl + Cl \qquad (3.30)$$
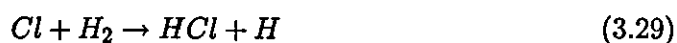
Such reactions comprise of a linear chain since each propagation step leaves the total number of active centres (H and Cl) unchanged.

Although linear chain propagation is normal, examples are known where chain branching may also occur, that is, in which one active species produces additional

species which are capable of continuing the chain. In the oxidation of hydrogen, the reaction

$$H = O_2 \rightarrow OH + O \tag{3.31}$$

brings about chain reactions since both OH and O can react with hydrogen molecules to continue the chain. Branching chain reactions are particulary important in many combustion reactions. This is discussed in Chapter 4.

Typical active species involved in hydrocarbon combustion are H, O, OH, CH_3 and CHO. Reactions of such species have low energy barriers and hence their rates are rapid even though concentrations of active species are low. With the exception of thermal ignition in general, reactions involving only molecular reactants are too slow to sustain combustion.

The behaviour of a complex reaction mechanism is described mathematically by a set of simultaneous differential equations, equal in number to that of the chemical species involved. Analytical solution of these equations is usually impossible, and therefore use is made of the stationary-state approximation in which the rates of change of concentrations of the active centres with respect to the time are set to zero [34]. In the hydrogen/chlorine example, involving equations (3.29 and 3.30) amongst other reactions leads to

$$\frac{d[H]}{dt} = \frac{d[Cl]}{dt} = 0 \tag{3.32}$$

This reduces a number of the differential equations to algebraic equations. It does not imply that the concentrations of radicals are invariant in the time, but only that they can be related algebraically to the concentrations of stable species, which have finite time derivatives. The algebraic equations can often be solved to give the steady-state concentrations of radical species. In some cases, when the state of reaction is very high, it is not possible to use stationary-state assumption [34].

3.4 How Chemical Kinetics can be Used for Combustion Related Problems

It is becoming increasingly important to ensure that combustion processes are performed in the most efficient manner. That they are geared towards increasing efficiency and reducing pollutant emission. Therefore, the study of combustion processes becomes an important area of research work, and it will remain so having regard to the requirements of society and to the demands of national and international legislation which control the environmental impact [34].

The need for compact models to represent the combustion of hydrocarbons has never been greater than it is today, as combustion scientist and engineers exploit computational methods for the design and prediction of performance of practical combustion systems, especially with regard to economical operation and the minimisation of atmospheric pollutants. Numerical studies form the link between experimental observations and fundamental interpretations of the various processes, such as combustion in internal combustion engines, industrial burners and furnaces and in atmospherically relevant reactions. They can also be used in gaining a valuable insight into the nature of the phenomena being explored.

The modelling of some technologically important processes may also result in the need to model other processes along-side with the combustion process, such as partial oxidation and pyrolysis processes. In that way modelling becomes very complex and involves hundreds of kinetically significant species, and with so many reactions it is very difficult to determine (experimentally) all the rates. In some cases the chemical kinetics is closely coupled with mixing and heat flows. Hence, significantly increasing the computational difficulty. It is generally not feasible for one designing a new engine, reactor, chemical process or product to invest the effort required to construct a detailed kinetic model capable of making accurate predictions or extrapolations for these complex systems.

In order to illustrate the complexity of hydrocarbons and other fuels, a short description of their nature will be presented in the following text.

The oxidation of hydrogen is represented by Equation 3.9 ($2H_2O + O_2 = 2H_2O$). The understanding of the kinetics and mechanism of this reaction, over a very wide temperature range (700-3000 K), is central to the understanding of the mechanisms involved in the combustion of complex fuels. Equation 3.9 represents the overall process, and the kinetic detail which describes the complete behaviour of hydrogen oxidation comprises nearly 100 reversible elementary reactions [34].

Methane (CH_4) is the simplest of hydrocarbon fuels and is the major constituent of natural gas ($\approx$ 93-96% by volume). There exists some variations in composition depending on source, and other components which can be found in natural gas. These are mainly *ethane* (C_2H_6), *propane* (C_3H_8) and *butane* (C_4H_{10}). These components do not strongly influence the released energy from combustion, but they have a strong impact on spontaneous ignition (auto-ignition). For a fair representation of complete kinetics of natural gas combustion, it is necessary to include several hundreds of elementary reactions [35, 87].

Even though there are some similarities, the chemistry of methane combustion is not strictly typical for all alkanes, throughout the whole temperature range of general interest (500-2500 K). In order to understand more about alkanes in general, it is necessary to begin investigations with butane, taking into account differences between two isomeric structures, normal butane $CH_3(CH_2)_2CH_3$ and isobutane $(CH_3)_3CH$.

Liquid hydrocarbon fuels consist of huge numbers of components that are classified into several groups. These groups are alkanes, alkenes, alkynes and aromatic compounds [34, 88]. A chemical analysis of the fuel does not provide sufficient information for the prediction of combustion characteristic or performance. The reason for this is that the physicochemical interactions involved in combustion are not derived in a way that it is proportionate to the mass or volume fraction of each component.

Blends of petrol (gasoline) are drawn mainly from the fraction of crude oil in the normal boiling point of about 320-450 K. This can include components of carbon number distributed between C_4 and C_{10}, with the main constituents being approximately C_8. The aromatics may be up to 40% (by volume) of this type of fuel, with alkanes around 30-40%, and the remainder being unsaturated hydrocarbons, the alkenes. For representation of detailed chemical kinetics of combustion of higher hydrocarbons fuels, such as primary reference fuels n-heptane (C_7H_{16}) or iso-octane (C_8H_{18}), several thousands of elementary reactions have to be included [89, 90].

Another type of fuel, commercial jet aircraft fuel (kerosene) is made from a slightly lower volatility fraction than petrol (normal boiling range 430-550 K) , and consists of hydrocarbons in the range C_{10}-C_{16}. On the other hand typical diesel fuels are taken from the slightly higher boiling fraction (550-750 K) and they are distinguished by the predominance of the strait chain alkanes, n-$C_{11}H_{24}$ to n-$C_{24}H_{50}$. Diesel fuels are not without aromatic compounds, comprising a few percent of napthalenes, fluorenes and phenanthrenes [34]. Sulphur containing and nitrogen containing compounds are also present in small portions, but sufficient to be a concern in relation to pollutant formation.

Chapter 4

Phenomenology of Auto-ignition Process

In many practical steady combustion system, the *ignition* is simply means of starting the system on its way to a steady state. Performance and emissions are essentially independent of the ignition in such system as boilers, furnaces and burners. On the other hand, in other practical problems, such as internal combustion engines, the ignition has a great influence on performance, emissions and other characteristic, and also ignition can explain the performance of entire system [20].

The ignition can depend on physical, chemical, mixing and transport features of a problem, and in some cases on heterogeneous phenomena. Detail reviews of ignition and its features can be found in [34, 35, 88].

The ignition can be defined as a time dependent process, which starts from reactants (usually fuel and air) and evolves, in time, towards a steadily burning flame [35]. Examples of ignition processes include *induced ignition* (such as occurs in the spark engines), *auto-ignition* (such as occurs in the diesel engines), and *photo-ignition* caused by photolytic generation of radicals.

Further discussion of ignition phenomena will be concentrated on the *auto-ignition* process and its main characteristic and features. This includes:

- The reaction chain processes

- The auto-ignition limits and oscillatory cool flames

- The ignition delay

- High and low temperature chemistry of auto-ignition

- Negative temperature coefficient (NTC) behaviour.

This Chapter is organised so that characteristics and types of auto-ignition process will be presented first, followed by a description of chain reactions in the chain-thermal auto-ignition processes. Auto-ignition limits and oscillatory cool flames of hydrocarbons together with the ignition will be discussed. The explanations of the high and low temperature chemistries of the auto-ignition and combustion in hydrocarbon fuels will be presented. The negative temperature coefficient behaviour will be explained. The chapter concludes with the summary of the phenomenology of auto-ignition process.

4.1   Characteristics of Auto-ignition Process

Auto-ignition process in a closed system during the changes in the temperature and pressure, may arise from various phenomena such as thermal feedback, chain reactions or combination of these two [35]. In that way the behaviour and controlling of the auto-ignition process may be different and division into three typical types of the auto-ignition process can be make:

1. The thermal auto-ignition[1]

2. The chain-branching auto-ignition

3. The chain-thermal auto-ignition with negative temperature dependence (NTC) behaviour.

---

[1]With some qualifications the thermal auto-ignition process is rather termed as the spontaneous auto-ignition process.
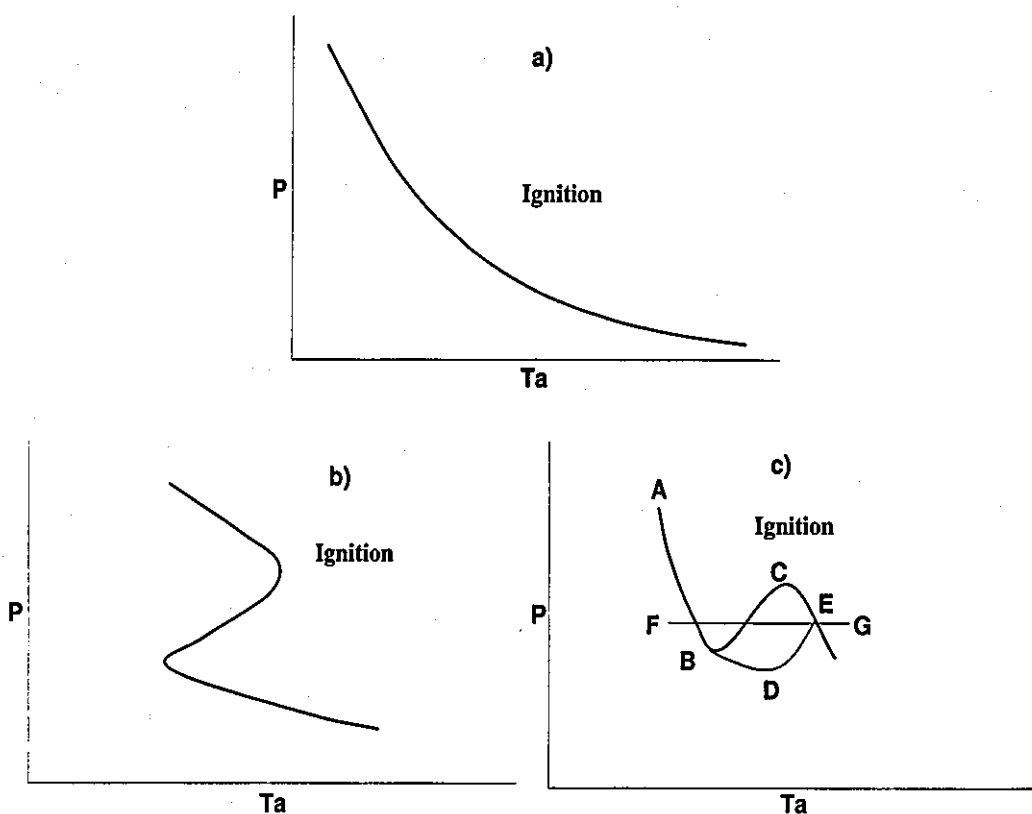
Figure 4.1: Pressure-temperature diagrams representing the boundaries for the auto-ignition of gases when reaction occurs as a result of (a) thermal feedback alone, (b) chain branching interaction of the kind involved in hydrogen oxidation, (c) chain-thermal interactions of the kind involved in alkane oxidation [91].

Auto-ignition processes are usually represent in the form of the p-T_a ignition diagram. Figure 4.1 shows forms of the p-T_a diagrams for auto-ignition processes that are encountered in the combustion systems. These diagrams summarise the conditions at which different modes of auto-ignition behaviour are observed when a particular reactant mixture is introduced to a uniformly heated vessel (wall temperature T_a) at specified pressure (p). The regions in which ignition takes place are separated by a curve from the regions where no ignition occurs. [91]. The existence of clearly defined boundaries signifies a parametric 'sensitivity' to the conditions at which critical transition occurs from one mode of behaviour to another. The three

types of ignition diagram shown in Figure 4.1 represent the typical behaviour:

1. As a result of thermal ignition (as in di-t-butyl peroxide decomposition [92])–Figure 4.1 (Diagram (a)).

2. In the chain-branching reactions (typified by the oxidation of hydrogen and of carbon monoxide [93, 94, 95])–Figure 4.1 (Diagram (b)).

3. The chain-thermal interactions in which an overall negative temperature coefficient (NTC) of reaction rate occurs (as is most familiar in alkane oxidation [96]–Figure 4.1 (Diagram (c)).

The first two types of ignition diagram (Figure 4.1, Diagrams (a) and (b)) will be discussed briefly, since they not represent a typical auto-ignition behaviour of the hydrocarbon fuels in the internal combustion engines. Third type of the ignition diagram (Figure 4.1, Diagrams (c)), represents a typical auto-ignition behaviour of alkane fuels in the internal combustion engines, and therefore is discussed in detail in Section 4.3.

The *thermal auto-ignition*, shown in Figure 4.1 (Diagram (a)), is driven solely by the rate of energy release through thermal feedback. The criterion for occurrence of the thermal auto-ignition is related to the net rate of heat gain or loss in a volume of the reacting system. If the rate of heat loss owing to conduction, convection and radiation remains equal to the rate of heat generation by reaction, then a stable temperature distribution will be established. On the other hand, if the rate of heat loss cannot keep pace with the heat generation, then 'thermal runaway' to ignition will occur [34].

In the thermal auto-ignition the heat generation occurs only due to chemistry (driven by temperature) without the influence of the chain branching, i.e. the increase in temperature results in the higher rate of heat release from chemical reactions.

Depending on the characteristics of a reaction system there exist two types of the thermal auto-ignition: (i) the homogeneous and (ii) heterogeneous. If the heat

exchange in the reaction system is fast enough in comparison to the heat exchange with surroundings (vessel surface, etc.), then the temperature of the reaction system is assumed to be uniform over the whole volume (the system is assumed to be well mixed–*homogeneous*). The ignition in this system is termed *homogeneous thermal auto-ignition* [97]. On the other hand, when the heat exchange with the surrounding is faster that the heat exchange within the system (due to the relatively low thermal conductivity within the reactants), the ignition is termed *heterogeneous thermal auto-ignition* [98]. The thermal auto-ignition phenomenon was recognised by van't Hoof [99] at the end of last century, while an elementary model for the quantitative explanation of homogeneous thermal auto-ignition phenomenon was developed by Semenov [97], at the beginning of 20th century. Several years latter, the elementary model for the quantitative explanation of the heterogeneous thermal auto-ignition phenomenon was developed by Kamenskii [98].

The major distinction in the origins of the ignition diagrams in Figure 4.1 (Diagram (b)), which represents the behaviour of some chain branching reactions, is that the heat release originates from complex chemical mechanisms that include chain branching. This type of ignition is termed the *chain-branching auto-ignition*. In Figure 4.1 (Diagram (b)) the chain-branching ignition of hydrogen is shown. It can be seen the existence of the first and second ignition limits which not exist for the thermal auto-ignition. These limits are due to the relative pressure dependencies of the chain branching and chain termination rates [91]. They are represented in the simplest form, at the first limit by the kinetic competition of H atom reactions as

$$H + O_2 \rightarrow OH + O \quad \text{chain branching} \tag{4.1}$$

$$H \rightarrow \text{inert at wall} \quad \text{chain termination} \tag{4.2}$$

at the second limit by

$$H + O_2 \rightarrow OH + O \quad \text{chain branching} \tag{4.3}$$

$$H + O_2 + M \rightarrow HO_2 + M \quad \text{chain termination} \tag{4.4}$$
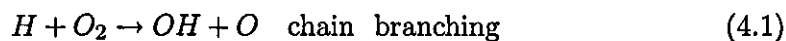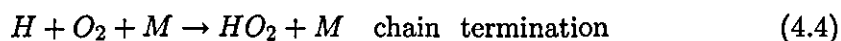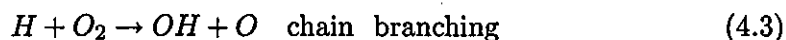
It is the respective temperature and pressure dependences of these pairs of elementary reactions that determine the gradient of the first or second ignition limit in the p-T_a ignition diagram. Neither of the terminating routes has a significant activation energy.

The third type of ignition, termed the chain-thermal auto-ignition is shown in Figure 4.1 (Diagram (c)). This type of the ignition is characterised with the occurrence of NTC behaviour, as is most familiar in the alkane oxidation and therefore in most of the commercial fuels for automotive applications.

To illustrate differences between the chain-branching auto-ignition and the chain-thermal auto-ignition with NTC behaviour, the analysis of their p-T_a diagrams is carried out.

If the horizontal 'ignition peninsula' in (Figure 4.1, Diagram (b)) arises from changes in the kinetics as a result of the different *pressure dependences* of the dominant reactions at a given temperature, then the vertical 'ignition peninsula' in (Figure 4.1, Diagram (c)) arises from changes in the kinetics as a results of different temperature dependences of the dominant reactions at a given pressure [91]. In particular, following the line FG, the low temperature oxidation is controlled by an overall non-branching reaction mode. That is, within the structure of elementary reactions, the termination rate exceeds the chain-branching rate. As the temperature is raised, chain propagation (or strictly, degenerate branching) is predominant at AB. At some higher temperature still, there is a second switch to another predominantly non-branching reaction mode at BC and so on. The important distinction in this case from that in (Figure 4.1, Diagram (b)) is that the kinetics cannot be separated from the thermal contributions. The behaviour results from a chain-thermal interaction. In that way, chain-thermal auto-ignition[2] can be defined as a requirement that the reacting system must experience exponential growth, both in temperature and number of chain carriers, and the exponential chain reaction must proceed for

---

[2]In further text this type of auto-ignition process will be discussed only, and for simplicity it is termed the *auto-ignition.*

a significant degree of fuel consumption [20].

In that way (chain-thermal) auto-ignition can be understood as a process of thermal activation of the local kinetic processes, which depends on two parameters: (i) the temperature and (ii) the concentration. Initially the process is dominated by the kinetic effect, which intensity depends on concentration. The enhanced exothermic kinetic reactions increase the temperature of the reacting mixture. A higher temperature further boosts kinetic reactivity and accelerates the fuel consumption. With increase in the temperature the rate of heat release grows. The growing heat release rate self-accelerates the fuel consumption. The dominant effect shifts from the concentration to the temperature during the energy release (the heat release).

4.2 General Characteristic of Chain Reaction Processes

Many interesting systems involve chain reaction processes, such as nuclear reactors, with neutrons as chain carriers. The chain termination is provided by neutron absorbers, and the chain branching is associated with the term 'supercritical', normally a condition to be avoided. Populations of living organisms obey the same reactivity laws. Organisms can grow exponentially via chain branching until limited availability of nutrients first stabilizes the population and eventually quenches the system via chain termination. The reaction system follows the general equation

$$\frac{dn(t)}{dt} = kn(t) \qquad (4.5)$$

where $n(t)$ is the number of chain carriers. This indicates that the change in number of neutrons in a reactor depends on the number of neutrons available to produce further neutrons. Also, it may be commented or as the change in the number of bacteria that depends on the number of bacteria which can reproduce, a reflection that the current population of chain carries produces the next generation of chain carries.

Solution of Equation (4.5) leads to the expression

$$n(t) = n(0) \exp(kt) \qquad (4.6)$$

When $k < 0$, the result is exponential decay, but when $k > 0$ the radical population experiences exponential growth. Thus $k \cong 0$ is equivalent to criticality or steady combustion (or population stability) [20]. In a chemically reactive system, the coefficient k is an average over all reactions taking place, including initiation, propagation, chain branching and termination reactions. As mentioned in Section 4.1, the *auto-ignition* can be defined as a requirement that the reacting system must experience the exponential growth both in temperature and number of chain carriers, and the exponential chain reaction must proceed with a significant degree of fuel consumption [20].

Therefore, the main feature of the chain branching reactions is an exponential growth in reaction rate as a result of the multiplication of the primary propagating species. These species are very reactive and are usually in the form of atoms or *free radicals*. Four different types of event can take place in the during the auto-ignition process.

1. **Initiation.** Atoms or radicals are often produced by the dissociation of either a reactant molecule or some substance (an initiator) added specifically to promote the reaction. The rate of initiation is slow because the activation energy of a unimolecular dissociation reaction is equal to, or grater than, the bond dissociation energy ($\approx$ 200-500 kJmol^{-1}). Bimolecular initiation reactions (for example, such as between fuel and oxygen) tend to have lower activation energies but also lower pre-exponential factors, and thus are not necessary significantly faster. Initiation may take place homogeneously, or heterogeneously at the walls of a reaction vessel. Initiation can be represented as

$$A \rightarrow 2X \quad \text{rate}, \nu_i = k_i[A] \tag{4.7}$$
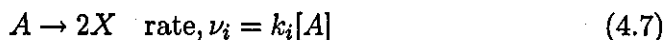
   where A denotes an initial reactant and X an active species (or free radical). In short, the **initiation** is the formation of the active species (or free radicals) from the stable species.

2. **Propagation.** The propagation reaction step is where the active species react with stable species and form another reactive species. The propagation reaction is important because it governs the rate at which the chain continues. The requirement is for a free radical X to react with a stable species A and to produce a second free radical

$$X + A \rightarrow Y + P \quad \text{rate}, \nu_p = k_p[X][A] \tag{4.8}$$
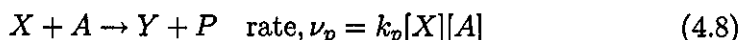
where A is a molecule (normally a reactant) and P is a stable product. It is unlikely that X and Y will be identical, so the chain normally propagates by a 'shuttle' between two or more types of free radicals [34]

$$Y + A \rightarrow X + P \tag{4.9}$$
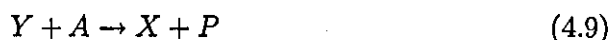
The reactant and product molecules in Equation (4.7) and Equation (4.8) may not be same in practice. For most propagation reactions of importance in combustion, activation energies lie between 0 and 60 $kJmol^{-1}$, [34, 91].

3. **Branching.** Chain branching step is where an active species reacts with a stable species forming two reactive species. In a chain branching reaction three free radicals are formed from the reaction of one free radical, so the net gain is two free radicals

$$X + A \rightarrow 3Y + \dots \quad \text{rate}, \nu_b = k_b[X][A] \tag{4.10}$$
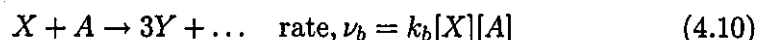
This reaction may be responsible for the *branching chain explosion* and is termed *quadratic branching*, because there is an overall second order dependence of the reaction rate on species concentration. The activation energy for the branching reactions may be considerably higher than that of the ordinary propagation reactions. *Linear branching* involves decomposition of a stable intermediate product to give free radicals

$$P \rightarrow 2P + \dots \quad \text{rate}, \nu_b = k_b[P] \tag{4.11}$$
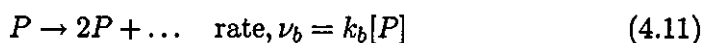
This is a relatively slow process, and it is termed *degenerate branching* (or secondary initiation). This phenomenon has been discussed in detail in [34, 35, 91].

4. **Termination.** Combinations of the above processes (initiation, propagation and branching) would cause the overall reaction rate to accelerate without limit were it not for competition for the free radicals by reactions which terminate the chains. Gas-phase termination occurs either by recombination of two radicals to give a stable molecule, or by reaction of radical of lower reactivity which is unable to propagate the chain. Since each of these processes is exothermic, a *third body* is often required to take up the energy released and prevented dissociation, as discussed in Section 3.3.5 (Chapter 3),

$$X + X + M \rightarrow X_2 + M \quad \text{rate}, \nu_{t1} = k_{t1}[X]^2[M] \tag{4.12}$$

$$X + S + M \rightarrow XS + M \quad \text{rate}, \nu_{t2} = k_{t2}[X][S][M] \tag{4.13}$$
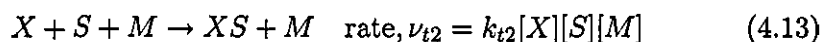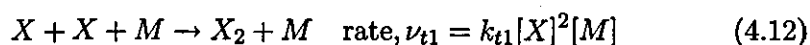
Removal of radicals at the wall can take place in a variety of processes, the details of which are usually unimportant since the rate controlling step is normally diffusion through the gas

$$X \rightarrow \frac{1}{2}X_2 \quad \text{rate}, v_{t3} = k_{t3}[X] \tag{4.14}$$
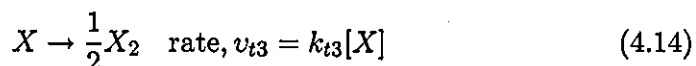
Equation (4.13) and Equation (4.14) are referred to as linear termination (with respect to [X]), and Equation (4.12) as quadratic termination.

4.3 Oscillatory Cool Flames of Hydrocarbons

The p-T_a ignition diagram for the chain-thermal ignition shown in Figure 4.1 (Diagram (b)), is characterised by two regions, the region of 'slow combustion' and the region of 'ignition'. These regions are separated by a critical boundary. Although in the diagram for the chain-thermal ignition (Refer to Figure 4.1, Diagram (c)), there exists similar sharp boundary beyond which ignition occurs there are

qualitative differences. The boundary in the chain-thermal auto-ignition comprises three branches, the middle one of which exhibits an increase of the critical pressure as the vessel temperature is raised. This results from the *negative temperature coefficient-NTC* in the heat release, the kinetic basis of which is described in Section 4.6.3. The subcritical region of the ignition diagram is also subdivided into different type of behaviour. Part of this represents slow combustion, but multiple (or oscillatory) cool flames occurs in a closed region bounded by the NTC branch of the ignition boundary. For a detail representation of the oscillatory cool flame effect in NTC region a new diagram is constructed and shown in Figure 4.2. The qualitative structure in Figure 4.2 is characteristic of alkanes and alkenes containing three or more carbon atoms, of acetaldehyde (ethanol) and higher molecular mass aldehydes, higher alcohols, ethers other than dimethyl ether, and a variety of other organic compounds that contain fairly large aliphatic groups [34]. Although there are some resemblances in the behaviour, the features of Figure 4.2 are not exhibited fully by methane, ethane, ethene or formaldehyde. Nor are they shown by the aromatics such as benzene, toluene or xylene. The features of Figure 4.2 are illustrated by referring to the temperature-time or pressure-time records that are obtained from the experimental measurements [34]. Insofar that the phenomena are non-isothermal, knowledge of the temperature history is extremely important, but qualitative insight is gained from the pressure record.

The curves in Figure 4.3 relate to a fixed vessel temperature with gradual increased initial pressures. Slow reaction takes place at the lowest pressures.

The pressure time curves are sigmoidal (Refer to Figure 4.3, curve (a)), as is characteristic of degenerate chain branching reactions. As the initial reactant pressure is increased (Refer to Figure 4.3, curves (b) and (c)) there are momentary pressure pulses which interrupt the smooth growth in pressure. At slightly higher pressures, the transition to ignition is marked by a reaction in which there is a massive and very rapid pressure rise. Within the ignition peninsula the ignition is preceded by a *cool flame.* This process is known as two-stage ignition (Refer to Figure 4.3, curve (d)).
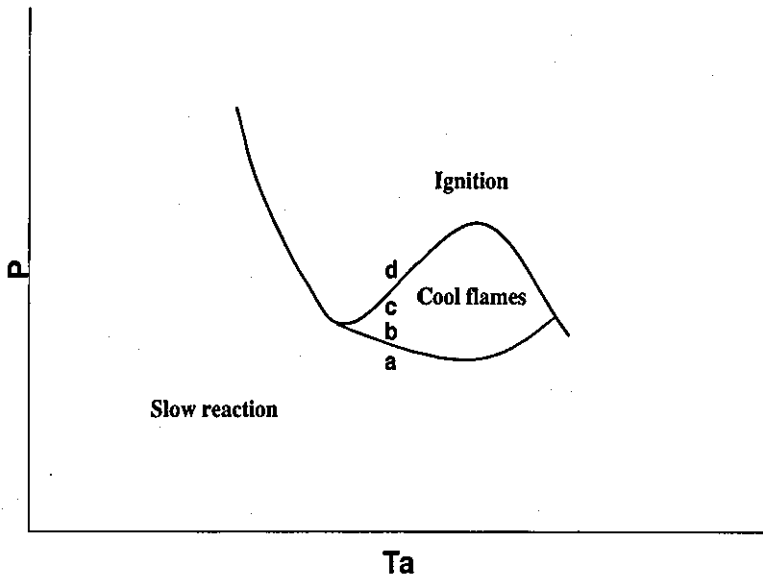
Figure 4.2: The oxidation of alkanes and other organic compounds in a closed vessel [34]. Points a-d relate to Figure 4.3.
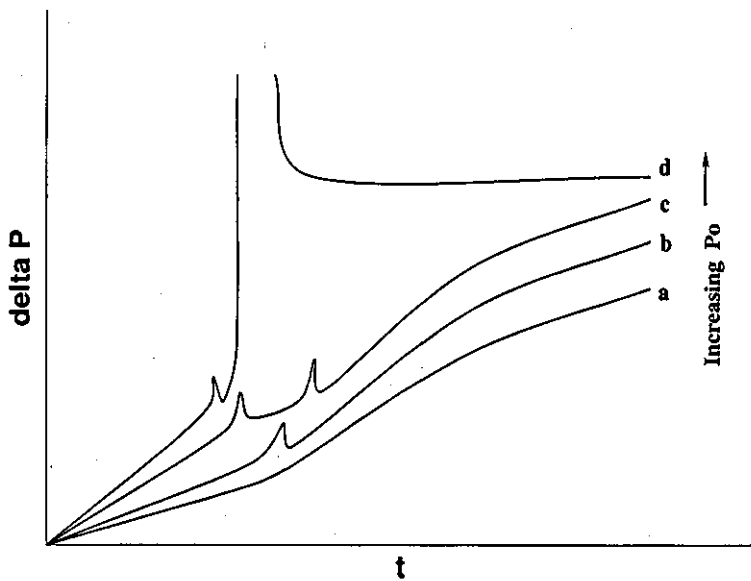
Figure 4.3: Typical pressure-time records obtained during the oxidation of alkanes in a closed vessel [34].

The multiple stage ignitions, that can occur adjacent to the negative temperature dependent branch of the ignition boundary, are detected as a succession of one or more cool flames preceding the two-stage ignition. A single stage event is observed elsewhere in the ignition region. The periodic pulses in the pressure records, caused by the cool flame, and the overshoot accompanying full ignition are a consequence of temperature increases.

To understand and to satisfactory model two-stage ignitions are of particular relevance to combustion process in internal combustion engines. Two-stage ignitions occur at the low temperature ignition limit and within the ignition peninsula ABC (Refer to Figure 4.1). The multiple-stage events are observed adjacent to the oscillatory cool flame region at the upper temperature boundary of the ignition peninsula (BC). Two-stage and multiple stage ignition are two different combustion processes.

Multiple-stage ignitions have been observed during the oxidation of only relatively few organic compounds, and like oscillatory cool flames, are an artifact of non-adiabatic conditions. By contrast, two-stage ignition is an extremely common and widespread phenomenon [91]. The underlying chemical kinetics lies in the thermokinetic evolution that permits the transition from the preliminary first, *'cool flame'* stage to the second, *'hot stage'* or *'main stage'*. The are two thermally related factors to note:

1. Firstly, the rates of temperature change in the first stage is appreciably slower than that in the second stage, which is a consequence of the different types of chemistry that prevail in each stage (the low-temperature and high-temperature chemistries that are discussed in Section 4.5 and Section 4.6 respectively).

2. Secondly, there is a limiting temperature at which the inflexion occurs between the first and second stages.

The transition may vary for different fuels or may be dependent on different pressures and compositions.

4.4 Ignition Delay Time

In comparison to pure thermal ignition processes, where the temperature increases at once, in the ignition of hydrogen or hydrocarbon-air mixtures the temperature increase (and therefore the explosion), takes place only after a certain induction time, the *ignition delay time*, as can be seen in Figure 4.4. The ignition delay is characteristic of radical-chain explosions, the chemical reactions governed by a chain-branching mechanism (as discussed in Section 4.2). During the ignition-delay
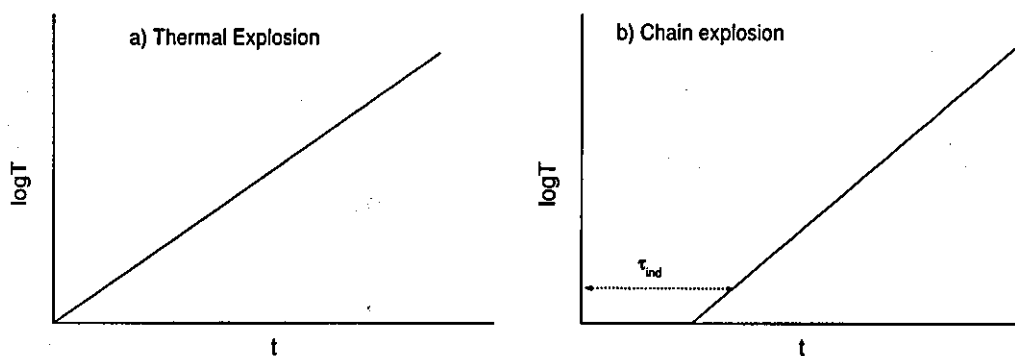
Figure 4.4: Simplified time behaviour of thermal and chain-thermal auto-ignitions in an adiabatic system.

period, the radical-pool population increases at an exponential rate. Nevertheless, during this process the amount of fuel being consumed, and thus the amount of the liberated energy is too small to be detected. Therefore, the important chemical reactions such as, chain branching or formation of radicals, take place during the induction time while the temperature remains nearly constant.

Finally, at the end of induction time, the radical pool becomes large enough to consume a significant fraction of the fuel, and therefore a rapid ignition takes place. The precise definition of induction time depends on the used criterion such as, the consumption of fuel, the formation of CO or OH, the increase of pressure in a constant volume vessel, the increase of temperature in an adiabatic vessel, etc [35].

Due to the temperature dependence of the underlying elementary reactions, the

ignition time depends strongly on the temperature. The *ignition delay* time depends exponentially on the reciprocal temperature

$$\tau = A \exp(\frac{B}{T}) \tag{4.15}$$

which reflects the temperature dependence (Arrhenius law-Equation 3.16) of the underlying elementary reactions that occur during the induction period.

4.5 High Temperature Auto-ignition and Combustion Chemistry

The temperature at which chemical processes involved in combustion occurs is divided at 'low temperature' and 'high temperatures' regimes. A division is made at approximately 1000 K between these two regimes, because there is a very clear distinction between the types of reaction that dominate the overall combustion processes as temperature rise from below 850 K to beyond 1200 K. The division itself is artificial. It does not imply the sudden switching off of one set of reactions and the switching on of another, and the choice of 1000 K as the threshold is one of convenience within a broad temperature range [34].

Apart from the qualitative structure of the mechanisms involved in the high temperature regime, it is important to gain some insight into relative importance of different processes under different conditions. Combustion reactions must be reasonable rapid since, in general, appreciable extents of reaction must occur in times within a broad range of 10^{-6} to 10^{-2} s.

The interpretation of combustion processes by modelling of detailed kinetic mechanisms requires a quantitative knowledge of the parameters of the rate constant for each elementary reaction involved in the combustion process, given as either

$$
\begin{aligned}
k &= A \exp(\frac{-E}{RT}) \quad \text{or} \\
k &= A T^n \exp(\frac{-E}{RT})
\end{aligned}
\tag{4.16}
$$

The parameters for a wide range of elementary reactions have been generated from experimental studies. Moreover, there a number of 'rate data assessment' computer programs, from which recommendations of the most suitable data for many elementary reactions can be obtained. Without these contributions many of the parameters would have to be estimated, or they may have too great an uncertainty for numerical computation to be meaningful [34].

4.5.1 Rates of the Elementary Reactions in High Temperature Regime

The free radical chain initiation processes are not normally predominant in the control of events, and the development of combustion falls to the chain propagation and branching characteristic of the reaction. Nevertheless, the alternative modes for the initiation of alkane combustion illustrate some of the underlying issues.

Consider the possibilities:

$$RH + O_2 \rightarrow R + HO_2 \quad k_1 = 1 \times 10^{14} \exp(\frac{-25000}{T}) cm^3 mol^{-1} s^{-1} \quad (4.17)$$

$$RH \rightarrow R_1 + R_2 \quad k_2 = 5 \times 10^{16} \exp(\frac{-42000}{T}) s^{-1} \quad (4.18)$$
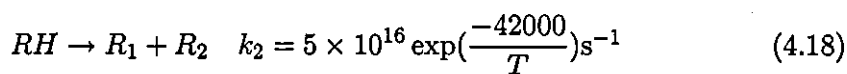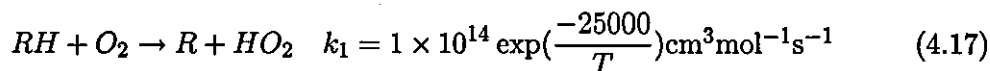
In the generalised representation of Equation (4.17), the oxidation of the fuel (RH) by hydrogen atom *abstraction* may yield a hydroperoxy radical (HO$_2$) and an alkyl radical (R) in which the carbon backbone of the alkane remains intact. By contrast, the *unimolecular decomposition* of the fuel (Equation 4.18) may yield two alkyl radicals (R$_1$ and R$_2$), as a result of which the carbon backbone of the alkane molecule is severed. Typical rate constants for these types of process are given in the simple Arrhenius form, and the relative rates of initiation are thus

$$\frac{\nu_1}{\nu_2} = 2 \times 10^{-3} \exp(\frac{17000}{T})[O_2] \quad (4.19)$$

Temperature has the greatest effect on which of these reactions dominates (Reaction 4.17 or Reaction 4.18), through the relative magnitudes of activation energies, but the concentration of oxygen is also important. Consider normal atmospheric

condition, for which the concentration of O_2 is approximately 2.5×10^{-6} mol cm^3 at 1000 K, and is inversely proportional to temperature [34]. The relative rates of initiation, given by equation (4.19) in the temperature range 800-1400 K for 200 K increments, are then 10.8, 0.12, 0.006 and < 0.001, respectively [91]. Thus the oxidation route to initiation would predominate at temperature somewhat below 1000K, and the carbon backbone structure of the fuel would remain intact. However, there is an increasing importance of the degradation route (Equation 4.18) as the temperature is raised, and it must be regarded to be virtually exclusive of mode of initiation above about 1400K.

This illustrates how, at high temperatures, reactions with a high activation energy and high pre-exponential factor (Equation 4.18) tend to be more important than those with lower activation energy but lower pre-exponential term (Equation 4.17). Many of the simpler bimolecular reactions have similar pre-exponential factors that differ only in their activation energies. Since the exponential term approaches unity at high temperatures, many of these reactions have similar rate constants at flame temperatures and so are of comparable importance. For this reason, the reactions associated with flames should be represented as reversible processes since, at T$>$ 1500 K say, there may be a sufficiently high reaction rate for both the forward and reverse processes that an equilibrium is established [34].

At lower temperatures, in many cases, the equilibrium is displaced so far to the right hand side that the reverse process may be disregarded. These circumstances pertain when high activation energies for the reverse reaction are involved, as in Equation (4.21) and Equation (4.23) given below.

Amongst bimolecular reactions, the most important ones are metathetical reactions involving an atom or simple radical $A + BC \rightarrow AB + C$. Such reactions do not usually involve complex rearrangements and therefore have high pre-exponential factors. The most common reactions in this category are H atom abstractions, for

example,

$$H + CH_4 \quad \Leftrightarrow \quad H_2 + CH_3 \qquad (4.20)$$

$$k_f \quad = \quad 8.49 \times 10^{14} \exp(\frac{-8205}{T}) \text{cm}^3\text{mol}^{-1}\text{s}^{-1}$$

$$k_r \quad = \quad 5.08 \times 10^{13} \exp(\frac{-11270}{T}) \text{cm}^3\text{mol}^{-1}\text{s}^{-1}$$

$$OH + CH_4 \quad \Leftrightarrow \quad H_2O + CH_3 \qquad (4.21)$$

$$k_f \quad = \quad 6.12 \times 10^{13} \exp(\frac{-3973}{T}) \text{cm}^3\text{mol}^{-1}\text{s}^{-1}$$

$$k_r \quad = \quad 6.90 \times 10^{12} \exp(\frac{-12400}{T}) \text{cm}^3\text{mol}^{-1}\text{s}^{-1}$$

The nature of species involved depends on the particular fuel-oxidant system but in virtually all systems in which elements H and O occur, the **OH** radical is an important and frequently dominant species causing oxidation. Reactions involving HO_2, H and O are also significant. The principal route to water as a final product of hydrocarbon combustion is from abstraction processes such as the reaction shown in Equation (4.21).

There are important shifts in emphasis of the main chain propagating radicals as the temperature is increased. In the "high temperature" range this may be attributed mainly to the competition between the chain branching (Equation 4.22) and non-branching (Equation 4.23) reaction modes

$$H + O_2 \quad \Leftrightarrow \quad OH + O \qquad (4.22)$$
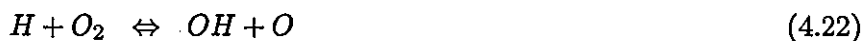
$$k_f \quad = \quad 2.00 \times 10^{14} \exp(\frac{-8455}{T}) \text{cm}^3\text{mol}^{-1}\text{s}^{-1}$$

$$k_r \quad = \quad 1.46 \times 10^{13} \exp(\frac{-252}{T}) \text{cm}^3\text{mol}^{-1}\text{s}^{-1}$$

$$H + O_2 + M \quad \Leftrightarrow \quad HO_2 + M \qquad (4.23)$$

$$k_f \quad = \quad 2.30 \times 10^{18} T^{0.8} \text{cm}^6\text{mol}^{-2}\text{s}^{-1}$$

$$k_r \quad = \quad 2.80 \times 10^{15} \exp(\frac{-23000}{T}) \text{cm}^3\text{mol}^{-1}\text{s}^{-1}$$

The relative rates of the forward reactions for equations (4.22 and 4.23) may be expressed as

$$\frac{\nu_1}{\nu_2} = 8.7 \times 10^{-5} T^{0.8} \exp(\frac{-8455}{T})[M]^{-1} \qquad (4.24)$$

and the pressure-temperature relationship at which the rates of these two reactions are equal is shown in Figure 4.5. The efficiency of the 'chaperone species' M in Equation (4.23) is assumed to be that of air, but [M] represents the total concentration of species in the system. The formation of OH and O predominates at temperatures above the line in Figure 4.5 and occurs at T< 1000K at pressures below 100kPa. A temperature in excess of 1400K is required at pressures exceeding 1 MPa, as is the case in reciprocating engine combustion.
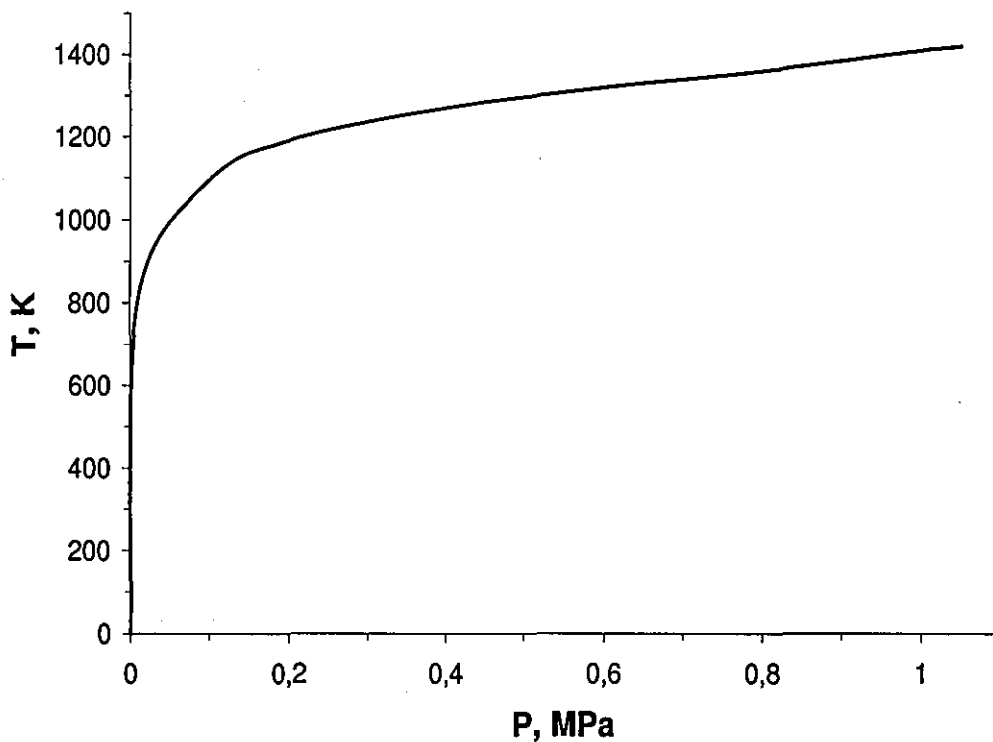
Figure 4.5: Pressure and temperatures at which the rate of Reaction (4.22) is equal to that of Reaction (4.23), given by Equation (4.24) [34].

The comparable rate parameters for the branching reaction shown in Equation (4.22)

and that of a typical abstraction process shown in Equation (4.20) indicate that the reaction of H atoms with oxygen is as important as the abstraction process, over the temperature range shown in Figure 6.1, except in very fuel-rich conditions. The importance of the switch in propagating species from HO_2 to OH is brought about by the competition between Equation (4.22) and Equation (4.23).

4.5.2   Mechanism of Alkane Oxidation

The underlying mechanistic structure for the high temperature combustion of methane and ethane is shown in Figure 4.6 [35].
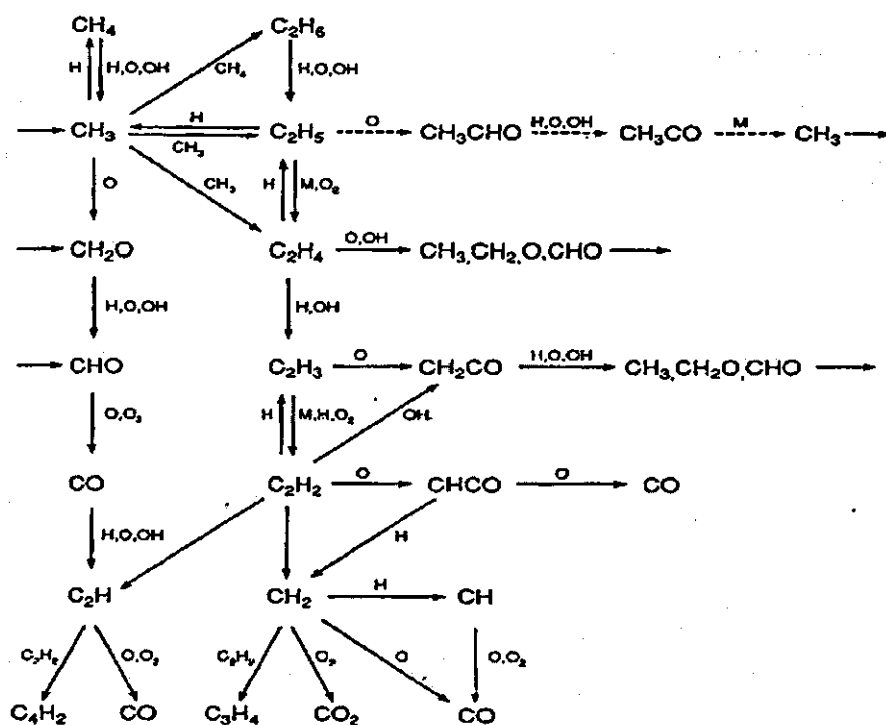
Figure 4.6: Schematic representation of a mechanism for methane oxidation at high temperatures.

In this scheme the main free propagating free radicals are shown as H, O, OH, HO_2 and CH_3. They are a number of key features:

a) The mechanisms of the two primary fuels are linked at an interplay between CH_3 and C_2H_6, C_2H_5 or C_2H_4. C_2-containing species are detected in methane flames, especially under fuel-rich conditions.

b) Formaldehyde (CH_2O) and formyl radicals (CHO) are the main partially oxygenated products of the C_1 and C_2 hydrocarbon fragments. Decomposition of the CHO can be a source of H atoms, via

$$CHO + M \quad \rightarrow \quad H + CO + M \tag{4.25}$$
$$k \quad = \quad 4.65 \times 10^{13} \exp(\frac{-7167}{T}) cm^3 mol^{-1} s^{-1}$$
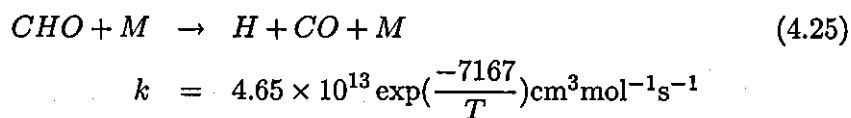
but its competitive oxidation is also a major source of HO_2 at all temperatures

$$CHO + O_2 \quad \rightarrow \quad CO + HO_2 \tag{4.26}$$
$$k \quad = \quad 3.01 \times 10^{12} cm^3 mol^{-1} s^{-1}$$
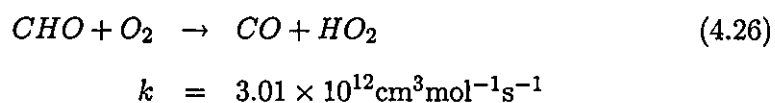
c) Carbon monoxide (CO) is the end product of virtually all of the chain sequences. This signifies that carbon monoxide is almost invariably a precursor to carbon dioxide, as the final product of combustion.

The combustion of higher alkanes is closely connected to the sequence of reactions shown in Figure 4.6, insofar that these processes are the final stages of the reaction chains involved, regardless of the molecular mass of the primary fuel. Degradation of the molecular structure of the fuel is favoured at high temperatures, yielding a predominance of free radicals and molecular intermediates which contain only small numbers of carbon atoms. In particular the formation of alkyl radicals in any free radical abstraction process, for example (X=O, OH, etc)

$$n - C_7H_{16} + X \rightarrow n - C_7H_{15} + HX \tag{4.27}$$

is followed by

$$nC_7H_{15} \quad \rightarrow \quad CH_3 + n - C_6H_{12} \quad \text{(alkene)} \tag{4.28}$$

$$n - C_7H_{15} \rightarrow C_2H_5 + n - C_5H_{10}$$

$$n - C_7H_{15} \rightarrow n - C_3H_7 + n - C_4H_8$$

$$n - C_7H_{15} \rightarrow n - C_4H_9 + n - C_3H_6$$
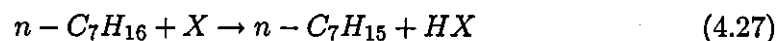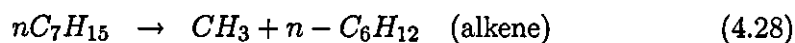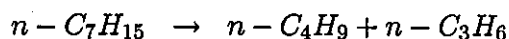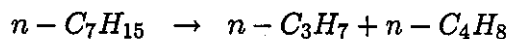
The alkyl radicals ($C > 2$) are themselves susceptible to a similar sequence of decomposition processes, and the molecular alkenes are susceptible to a free radical attack (O, OH, HO_2) at the double bond which leads to further degradation of the carbon structure. A typical activation energy for reactions of the type shown in Equation (4.28) is 120 kJ/mol, but because these are unimolecular reactions there is a high frequency factor associated with the rate constant. Thus, high temperatures tend to favour the unimolecular decomposition of the alkyl radicals rather than their bimolecular interaction with oxygen. Hydrogen atoms may also originate from alkyl radical decomposition via

$$RCH_2CH_2^\star \rightarrow H + RCH = CH_2 \quad \text{(alkene)} \tag{4.29}$$
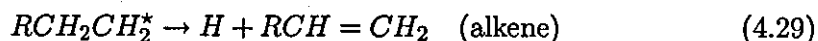
in which R represents a unit comprising C_nH_{2n+1}. Some typical Arrhenius parameters for the unimolecular decomposition of alkanes and alkyl radicals are given in [34, 35].

4.5.3 Principal Propagating Free Radicals and Reactions

At premixed flame temperature (T> 2000 K) the branching channel (Equation 4.22) to O and OH is the predominant reaction between H atoms and O_2, regardless of the pressure at which combustion takes place. This particular reaction, coupled to

$$O + RH \rightarrow OH + R \tag{4.30}$$

and the principal propagation reaction

$$OH + RH \rightarrow R + H_2O \tag{4.31}$$

are crucial to the branching chain-thermal interaction that gives rise to the self-sustaining properties of hydrocarbon flame propagation [34].

In pre-ignition stages, which may be at the beginning of spontaneous ignition or may be in the preflame zone of a propagating flame, the temperature and pressure govern whether or not the branching channel predominates. At temperatures below the line in Figure 4.5 the HO_2 radical formed in the reaction shown in Equation (4.23) becomes the principal propagating species, which reacts as follows:

$$RH + HO_2 \rightarrow R + H_2O_2 \tag{4.32}$$

$$H_2O_2 + M \rightarrow 2OH + M \tag{4.33}$$
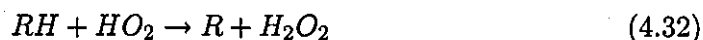
The temperatures at which the particular sequence is important are in range 800-1200K (Figure 4.6). Other reactions become important below 800K, and it will be discussed later in the text.

The reactions shown in Equation (4.32) and Equation (4.33) constitute a chain branching sequence, but with some qualification. The rate of development of reaction is moderated by the appreciably slower propagation via HO_2 radicals since the activation energies associated with reactions of the type (For example, Equation 4.32) fall in the range 40-60 $kJmol^{-1}$. Secondly, the branching rate is governed by the half-life of hydrogen peroxide. Although this is short ($\tau_{1/2} < 1ms$) at temperatures above 1000 K, it does not match the characteristic times associated with the radical branching route (Equation 4.22). This means that there is a much slower acceleration of rate when HO_2 propagation predominates, compared with that at higher temperatures.

4.5.4 The Importance of Reactions in Hydrogen and Carbon Monoxide Oxidation

Hydrogen is the simplest fuel that is able to undergo oxidation, and more is known about hydrogen combustion than any other comparable combustion system [34, 35, 81]. H atoms and OH, O and HO_2 radicals play a crucial role in hydrogen combustion but they are also formed in hydrocarbon combustion processes. Understanding of their elementary reactions in hydrogen oxidation is very important for the interpretation of chain propagation and branching, in the oxidation of all C-H-O containing

fuels. It is also worth to discuss carbon monoxide oxidation because the formation of virtually all CO_2 is via CO as its precursor.

4.5.4.1 The Combustion of Hydrogen

The oxidation of stoichiometric hydrogen/air mixture proceeds through the followings elementary reaction sequences:

$$H + O_2 \quad \rightarrow \quad OH + O \quad \text{(branching)} \tag{4.34}$$
$$k \quad = \quad 2.00 \times 10^{14} \exp(\frac{-8455}{T}) \text{cm}^3 \text{mol}^{-1} \text{s}^{-1}$$

$$O + H_2 \quad \rightarrow \quad OH + H \quad \text{(branching)} \tag{4.35}$$
$$k \quad = \quad 2.126 \times 10^{14} \exp(\frac{-6860}{T}) \text{cm}^3 \text{mol}^{-1} \text{s}^{-1}$$

$$OH + H_2 \quad \rightarrow \quad H_2O + H \quad \text{(propagation)} \tag{4.36}$$
$$k \quad = \quad 5.94 \times 10^{13} \exp(\frac{-3880}{T}) \text{cm}^3 \text{mol}^{-1} \text{s}^{-1}$$
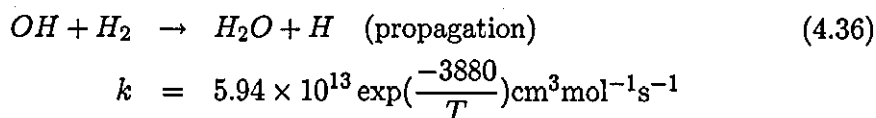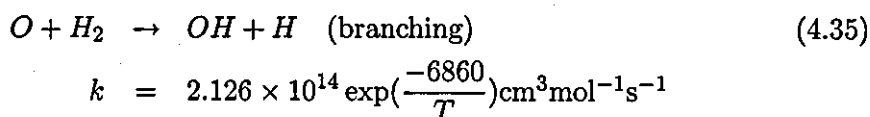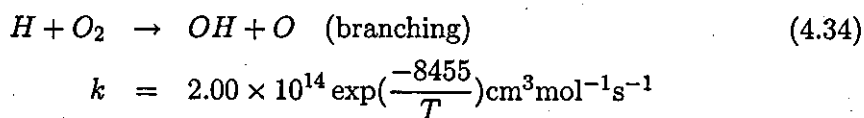
A complete cycle of these three elementary reactions begins with one hydrogen atom and leads to the production of three hydrogen atoms according to the proportions $H_2/O_2 = 3/1$, i.e.

$$H + 3H_2 + O_2 = 3H + 2H_2O \tag{4.37}$$
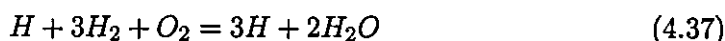
The stoichiometry is a correct representation of 'chemical autocatalysis' in which H atom regenerates itself. There is also a net gain of two free radicals in the autocatalytic cycle. This is a consequence of the separation of a pair of electrons in chemical bond to two individual individual entities, which are then capable of continuing the chain propagation.

The Equation (4.34) has an activation energy of ≈ 70 kJmol^{-1}, just slightly higher that its endothermicity. The activation energies of Equation (4.35) and Equation (4.36) are not as high, so the rate constant of Equation (4.34) is considerably lower than that of Equation (4.35) and Equation (4.36), at temperatures below 1000K

[34]. This causes Equation (4.34) to be rate determining and the OH and O concentrations remain in a stationary state with the respect to the H atom concentration throughout. This type of analysis is common in chain-branching reactions, although it must be used with caution [34, 35]. At higher temperatures the rate constant of Equation (4.34) and Equation (4.35) are much closer, and thus the rate determining role of Equation (4.34) is negligible.

Even though, these three reactions are responsible for the exponential increase in oxidation rate, they do not correspond to the stoichiometry for the complete oxidation of hydrogen

$$2H_2 + O_2 = 2H_2O \tag{4.38}$$

and therefore other reactions become important as reaction proceeds. In premixed flames, for example, the chain-branching reaction ceases when the reverse reactions shown in Equation (4.34), Equation (4.35) and Equation (4.36) become significant

$$OH + O = H + O_2 \tag{4.39}$$

$$OH + H = O + H_2 \tag{4.40}$$

$$H + H_2O = OH + H_2 \tag{4.41}$$
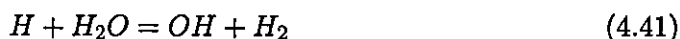
A quasi-equilibrium is then established in which the reaction has proceeded about three-quarters of the way to completion, but a large proportion of the available enthalpy is still contained in the high atom and radical concentrations [34]. This energy is then released by third order recombination reactions that take place on a longer time scale than the second order processes above. In the post flame gases of fuel rich mixtures the dominant reactions are

$$H + OH + M = H_2O + M \tag{4.42}$$

$$H + H + M = H_2 + M \tag{4.43}$$
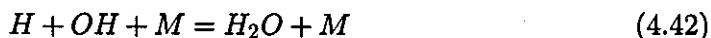
In fuel lean conditions, processes involving the HO_2 radicals become important

$$OH + HO_2 = H_2O + O_2 \tag{4.44}$$

$$H + HO_2 = H_2 + O_2 \qquad (4.45)$$

Many of the reactions in hydrogen oxidation that are also relevant to hydrocarbon combustion can be found in [34, 35].

4.5.4.2 The Oxidation of Carbon Monoxide

From a practical point it is difficult to free CO from all traces or hydrogenous material for the purpose of investigating the oxidation of the pure substance. This arises mainly from the production of cylinder-gas CO by fractionation: there are often parts per million (ppm) traces of CH_4 (boiling temperature at 109 K) in CO (boiling point at 81 K). It is likely that methane is the main impurity but, for historical reasons, the common terminology is to describe impure carbon monoxide (with the respect to hydrogenous material) as 'wet CO' [100], alluding to the possible presence of water vapour. The oxidation of hydrogen (or methane) involves OH and HO_2 radicals. Thus, if there are small quantities of either H_2 or CH_4 also present, chain propagation and branching in CO oxidation is promoted via the following reactions:

$$CO + HO_2 \rightarrow CO_2 + OH \quad \text{(propagation)} \qquad (4.46)$$

$$CO + OH \rightarrow CO_2 + H \quad \text{(propagation)} \qquad (4.47)$$

followed by

$$H + O_2 \rightarrow OH + O \quad \text{(branching)} \qquad (4.48)$$

or

$$H + O_2 + M \rightarrow HO_2 + M \quad \text{(propagation)} \qquad (4.49)$$

and also by

$$CO + O + M \rightarrow CO_2 + M \quad \text{(termination)} \qquad (4.50)$$
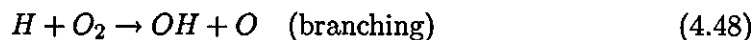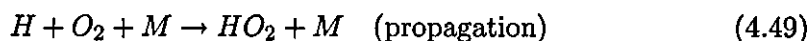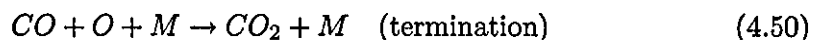
Apart from the contribution to chain propagation, there is also a supplementary branching step which involves the impurity, for example

$$O + CH_4 \rightarrow CO_2 + M \quad \text{(propagation)} \qquad (4.51)$$

Despite the very small impurity concentrations, these steps are competitive with the termolecular termination of Equation (4.50) because it has such a low probability. Moreover, only exceedingly small amounts of hydrogen-containing compounds need to be present because the hydrogen atom is recycled via the reactions shown in Equation (4.46) and Equation (4.47). H atoms are lost only if they are removed in the termination processes in which water is formed, or by adsorption at a surface of the reaction vessel.

Equation (4.46), Equation (4.47) and Equation (4.50) are the main processes by which carbon monoxide is oxidised to carbon dioxide in the combustion of all carbon-containing fuels, Equation (4.47,) being by far the most important. In general, carbon dioxide cannot be formed as a final product of hydrocarbon combustion without carbon monoxide being a precursor to it. Therefore, any interference with the ability of OH, HO_2 or O to react with CO, must reduce the efficiency of combustion and exacerbate the problem of carbon monoxide pollutant emissions. Equation (4.47) is relatively slow compared with H atom abstraction by OH, and so it cannot compete very successfully with hydrocarbon fuels in reaction with OH radicals. For example from

$$CH_4 + OH \rightarrow CH_3 + H_2O \qquad (4.52)$$
$$k_1 = 1.56 \times 10^7 T^{1.83} \exp(\frac{-1400}{T}) cm^3 mol^{-1} s^{-1}$$

$$CO + OH \rightarrow CO + H_2 \qquad (4.53)$$
$$k_2 = 6.32 \times 10^7 T^{1.5} \exp(\frac{250}{T}) cm^3 mol^{-1} s^{-1}$$

the ratio of the rate constants, k_1/k_2 is 4.6 at 1000 K, 9.2 at 1500 K and 13.3 at 2000 K. CO may remain as long as there is still unreacted fuel in the system, and the formation of carbon monoxide as a final product of combustion is inevitable under fuel-rich conditions.

4.6 Low Temperature Auto-ignition and Combustion Chemistry

As the auto-ignition was explained as a kinetically driven process of the low temperature oxidation (Refer to Section 4.1), understanding of the low temperature chemistry plays an important role. Although an understanding of the kinetics and mechanisms of methane combustion at T> 1000 K is relevant to the detailed interpretation of the high temperature combustion of higher alkanes and other hydrocarbons, there is only a limited relationship between methane oxidation at T< 1000 K and that of higher alkanes. This distinction arises because so much of the low temperature chemistry of hydrocarbons is governed by the size and structure of carbon backbone. The kinetics and mechanism of higher alkanes have yielded to quantitative interpretations in recent years. The common ground does not begin to emerge until there are four or more carbon atoms in the fuel molecule [34].

4.6.1 The Low Temperature Oxidation of Methane

The oxidation of methane is extremely slow at temperatures below 700 K, at normal pressures. Only at exceptionally high pressures (> 3 MPa), is there a reasonably significant reaction rate of oxidation at lower temperatures. There are some similarities with respect to ethane and ethene. There is useful common ground with the chemistry of other alkanes at temperatures in the range from about 750 K.

The initiation of methane oxidation in the gas phase starts by

$$CH_4 + O_2 \rightarrow CH_3 + HO_2 \tag{4.54}$$

After that HO_2 radicals may either attack methane

$$CH_4 + HO_2 \rightarrow CH_3 + H_2O_2 \tag{4.55}$$
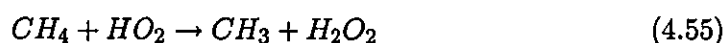
or undergo a radical recombination reaction such as

$$HO_2 + HO_2 \rightarrow H_2O_2 + O_2 \tag{4.56}$$

or

$$CH_3O_2 + HO_2 \rightarrow CH_3OOH + O_2 \qquad (4.57)$$
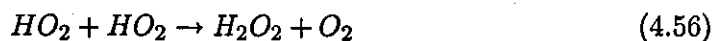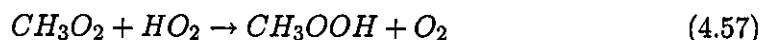
The oxidation of methyl radicals plays an important part in the overall process, and occurs at relatively low temperatures by

$$CH_3 + O_2 + M \Leftrightarrow CH_3O_2 + M \qquad (4.58)$$
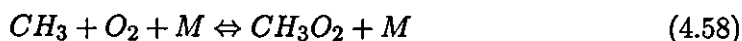
Both forward and reverse processes are relevant at temperatures below 1000 K. The equilibrium is displaced to the right hand side at 750K or below, so that reactions of CH_3O_2 are dominant.

Propagation through H atom abstraction by CH_3O_2 is possible,

$$CH_3O_2 + CH_4 \rightarrow CH_3OOH + CH_3 \qquad (4.59)$$
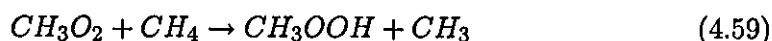
but this reaction has a relatively high activation energy ($E > 60$ kJ/mol) because the primary C-H bond of methane is amongst the strongest of the C-H single bonds. Consequently, in the low temperature range the favoured alternatives are radical-radical interactions of the following kind:

$$CH_3O_2 + CH_3O_2 \rightarrow CH_3O + CH_3O + O_2 \qquad (4.60)$$

$$CH_3O_2 + HO_2 \rightarrow CH_3O + OH + O_2 \qquad (4.61)$$

$$CH_3O_2 + HO_2 \rightarrow CH_3OOH + O_2 \qquad (4.62)$$

$$CH_3O_2 + CH_3 \rightarrow CH_3O + CH_3O \qquad (4.63)$$
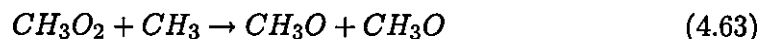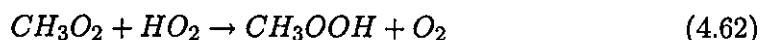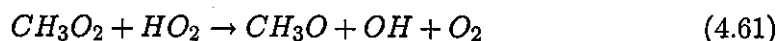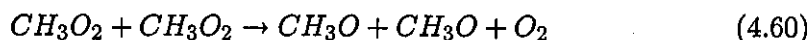
The main molecular products of the methyl + oxygen reaction are known to be methanol and formaldehyde, the proportions of which depend on the reaction conditions. The reaction

$$CH_3O_2 + CH_3O \rightarrow CH_3OH + CH_2O \qquad (4.64)$$
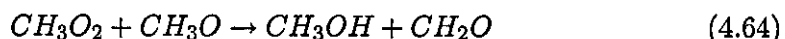
yields equal proportions of methanol and formaldehyde. An excess of methanol would suggest the reaction

$$CH_3O + CH_4 \rightarrow CH_3OH + CH_3 \qquad (4.65)$$
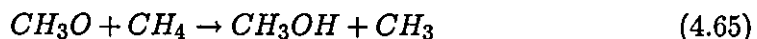
while an excess of formaldehyde in the products would suggest the reactions

$$CH_3 + M \to CH_2O + H + M \tag{4.66}$$
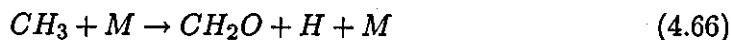
The equilibrium shown in Equation (4.58) is displaced to the left hand side at T> 850 K, which favours methyl radical reactions, either as the recombination

$$CH_3 + CH_3 + M \to C_2H_6 + M \tag{4.67}$$

or oxidation,

$$CH_3 + O_2 \to CH_2O + OH \tag{4.68}$$
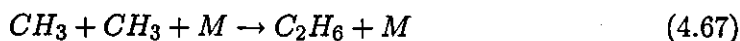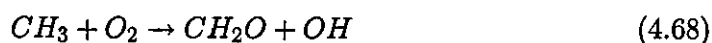
Equation (4.68) is not a simple bimolecular process but probably involves the methylperoxy radical that undergoes an intramolecular hydrogen atom transfer

$$CH_3O_2 \to [CH_2OOH] \to CH_2O + OH \tag{4.69}$$
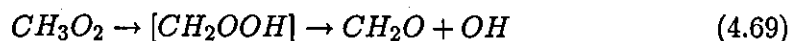
Since a primary C-H bond and a four-membered transition state ring are involved, this path has a high energy barrier and so it can become important only at higher temperatures. Chain propagation by hydroxyl radicals produced in Equation (4.68) occurs by

$$CH_4 + OH \to H_2O + CH_3 \tag{4.70}$$
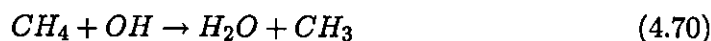
leading to formaldehyde and water as the molecular products of Equation (4.68) and Equation (4.70). Equation (4.67) is the *principal chain terminating* process in methane oxidation. During slow oxidation in closed vessels, reaction chains may also terminate at the walls probably by removal of species such as HO_2.

This overall sequence of reactions probably gives a fair representation of the main elementary reactions that occur in *methane* at T< 850K, but there are further possibilities. The more important features are governed by the reactivity of the molecular intermediates. Formaldehyde is able to offer a very labile H atom (the destruction energy of the C-H bond is 368 kJ/mol in formaldehyde compared with 435 kJ/mol in methane). Therefore, not only is a secondary initiation of reaction possible by

$$CH_2O + O_2 \to CHO + HO_2 \tag{4.71}$$
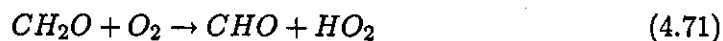
but also radical attack by OH and HO_2 is favoured

$$OH + CH_2O \rightarrow H_2O + CHO \qquad (4.72)$$

$$HO_2 + CH_2O \rightarrow H_2O_2 + CHO \qquad (4.73)$$

However, the difference between the reactivities of Equation(4.70) and Equation (4.72) is not very significant, the rate constant of Equation (4.73), for which $E \approx$ 42kJ/mol, is considerably lower that for Equation (4.55), $E > 60$kJ/mol. Subsequent reactions of the formyl radical (CHO) are

$$CHO + O_2 \rightarrow CO + HO_2 \qquad (4.74)$$

and

$$CHO + M \rightarrow CO + H + M \qquad (4.75)$$
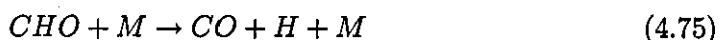
and the oxidation of CO to CO_2 and H to HO_2 may also occur.

The additional formation of HO_2 in Equation (4.74) sustains the hydroperoxy radical as a propagating species and the formation of hydrogen peroxide either in the abstraction reactions of Equation (4.55) and Equation (4.73) or the radical recombination of Equation (4.56). Hydrogen peroxide decomposes quite readily, as follows:

$$H_2O_2 + M \rightarrow 2OH + M \qquad (4.76)$$

In this way, the relatively unreactive HO_2 radicals are converted to highly reactive OH radicals, and if the major route to H_2O_2 is via the abstraction reactions of Equation (4.55) and Equation (4.73, this also constitutes a chain branching sequence. The overall reaction is not a chain branching sequence if Equation (4.56) is the sole source of H_2O_2, because two HO_2 radicals are involved in the formation of two OH radicals.

Taking the rate constant for the unimolecular decomposition to be in the first-order (high pressure) limit, for which $k = 3.0 \times 10^{14} \exp(-24400/T)$ s^{-1}, the half life for the H_2O_2 decomposition is 3.2 s at 700 K, 40 ms at 800 K and 1.4 ms at 900 K.

Thus, the rate of acceleration of reaction as a result of this chain branching process is very strongly temperature dependent. Development on such a slow timescale as that at low temperature relative to the normal propagation rate was called a *degenerative chain branching reaction* by Semenov [97]. In this type of reaction the rate accelerates rather slowly to a maximum and then decays. The controlled development, as opposed to a chain branching explosion, arises because there is a significant depletion of the reactant concentration owing to concurrent propagating reactions.

There is another possibility of degenerative branching during methane oxidation, but it is likely to be prevalent only at conditions in which reaction is promoted at temperatures below 700 K. These include reaction in very fuel-rich conditions at high pressure or when there is a catalyst (such as hydrogen bromide- HBr, which accelerates the reaction rate) present, and results from the formation and decomposition of methyl hydroperoxide, as

$$CH_3O_2 + CH_4 \rightarrow CH_3OOH + CH_3 \qquad (4.77)$$

or more favourably

$$CH_3O_2 + CH_2O \rightarrow CH_3OOH + CHO \qquad (4.78)$$

followed by

$$CH_3OOH \rightarrow CH_3O + OH \qquad (4.79)$$
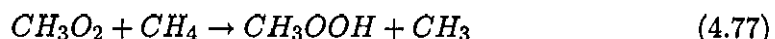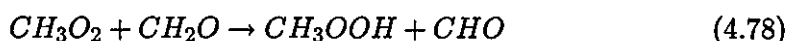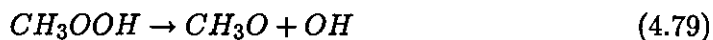
The first-order rate constant for methyl hydroperoxide decomposition is believed to be $\approx 8 \times 10^{14} \exp(-21500/T)$ s^{-1}, which gives a half-life of 3.2 s at 600 K and 19 ms at 700 K. However, the primary H atom abstraction (Equation 4.59) is not strongly favoured so this mode of chain branching is more strongly affected by the formation of formaldehyde as an molecular intermediate if the reaction is not catalysed by additives.

Hydrogen bromide is an effective catalyst because it is able to offer a labile H atom

$$CH_3O_2 + HBr \rightarrow CH_3OOH + Br \qquad (4.80)$$
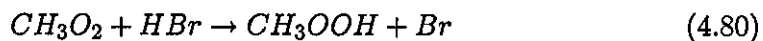
The activation energy for the Equation (4.80) is approximately 30 kJ/mol. The catalytic nature arises because hydrogen bromide may be regenerated in the reaction

$$Br + CH_4 \rightarrow HBr + CH_3 \qquad (4.81)$$
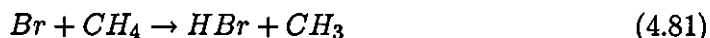
The supplementary reactions that can occur during methane oxidation depend on the reactant temperature.

4.6.2 The Oxidation of Higher Alkanes

The low temperature oxidation of an organic component involves a considerable variety of reactive intermediates[3] and there is correspondingly larger number of molecular product. There is a coherent structure to the elementary reaction involved, which can be coordinated in a formal structure for the kinetics. Higher alkanes refer basically to the series starting with normal butane and iso-butane. The limited overlap with the behaviour of propane exists [34]. The main gaseous reaction pathways over the temperature range of approximately 500-850 K are shown in Figure 4.7, taking butane as a representative case. Oxidation can also take place at temperatures below 500K, and the qualitative kinetics features are characterised by the very lowest temperature branch that is shown in Figure 4.7. The reaction rates becomes exceedingly slow and it relates mainly to the liquid-phase oxidation of much higher hydrocarbons, especially with regard to oxidative degradation when they are used as lubricants or the long term stability of animal or vegetable oils and fats [34]. Oxidation also progresses steadily at temperatures above 850K, but there is an increasing influence of the alkyl radical decomposition reactions (Equation 4.28), which lead eventually to 'high temperature' mechanisms. If the temperature is sufficiently high for rapid alkyl radical decomposition, the overall process may be characterised by the oxidation of a lower molecular mass alkene.

It can be seen in Figure 7.1 there is division into three temperatures regimes that signify the shift in the predominant reaction modes as the temperature is changed.

---

[3]The chemical substances that are produced by one elementary step and then consumed by another, so that they do not occur as a part of the overall products, are termed *intermediates*.
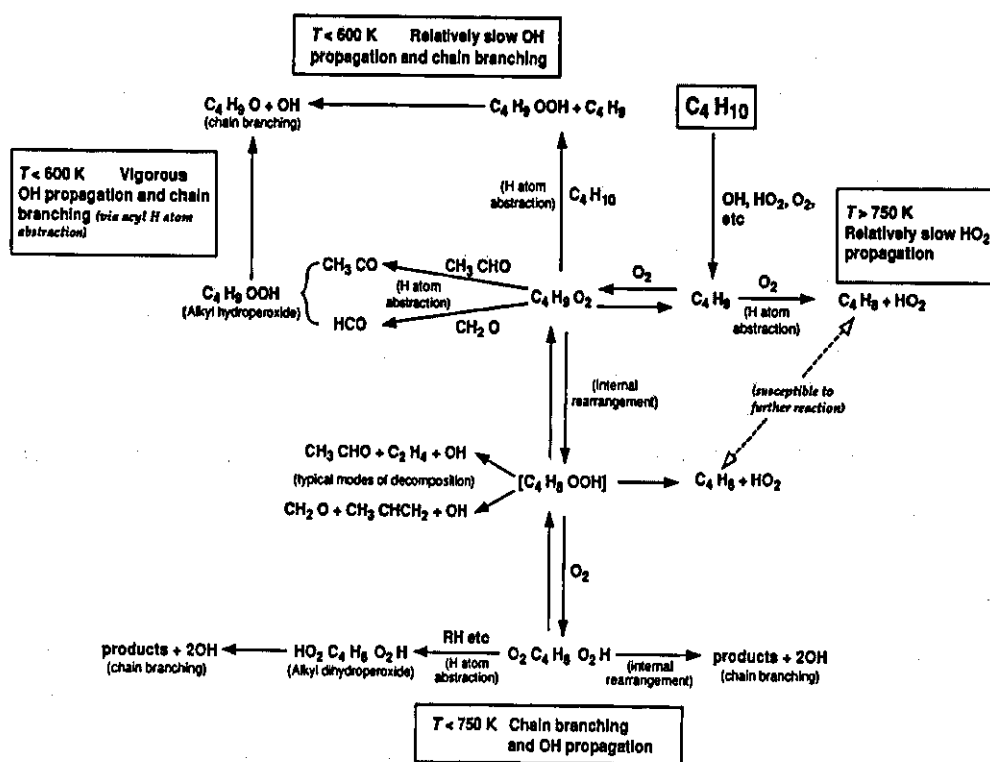
Figure 4.7: Schematic representation of normal butane oxidation in the temperature range 500-800K. An example on typical mechanisms involved in the oxidation of alkanes with four or more carbon atoms [34].

Each alkane, or its alkyl derivative, responds in ways that correspond qualitatively to the reaction shown. Quantitative differences in the kinetics are reflected in different transitional temperatures. The detailed explanations of this phenomenon can be found in [34, 35, 91, 96].

It can be seen in the middle of Figure 7.1 a simplified construction of the $R+O_2/RO_2$ equilibrium and its competition with the overall abstraction process yielding an alkene. As long as the oxidation to alkylperoxy radicals is favoured by $R+O_2/RO_2$ equilibrium, reaction is propagated by OH radicals. Not only is this vigorous because the associated activation energies are negligible, but it also tends to be quite strongly exothermic for an alkane

$$RH + OH \rightarrow R + H_2O \quad \Delta H^{\ominus}_{298} \approx -50\text{kJmol}^{-1} \tag{4.82}$$
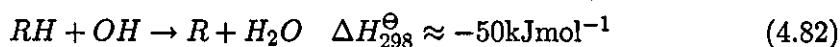
The subsequent oxidation of the alkyl radical gives considerably more heat, especially when carbon oxides are eventually formed. Degenerate chain branching modes also follow from the alkylperoxy radical reaction route.

By contrast, if the equilibrium is displaced towards the dissociation of alkylperoxy, the way is left open for an H atom abstraction process of the kind

$$R + O_2 \rightarrow \text{alkene} + HO_2 \qquad (4.83)$$

which gives rise to predominance of HO_2 radical propagation of the form

$$RH + HO_2 \rightarrow R + H_2O_2 \qquad (4.84)$$

Not only is this reaction relatively slow due to the associated activation energies (E>60 kJmol^{-1} at a primary C-H bond, >50 kJmol^{-1} at a secondary C-H bond and >40 kJmol^{-1} at a tertiary C-H bond), but there is also a little contribution of branching from hydrogen peroxide at temperatures below 750 K [34]. In addition, the stoichiometry from Equation (4.83) and Equation (4.84) is virtually thermoneutral

$$RH + O_2 = \text{alkene} + H_2O_2 \qquad (4.85)$$
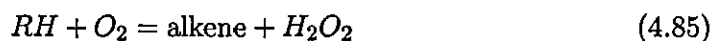
The overall feature of alkane oxidation and of other organic compounds is a transition from fairly vigorous, chain branching, exothermic oxidation to an essentially non-branching reaction of rather low exothermicity, as the temperature is raised through a certain range.

The main processes at the lowest temperatures (typically T<650K) are attributed to intermolecular H atom abstraction by alkylperoxy radicals of the form

$$RH + RO_2 \rightarrow R + ROOH \qquad (4.86)$$
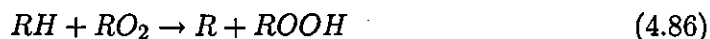
where ROOH represents molecular, *alkyl hydroperoxide*. The activation energies of these types of processes are believed to be rather similar to the corresponding reactions for HO_2 radicals, which means that chain propagation is relatively slow.

As for the decomposition of CH_3OOH (Equation 4.79), the alkyl hydroperoxides are appreciably less stable than hydrogen peroxide (E~170-180 kJ/mol). Degenerate chain branching is possible, but the acceleration of the reaction rate will not be fast since, the half life for the decomposition is 3 s at 600 K falling to about 20 ms at 700 K. These times may seem short, but combustion processes are known for their rapidity, and there are applications, such as diesel engines and CAI engines, for which this is too slow (from 0.6 to 3 ms for diesel engines and from 0.5 to for CAI engines[4]) [20, 21].

The decomposition of the alkyl hydroperoxide is promoted at the weak peroxide bond

$$ROOH \rightarrow RO + OH \qquad (4.87)$$

so that the subsequent propagation occurs via the hydroxyl and alkoxyl radicals. The alkoxyl radical could be a source of and alcohol as an intermediate molecular product, by

$$RO + RH \rightarrow ROH + R \qquad (4.88)$$

and this is the simplest means of reverting to alkyl and alkylperoxy radical propagation. A relatively high activation energy for Equation (4.88) allows the occurrence of some alternative reactions [34].

The most complicated kinetic region displayed in Figure 7.1 is associated with the *intermediate temperature range*, usually assigned as 650-750 K [20, 34]. Additional reactions are possible because the alkylperoxy radical is able to undergo an internal re-arrangement or *isomerisation* that involves an intramolecular H atom transfer

$$RO_2 \Leftrightarrow QOOH \qquad (4.89)$$

The product of this reaction (commonly assigned as QOOH in general terms) is represented as C_4H_8OOH, which signifies that a hydroperoxide linkage has been

---

[4]Auto-ignition timing depends of engine operating conditions, such as the compression ratio, intake temperature and intake pressure.

created and that the free radical site is then associated with a carbon atom some-where further along the structure [34]. The isomerisation reaction of Equation (4.89) is regarded to be reversible. QOOH is a free radical which also includes the weak O-O bond and therefore it is very reactive.

Two possible modes of decomposition of C_4H_8OOH are shown in Figure 7.1, but there may be a number of alternatives, which are governed by the relative locations of the free radical site and the–OOH moiety, represented generally as

$$QOOH \rightarrow AO + OH \qquad (4.90)$$

The dissociation of the peroxide group is inevitable, yielding a partially oxygenated molecular intermediate (AO) and a hydroxyl radical. These products are represented as aldehydes in Figure 7.1, because they may be contributory to one of the important, kinetic features in this particular regime, namely

$$RCHO/CH_2O + RO_2 \rightarrow RCO/CHO + ROOH \qquad (4.91)$$
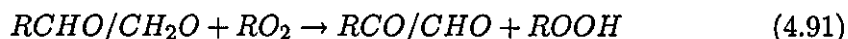
Equation (4.91) is distinguished from Equation (4.86) by the low activation energy ($E \approx 40$ kJmol^{-1}) which results from the weak acyl C-H bond in the aldehydes. The ability of the alkylperoxy radical to isomerise and to generate molecular intermediates that are more reactive than the primary fuel greatly facilitates a route to the alkyl hydroperoxide, and chain branching [34].

Further oxidation of QOOH may also yield alkyl dihydroperoxides in the low temperature of heptane. Their formation is believed to include the reversible addition of molecular oxygen

$$QOOH + O_2 \Leftrightarrow O_2QOOH \qquad (4.92)$$
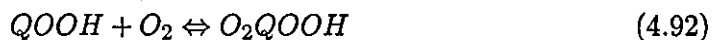
followed by either further, reversible, intramolecular rearrangement (Equation 4.93) or intramolecular H atom abstraction (Equation 4.94). The former would lead to another free radical (designated as HOOQ'OOH below), which is then likely to decompose to give a chain branching (Equation 4.93). The latter also gives degenerate chain branching as a result of the decomposition of the dihydroperoxide itself

(Equation 4.95).

$$O_2QOOH \Leftrightarrow HOOQ'OOH \rightarrow 2OH + \text{other products} \qquad (4.93)$$

$$O_2QOOH + RH \rightarrow HOOQOOH + R \qquad (4.94)$$

$$HOOQOOH \rightarrow 2OH + \text{diketone or other products} \qquad (4.95)$$
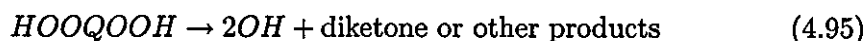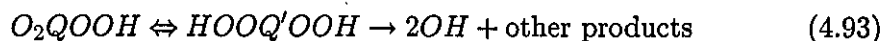
Diketone and hydroxyketo derivatives have been indentified from the low temperature combustion of heptane and other alkanes [34].

The decomposition of the isomerised free radical HOOQ'OOH (Equation 4.93) is likely to be similar to that of for the hydroalkylperoxy radical, QOOH (Equation 4.90), so that degenerate chain branching via Equation (4.93) is able to occur much more rapidly than through the molecular, organic peroxyde intermediates.

The activation energies associated with the alkylperoxide/hydroalkylperoxy isomerisation fall in the range 90-150 kJ/mol according to the mode of internal rearrangement [34]. It is *this energy barrier* that prohibits the isomerisation pathways from being the dominant chain branching route throughout the whole range at temperature below 750 K. Although complicated by the various equilibria involved, this is another example of the gradual transition of one predominant reaction route to another, as a consequence of competition between a bimolecular interaction (Equation 4.86) and a unimolecular reaction (Equation 4.90) which has a higher activation energy.

4.6.3 Negative Temperature Coefficient

The negative temperature coefficient-NTC occurs at temperatures around 700-800K. The NTC behaviour depends of the fuel molecular size and structure, and it is observed at some fuels that have two-stage ignition process, such as alkanes (paraffins). The NTC arises from the degenerative chain branching process, where radicals decompose back to reactants, which results in stopping the chain branching process. The region of NTC is characterised by the fact that a temperature increase causes

an increase of the ignition delay, instead of the usual temperature dependence where delay time should decrease.

The observation of a NTC during hydrocarbon oxidation was identified by Pease [101, 102]. The kinetic explanation of this phenomenon is well understand and can be summarised as follows:

- At low temperatures the $R + O_2/RO_2$ is displaced towards the formation of RO_2. The oxidation proceeds via alkyl hydroperoxide formation and, involving RO_2 isomerisation, the formation of dihydroperoxy species.

- As the temperatures rises, a decreasing fraction of alkyl radicals are converted to alkylperoxy radicals. This displacement of the predominant mode is virtually complete by 750 K. The system is then at its minimum reactivity because the prevailing radical concentration is exceedingly low.

- As the temperature is raised beyond 750K, an increased reactivity becomes possible through further reaction of the molecular intermediates, such as CH_2O and an increasing rate of decomposition of H_2O_2 that may promote autocatalysis.

4.7 Summary

The auto-ignition process is important as it precedes the combustion process and influences the performance, emissions and characteristics of the entire system. In a closed system, the auto-ignition may arise from various phenomena such as, thermal feedback, chain reactions or combination of these two. With regard to this, a division on three typical types of the auto-ignition process can be made:

1. The thermal auto-ignition

2. The chain-branching auto-ignition

3. The chain-thermal auto-ignition.

The chain-thermal auto-ignition, which can be defined as the requirement that the reacting system must experience exponential growth, both in temperature and number of chain carriers, is the most familiar in the alkane oxidation and therefore in the most of commercial fuels for automotive applications. Therefore, the auto-ignition in the internal combustion engines can be understand as a process of the thermal activation of the local kinetic processes, which depends of two parameters, (i) the temperature and (ii) the concentration. Initially the process is dominated by the kinetic effect, in which intensity depends on the concentration. The enhanced exothermic kinetic reactions increase the temperature of the reacting mixture. A higher temperature further boosts kinetic reactivity and accelerates the fuel consumption. With increase in temperature the rate of heat release grows. The growing heat release self-accelerates the fuel consumption. The dominant effect shifts from the concentration to the temperature during the energy release.

Automotive fuels, which have different structure and composition, leads to a very different behaviour of the auto-ignition process. These differences are explained by comparing the low temperature oxidation chemistry of methane and higher alkane fuels. After, the phase of the low temperature oxidation, the auto-ignition reaches the high temperature phase where differences in behaviour amongst hydrocarbon fuels are much less pronounced.

The differences in the low temperature auto-ignition chemistry amongst hydrocarbon fuels are expected to play a very important role in the CAI combustion process, as it is controlled by the chemical kinetics of air/fuel mixture. This will be discussed in Chapters 6, 7 and 8.

Chapter 5

Simulation Model

The basic characteristic of CAI combustion is that auto-ignition occurs at many points simultaneously, and that further combustion proceeds uniformly, with no flame propagation. CAI combustion is mainly controlled by the chemical kinetics of air-fuel mixture, with no influence of turbulence. The insensitivity towards turbulence makes it possible to use a chemical kinetics approach for accurate CAI modelling as discussed earlier in Chapter 2.

5.1 Description of the Simulation Model

In selection of the computational model for the simulation of an internal combustion engine with CAI combustion, it is necessary that the model has to satisfy the following demands:

1. To perform a detailed chemical kinetics analysis.

2. To be able to accurately predict the start of combustion process (ignition timing), heat release rate, peak cylinder pressure, indicated power and NO_x emission.

3. To have the possibility to perform a parametric analysis of the influence of engine parameters and fuel types.

4. To have a reasonably short computational time.

Based on these demands, and from the analysis of various simulation studies performed in Section 2.2, the author decided to use the detailed chemical kinetics approach with a single-zone model. It offers good accuracy in prediction of ignition timing, heat release rate, peak cylinder pressure, indicated power and NO_x in relatively short computational time.

The Aurora application from the Chemkin III modelling package [67] is chosen for the modelling of the CAI engine. The package considers the cylinder as a single-zone, homogeneous reactor with a variable volume. The volume is varied with time according to the slider-crank relationship [21].

The present model assumes mixture in the cylinder as a perfect gas, with uniform thermodynamic properties and evenly distributed mixture composition. The heat transfer loss is taken into account by using Woschini's heat transfer correlation [1]. This correlation treats the heat loss as a distributed heat transfer, proportional to the temperature difference between the average gas temperature and a time averaged wall temperature. The other losses, such as radiation heat losses to the engine cylinder walls, blowby, fuel trapping in crevices volume and other processes are not considered.

5.2 Governing Equations

In this section description of the model's governing equation will be presented.

The employed Aurora application considered the cylinder as a single-zone closed volume, filled with homogeneous mixture, which acts as a perfect gas and conservation of mass, energy and species are applied.

Conservation of Mass

The total mass of the mixture in a closed system with no mass crossing the boundary

is presented by:

$$m = \sum_{j=1}^{J} m_j \qquad (5.1)$$

and changing the mass during the time by:

$$\frac{dm}{dt} = 0 \qquad (5.2)$$

This means that mass is constant. The m_j is the mass of j-th species and J is the total number of species in the mixture.

Conservation of Species

The individual species are produced or destroyed according to

$$\frac{dm_j}{dt} = V\dot{\omega}_j M_j \qquad (5.3)$$

where t is time, $\dot{\omega}_j$ is the molar production rate of the j-th species by the elementary reaction, M_j is the molar mass of the j-th species and V is the volume of the system. Volume of the system varies with the time according to the slider-crank relationship (Equation 5.25). As the total mass in the system is constant Equation (5.3) can be written in the terms of the mass fractions

$$\frac{dY_j}{dt} = v\dot{\omega}_j M_j \qquad (5.4)$$

where Y_j is the mass fraction of the j-th species represented by

$$Y_j = \frac{m_j}{m} \qquad (5.5)$$

and v is the specific volume represented by

$$v = \frac{V}{m} \qquad (5.6)$$

Conservation of the Energy

The first law of the thermodynamic applies to a closed system yields to:

$$\underbrace{\frac{dQ_{ht}}{dt}}_{\text{Heat Transfer}} = \underbrace{\frac{dU}{dt}}_{\text{Internal Energy}} + \underbrace{p\frac{dV}{dt}}_{\text{Displacement Work}} \qquad (5.7)$$

where p is the pressure and V instantaneous cylinder volume.

The internal energy for the mixture of ideal gasses is given by:

$$U = m(\sum_{j=1}^{J} Y_j u_j) \tag{5.8}$$

where m denotes the total mass within the cylinder, Y_j the mass fraction of the j-th species and u_j is the specific internal energy of the j-th species.

Substituting Equation (5.8) into Equation (5.7) leads to

$$\frac{dQ_{ht}}{dt} = (\sum_{j=1}^{J} Y_j \frac{du_j}{dt} + \sum_{j=1}^{J} u_j \frac{dY_j}{dt}) + p\frac{dV}{dt} \tag{5.9}$$

Assuming perfect gas, du_j can be written as

$$du_j = c_{v,j} dT \tag{5.10}$$

where T is the temperature of the mixture and $c_{v,j}$ is the specific heat of the j-th species evaluated at evaluated at constant volume. The mean specific heat of the mixture then becomes

$$\bar{c}_v = \sum_{j=1}^{J} Y_j c_{v,j} \tag{5.11}$$

Substituting Equations (5.4) and (5.11) into Equation (5.9) gives

$$\frac{dQ_{ht}}{dt} = \bar{c}_v \frac{dT}{dt} + v\sum_{j=1}^{J} u_j \dot{\omega}_j M_j + p\frac{dV}{dt} \tag{5.12}$$

The pressure p is calculated by using the perfect gas equation of state

$$p = \frac{\rho \tilde{R} T}{\bar{M}} \tag{5.13}$$

where ρ is the mass density of the mixture, $\tilde{R}$ universal gas constant and $\bar{M}$ is the mean molar mass of the mixture.

The heat transfer considers convection losses from the gas mixture to the cylinder walls according to

$$Q_{ht} = hA(T - T_{wall}) \tag{5.14}$$

where h is the heat transfer coefficient, A is the heat transfer area, T and T_{wall} is time averaged gas temperature and cylinder wall temperature respectively.

Heat transfer coefficient h is obtained from the Woschini's heat transfer correlation [1]

$$Nu = aRe^b Pr^c \qquad (5.15)$$

where N is the Nusselt number for heat transfer, Re is the Reynolds number and Pr is the Prandtl number. These number are defined according to

$$
\begin{aligned}
Nu &\equiv \frac{hD}{\lambda} \\
Re &\equiv \frac{D\bar{S}_p \rho}{\mu} \\
Pr &\equiv \frac{c_p \mu}{\lambda}
\end{aligned}
\qquad (5.16)
$$

where D is the characteristic length in this case it is cylinder bore, λ is the gas conductivity, $\bar{S}_p$ is the mean piston speed define in equation (5.17) and μ is the gas viscosity.

The mean piston speed $\bar{S}_p$ is defined as

$$\bar{S}_p = 2L\Omega \qquad (5.17)$$

where L is the piston stroke and Ω is the rotational speed of crankshaft.

The area available for heat transfer A includes the cylinder walls area A_{liner}, which is time-dependent and end surfaces area (piston and head surface area) A_{surf}:

$$
\begin{aligned}
A &= A_{liner} + A_{surf} \qquad (5.18) \\
A_{liner} &= \frac{\pi DL}{2}(R + 1 - \cos\theta - \sqrt{R^2 - \sin^2\theta}) \\
A_{surf} &= A_p + A_h \approx \frac{2\pi D^2}{4}
\end{aligned}
$$

where R is the ratio of connecting rod length to crank radius and θ crank angle. These parameters together with all other relevant parameters will be explained in the following text.

Other Governing Equations

Other equations are used to define the geometrical properties of the engine and the net species production rate.

Engine geometrical properties equations

Compression ratio **CR** is defined as

$$CR = \frac{\text{Maximum cylinder volume}}{\text{Minimum cylinder volume}}$$

$$CR = \frac{V_d + V_c}{V_c} \tag{5.19}$$

where V_d is displaced or swept volume and V_c is the clearance volume.

Ratio of connecting rod length to crank radius **R** is

$$R = \frac{l}{a} \tag{5.20}$$

The stroke L and crank radius a are related by

$$L = 2a \tag{5.21}$$

The rotation speed of the crankshaft Ω is represented by changing of the crank angle θ in time

$$\Omega \equiv \frac{d\theta}{dt} \tag{5.22}$$

The cylinder volume at any crank angle position is

$$V = Vc + \frac{\pi D^2}{4}(l + a - s) \tag{5.23}$$

where s is the distance between the crank axis and the piston axis [21], and is given by

$$s = a\cos\theta + \sqrt{l^2 - a^2\sin^2\theta} \tag{5.24}$$

Substituting Equation (5.24) into Equation (5.23) and re-arranging leads to

$$\frac{V(t)}{V_c} = 1 + \frac{(CR-1)}{2}(R + 1 - \cos\theta - \sqrt{R^2 - \sin^2\theta}) \tag{5.25}$$

Differentiation of Equation (5.25) with respect to time (t) gives

$$\frac{d(V/V_c)}{dt} = \Omega\frac{(CR-1)}{2}\sin\theta(1 + \frac{\cos\theta}{\sqrt{R^2 - \sin^2\theta}}) \tag{5.26}$$

which represents the changing of the volume in time.

Governing equations for species production rate

The rates of creation/destruction of chemical species are represented by using mass-action kinetics as explained in Section 3.3. An elementary reaction that involves J' chemical species in I' reactions can be represented in the form

$$\sum_{j=1}^{J} \nu'_{ji} X_j \Leftrightarrow \sum_{j=1}^{J} \nu''_{ji} X_j \tag{5.27}$$

where ν'_{ji} and ν''_{ji} are the stoichiometric coefficient for the forward and reverse stages respectively.

The species molar production rate $\dot{\omega}_j$ is defined as

$$\dot{\omega}_j = \sum_{j=1}^{J} (\nu''_{ji} - \nu'_{ji}) q_i \tag{5.28}$$

where q_i is the process progress variable

$$q_i = k_{f_i} \prod_{j=1}^{J} (\rho \frac{Y_j}{M_j})^{\nu'_{ji}} - k_{r_i} \prod_{j=1}^{J} (\rho \frac{Y_j}{M_j})^{\nu''_{ji}} \tag{5.29}$$

where k_{f_i} and k_{r_i} are the forward and reverse reaction rate constants respectively.

The reaction rate constant is expressed in the Arrhenius form

$$k_{f_i} = A_i T^{\beta_i} \exp(\frac{-E_i}{RT}) \tag{5.30}$$

where A_i is pre-exponential factor, β_i is the temperature exponent and E_i is the activation energy of the i-th reaction. Detailed discussion about this equation and its parameters are given earlier in Section 3.3.

5.3 Numerical Solution Method

The system of ordinary differential equations used for modelling of the CAI engine cylinder environment, described in the previous section, is generally stiff (problematic for simultaneous solution). One of the efficient ways to solve stiff system of

ordinary differential equations is to use an implicit technique. A software package called Differential Algebraic Sensitivity Analysis Code (DASAC), based on the Differential/Algebraic System Solver (DASSL) is used. This solver performs the time integration using the backward differentiation formula [67].

5.4   Engine Description

The engine is assumed to have bore 80.5 *mm*, stroke 88.2 *mm*, and a connecting rod length 132 *mm* with displacement of 450 *cm*^{3}. The engine is assumed to have fully variable valve train (FVVT) system, instead of conventional camshafts, which allows the trapping of a large amount of exhaust gases (up to 80% by volume) and quick changes in trapped percentage in comparison to the engine with camshaft [42]. This arrangement allows near adiabatic exhaust gas recirculation (*EGR*) process , which means that the mixture temperature increases with the increase in *EGR* percentage. Trapping the exhaust gases on this way is termed *'internal exhaust gas recirculation'- IEGR* process. The engine is assumed to be un-throttled at all operational points with a volumetric efficiency of 100 percent.

5.5   Validation of the Model

The results obtained by using the computational model are validated against the experimental results. The experiment was performed with a single cylinder, 4-stroke engine equipped with AVT-Lotus' Research Active Valve Train System[1] and fuelled with *n-heptane* and *iso-octane* fuels. The experimental engine and AVT are discussed in detail in [43, 103]. Test conditions are summarised in Table 5.1.

The simulation starts at the beginning of compression stroke BDC point (IVC point) and finishes at the end of expansion stroke with the time step of 1° crank angle. The engine operational parameters are those specified in Table 5.1. The heat release rate is calculated from the pressure values at each time step by using Kinalc post

---

[1]The FVVT system is also called Active Valve Train System-AVT.

Table 5.1: Engine specification and test conditions

Bore	80.5 mm
Stroke	88.2 mm
Swept volume	450 cm^3
Number of valves per cylinder	4
Valves Control	Electro-hydraulic Lotus AVT system
IMEP	3 bar
Compression Ratio	10.5:1
Speed	2000 rpm
Inlet Pressure	Naturally Aspirated
IEGR	55 %(by volume)
Fuel	n-heptane and iso-octane
Equivalence air-fuel ratio	Stoichiometric

processor code [104]. Kinalc can also perform the sensitivity analysis and the life time analysis for characteristic species and reactions. Detailed explanation of Kinalc's code performances can be founded in [104].

The *IEGR* is assumed to consist mainly of water vapour, carbon dioxide, molecular nitrogen and oxygen from previous engine cycles[2] and to be fully mixed with the fresh un-reacted air-fuel mixture. The newly formed resulting charge (air/fuel/IEGR) is assumed homogeneous with a uniform composition and thermodynamic properties.

The temperature of the resulting charge (trapped IEGR and fresh air/fuel charge) is estimated assuming the mixing of the ideal gases by the published procedure in [21]. This is presented in Appendix B.

The air-fuel equivalence ratio (λ) is defined as that of the incoming charge in the cylinder (fresh un-reacted air-fuel charge) and not that of the resulting charge in the cylinder (air/fuel/IEGR) which can be leaner due to the residual oxygen.

The cylinder wall, piston and head are all assumed to be at the uniform temperature, with 450 K using *n-heptane* fuel and 500 K using *iso-octane* fuel. The difference of

---

[2]The concentration of IEGR components are calculated from the overall combustion equation [105]. For an example, with *iso-octane* fuel, the IEGR composition is $CO_2=12.3\%$, $H_2O=13.8\%$, $N_2=71.8\%$ and $O_2=2.1\%$, while with *n-heptane* fuel the IEGR composition is $CO_2=12.2\%$, $H_2O=14\%$, $N_2=72\%$ and $O_2=2.2\%$. Detailed explanation is given in Appendix B.

50K is assumed based on experimental results where measured exhaust gas temperature in the exhaust manifold was 50K higher with iso-octane than with n-heptane fuel [43, 103].

The chemical kinetic mechanisms used for n-heptane and iso-octane simulation are those developed by the Lawrence Livermore National Laboratory [89, 90]. The mechanism for *n-heptane* consists of 618 species and 2695 reactions, while *iso-octane* mechanism consists of 910 species and 3761 reactions. The NO$_x$ chemistry, which consists of 53 species and 155 reactions is included in the given reaction set.

These mechanisms have been validated through extensive comparisons with experimental data obtained from the measurement conducted in flow reactors, shock tubes and rapid compression machines [72, 89, 90, 106].
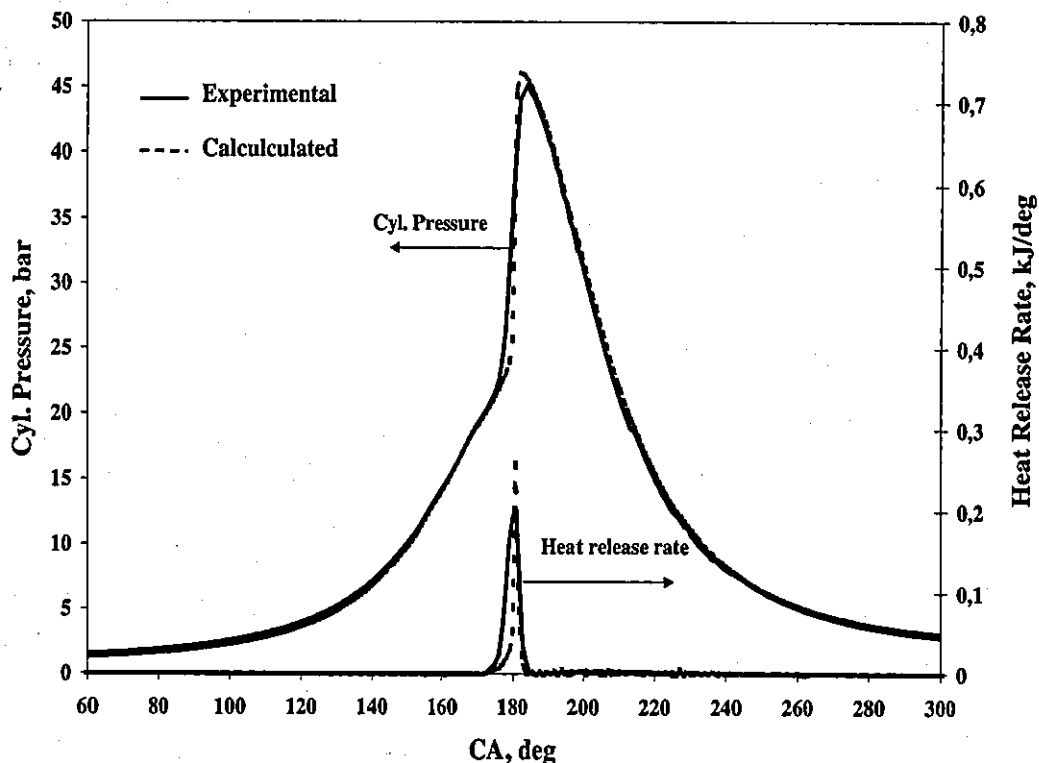
Figure 5.1: Comparison of calculated and experimental cylinder pressure and heat release rate curves for *n-heptane* fuel. Dotted lines represent calculated results and solid lines experimental results.

Figure 5.1 shows a comparison between the calculated and measured cylinder pressure and heat release rate curves for n-heptane fuel and Figure 5.2 for iso-octane fuel.
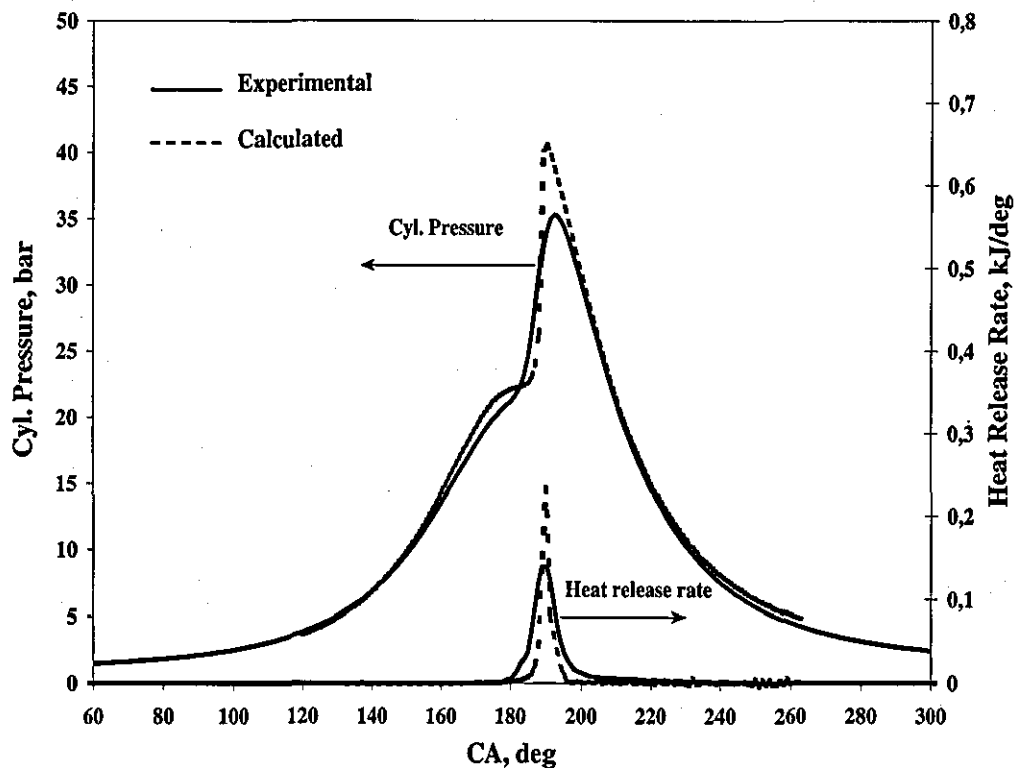
Figure 5.2: Comparison of calculated and experimental cylinder pressure and heat release rate curves for *iso-octane* fuel. Dotted lines represent calculated results and solid lines experimental results.

It can be seen that for both fuels the general shape of the calculated cylinder pressure curves correspond rather well to the experimental ones. Calculated values for cylinder pressures before ignition points are slightly higher than experimental ones ($\approx 5\%$ difference for iso-octane fuel and $\approx 2\%$ difference for n-heptane fuel), because in simulation IVC is assumed to be at 180 BTDC, while in experiment it was later, 145 BTDC. The peak cylinder pressures are over predicted due to the deficiency of single-zone assumption to model temperature gradient within the mixture.

Due to the nature of the single-zone model the fuel in the cylinder volume burns

simultaneously. Therefore, the peak cylinder pressure is over-predicted ($\approx 10\%$) and the pressure gradient after ignition is too high. However, the time of auto-ignition is accurately predicted (within a difference of $\approx +0.5$ CA degrees).

The overall trend of heat release curves are matched for both fuels, but the calculated values are over-predicted (≈ 15-30%) and durations are under-predicted (≈ 10-20%). This is due to the assumption (of single-zone model) that the whole mixture inside the cylinder will burn almost simultaneously and completely, together with inability of single-zone model, to model a temperature gradient within cylinder[3].

In reality a boundary layer which contains significant mass will exist and it will be at a lower temperature than the bulk gas near TDC. Consequently, the boundary layer will always burn last and extend the heat release rate compared to this simulation. Also, an amount of fuel will be captured in crevices and will not be burned. Thus the heat release rate will be extended more in time.

As a consequence of the assumption that the whole mixture burns simultaneously and completely, the indicated mean effective pressure IMEP[4] and NO_x emission are over-predicted for both fuels. The ratio of experimental/calculated values for IMEP is:

- 2.89bar/3.15bar for *n-heptane*.

- 3.24bar/3.47bar for *iso-octane*.

The ratio of experimental/calculated values for NO_x emission is:

- 75ppm/120ppm for *n-heptane*.

- 220ppm/310ppm for *iso-octane*.

---

[3]Since the rate of heat release is obtained by analysing the pressure traces any inaccuracies in the pressure will therefore, result in a considerable differences in predicted heat release rates.

[4]IMEP is compared only for the 'power stroke', i.e. for the compression and expansion strokes.

As the NO_x emission in the IC engines originates mainly from 'thermal NO_x', then even a small over-prediction in the cylinder temperature will result in its over-prediction.

The CO and HC emissions, which have been explained as dependant on the crevices in Section 2.2, cannot be accurately predicted with this model.

The author recognises that model assumptions are the over-simplification of the actual condition within the engine cylinder which leads to over-estimation of peak cylinder pressure and rate of pressure rise, under-estimation of burn duration and inability to accurately predict HC and CO emissions. On the other hand prediction of the start of ignition, pressure traces and heat release rate trends are shown to be accurate. Therefore, the Aurora application will be used for the further numerical investigation of the fuel composition effect (Chapter 6), engine parameters effect (Chapter 7) and IEGR effect (Chapter 8) on CAI combustion.

Chapter 6

Effect of Fuel Composition on CAI Combustion

CAI combustion is a process characterised by uniform and homogeneous auto-ignition controlled by the chemical kinetics of air-fuel mixture. It could be said that CAI combustion has many similarities with the 'end gas' auto-ignition in spark engines that is responsible for the knock effect [20].

From a characteristic of the auto-ignition process and chemical kinetics discussed in Chapter 4 and Chapter 3 respectively, and from research studies focused on knock onset in a motored engine using homogeneous charge of various fuels [20, 107, 108, 109, 110], it can be concluded that the controlling parameters in the initiation of auto-ignition process are the fuel properties, temperature, pressure and composition of the air-fuel mixture.

In this Chapter the effects of fuel composition on the onset/timing of auto-ignition and heat release rate in a CAI combustion will be discussed.

The other parameters that influence CAI combustion characteristics (such as temperature, pressure and composition of air-fuel mixture), depend of engine operational parameters. This will be discussed in Chapter 7.

In this chapter the fundamental understandings of the auto-ignition process in a CAI engine will be presented, followed by the effect of fuel composition on the

onset/timing of auto-ignition and rate of heat release. The investigated fuels are *n-heptane, iso-octane, ethanol* and *methane*. N-heptane and iso-octane are primary reference fuels (PRF's) and they are selected because their ignition chemistry spans the range of cetane and octane numbers of diesel and gasoline fuel. Ethanol and methane are chosen as potentially interesting fuels for use in CAI engine. Ethanol is chosen as a representative of an alcoholic type of fuel and methane is representative of a gaseous type of fuel. The chapter concludes with the summary of auto-ignition behaviour of different investigated types of fuel in a CAI engine.

6.1 Fundamentals of Auto-ignition Process in CAI engine

Regarding the start of the auto-ignition process in a CAI engine there exists different opinions with radicals and reactions being the crucial ones. It is a well accepted fact that OH radicals are the most important and frequently dominant species in ignition process of any hydrocarbon fuel. As the most reactive and fastest propagation radicals, their reaction with fuel molecules are the dominant ones, resulting in producing water, heat, increasing the temperature of the reactive mixture and establishing self-sustaining properties of auto-ignition and combustion process.

Furutani et al [111] and Yumasaki et al [112] state that the starting of formaldehyde (CH_2O)decomposition is responsible for the start of auto-ignition in CAI combustion. It is the 'trigger' of the auto-ignition process. Analysis performed of all radicals production/destruction reactions for methane fuel shows that decomposition of (CH_2O) leads to formation of formyl radicals (HCO) and water, mainly via reaction with OH radicals [113]. After that, formyl radicals react with oxygen producing HO_2 radicals and CO intermediates. From these it can be concluded that (CH_2O) is the main source of HO_2 radicals that are considerably slower in propagation and less reactive in comparison with OH radicals. In that way, it is highly likely that (CH_2O) radicals have contribution to the heat release from the low temperature reactions (cool flame ignition) as the source of HO_2 radicals. HO_2 radicals are formed

in highly exothermic reactions, which play an important role in this stage of ignition [106, 108]. However, as the investigation was performed for methane fuel, which has not experienced the same low temperature ignition process as higher hydrocarbons fuels (discussed in Section 4.6), the possibility that (CH_2O) decomposition is genuinely responsible for the start of ignition in a CAI engine cannot be ruled out without further investigation.

Westbrook [20], and Aceves et al [29] claim that hydrogen-peroxide (H_2O_2) decomposition controls the start of the ignition process in a CAI engine. Start of the H_2O_2 decomposition produces an enormous number of OH radicals, which then start to react with fuel molecules producing water and heat and increasing the temperature of the reacting mixture. This sets in motion an effective chain branching sequence:

$$RH + HO_2 \Leftrightarrow R + H_2O_2 \qquad (6.1)$$

$$H_2O_2 + M \Leftrightarrow 2OH + M \qquad (6.2)$$

$$OH + RH \Leftrightarrow R + H_2O \qquad (6.3)$$

$$R + O_2 \Leftrightarrow \text{alkene} + HO_2 \qquad (6.4)$$

$$H + O_2 + M \Leftrightarrow HO_2 + M \qquad (6.5)$$
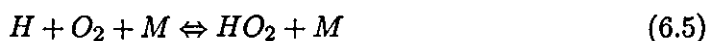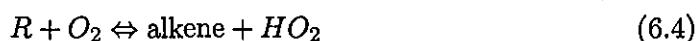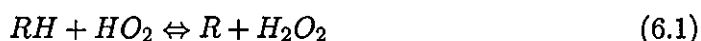
This reaction sequence proceeds rapidly until the temperature reaches certain values after which the high temperature chain branching sequence

$$H + O_2 \Leftrightarrow O + OH \qquad (6.6)$$

takes place and control of the remainder of combustion process. The same results have been obtained in the simulation studies of a CAI engine fuelled with methane, carried out by Chen and Milovanovic [114, 115].

The start of auto-ignition (SAI) in IC engines is readily seen, either, as a sharp increase in cylinder pressure or cylinder temperature [21]. For this study the SAI is defined as the crank angle (CA) degree at which maximum pressure rise is observed. As, has been previously discussed, ignition in a CAI engine is controlled by the start

of H_2O_2 decomposition. Thus SAI can also be determined by identifying the peak in H_2O_2 concentration. In Figure 6.1 it can be seen that the SAI occurs at the point of maximum pressure rise, which is at the same time point of the peak H_2O_2 concentration. (At 179 CAD in this case.)
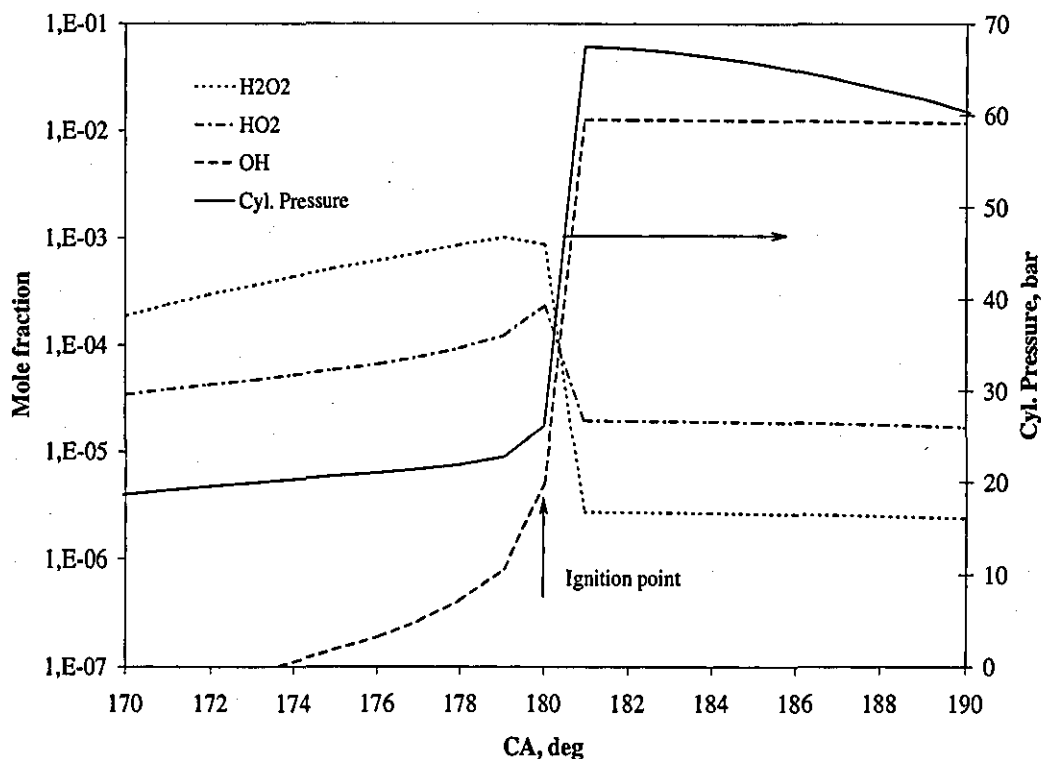
Figure 6.1: Start of the auto-ignition in a CAI engine. Solid line represents cylinder pressure, dotted line H_2O_2 radicals concentration, dashed line with dots HO_2 radicals concentration and dashed line OH radicals concentrations.

6.2 Effect of Different Fuels on Ignition Timing and Heat Release Rate in CAI engine

One of the advantages of a CAI engine in comparison to SI and CI counterparts is *fuel-flexibility*. Test results show that various fuels can be used in CAI [22, 116].

In this study the effects of four different types of fuels on onset/timing of auto-ignition and heat release rate in CAI engine are investigated. The investigated fuels

are:

- n-heptane (n-C_7H_{16}),

- iso-octane (i-C_8H_{18}),

- ethanol (C_2H_5OH) and

- methane (CH_4).

N-heptane and *iso-octane* are primary reference fuels, whose ignition chemistry spans the range of cetane and octane numbers of diesel and gasoline fuel. The cetane number (CN) of n-heptane is similar to CN of diesel fuel (CN$\sim$ 56). Iso-octane has octane number ON (100), which is similar to ON of gasoline.

Ethanol and *methane* are potentially attractive fuels for use in heavy-duty, agricultural and construction CAI engines. These fuels are 'environmentally clean' and have advantages for agriculturally based rather than oil based economy. The ethanol and methane are chosen as potentially interesting fuels for use in a CAI engine, and also to represent behaviour of alcohols and gaseous types of fuel. The ON of ethanol is ($\sim$ 107), while methane has ON ($\sim$ 120).

These four fuels, n-heptane, iso-octane, ethanol and methane, have different composition, molecular size and structure, which result in different values of cetane numbers (CN) and octane numbers (ON). Under CAI engine conditions these fuels will show quite different auto-ignition behaviour, and those differences will have the important consequences on further combustion and controlling processes.

6.2.1 Fuel Effects on the Auto-ignition Timing

The onset/timing of auto-ignition is clearly crucial to the operation of a CAI engine and should occur within 10^0 BTDC to 10^0 ATDC. Ignition timing should be controlled so that heat is released at the appropriate time in the engine cycle [21]. For the optimal engine efficiency ignition should occur around TDC .

The engine parameters for this study are those summarised in Table 6.1. The chemical kinetic mechanisms used for n-heptane, iso-octane and ethanol are those developed by Lawrence Livermore National Laboratory [89, 90], while for methane it is the GRI-Mech 3.0 mechanism [87]. The mechanism for *n-heptane* consists of 565 species and 2540 reactions, for *iso-octane* of 875 species and 3606 reactions, for *ethanol* of 57 species and 383 reaction and for *methane* of 53 species and 325 reactions. These mechanisms have been validated through extensive comparisons with experimental data obtained from the measurement conducted in flow reactors, shock tubes and rapid compression machines [72, 89, 90, 106]. In Figure 6.2 the

Table 6.1: Engine parameters specification

Bore	80.5 mm
Stroke	88.2 mm
Swept volume	450 cm^3
Compression Ratio	10.5:1
Speed	2000 rpm
Inlet Pressure	Naturally Aspirated
Fuel	n-heptane,iso-octane,ethanol and methane
Equivalence air-fuel ratio	Stoichiometric
Cylinder wall temperature	500K

cylinder pressures curves for these four fuels are shown while Figure 6.3 shows the cylinder temperatures curves. Due to the different structures of the fuels and in order to obtain ignition near TDC, the inlet air temperature was adjusted for each fuel separately.

It can be seen that *n-heptane* needs the lowest inlet temperature, while *methane* needs the highest. *Iso-octane* needs a much higher inlet temperature than n-heptane, but lower that that for methane. *Ethanol* has a slightly higher inlet temperature than iso-octane. It can be concluded that inlet temperature depends on fuel ON, the fuel with lower ON needs a lower inlet temperature for auto-ignition and vice versa. The relationship between ON and inlet temperature is given in Figure 6.4. These results are in agreement with the experimental results obtained by Christensen et
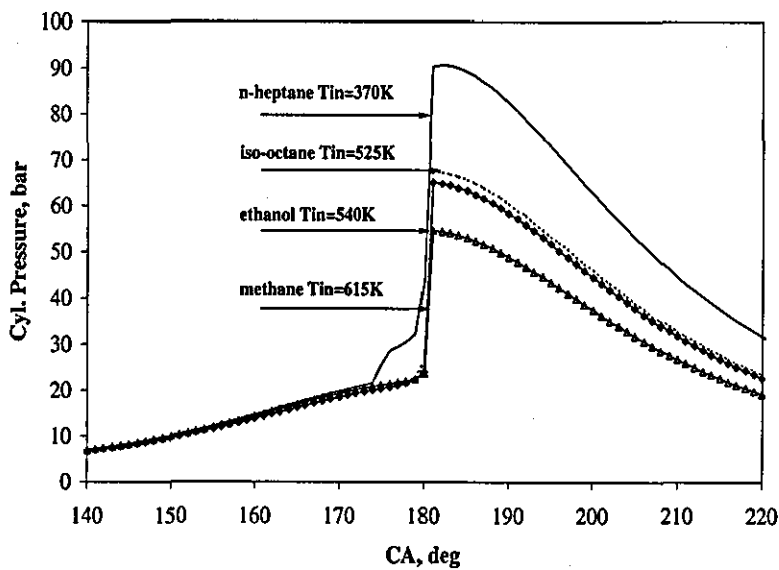
Figure 6.2: Cylinder pressure as a function of crank angle for analysed fuels. Solid line represents *n-heptane*, dashed *iso-octane*,(◇) ethanol and (△) methane.
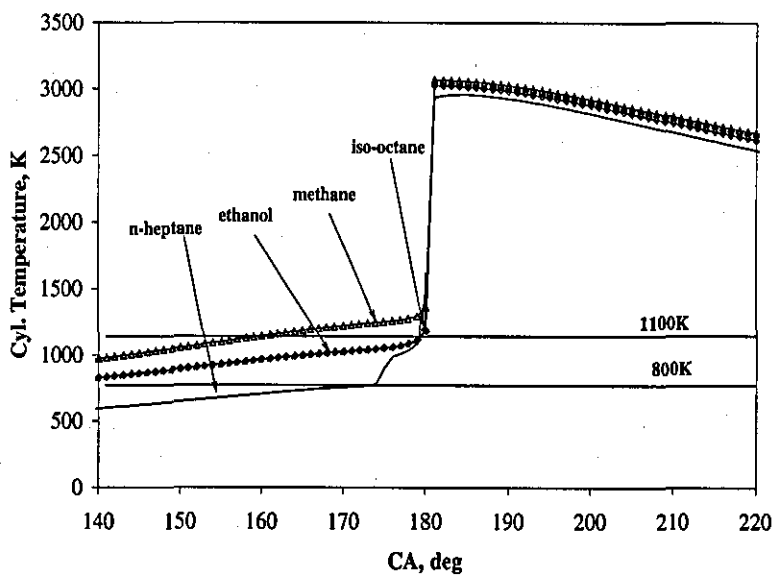
Figure 6.3: Cylinder temperature as a function of crank angle for various fuels. Solid line represents *n-heptane*, dashed *iso-octane*,(◇) ethanol and (△) methane.

al [22] and Aroonsrisopon et al [116].
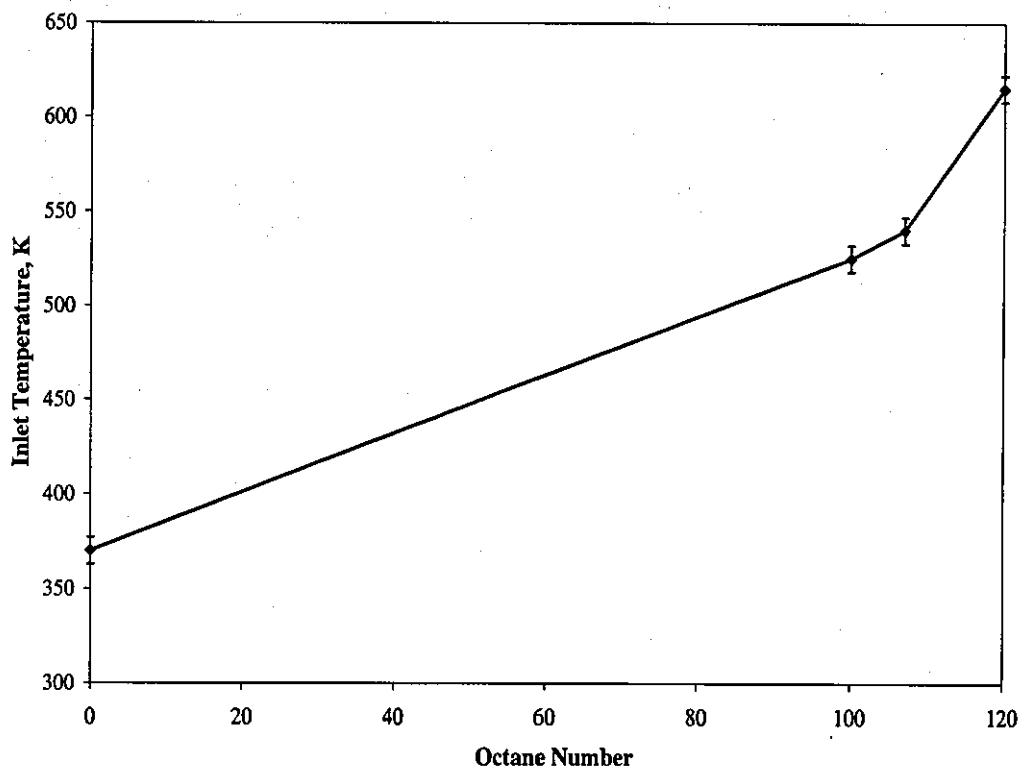
Figure 6.4: Inlet temperature as a function of Octane number for analysed fuels.

It can be seen in Figures 6.2 and 6.3 that fuels investigated show different auto-ignition behaviour. *N-heptane* exhibits *two stage ignition*, with cool-flame (CF) or low-temperature ignition, negative temperature coefficient (NTC) behaviour and main ignition (MI) or high temperature ignition. On the other hand *iso-octane, ethanol and methane* undergo *single stage ignition* only.

N-heptane is a long straight-chain paraffin with many weakly bonded H atoms, and with high isomerization rates, which leads to rapid ignition. The first stage of ignition CF is started at about 800K, causing the step rise in pressure and temperature (Refer to Figure 6.2 and Figure 6.3). The cool-flame ignition is mainly due to presence of C_7H_{15} radicals, which ultimately leads to a relatively high rate of chain branching from ketohydroperoxide decomposition [106, 117].

This chain branching sequence results in an enhanced yield of OH radicals which starts to consume fuel, release heat and increases the temperature of the mixture. Therefore, due to the presence of C_7H_{15} radicals *n-heptane* has a low activation energy, and thus needs relatively low inlet temperature to start auto-ignition.

It can be seen, from Figure 6.3, that between the cool-flame and the main ignition there exists an 'induction period' or NTC behaviour which corresponds to intermediate temperature zone (900-1100K). The induction period is associated with the competition of the fast chain branching reactions and relatively slower chain propagation reactions (as discussed in Chapter 4). In this period chain propagation reactions dominate, causing the slow-down of n-heptane reactivity, which results in a reduction of the rate of heat release (Refer to Figure 6.5). Therefore, only a gradual accumulation of the radicals' pool and gradual temperature rise occur.

When the temperature has reached a value of around 1100 K, the high temperature chain branching reactions start to dominate again and the main ignition occurs. The main high temperature chain branching reaction, which dominates the further ignition process, is reaction (6.6).

On the other hand, *iso-octane*, a branched-chain paraffin, has a much lower reactivity than n-heptane, and thus needs a higher inlet temperature to start auto-ignition.

Lower reactivity of the *iso-octane* is not only due to a large number of less reactive methyl groups but also from the presence of tertiary and quaternary C atoms in its structure. The homolysis reactions of tertiary and quaternary structures compete with ketohydroperoxide formation contributing to the lower activity of branched-chain paraffins [118]. As a result, virtually all of the isomerization pathways which produce OH radicals at temperatures below 1000K are inhibited, because some or all of the steps require abstraction of primary H atoms with their relatively large energy barriers. Therefore, for iso-octane, the heat release from low temperature ignition (cool flame ignition) is omitted, and thus the much higher inlet temperature is needed for auto-ignition in comparison to n-heptane.

Lower reactivity of iso-octane results in lower amounts of heat release from MI in comparison to n-heptane, as it can be seen in Figure 6.5 and Figure 6.6.

Ethanol as a alcohol type of fuel, is characterised by lower specific energy but higher heat of vaporization than gasoline.

The ignition process in ethanol is very much influenced by the weaker C-C bond in comparison to C-OH bond, with the result that the OH group is not displaced in the initiation step [88]. Therefore, the initiation starts with breaking the C-C bond in the reaction

$$C_2H_5OH + M \Leftrightarrow CH_3 + CH_2OH + M \tag{6.7}$$

Since the activation energy of breaking the C-C bond is slightly higher than that of abstraction of the primary H-atom site in iso-octane, the intake temperature for ethanol is close but slightly higher than that of iso-octane (Refer to Figure 6.2). Ethanol has a slightly higher ON (107) than that of iso-octane. The ignition and heat release rate of ethanol, is also characterised with single-stage only, as can be seen in Figure 6.2 and Figure 6.7.

Methane exhibits certain oxidation characteristics that are different from all other hydrocarbons, as was discussed in Section 4.6. Methane is the most difficult fuel to ignite, and therefore needs the highest intake temperature amongst the fuels investigated. The difficulties in methane ignition is a consequence of a very slow low temperature oxidation, which is governed mainly by reaction (Equation 4.67). This reaction is a termination reaction, which reduces the number of radicals and decreases the temperature in the system and thus leads to inhibition of fuel reactivity. (The overall rate of ignition.) In this way, the required inlet temperature for methane to start the auto-ignition around TDC is 615K, which is the highest amongst the fuels being analysed. Methane, like iso-octane and ethanol, exhibits single-stage ignition and heat release rate, as can be seen in Figure 6.2 and Figure 6.8 respectively.

Figure 6.3 shows the calculated cylinder temperature for analysed fuels. It can be seen that main ignition starts for all fuels when the temperature reaches the value

over 1100K. At this *temperature*, high temperature chain branching sequences takes place, controlled by the single reaction (Equation 6.6). This reaction dominates the further ignition process, and it is essentially *independent* of the type of fuel [20, 109].

This constant value of the temperature of main ignition shows a distinctive feature that the high temperature chain branching reaction (Reaction 6.6) is independent from the type of fuel. However, methane ignites at a slightly higher temperature due to the domination of termination reaction in low temperature chemistry.

6.2.2 Fuel Effect on the Heat Release Rate

In Figure 6.5 and Figure 6.6 the heat release rate curves for *n-heptane* and *iso-octane* fuels are presented, while in Figure 6.7 and Figure 6.8 for *ethanol* and *methane* fuels respectively.

It can be seen that n-heptane exhibits a two-stage heat release behaviour, where the first stage is a result of cool-flame combustion (low temperature oxidation) and the second stage is due to main combustion event (high temperature oxidation). Even though the heat release from cool-flame is modest in comparison to main heat release (Refer to Figure 6.5), it plays an important role in combustion process. The importance, of the first stage (low temperature oxidation period), is that it provides heat release early in the reaction history, so the reactive air-fuel mixture arrives at the main ignition temperature (>1100K) earlier than would have occurred without that early heat release rate [20].

In that way fuels with two-stage ignition process, such as *n-heptane*, exhibit release energy early in the compression stroke, which increases the temperature of the air-fuel mixture and thus a lower intake temperature is needed to start the main combustion process than for fuels with a single stage ignition process (*iso-octane, ethanol* and *methane*).

Also, it can be noticed that n-heptane has the highest heat release rate value, while methane has the lowest. Iso-octane and ethanol have similar values of heat release
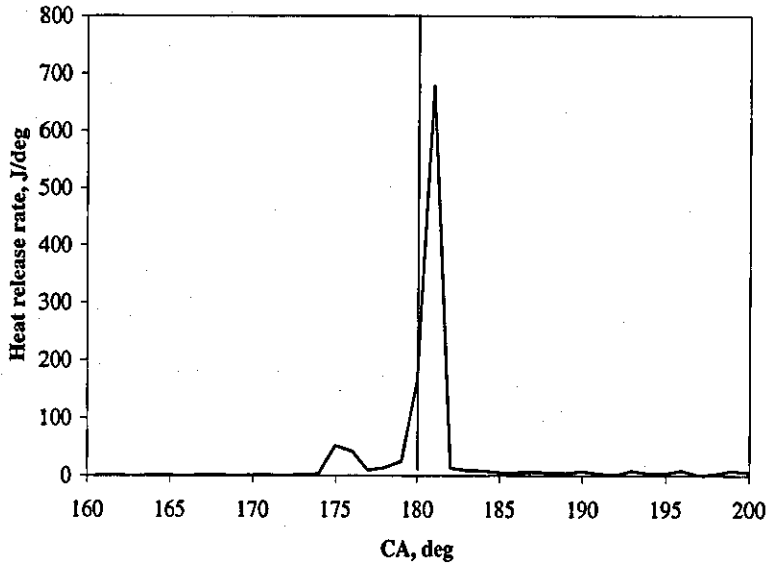
Figure 6.5: Heat release rate curve as a function of crank angle for *n-heptane* fuel.
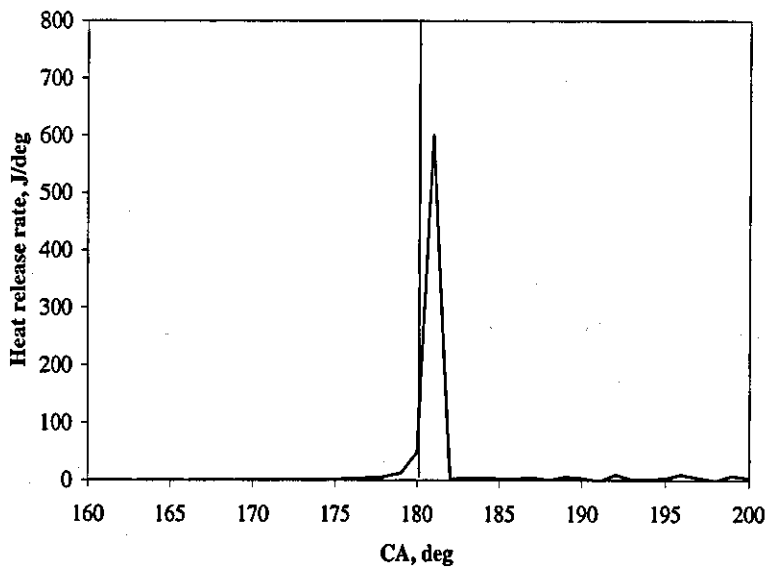
Figure 6.6: Heat release rate curve as a function of crank angle for *iso-octane* fuel.
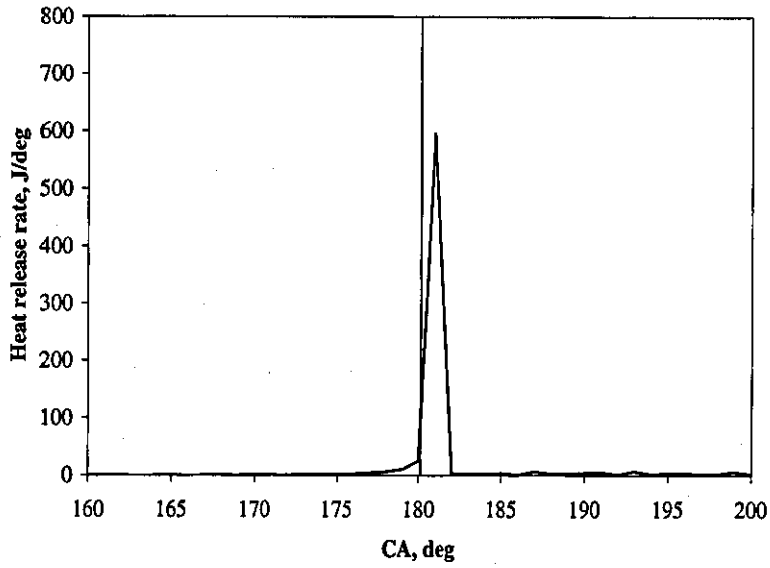
Figure 6.7: Heat release rate curve as a function of crank angle for *ethanol* fuel.
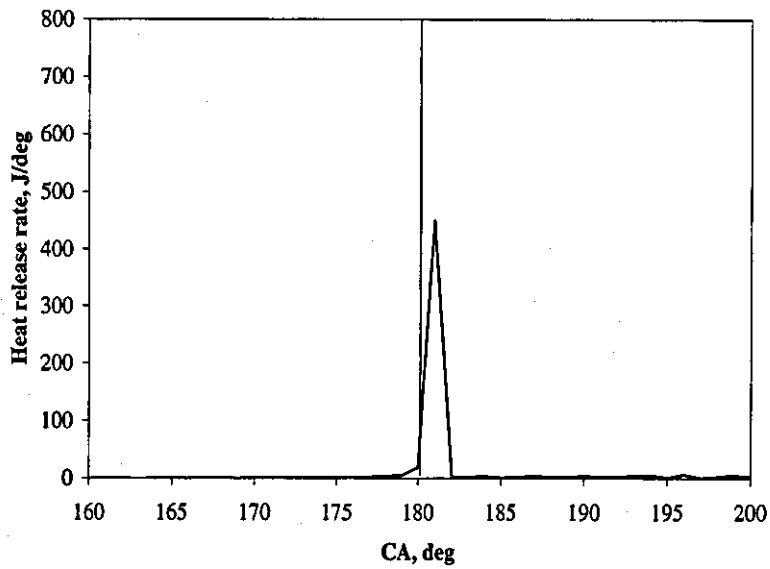
Figure 6.8: Heat release rate curve as a function of crank angle for *methane* fuel.

rate, which are lower in comparison to n-heptane, but considerably higher than that for methane[1].

6.3 Summary of the Effect of Fuel Composition on CAI Combustion

The characteristics of CAI combustion are that homogeneous air-fuel mixture auto-ignites uniformly and simultaneously and it is controlled by chemical kinetic. Auto-ignition in a CAI engine has many characteristics of end gas auto-ignition in spark engines, which is responsible for knock effect.

The onset/timing of auto-ignition and heat release rate are clearly crucial for operation and controlling of a CAI engine. These processes are a function of the complex chemistry, the temperature-pressure history of the charge in the pre-ignition and ignition processes. The chemistry includes both 'low temperature' reactions, with 'cool flame'/'negative temperature coefficient' behaviour, and 'high temperature' chemistry.

In this way the auto-ignition behaviour of fuel in a CAI engine depends largely upon fuel composition, molecular size and structure. *N-heptane* is reactive straight-chain paraffin, which has a low octane number and it is characterised with two-stage ignition, ('cool flame') with NTC behaviour followed by main ignition stage. On the other hand *iso-octane* is a less reactive branched-chain paraffin with a high octane number which undergoes single-stage ignition only. *Ethanol* and *methane* fuels also exhibit single-stage ignition process.

In fuels characterised with single-stage ignition process (and high ON), such as iso-octane, ethanol and methane, little heat is released prior to the main ignition event, which takes place over 1100K . On the other hand, fuels with two-stage ignition process (and low ON-high CN), like n-heptane, significant heat is released from low

---

[1]In a real engine the total in-cylinder mass is reduced when the temperature is increased for a fixed intake pressure. This results that the total heat release rate is reduced for a fixed stoichiometry. However, this effect has been removed from the heat release plots presented here because the heat release rate is normalized by the total mass.

temperature reactions at about 800 K. Although, the amount of liberated energy is too small to be considered ignition, these low temperature reactions quickly bring the air-fuel mixture up to the temperature of 1050-1100 K, a temperature necessary for H_2O_2 decomposition and start of the main ignition. It is this effect that causes CAI combustion to be sensitive to fuel types. Therefore, fuel with a low octane number and two-stage ignition will need a lower intake temperature to start the main ignition in comparison to high-octane fuels with single-stage ignition.

The main ignition starts when the temperature increases above 1100K, then high temperature chain branching sequence (reaction 6.6) takes place and further dominates the remainder of the overall reactions in combustion process-*heat release rate*. This reaction is essentially independent of the fuel type, and for *all hydrocarbon fuels, the main ignition occurs at approximately the same temperature (> 1100K)*.[2]

Finally, it can be concluded that in a CAI engine, the *start of auto-ignition* is identified by the start of hydrogen peroxide decomposition, while the remainder of combustion process by high temperature chain branching reaction (Reaction 6.6). In this way, any variation in any engine parameters that bring a reactive air-fuel mixture earlier to the hydrogen peroxide decomposition temperature (1050-11000K) will advance ignition, and anything that delays reaching that temperature will retard ignition.

The effects of engine parameters on ignition timing of a CAI engine will be presented in the Chapter 7.

---

[2]Methane exhibits a slightly different behaviour to other hydrocarbon fuels due to the domination of termination reactions in the low temperature chemistry and therefore the main ignition starts at a slightly higher temperature.

Chapter 7

Effect of Engine Parameters on CAI Combustion

In practical transport applications, a CAI engine will be the same as SI and CI engines in that there will be frequent changes between operation in idle, acceleration, de-acceleration and steady cruise modes. These changes in operational mode are accomplished by changes in engine power output (load) and speed. In that way it is expected that the CAI engine has to be able to work over a wide range of loads and speeds.

In order to make it possible for a CAI engine to work with a wide range of loads and speeds, the timing of auto-ignition and heat release rate have to be properly phased (controlled). Controlling the operation of a CAI engine over a wide range of speeds and loads is probably the major difficulty facing CAI engines. As CAI combustion is controlled by the chemical kinetics of charge mixture, the ignition is determined by its composition, and its temperature and pressure histories[1], as discussed in Chapter 3 and Chapter 4. Changing the load of a CAI engine requires a change in the fuelling rate, therefore in the charge composition. As a result, the charge temperature has to be adjusted to maintain proper ignition timing and heat release rate.

---

[1]The influence of pressure is smaller in comparison to the influences of charge mixture composition and its temperature history.

Similarly, changes in the engine speed changes the amount of time for the auto-ignition chemistry to occur relative to the piston motion[2]. To compensate for this, the charge temperature has to be adjusted again. In the rapid transient mode, during the engine accelerations and de-accelerations, compensation of load and speed effect becomes very demanding.

To encounter the effect of the engine operational parameters on ignition timing in the CAI engine, various parameters are investigated:

- Inlet mixture temperature

- Compression ratio

- Fuel-air ratio

- Engine speed

The range of fuels used in this investigation is wider in comparison to the range used in Chapter 6. Hence, the followings fuels are analysed:

- n-heptane (n-C_7H_{16}),

- iso-octane (i-C_8H_{18}),

- ethanol (C_2H_5OH) and

- methane (CH_4)

- dimethyl ether ((CH_3)$_2O$)

- methyl butanoate ($C_5H_{10}O_2$)

- methyl formate (CH_3OCHO)

---

[2]The auto-ignition chemistry has a fixed time scale independent on engine speed, but the piston motion becomes faster with an increase in the engine speed. This results in a reduction of the engine cycle duration and therefore in a shorter time base for the auto-ignition chemistry

Dimethyl ether (DME), methyl butanoate (MB) and methyl formate (MF) are diesel-like types of fuel. These fuels are included in the investigation due to increased interests for their use as an alternative fuel in medium and heavy-duty CAI engine applications in lorries and agricultural vehicles.

Dimethyl ether (DME) represents a clean alternative fuel for diesel engine due to its smokeless combustion characteristics and favorable ignition properties (high cetane number CN~70) [58, 119, 120]. Moreover, the non-corrosive nature of DME does not require special materials for the fuel injection equipment. The problem of using DME as a fuel in engines are its high vapour pressure, low viscosity and density, and reduced heat of combustion.

Biodiesel fuels can be derived from vegetable oils and animal fats. These fuels offer benefits in their low sulfur content and possibility to be renewable in comparison to common diesel fuels. Furthermore, biodiesel fuels are attractive because their content is about 10% of oxygen by mass which can provide soot reduction similar to those observed for other oxygenated fuels and additives. For engine applications, biodiesel fuels derived from fatty acid have to be converted into methyl or ethyl esters in order to improve their physical properties such as viscosity, melting and boiling points [121]. Typical biodiesel fuels consist of mixtures of saturated and unsaturated methyl esthers. *Methyl butanoate* (MB) is chosen as a surrogate for heavy bio-diesel fuels, while *methyl formate* (MF) for light bio-diesel fuels.

In choosing the engine parameters and fuels for this research, it is considered that in the current state of technological development of a CAI engine (discussed in Chapter 2), it is not possible to run an engine in CAI combustion mode throughout entire load and speed range. Therefore, it is highly likely that the first step in introducing a CAI engine in practical use will be hybrid SI/CAI and CI/CAI concept as proposed in [10, 25]. In these concepts engines would operate in CAI mode at low power and in SI or CI at high power. The hybrid concept will take advantage of the high efficiency, low NO_x and particulate emissions of CAI engine at low power conditions, while eliminating the power limitations and startability problems of CAI

engine.

In that way it was concluded that n-heptane, *iso-octane, ethanol* and *methane* fuel will be more interesting to investigate in the frame of a future hybrid SI/CAI engine concept. For a future hybrid CI/CAI engine concept, diesel-like types of fuel, *n-heptane, dimethyl ether* and bio-diesel fuels, *methyl butanoate* and *methyl formate* will be investigated.

The SI/CAI concept has to be able to run in near stoichiometric SI operation at high loads to maintain maximum power and torque output of a conventional 4-stroke gasoline engine, as well as other conditions under which CAI cannot be achieved. This dictates that the engine's compression ratio should be kept the same as conventional SI spark engines in order to avoid any torque limitation by knocking combustion under full-load operation. The use of a stoichiometric mixture permits the use of a standard three-way catalyst to reduce any exhaust emissions generated from part-load CAI combustion as well as those from high-load SI combustion operation.

The CI/CAI concept is expected to run on a lean mixture and to use a higher compression ratio than in SI/CAI concept (similar to those in existing CI engines). Fuel supply systems in CI/CAI concept will be the same as the existing one in the direct injection CI engine. Therefore, no additional costs will be added.

The engine operational conditions, for both concepts are those summarised in Table 7.1.

The chemical kinetic mechanisms employed for n-heptane, iso-octane, ethanol and dimethyl ether (DME) are those developed by Lawrence Livermore National Laboratory [89, 90], while for methane is GRI-Mech 3.0 mechanism [87] and for methyl butanoate (MB) and methyl formate (MF) mechanism are those developed by Fisher et al [121]. The mechanism for *n-heptane* consists of 565 species and 2540 reactions, *iso-octane* 875 species and 3606 reactions, *ethanol* 57 species and 383 reaction and for *dimethyl ether* (DME) 78 species and 336 reactions.

Table 7.1: Engine operational conditions for the analysis of the engine parameters effects on the CAI combustion.

Bore	80.5 mm
Stroke	88.2 mm
Swept volume	450 cm^3
Compression Ratio	Varied
Speed	Varied
Equivalence fuel-air ratio	Varied
Intake Temperature	Varied
Inlet Pressure	Naturally Aspirated
Cylinder wall temperature	500K
Fuel	n-heptane,iso-octane,ethanol, methane dimethyl ether (DME),methyl butanoate (MB) and methyl formate (MF)

The mechanism for *methane* consists of 53 species and 325 reactions, *methyl butanoate* (MB) 264 species and 1219 reactions and for *methyl formate* (MF) 193 species, 925 reactions.

All these mechanisms have been validated through extensive comparisons with experimental data obtained from the measurement conducted in flow reactors, shock tubes and rapid compression machines [72, 87, 89, 90, 106, 121].

Due to a large number of analysed fuels in different engine concepts, discussion of the engine parameters effect on ignition timing will be carried out separately for each engine concepts and associated fuels:

1. *SI/CAI concept fuels*:n-heptane, iso-octane, ethanol and methane.

2. *CI/CAI concept fuels*:n-heptane, dimethyl ether (DME), methyl butanoate (MB) and methyl formate (MF).

The effect of each parameter on ignition timing was analysed by means of varying that parameter while keeping other parameters unchanged. For example, if compression ratio effect was analysed, than compression ratio is varied while other parameters remain unchanged. The results obtained are presented in diagrams where

the x-axis assigns the independent variable (engine parameter) and the y-axis the dependent variable (ignition timing).

7.1 Effect of Inlet Temperature

As discussed in Chapter 2, a common approach in many experimental studies has been to use high inlet temperature to initiate combustion in a CAI engine. To assess this effect, the inlet temperatures is varied while other engine parameters are kept unchanged as follows:

- Engine speed–2000 rpm

- Compression ratio

  10.5 for SI/CAI fuels,

  14 for CI/CAI fuels.

- Fuel-air equivalence ratio

  Stoichiometric ($\phi = 1.0$) for SI/CAI fuels,

  Lean ($\phi = 0.5$) for CI/CAI fuels.

- Inlet pressure–naturally aspirated for both concepts, SI/CAI and CI/CAI.

Reasons for using different values of compression and fuel-air ratios in SI/CAI and CI/CAI concepts were discussed at the beginning of this Chapter.

Figure 7.1 shows the variation of ignition timing while varying the inlet temperature for *SI/CAI fuels*, while Figure 7.2 for *CI/CAI fuels*. It can be seen that the higher inlet temperature advances the ignition timing for all fuels examined, due to increased reaction rates (Refer to Chapter 3). Higher temperatures boost kinetic reactivity, the heat release grows and auto-ignition is accelerated. On the other hand, decrease of inlet temperature delays ignition and it can be noticed that for each of the analysed fuels there exists a minimum inlet temperature, below which ignition

cannot be initiated. This temperature represents the ignitability limit for a given fuel. It is also interesting to note in Figure 7.3, where the ignition of n-heptane
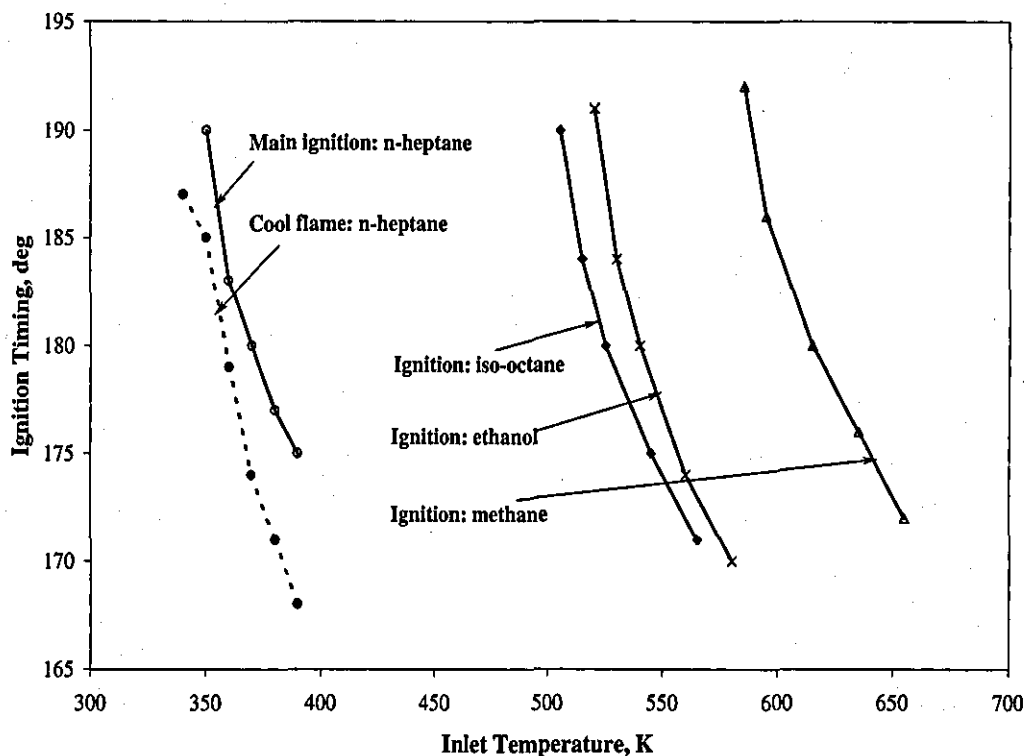
Figure 7.1: Effect of inlet temperature on ignition timing for n-heptane, iso-octane, ethanol and methane fuel in the SI/CAI concept. Symbol (○) represents *n-heptane* main ignition, (●) *n-heptane* cool flame ignition, (◇) *iso-octane*,(×) *ethanol* and (△) *methane* main ignition. Solid line corresponds to the main ignition while dashed line to the cool flame ignition.

and DME are separately shown, that the induction period for n-heptane and DME becomes longer with inlet temperature increase.

It is likely that this is a consequence of several effects that take place simultaneously:

- With higher inlet temperature the magnitude of energy release from cool flame (CF) ignition decreases due to a reduction in the mass trapped in the cylinder. Reduced energy release from cool flame ignition therefore results in a longer duration for the induction period [122].

Figure 7.2: Effect of inlet temperature on ignition timing for n-heptane, DME, MB and MF fuel in the CI/CAI concept. Symbol (○) represents *n-heptane* main ignition, (•) *n-heptane* cool flame ignition, (+) and solid line *DME* main ignition , (+) and dashed line *DME* cool flame ignition, (△) MB and (◇) MF. Solid line corresponds to the main ignition while dashed line to the cool flame ignition.

- With higher inlet temperature the in-cylinder mixture reaches the cool flame ignition temperature at an earlier crank angle, and thus at lower values of cylinder pressure. The chemical kinetics, responsible for NTC behaviour (in induction period) is strongly pressure dependent. Therefore, the occurrence of the CF ignition earlier in the compression stroke results in a lower overall energy release during induction period, due to lower cylinder pressure values, and consequently in longer induction period.

- With higher inlet temperatures, the mixture reaches critical temperature for the start of cool flame ignition at earlier crank angles (Refer to Figure 7.2).
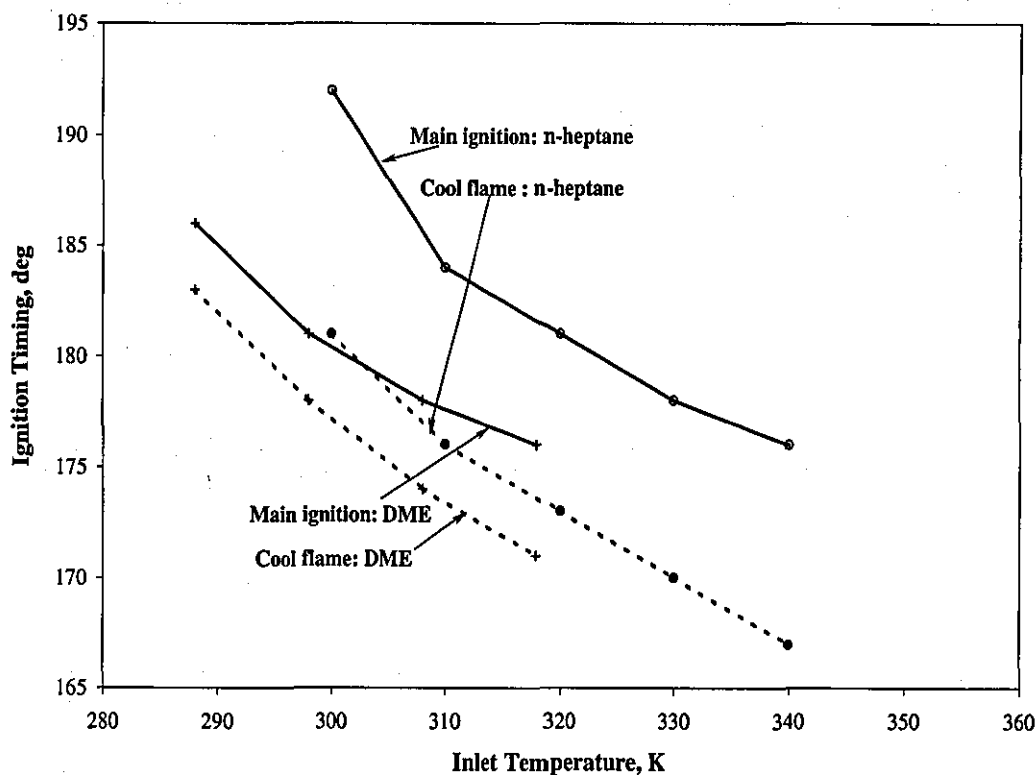
Figure 7.3: Effect of inlet temperature on ignition timing for n-heptane and DME in the CI/CAI concept. Symbol (o) represents *n-heptane* main ignition, (•) *n-heptane* cool flame ignition, (+) and solid line *DME* main ignition , (+) and dashed line *DME* cool flame ignition. Solid line corresponds to the main ignition while dashed line to the cool flame ignition.

The magnitude of the cool flame energy release decreases with higher inlet temperatures due to a reduction in trapped mass in the cylinder. On the other hand, the main ignition is a function of the accumulated thermal energy during the induction period. If the CF ignition starts early, the contribution from piston compression is less, and therefore a longer time is required to accumulate sufficient thermal energy to initiate the main combustion.

It is important to emphasis that the increased inlet temperature will negatively affect the indicated thermal efficiency, volumetric efficiency and trapped mass. An increase in the inlet temperature reduces trapped mass and volumetric efficiency,

which in turn adversely affects torque and power output [123]. Also, advanced ignition increases compression effort and combined with reduced volumetric efficiency leads to the reduction in net indicated efficiency.

7.2   Effect of Compression Ratio

Another way to increase the in-cylinder air-fuel mixture temperature to reach auto-ignition value is to increase the compression ratio.

A higher compression ratio increases the temperature of the in-cylinder charge during the compression process and therefore advances the CF and main ignition (MI) timings. This is a result of more elevated temperature histories earlier in the cycle which enhances chemical reaction rates and therefore the charge reaches the main ignition temperature earlier. Figure 7.4 shows the influence of compression ratio on ignition timing for *SI/CAI fuels*, while Figure 7.5 for *CI/CAI fuels*. It can be seen that a higher compression ratio advances both the cool flame ignition and the main ignition.

It can be noticed in Figure 7.5 that for fuels with two-stage ignition behaviour, n-heptane and DME, the induction period becomes shorter as the compression ratio increases, which is the result of the elevated charge temperature.

A negative effect of the higher compression ratios is the higher values of peak cylinder pressure. Figure 7.6 shows peak cylinder pressure for various compression ratios for n-heptane fuel, while Figure 7.7 for MF fuel[3].

Early start of the CF and MI timing for n-heptane and MI timing for methyl formate (MF), relative to TDC, causes elevated pressures during the compression stroke. This increases the compression work, which in turn reduces the net piston work, and leads to a reduction in net efficiency.

---

[3]The effect of compression ratio on the peak cylinder pressure for other investigated fuels (in both concepts), is the same as for these two fuels and therefore an additional figures are not presented.

Figure 7.4: Effect of compression ratio on ignition timing for n-heptane, iso-octane, ethanol and methane fuel in the SI/CAI concept. Symbol (○) represents *n-heptane* main ignition, (●) *n-heptane* cool flame ignition, (◇) *iso-octane*, (×) *ethanol* and (△) *methane* main ignition.
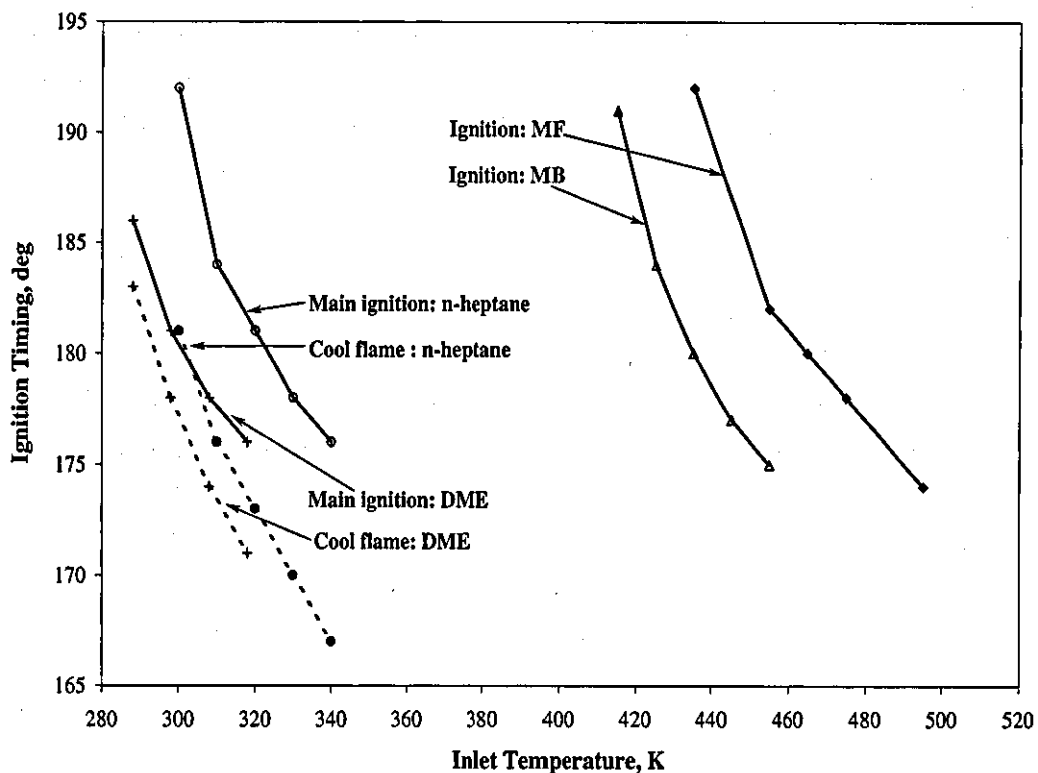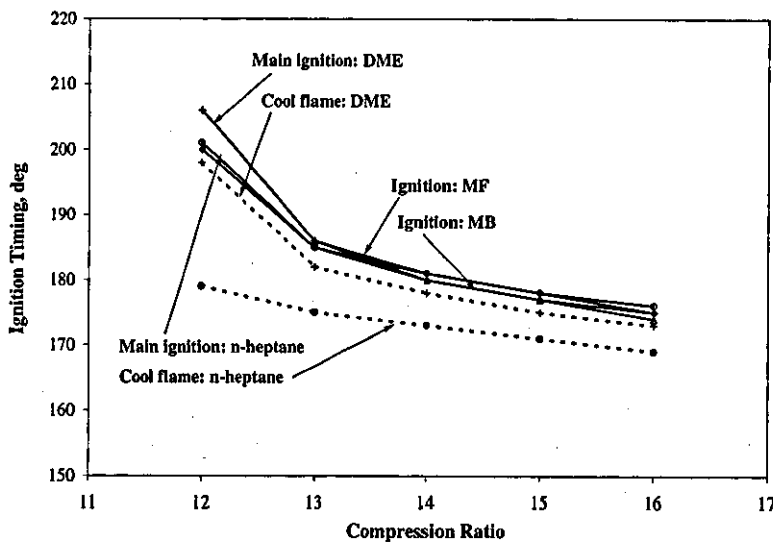

Figure 7.5: Effect of compression ratio on ignition timing for n-heptane, DME, MB and MF fuel in the CI/CAI concept. Symbol (○) represents *n-heptane* main ignition, (●) *n-heptane* cool flame ignition, (+) and solid line *DME* main ignition , (+) and dashed line *DME* cool flame ignition, (△) *MB* and (◇) *MF* main ignition.
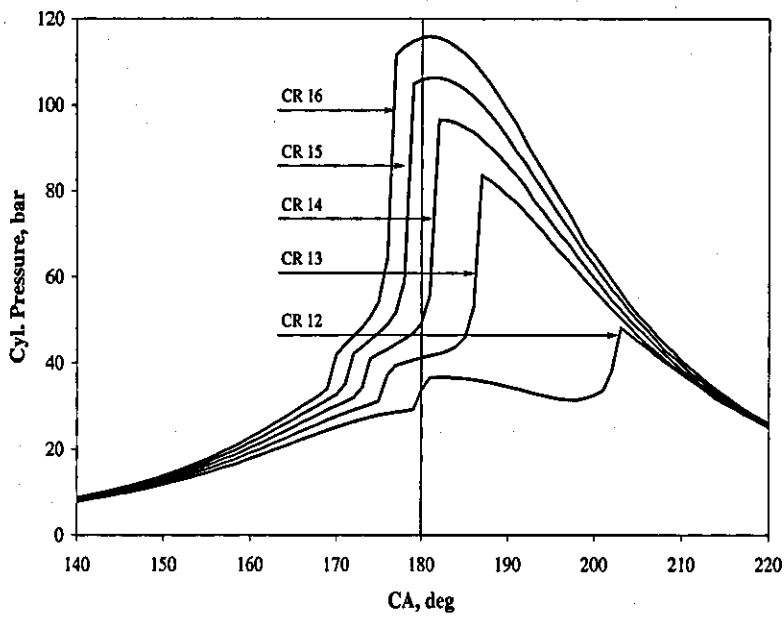
Figure 7.6: Effect of compression ratio on cylinder pressure for *n-heptane* fuel in the CI/CAI concept.
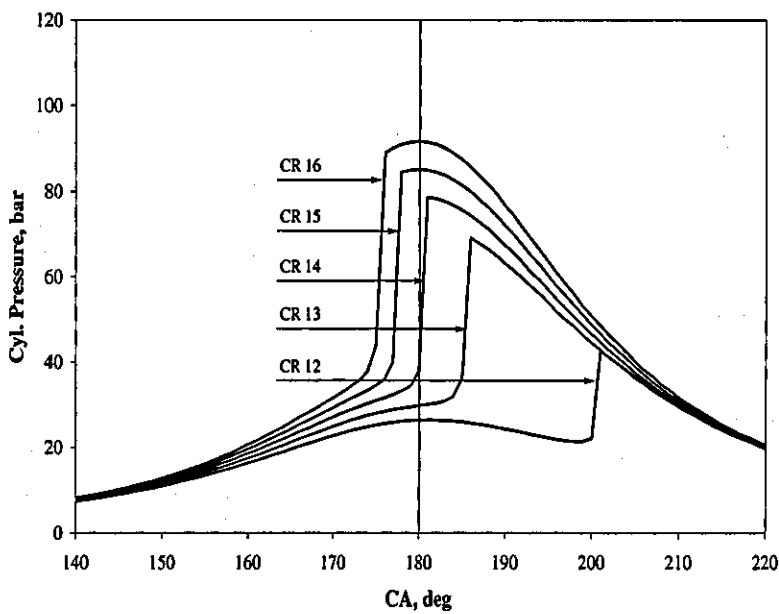
Figure 7.7: Effect of compression ratio on cylinder pressure for *MF* fuel in the CI/CAI concept.

7.3 Effect of Fuel-Air Equivalence Ratio

Load variation in a CAI engine is studied by varying the equivalence fuel-air ratio (ϕ). Changing the load of a CAI engine requires a change in the fuelling rate and thus in the charge composition. Due to the auto-ignition of the fuel by piston compression work no centralised ignition source is required and therefore considerably fuel lean mixtures can be employed in a CAI engine ($\phi \approx 0.2$) [22] .

Figure 7.8 shows the influence of different (ϕ) on the ignition timing for *CI/CAI fuels*, while Figure 7.9 for *SI/CAI fuels*. Inlet temperatures and other engine parameters remain unchanged from the values stated in Section 7.1.

Figure 7.8: Effect of equivalence fuel-air ratio on ignition timing for n-heptane, DME, MB and MF fuel in the CI/CAI concept. Symbol (o) represents *n-heptane* main ignition, (•) *n-heptane* cool flame ignition, (+) and solid line *DME* main ignition, (+) and dashed line *DME* cool flame ignition, ($\triangle$) MB and ($\diamond$) MF. Solid line corresponds to the main ignition while dashed line to the cool flame ignition.
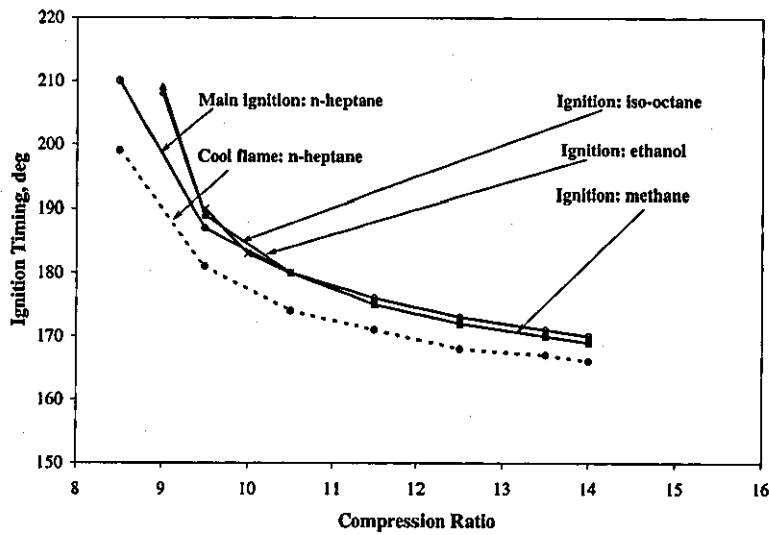
Figure 7.9: Effect of equivalence fuel-air ratio on ignition timing for n-heptane, iso-octane, ethanol and methane fuel in the SI/CAI concept. Symbol (○) represents *n-heptane* main ignition, (●) *n-heptane* cool flame ignition, (◇) *iso-octane,* (×) *ethanol* and (△) *methane* main ignition. Solid line corresponds to the main ignition while dashed line to the cool flame ignition.

It can be noted that (ϕ) has rather different effects on the ignition timing of analysed fuels which depends on fuel auto-ignition behaviour. For fuels with two-stage ignition, such as *n-heptane* and *DME*, changing (ϕ) has an impact on the onset of cool flame and main ignition, magnitude of the initial temperature/pressure increase, and duration of the induction time (Refer to Fig. 7.8). On the other hand, for fuels with single-stage ignition, such as *iso-octane, ethanol, methane, MB* and *MF*, only the onset of main ignition is affected with ϕ (Refer to Figure 7.9 and Figure 7.8). In further discussions the effect of (ϕ) on ignition timing of fuels with two-stage will be discussed, followed by comments on the effect on fuels with single-stage ignition process.

Effect of Fuel-Air Equivalence Ratio (ϕ) on Fuels with Two-stage Ignition Behaviour In order to represent variations in all phases of two-stage ignition process with changes in ϕ, the in-cylinder mixture temperature histories as a function of crank angle degree for different values of ϕ are shown for n-heptane fuel in Figure 7.10 and for DME fuel in Figure 7.11. As (ϕ) increases, the ratio of specific
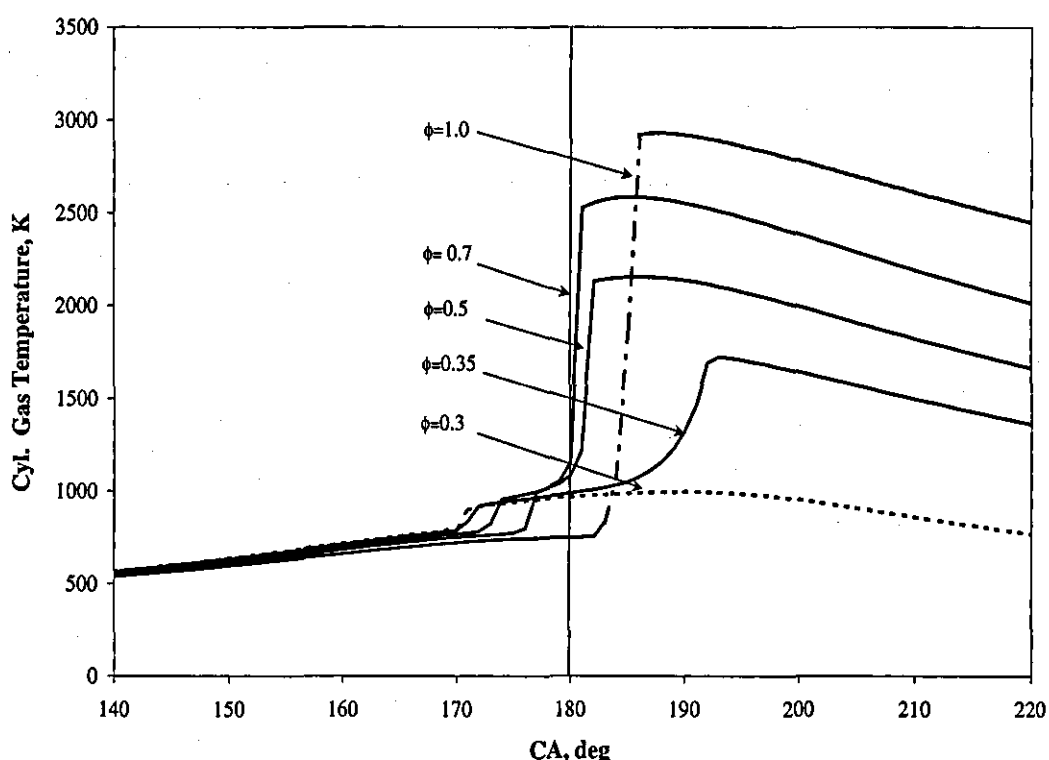
Figure 7.10: In-Cylinder gas temperature as a function of crank angle and ϕ for *n-heptane* fuel in the CI/CAI concept.

heats (γ) for the mixture decreases, reducing the amount of compression heat of the mixture. Therefore, a near stoichiometric mixture has to be compressed further than a lean mixture in order to attain a temperature sufficient to initiate the CF ignition. Increases in (ϕ), from 0.3 to 1.0 for *n-heptane*, results in a delay of the CF timing of approximately 12 crank angle degrees (CAD) , while for *DME*, increasing (ϕ) from 0.25 to 0.95, delays CF for approximately 27 CAD, as can be noted in Figure 7.12. It is obvious that the CF ignition timing of DME is affected more with
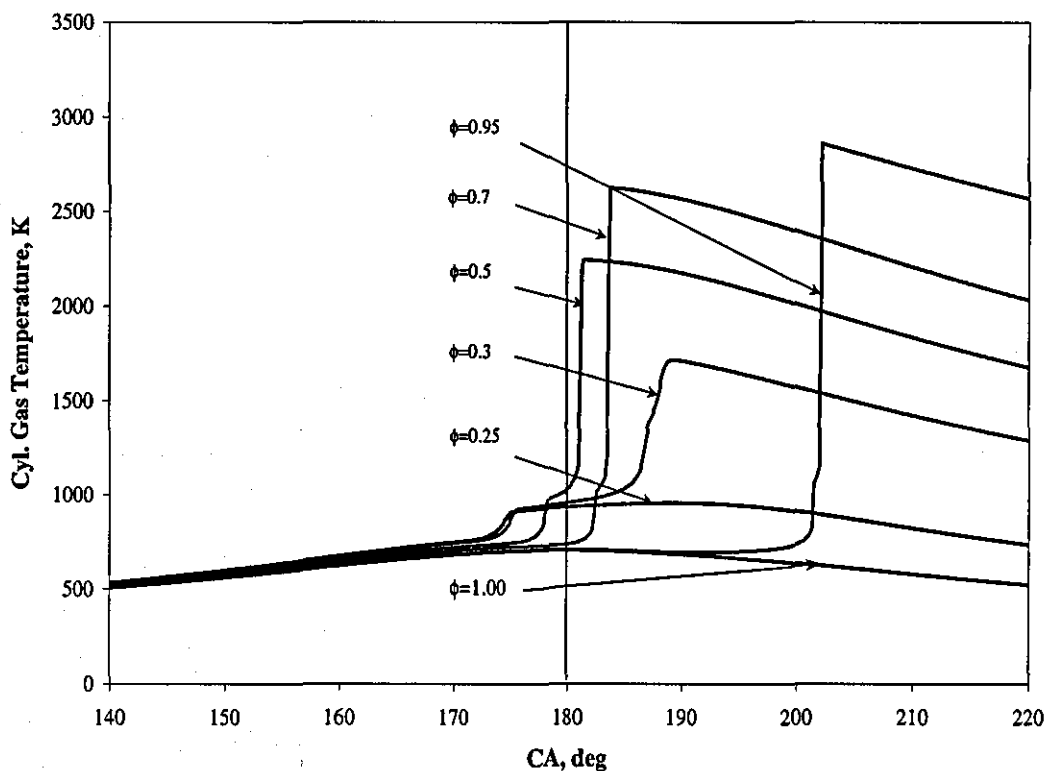
Figure 7.11: In-Cylinder gas temperature as a function of crank angle and ϕ for *DME* fuel in the CI/CAI concept.

a change in equivalence ratio. This is due to the nature of the low temperature chain branching processes, responsible for the cool flame ignition in DME and n-heptane. The peroxy radicals' chemistry controls the low temperature chain branching process in DME, while C_7H_{15} radicals' chemistry in the n-heptane. The production of peroxy radicals is more sensitive to the changes in temperature and fuel concentration than the production of C_7H_{15} radicals. Therefore, a reduced temperature rise and increased fuel concentrations will have more pronounced influence on cool-flame ignition in DME.

The magnitude of the cool-flame ignition temperature rise depends on (ϕ). Excess air acts as a diluent which absorbs heat and reducing the temperature rise from cool flame reactions as the mixture becomes leaner (ϕ decreases). Therefore, in order
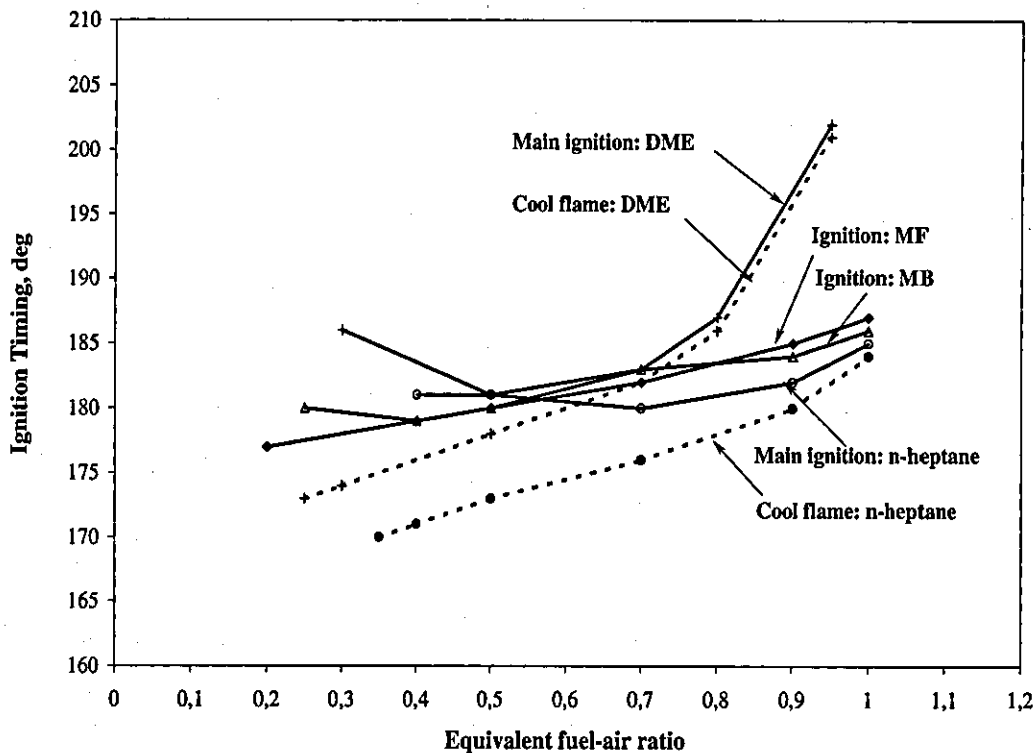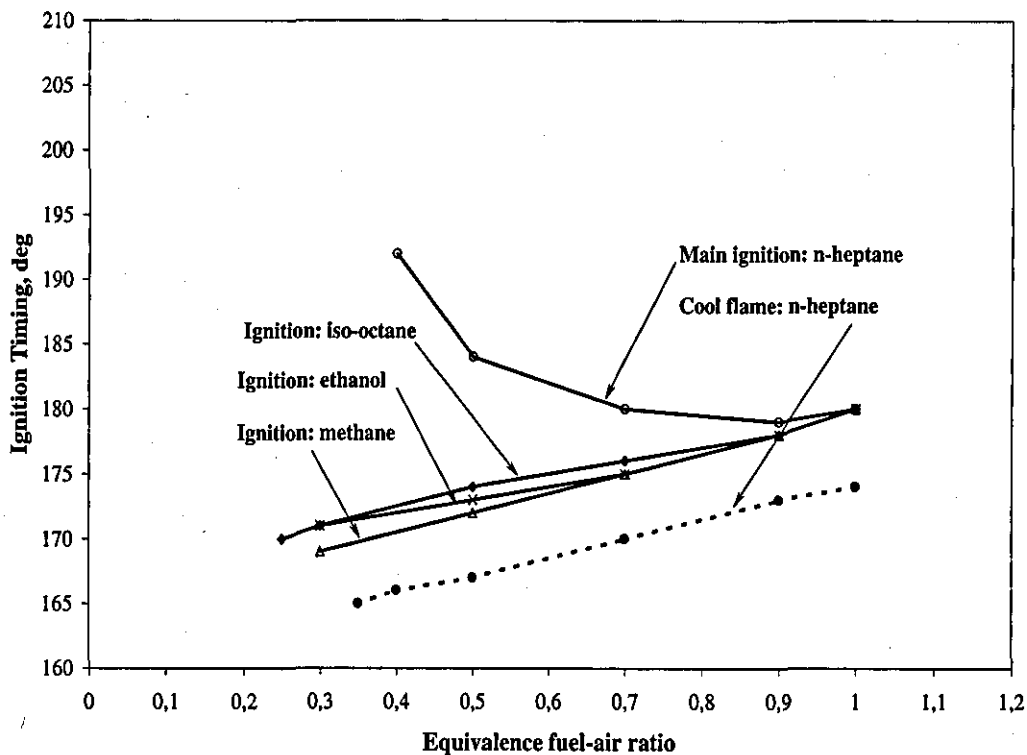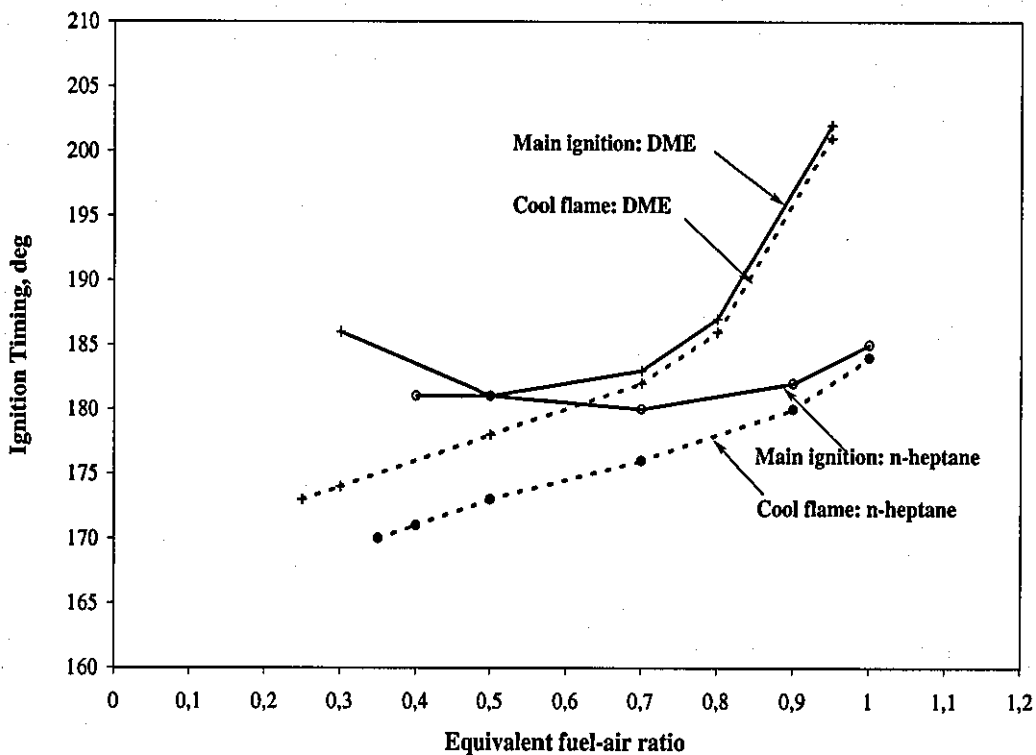
Figure 7.12: Effect of equivalence fuel-air ratio on ignition timing for *n-heptane* and *DME* fuel in the CI/CAI concept. Symbol (o) corresponds to *n-heptane*, (+) to *DME*. Solid line represents main ignition while dashed cool flame ignition.

to reach the temperature of MI stage (1100K), more heating is required during the induction period for leaner mixtures. During this period, heat is slowly generated by the chemical reactions, and the temperature is further raised by compression (prior to TDC). The net result is an increase in the induction period, as the mixture becomes leaner.

Therefore, it can be said that, the overall ignition timing of n-heptane and DME is affected by the (ϕ), throug two competing effects:

- The strength of the cool flame ignition reactions–*heat released by low temperature oxidation.*

- The amount of compression heating due to the changes in the mixture specific

heat (γ)–*heat released by piston compression work.*

The effect of ϕ on ignition timing of n-heptane fuel in the SI/CAI concept is shown in Figure 7.9. It can be noted that the auto-ignition behaviour with changes in ϕ is the same as previously discussed for the n-heptane behaviour in the CI/CAI concept. The CF ignition is less affected than the main ignition, which depends on the induction period and thus is a function of two competing effects: the heat release from cool flame ignition and the heat released from the piston compression work.

The main ignition timing curves, presented in Figure 7.8 and Figure 7.9, look different, which is due to the different basic ϕ used in CI/CAI and SI/CAI concept. In CI/CAI concept basic ϕ=0.5 (lean mixture), while in SI/CAI concept basic ϕ=1 (stoichiometric).

As shown in Figure 7.10 and Figure 7.11, the earliest CF ignition occurs for the (ϕ) 0.3 for n-heptane and 0.25 for DME, but the associated temperature rise is not sufficient to lead to main ignition. When (ϕ) is increased to 0.35 for n-heptane and to 0.3 for DME, the MI occurs, although after TDC. As (ϕ) continues to increase, the CF ignition occurs later, but the induction period becomes shorter. The result is that MI occurs at the earliest time for (ϕ) equal to 0.7 for n-heptane. However, MI becomes retarded again at higher equivalence ratios. The onset of main ignition for DME fuel exhibits similar behaviour as that for n-heptane fuel. At first it advances as (ϕ) increases, but later, for higher (ϕ) it retards again. Additionally, it must be noted that DME neither exhibits cool flame nor main ignition for the (ϕ) equal to 1 (stoichiometric mixture). This is highly likely since the inlet temperature is below the value necessary to initiate CF ignition event.

It can be noted that the applicable range for n-heptane is extended towards higher (ϕ) values than DME, while DME exhibited lower flammability limit than n-heptane.

Effect of Fuel-Air Equivalence Ratio (ϕ) on Fuels with Single-stage Ignition Behaviour In the case of *iso-octane, ethanol, methane, MB* and *MF*, fuels with single-stage ignition behaviour, the ignition timing is also affected with (ϕ), as can be seen in Figure 7.9 and Figure 7.8. Due to the fact that their ignition is characterised by a single stage process, ignition timing is mainly affected by the changes in heat capacity and the proportional changes in compression temperature. Therefore, the ignition time becomes delayed as ϕ increases.

For *SI/CAI fuels* with single-stage ignition, iso-octane, ethanol and methane it can be noticed from Figure 7.9, that the ignition timing is almost a linear function of ϕ. Among these fuels it appears that methane is the most sensitive to changes in ϕ, while iso-octane and ethanol exhibits similar and lower sensitivity than methane. Increasing the values of ϕ from 0.3 to 1 results in an ignition delay of approximately 13 CA degrees for methane and 9 CA degrees for iso-octane and ethanol. The main ignition timing of n-heptane fuel in SI/CAI concept, is not a linear function of ϕ, while the CF ignition timing shows linear dependence. Increasing the values of ϕ from 0.4 to 1 results in the main ignition delay of approximately 12 CA degrees for n-heptane fuels.

It can be noticed that iso-octane has the lowest flammability limit amongst SI/CAI fuels. Iso-octane can ignite and sustain complete combustion for $\phi=0.25$, while methane and ethanol cannot be ignited below $\phi=0.3$. N-heptane fuel has the worst flammability limit in comparison to other fuels. It cannot be ignited and sustain complete combustion below $\phi=0.4$.

In the CI/CAI concept, increases in ϕ, from 0.2 to 0.5 has virtually no effect on the ignition timing of MB fuel (Refer to Figure 7.8). When the higher equivalence ratio is employed (> 0.5), the ignition becomes delayed. Therefore, for the MB fuel increasing in ϕ from 0.2 to 1 results in an ignition delay of approximately 7 CA degrees.

The ignition timing for MF fuel is slightly more affected with the changes in equivalence ratio in comparison to MB fuel, resulting in delays of 10 CA degrees over the

range of ϕ from 0.15 to 1 as can be seen in Figure 7.8.

In can be noticed from Figure 7.8, that MB and MF fuels have lower flammability limits in comparison to n-heptane and DME fuel, since they can sustain complete combustion for ϕ lower than 0.3. Alongside this, the changes in ignition timing for MB and MF fuels over the applicable ϕ range are much lower (7 CA degrees and 10 CA degrees, respectively) than that for n-heptane and DME fuels. Moreover, MB and MF can ignite even for lower equivalence ratio up to $\phi=0.05$ (not shown), but this leads to incomplete or partial combustion.

A commercial CAI engine, either for SI/CAI concept or CI/CAI concept, would need to operate over a range of equivalence ratios from 0.1 or less (idle) to about 1. The competing factors presented in the two stage-ignition processes of *n-heptane* and *DME*, indicate that controlling the ignition timing with changes in fuel loading (ϕ) will be more difficult in these fuels than in the *iso-octane, ethanol* and *methane* fuels or *MB and MF* fuels. Also, a significant increase in the cylinder temperature would be required to maintain combustion at low loads ($\phi < 0.3$) for the *n-heptane* and *DME* fuels.

7.4 Effect of Engine Speed

In operation a CAI engine will face frequent de-acceleration and acceleration. Hence, a change of speed. Changing of the engine speed changes the amount of time for the auto-ignition chemistry to occur relative to the piston motion.

The chemical reaction rates are sufficiently slow (relative to the engine speed), causing all analysed fuels ignition timings to be delayed with the increase in engine speed. The ignition is retarded with respect to crank angle degree[4]. Figure 7.13 shows the influence of engine speed on ignition timings for *SI/CAI fuels*, while Figure 7.14 for *CI/CAI fuels*.

---

[4]The auto-ignition chemistry has a fixed time scale independent on engine speed, but the piston motion becomes faster with an increase in the engine speed, which in turn reduces the engine cycle duration and therefore a time base for the auto-ignition chemistry
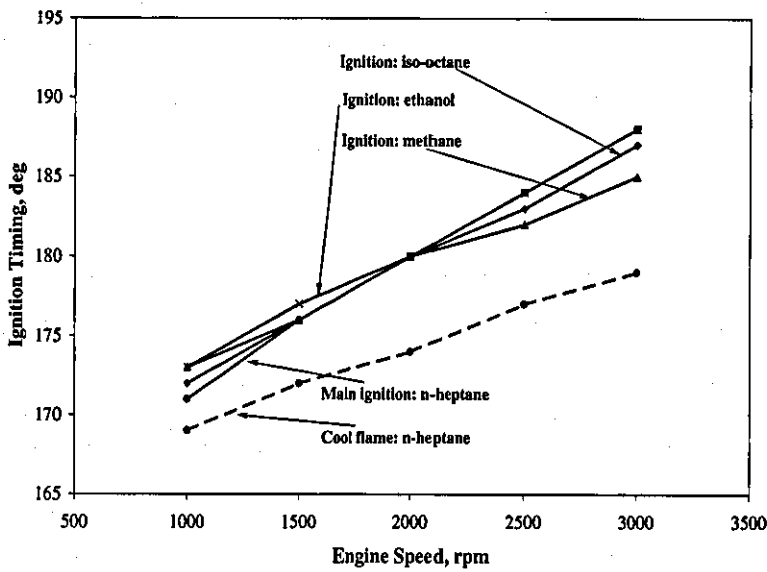
Figure 7.13: Effect of engine speed on ignition timing for n-heptane, iso-octane, ethanol and methane fuel in the SI/CAI concept. Symbol (○) represents *n-heptane* main ignition, (●) *n-heptane* cool flame ignition, (◇) *iso-octane,*(×) *ethanol* and (△) *methane* main ignition.
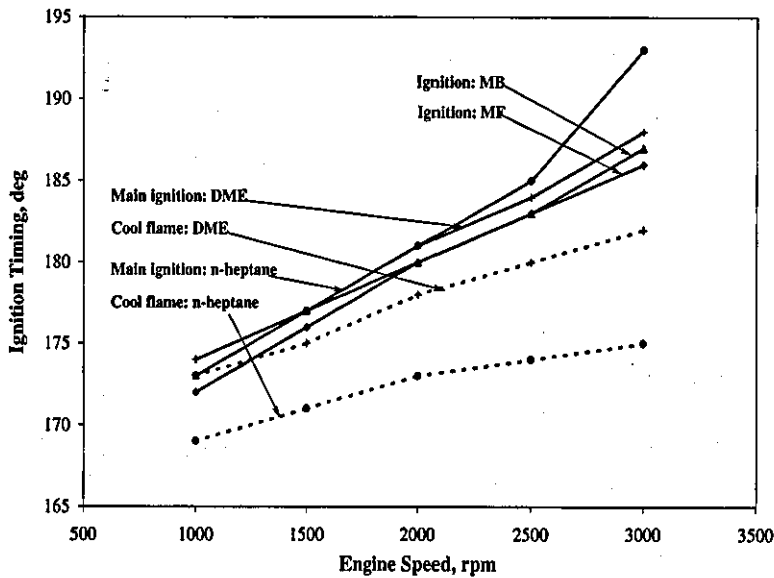
Figure 7.14: Effect of engine speed on ignition timing for n-heptane, DME, MB and MF fuel in the CI/CAI concept. Symbol (○) represents *n-heptane* main ignition, (●) *n-heptane* cool flame ignition, (+) and solid line *DME* main ignition , (+) and dashed line *DME* cool flame ignition, (△) MB and (◇) MF.

It can be seen that the engine speed has a rather different effect on ignition for fuels with a two-stage ignition behaviour, than it has on fuels with single-stage ignition behaviour. Similar to equivalence fuel-air ratio effects (Section 7.3), the discussion of engine speed effect (on ignition timing for examined fuels) will be discussed separately. First for fuels with two-stage ignition behaviour, and secondly for fuels with single-stage ignition behaviour.

Effect of Engine Speed on Fuels with Two-stage Ignition Behaviour The engine speed effect on the ignition timings of n-heptane and DME fuels in CI/CAI concept is shown separately in Figure 7.15. It can be seen, that as the engine speed increases, the CF ignition occurs at later crank angles (but earlier in real time). The induction time is also longer as speed increases, and thus MI timing is
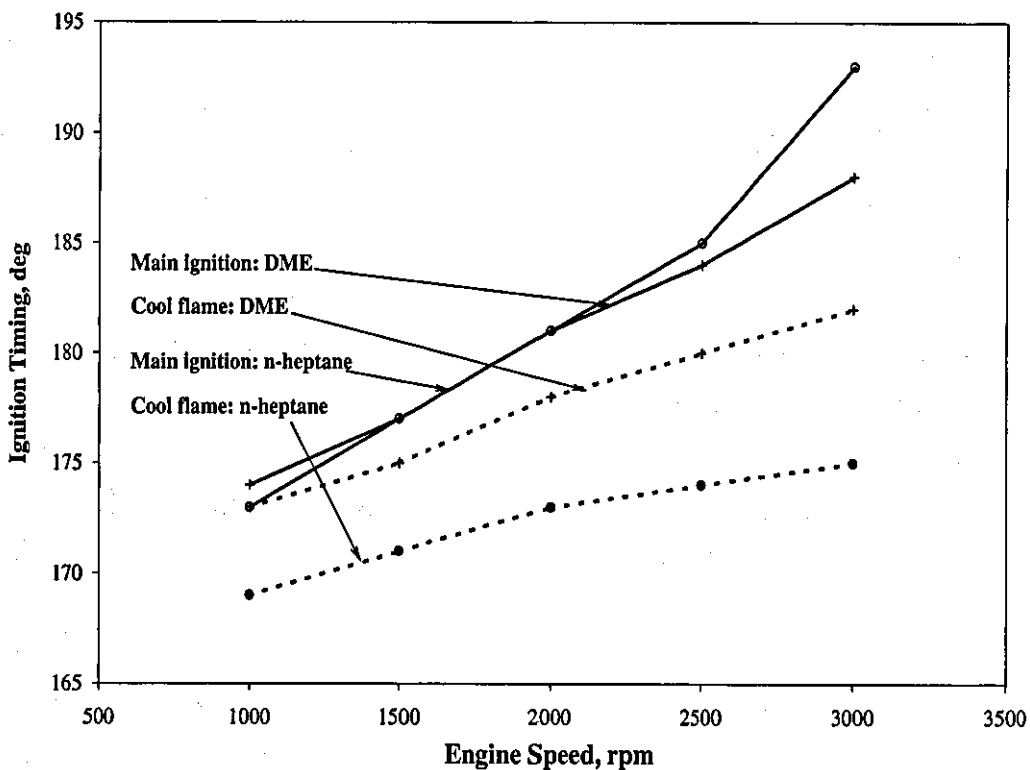
Figure 7.15: Effect of equivalence fuel-air ratio on ignition timing for n-heptane and DME fuel in the CI/CAI concept. Solid line represents *n-heptane*, dashed *DME*.

further retarded. If ignition occurs before TDC, the charge temperature rise from compression compensates this effect by reducing the induction period. However, for the ignition after TDC, the induction period increases since expansion slows down the temperature rise. For the conditions at this simulation, the difference in ignition timing, for the engine speed range from 1000 to 3000 rpm, is 21 CA degrees for *n-heptane* and 13 CA degrees for *DME.*

The effect of engine speed on ignition timing of *n-heptane* fuel in a SI/CAI concept is shown in Figure 7.13. It can be noted that n-heptane auto-ignition behaviour with changes in engine speed follow the same trend as n-heptane behaviour in a CI/CAI concept. The CF ignition, induction period and main ignition are delayed as engine speed increases.

Effect of Engine Speed on Fuels with Single-stage Ignition Behaviour
The dependence of ignition on engine speed for *iso-octane, ethanol* and *methane* fuels is presented in Figure 7.13, and for *MB* and *MF* fuels in Figure 7.14.

The trend is similar to that for n-heptane and DME, but with less variation in ignition timing. The reason for this is the nature of the chemistry which leads to single-stage ignition of these fuels. This chemistry proceeds faster once the temperature reaches the value of high temperature chain branching reactions. Then the main high temperature chain branching reaction (Equation 4.22), (which is essentially independent of the types of fuel), takes over control of the further ignition process. Therefore, the ignition in iso-octane, ethanol, methane, MB and MF fuels is not affected with the changes in the cool-flame stage. As a result, the differences in ignition timings for these fuels over the examined range of engine speed are less than that for n-heptane fuel.

In a SI/CAI concept the delay in ignition timing over the range of engine speed from 1000 to 3000 rpm, is approximately 16 CA degrees for n-heptane, 14 CA degrees for iso-octane, 13 CA degrees for ethanol and 11 for methane fuel. Based on this, it appears that methane is the least sensitive on changes in engine speed, followed

by iso-octane and ethanol, which have a similar sensitivity, while n-heptane has the highest sensitivity.

In a CI/CAI concept DME fuel exhibits the lowest variation of ignition timings with changes in engine speed due to its fast peroxy chemistry as discussed in Section 7.3, followed by MB and MF fuels. The changes in ignition timings for MB and MF fuels, over the engine speed range from 1000 to 3000 rpm, are 14 and 16 CA degrees, respectively (Refer to Figure 7.14). As in the SI/CAI concept, n-heptane has the highest variations (sensitivity) in ignition timing with changes in engine speed.

Although fuels with single stage ignition process in both engine concepts, have less variation in ignition timing with changes in engine speed than n-heptane has, some adjustment is required for each of the fuels to maintain the optimum ignition timing. This could be accomplished by adjusting the operational parameters such as intake temperature and pressure or compression ratio. In a practical case, intake temperature could be controlled by exhaust gas recirculation, which will be explained in the Chapter 8.

7.5   Summary of Engine Parameters Effects on CAI Combustion

From the analysis performed on the effects of engine parameters on CAI combustion the following can be highlighted:

- *Inlet temperature* has the greatest influence on ignition timing of CAI combustion. Small changes in inlet temperature (10K) have appreciable impact on ignition timing. A higher intake temperature promotes chemical reaction rates and thus advances ignition timing and vice versa. For each of the fuels analysed, under each examined set of operational conditions, there exists a minimum temperature below which ignition cannot be initiated.

- *Compression ratio* has a similar effect on ignition timing as inlet temperature. Higher compression increases the charge temperature and thus advances

the ignition timing. On the other hand, lower compression ratio retards ignition timing. There exists a minimum compression ratio under given engine operational parameters below which ignition cannot be initiated.

- *Fuel-air ratio* is used to analyse load variation in a CAI engine. In general, leaner fuel-air mixture is more favourable for auto-ignition independently of the type of fuel. A leaner mixture ignites earlier because it requires lower thermal charge energy (inlet temperature) for initiation. However, if the mixture is too lean it ignites later due to higher dilution, which reduces temperature rise from compression heating.

- *Engine speed* is the parameter which is expected to change frequently during operation of the CAI engine. Changing engine speed changes the amount of time for the auto-ignition chemistry to occur relative to the piston motion. Ignition timing retards as engine speed increases and vice versa.

From an engine design point of view, the inlet temperature and compression ratio are, in some sense, pre-determined parameters by engine design. In that way, in the engine operational mode, changes of the engine load and speed are expected to be frequent and to affect ignition timing.

Changing the load of a CAI engine requires a change in the fuelling rate, therefore in the charge composition. As a result, the charge temperature has to be adjusted to maintain proper ignition timing and combustion phasing.

Similarly, changes in the engine speed, changes the amount of time for the auto-ignition chemistry to occur relative to the piston motion. To compensate for this, the charge temperature has to be adjusted again . In the rapid transient mode, during the engine accelerations and de-accelerations, compensation of load and speed effect becomes very demanding.

Concerning the effects of the various engine parameters on different types of analysed fuels (n-heptane, DME, iso-octane, ethanol, methane, MB and MF), the followings are revealed:

- Significant differences in the behaviour of the fuels characterised with two-stage ignition *n-heptane* and *DME* and fuels with single-stage ignition, *iso-octane, ethanol, methane, MB* and *MF.* These differences have strong influence on the ignition timing and further combustion events during various engine load/speed conditions.

- Fuels with single-stage ignition have considerably less variation in ignition timing with changes in fuel loading (equivalence air-fuel ratio) than fuels with two-stage ignition.

- Iso-octane, ethanol and bio-diesel fuels allow the use of very lean mixture, under given conditions in SI/CAI and CI/CAI concept, while keeping combustion process complete, .

- Variations in ignition timing with changes in engine speed are substantially less with fuels characterised by single-stage ignition than with fuels characterised by two-stage ignition.

- Fuels with single-stage ignition behaviour require less adjustment of engine parameters to maintain optimal ignition timing over the required load/speed range of a CAI engine.

Chapter 8

Effect of Exhaust Gas Recirculation (EGR) on CAI Combustion

CAI combustion is a process which is mainly controlled by the chemical kinetics of hot air-fuel mixtures. It is achieved by controlling the temperature, pressure and composition of the air-fuel mixture, so that it spontaneously auto-ignites in the engine. The ignition and heat release rate are determined by the charge mixture and its temperature and pressure history. Therefore, direct controlling methods, as in SI and CI combustion, are not suitable for CAI combustion.

A number of different methods, which have the potential to control the start of auto-ignition and the heat release rate of the CAI combustion, together with their effectiveness and practical feasibility, have been discussed in Section 2.1 (Chapter 2).

The exhaust gas recirculation (EGR), obtained by trapping the hot exhaust gases in the cylinder (*internal EGR-IEGR*) or recycling them into the intake manifold (*external EGR-EEGR*) appear to have the potential to control CAI combustion in certain load/speed ranges. IEGR obtained by a fully variable valve train (FVVT) system gives much better results in controlling the CAI combustion process than using EEGR [42, 124, 125].

An engine with FVVT allows trapping of a large amount of the IEGR (up to 80%

by volume) and quick changes in the trapped percentage of IEGR in comparison to an engine with a camshaft [42].

When using the IEGR technique, a fresh air-fuel charge is mixed with hot trapped exhaust gases, increasing the temperature and changing the composition of the newly formed charge mixture (air/fuel/IEGR) and thus influencing the ignition timing and heat release rate. In order to initiate auto-ignition and maintain CAI combustion a certain amount of IEGR has to be captured. This amount depends on engine operating conditions (engine load and speed), and it is accomplished by adjusting the exhaust and inlet valves timing.

IEGR or hot trapped EGR, consists of many species such as the products of complete combustion (CO_2, H_2O, N_2), incomplete combustion (CO), excess oxygen (O_2), particulate matter–PM, unburned hydrocarbons–HC, NO_x and possibly some residual radicals (intermediate products). Different species have different heat capacities and chemical reactivity, and hence different effects on ignition timing and the heat release rate of CAI combustion.

Therefore, it could be said that IEGR has two effects, a *thermal effect* and a *chemical effect*. These distinct features of hot trapped exhaust gases (IEGR) have been recongised in experimental and theoretical studies of CAI combustion [103, 125, 126, 127, 128].

The *thermal effect* of IEGR consists of raising the temperature of inlet charge (fresh air-fuel charge) in the mixing process with hot exhaust gases inside the cylinder. In that way the start of auto-ignition (SAI) and further combustion are influenced. It was reported that higher temperatures of the resulting charge mixture (fresh air/fuel+IEGR) advanced the SAI and vice versa [42, 54, 129]. The thermal effect of the IEGR is a positive feature of the CAI engine since it reduces the necessity for the inlet air preheat or dependence on the operating conditions.

Although the role of the thermal effect is clear enough, there are a lot of uncertainties concerning the role of the *chemical effect*.

It could be considered that the chemical effect of IEGR actually consists of several different effects, which take place simultaneously[1]:

- **Heat capacity effect.** IEGR increases the specific heat of the charge mixture (air/fuel/IEGR) due to the presence of exhaust gas species which have higher heat capacity than a fresh air-fuel charge.

- **Dilution effect.** The introduction of exhaust gases into the cylinder results in the dilution of the charge mixture. Dilution may be up to 80% of cylinder volume. The introduction of exhaust gases into the cylinder displaces some air from fresh air-fuel charge. Hence, reduces the oxygen concentration in the resulting charge mixture. At the same time some fuel is displaced from the fresh air-fuel charge. In that way the charge mixture becomes diluted. Reduction in oxygen and fuel concentrations together with added exhaust gases will result in a changed air-to-fuel ratio in the resulting charge mixture.

- **Increasing the concentration of some exhaust gas species.** IEGR raises the concentration of water vapour and carbon dioxide which tends to reduce their net production rate.

- **Influencing the radicals' production and destruction reactions.** Some exhaust gas species, particularly residual (active) radicals (such as H, OH, HO_2), may influence the production and destruction reactions of some radicals. Also, water vapour as an effective third body may affect reactions where a third body plays an important role, such as in termination reactions.

In this chapter the thermal and chemical effects of IEGR on CAI combustion will be discussed.

This chapter first sets out the experimental results showing the effect of IEGR effect on CAI combustion carried out using Lotus AVT variable valve timing. After

---

[1]This division may be arguable. Some authors [126, 127] claimed that there are five different effects of IEGR: thermal, heat capacity, dilution, the effect of increasing H_2O and CO_2 concentration and the effect of IEGR constituents on some reactions.

that a simulation to investigate the thermal and chemical effects of IEGR on CAI combustion is described. The selection of engine parameters and fuels is performed in the same way as in Chapter 7 with two types of engine concept, SI/CAI and CI/CAI, and the corresponding sets of fuels analysed:

- SI/CAI fuels: n-heptane, iso-octane, ethanol and methane,

- CI/CAI fuels: n-heptane, dimethyl ether (DME), methyl butanoate (MB) and methyl formate (MF).

The chapter ends with the summary and the conclusions drawn.

8.1   Effect of Trapped Hot EGR-IEGR

Trapping hot exhaust gases (IEGR) inside a cylinder increases the temperature of the entire charge when it is mixed with a fresh air-fuel mixture. Therefore, by tuning the quantity of IEGR, the charge composition, temperature and pressure can be adjusted. In this way, by tuning the quantity of IEGR the ignition timing of CAI combustion can be adjusted.

The engine with FVVT allows the trapping of a large amount of the IEGR (up to 80% by volume) and quick changes in the trapped percentage of IEGR in comparison to an engine with camshaft.

The variable valve timing strategy is accomplished by the Lotus AVT system (FVVT system). The AVT system allows trapping of a pre-defined quantity of IEGR. The open and closing timing of each of the four electro-hydraulically driven valves are independently variable and can be digitally controlled. Detail explanation of the AVT system has been given in [42, 43].

Trapping of a set IEGR quantity is accomplished by a combination of an early exhaust valve closing (EVC) event (in exhaust stroke) and a late inlet valve opening (IVO) event (in induction stroke). The trapped gas in the cylinder is compressed

during the final stage of the exhaust stroke. As the piston descends on the next induction stroke, inlet valves are opened and fresh air-fuel mixture is drawn into the cylinder, which is partially filed with exhaust gases. At the end of the induction stroke, inlet valves are closed and a fresh charge and exhaust gas mixture is then compressed in the next compression stroke. The CAI combustion occurs as the mixture temperature increases in the final stage of the compression stroke. Once CAI has occurred, the power stroke drives the piston down and the cycle is thus repeated. This method is known a the *sequential method* and it is used in this investigation. One more method for achieving CAI combustion, the *simultaneous method*, has also been derived. Generally, in this method, as the piston reaches BDC from the power stroke, the exhaust valves are opened and all of the exhaust gases are expelled from the cylinder. As the piston passes TDC, on the induction stroke, both inlet and exhaust valves are opened simultaneously and fresh charge and exhaust gas are together drawn into the cylinder. Again, the CAI combustion occurs as the mixture temperature increases in the final stage of the compression stroke. Once CAI has occurred, the power stroke drives the piston down and the cycle is thus repeated. Detail explanations of the *simultaneous method* can be found in [42, 43].

Valve timing with early exhaust closing and delayed inlet opening, retains the exhaust gas in the cylinder, then compressing and expanding it again. The compression phase keeps the IEGR temperature up, despite the influence of the expansion effect, and thus IEGR will still have a high temperature at the beginning of mixing process with the fresh air-fuel gaseous mixture.

In Figure 8.1 cylinder pressure traces obtained on an experimental single-cylinder engine fitted with the Lotus AVT system are shown. The engine specification and operational parameters used in that experiment were those summarised in Table 5.1 (Refer to Chapter 5) and the fuel used was gasoline with 95RON.

It can be seen that increasing the quantity of IEGR advances the start of auto-ignition. It can also be seen that there is a minimum quantity of IEGR below which
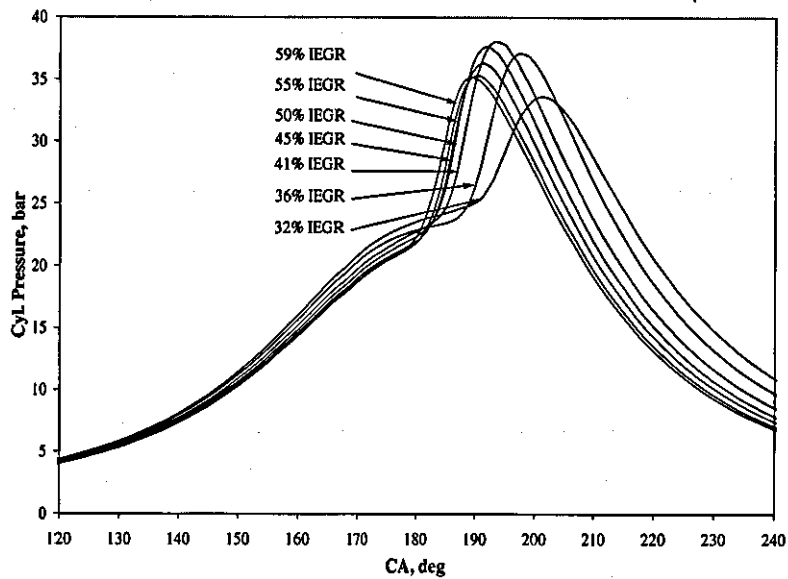
Figure 8.1: Cylinder pressure traces for different IEGR quantities, recorded in single-cylinder engine fitted with the Lotus AVT system.
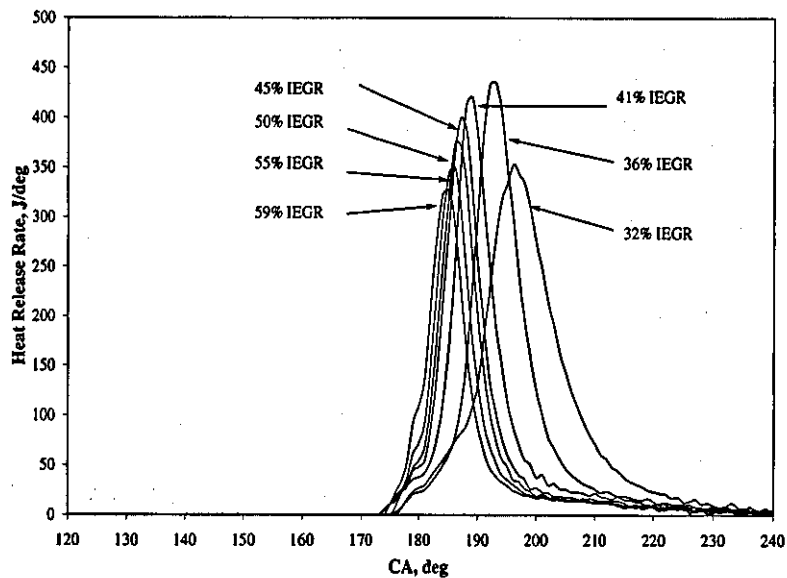
Figure 8.2: Heat release rate curves for a various IEGR quantities, obtained in single-cylinder engine fitted with the Lotus AVT system.

initiation of ignition is not possible. This amount is $\approx 36\%$IEGR (by volume) for this fuel and given set of operational conditions[2].

It could be said that the effect of IEGR on ignition timing of CAI combustion is similar to the inlet temperature effect, as explained in Section 7.1. However, with using IEGR there is no need to use the additional equipment for pre-heating the inlet air. Also, it is worth noting in Figure 8.2, that with higher IEGR quantities, the gradient of cylinder pressure decreases and the heat release rate seems to be reduced. This implies that IEGR slows down the overall combustion rate which results in the heat release rate being spread more over time.

Based on the above-mentioned observations that increasing IEGR quantities influences the ignition timing and heat release rate, it can again be concluded that IEGR has two effects:

- *Thermal effect.* The high temperature of trapped exhaust gases increases the temperature of the resulting charge in the mixing process with the fresh air-fuel mixture and accelerates the start of auto-ignition.

- *Chemical effect.* The chemical effect of the IEGR, which consists of four different effects that take place simultaneously, affects the composition, temperature and pressure of the resulting charge mixture. Hence, the ignition timing and heat release rate.

Simulation of IEGR effects on CAI combustion is carried out using the same model used for analysing the effect of fuel composition and effects of operational parameters in Chapter 6 and Chapter 7 respectively. The model was explained in detail in Chapter 5.

As mentioned previously, IEGR consists of many species which have different thermodynamic properties and chemical reactivity. The composition on IEGR depends of the fuel used. In order to model accurately the influence of the IEGR on CAI

---

[2]The cylinder pressure trace (Refer to Figure 8.1) and the heat release rate curve (Refer to Figure 8.2) for 32% IEGR were obtained for a 'spark assisted' CAI combustion.

combustion, all species, including the trace species, have to be considered. However, this creates a considerable increase in computational time especially when fuels with a complex chemical kinetics such as n-heptane and iso-octane are used. Moreover, some of the trace species have a negligible effect on the auto-ignition and actually represent ballast in the IEGR composition.

In this study seven different types of fuel will be investigated leading to seven different compositions of IEGR. It emerges that the 'standard' IEGR composition (surrogate) is needed, so that comparison of IEGR effect on each of the analysed fuels can be evaluated on the same basis. Therefore, it is decided that the IEGR consists of the products of complete combustion (carbon dioxide, water vapour and nitrogen) and when the fresh air-fuel charge is lean, oxygen is included.

The author recognises that by simulating IEGR in this manner the potential effects of carbon monoxide, trace species (HC and OHC compounds) and active radicals (H, OH and HO_2), which may be present in real IEGR are neglected. Carbon monoxide is excluded because only complete stoichiometric and lean combustion will be investigated. It is significant that, although concentrations of trace and active radical species are low, some of them, especially active radicals, may affect ignition timing[3]. This will be investigated in future projects.

The concentration of IEGR components are calculated from the overall combustion equation by the published procedure [105] which is given in Appendix B.

The mixed temperature of the IEGR and fresh air-fuel charge is estimated assuming the mixing of the ideal gases by the published procedure [21] which is presented in Appendix B.

The fuel-air equivalence ratio (ϕ) is defined as that of the incoming charge in the cylinder (fresh un-reacted air-fuel charge) and not that of the resulting charge in the cylinder (air/fuel/IEGR) which can be leaner due to the residual oxygen.

---

[3]There are currently divided opinions among scientific society regarding the role of active radicals. Some of them claim that they cannot survive the exhaust and induction strokes and thus have no influence on ignition timing of the newly formed charge mixture (air/fuel/IEGR) [16], others claim that they can survive and affect ignition timing of the newly formed charge mixture [31].

Table 8.1: Engine design and operational parameters of SI/CAI concept for analysis of the IEGR effects

Bore	80.5 mm
Stroke	88.2 mm
Swept volume	450 cm^3
Compression Ratio	10.5
Speed	2000 rpm
Equivalence fuel-air ratio	Stoichiometric
Intake Temperature	298K
IEGR Temperature	900K
IEGR Quantity	Varied
Inlet Pressure	Naturally Aspirated
Cylinder wall temperature	500K
Fuel	n-heptane,iso-octane,ethanol and methane

Table 8.2: Engine design and operational parameters of CI/CAI concept for analysis of the IEGR effects

Bore	80.5 mm
Stroke	88.2 mm
Swept volume	450 cm^3
Compression Ratio	14
Speed	2000 rpm
Equivalence fuel-air ratio	Lean ($\phi = 0.5$)
Intake Temperature	298K
IEGR Temperature	800K
IEGR Quantity	Varied
Inlet Pressure	Naturally Aspirated
Cylinder wall temperature	500K
Fuel	n-heptane,dimethyl ether (DME), methyl butanoate (MB)and methyl formate (MF)

Investigation of IEGR effects on a CAI engine is carried out in a similar way to the investigation of the engine parameters effect on CAI combustion presented in Chapter 7. Therefore, there will be two different engine concepts and corresponding fuels. The SI/CAI concept with parameters is summarised in Table 8.1 and the CI/CAI concept with parameters in Table 8.2.

The temperature of the hot IEGR is assumed to be 900K for the SI/CAI concept's fuels and 800K for the CI/CAI concept's fuels. This may seem to be opposite to that the one would expect, since the CI/CAI concept has a higher compression ratio than the SI/CAI concept. However, a much leaner mixture is used in the former concept than in the latter which results in a lower temperature of IEGR. The same trend is observed in experimental tests carried out in [23, 58, 116] and numerical simulation carried out in [73, 78].

Due to the different chemical reactivity of the analysed fuels, it can be expected that a different IEGR quantity is necessary to initiate the ignition process in each of these fuels under given conditions. Discussion of simulation results on analysed fuels will be performed separately for each of the engine concepts.

Effect of IEGR on fuels for SI/CAI Concepts Figure 8.3 shows the influence of IEGR on cylinder pressure for *n-heptane* fuel. It can be seen that with trapping a higher quantity of IEGR, the cool-flame (CF) and main ignition (MI) timings are advanced. The CF timing is more affected than the MI timing as the result of charge dilution and the elevated charge temperature history earlier in the cycle. The MI timing, as discussed previously in Section 7.3 (Chapter 7), depends of the two competing factors, the amount of compression heating and the strength of the low temperature reactions. It can be noticed that the minimum amount of IEGR needed for auto-ignition is 30%IEGR, and that below this value it is not possible to initiate auto-ignition and to sustain complete CAI combustion, under the given engine operational conditions.

Figure 8.3: Cylinder pressure traces as a function of different IEGR quantities for *n-heptane* fuel in the SI/CAI concept.

Figure 8.4: Cylinder pressure traces as a function of different IEGR quantities for *iso-octane* fuel in the SI/CAI concept.

Figure 8.5: Cylinder pressure traces as a function of different IEGR quantities for *ethanol* fuel in the SI/CAI concept.

Figure 8.6: Cylinder pressure traces as a function of different IEGR quantities for *methane* fuel in the SI/CAI concept.

As iso-octane, ethanol and methane fuels have lower reactivity, higher inlet temperatures are needed to initiate the ignition process in these fuels, as discussed in Section 7.3 (Chapter 7), and thus a higher amount of IEGR has to be employed. The amount of IEGR needed for *iso-octane* fuel is *55%*, for *ethanol 60%* and for *methane 70%*, as it shown in Figure 8.4, Figure 8.5 and Figure 8.6 respectively.

It can be seen, as with n-heptane fuel, that the higher amount of IEGR advances the ignition timings of these fuels.

A considerably lower amount of IEGR is needed for *n-heptane* fuel to start auto-ignition and to sustain complete combustion than for all other fuels analysed. This is due to the fact that *n-heptane* has a two-stage ignition process, while other fuels undergo a single-stage ignition process. The first stage of the ignition process ('cool flame ignition'), provides the reactive mixture with additional heat which increases its temperature and brings the reactive mixture earlier to the main ignition temperature. In the other fuels analysed (*iso-octane*, *ethanol* and *methane*), there is no cool flame ignition and hence no additional heat release from the first stage of ignition. Therefore, a higher amount of IEGR has to be employed to increase the temperature of the reactive mixture to the main ignition temperature.

The IEGR amounts obtained (30% for n-heptane, 55% for iso-octane, 60% for ethanol and 70% for methane fuel) represent the minimum values necessary for the start of auto-ignition and sustained complete combustion. Hence, the ignitability limits for these fuels under the given operational conditions.

Effect of IEGR on fuels for CI/CAI Concepts Due to different operational conditions in the CI/CAI concept (leaner mixture and higher compression ratio) than in the SI/CAI concept, it is expected that lower quantities of IEGR will be needed for initiation of auto-ignition in the analysed fuels.

Figure 8.7 shows the influence of IEGR on cylinder pressure for *n-heptane* fuel and Figure 8.8 for *DME* fuel.
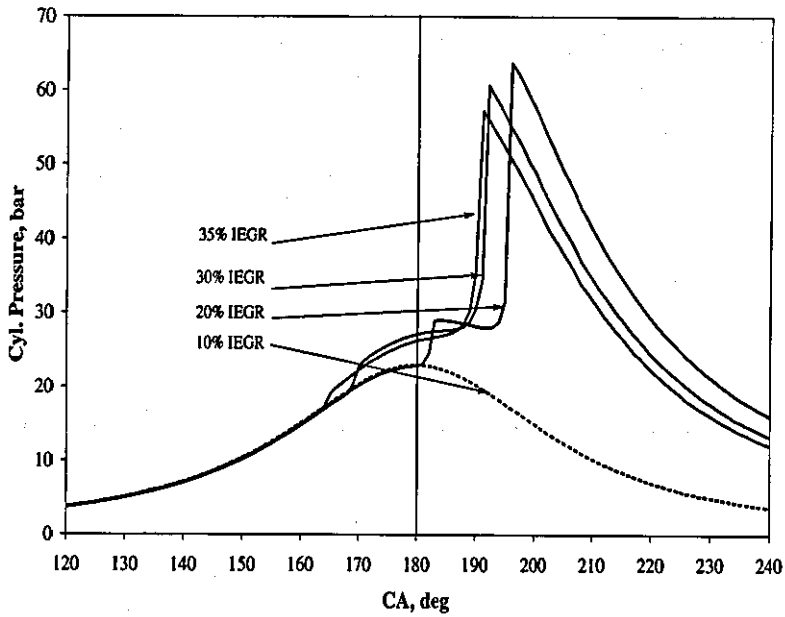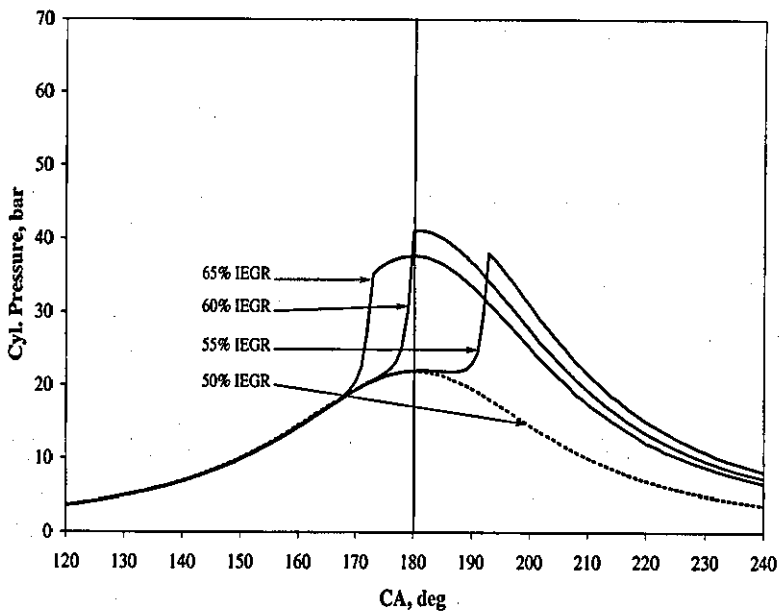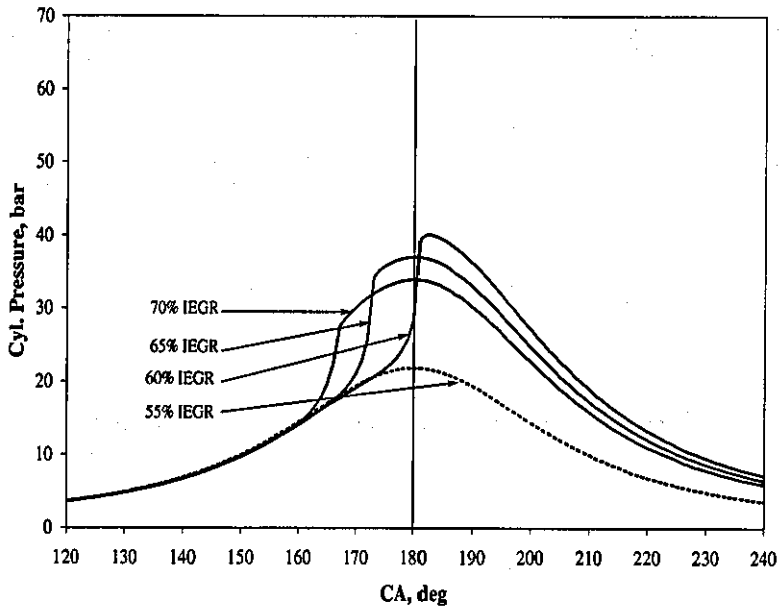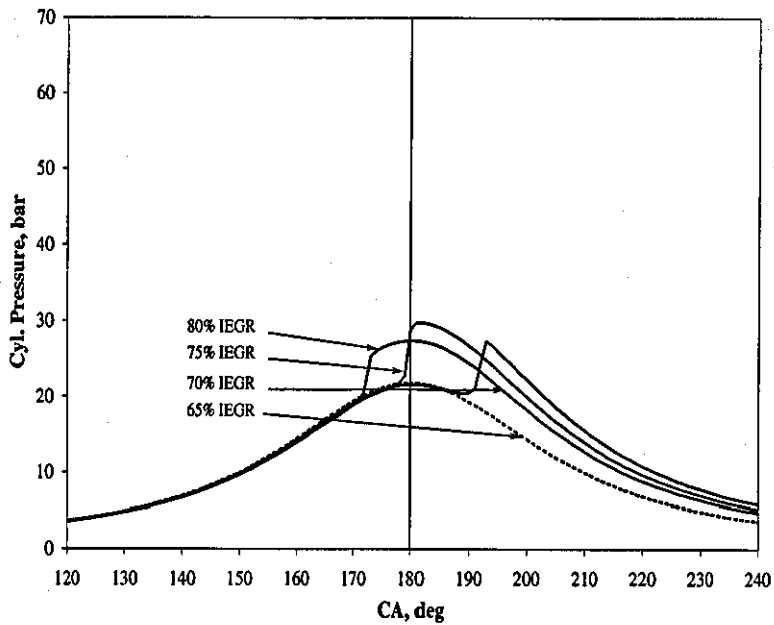
Figure 8.7: Cylinder pressure traces as a function of different IEGR quantities for *n-heptane* fuel in the CI/CAI concept.
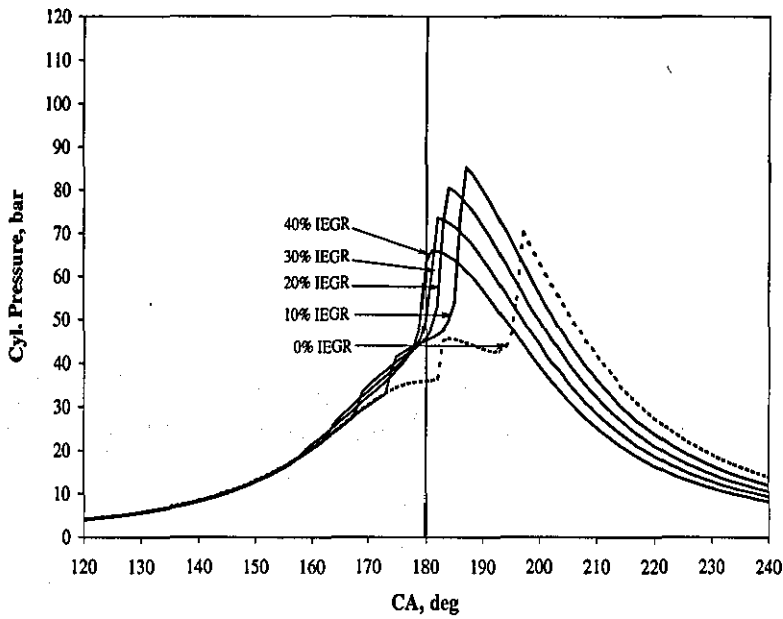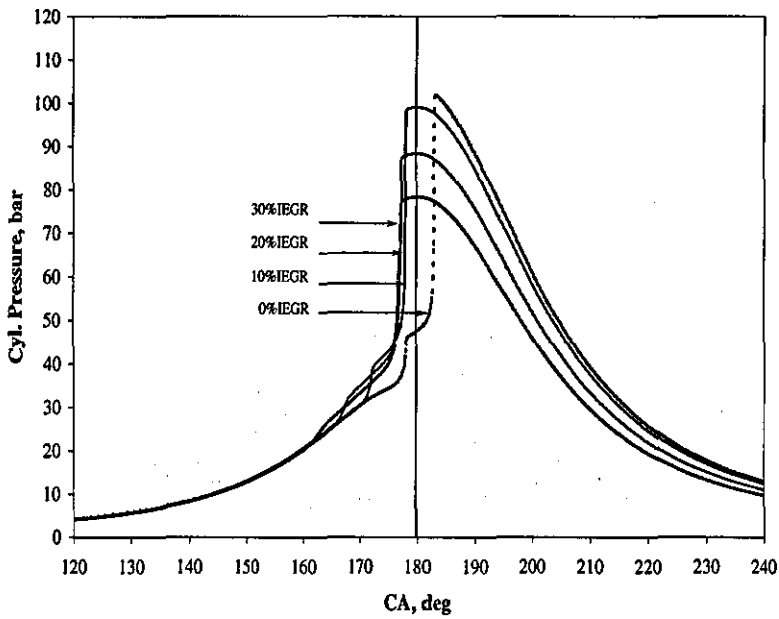

Figure 8.8: Cylinder pressure traces as a function of different IEGR quantities for *DME* fuel in the CI/CAI concept.
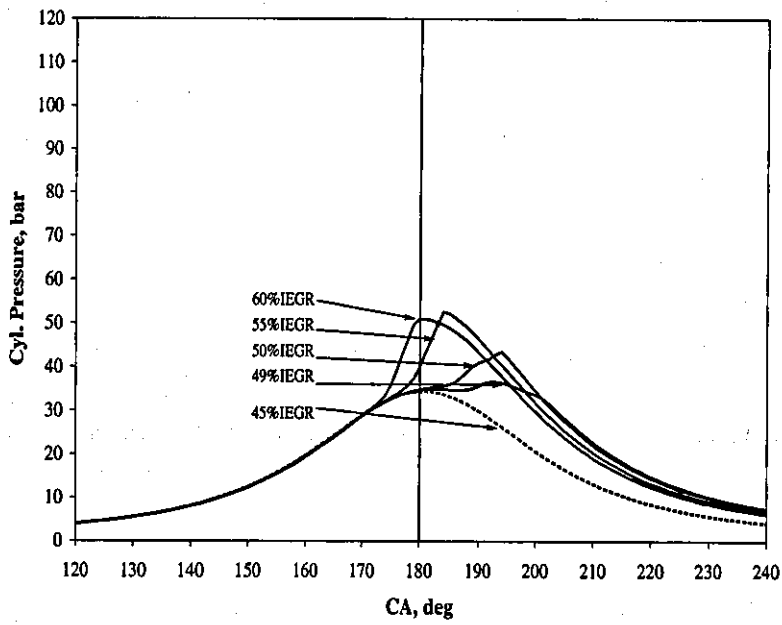
Figure 8.9: Cylinder pressure traces as a function of different IEGR quantities for *MB* fuel in the CI/CAI concept.
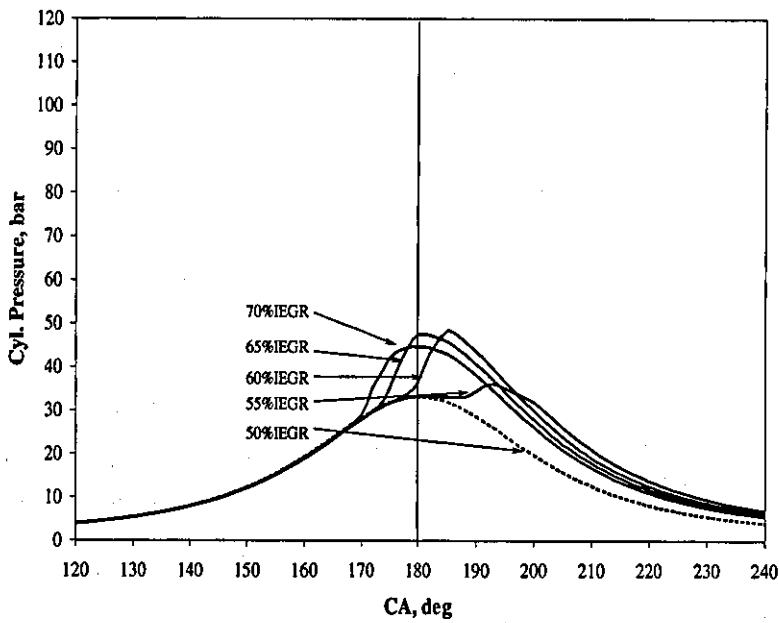
Figure 8.10: Cylinder pressure traces as a function of different IEGR quantities for *MF* fuel in the CI/CAI concept.

It can be seen that with trapping a higher IEGR percentage, the CF and MI timings for both fuels are advanced. The CF timing is more affected than the MI timing as the result of the elevated charge temperatures earlier in the cycle. The MI timing, as discussed in Section 7.3 (Chapter 7), depends on two competing factors, namely the amount of compression heating and the strength of the low temperature reactions.

As MB and MF have lower reactivity, relatively high intake temperatures are needed to the initiate ignition process in these fuels. Therefore, a high amount of IEGR has to be employed, 49% for MB and 55% for MF. The changing of cylinder pressure with IEGR for MB fuel is shown in Figure 8.9, and for MF fuel in Figure 8.10.

These IEGR quantities represent the minimum values necessary for complete combustion of MB and MF fuels, and thus their ignitability limits under given operational conditions.

It can be seen that for all fuels analysed in either the SI/CAI or the CI/CAI concept, the peak cylinder pressure decreases with the trapping of a higher IEGR percentage. In order to reveal this phenomena, cylinder pressure traces obtained for the auto-ignition initiated $\approx$ TDC with and without IEGR (with inlet charge pre-heating) are compared, and presented in Figure 8.11 for *iso-octane* and *ethanol* fuels in the the SI/CAI concept and in Figure 8.12 for *n-heptane* and *MB* fuels in the CI/CAI concept.

It can be seen that using IEGR for initiation of auto-ignition instead of inlet air pre-heating leads to the same effect, but with significantly reduced values of peak cylinder pressure[4]. This is due to the dual (thermal and chemical) effects of the IEGR. In the following text an explanation of these two effects and their influence on the ignition timing and heat release rate will be presented.

---

[4]The same effect is noticed for the other fuels, *n-heptane, methane* and *DME, MF* in the SI/CAI and CI/CAI concepts respectively, but it is not shown.
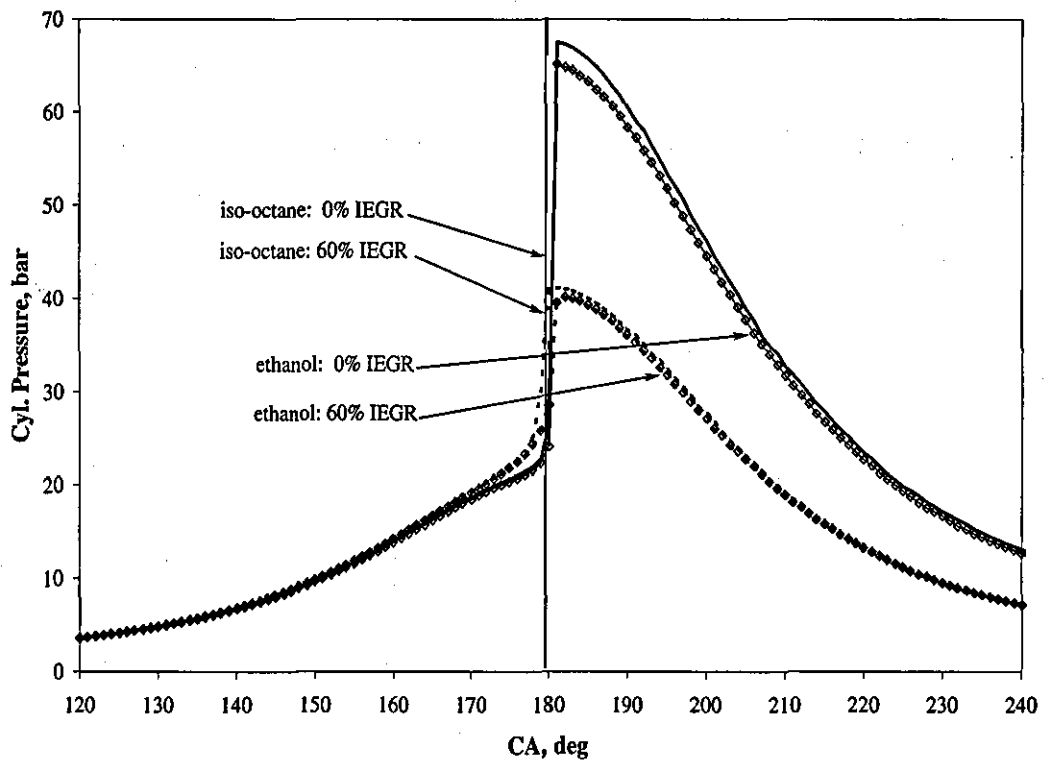
Figure 8.11: Comparison of cylinder pressure traces obtained from ignition initiated with IEGR and without IEGR for *iso-octane* and *ethanol* fuels in the SI/CAI concept. Symbol (◇) corresponds to *ethanol* fuel. Solid lines represent the auto-ignition initiated without IEGR , while dashed lines with IEGR.
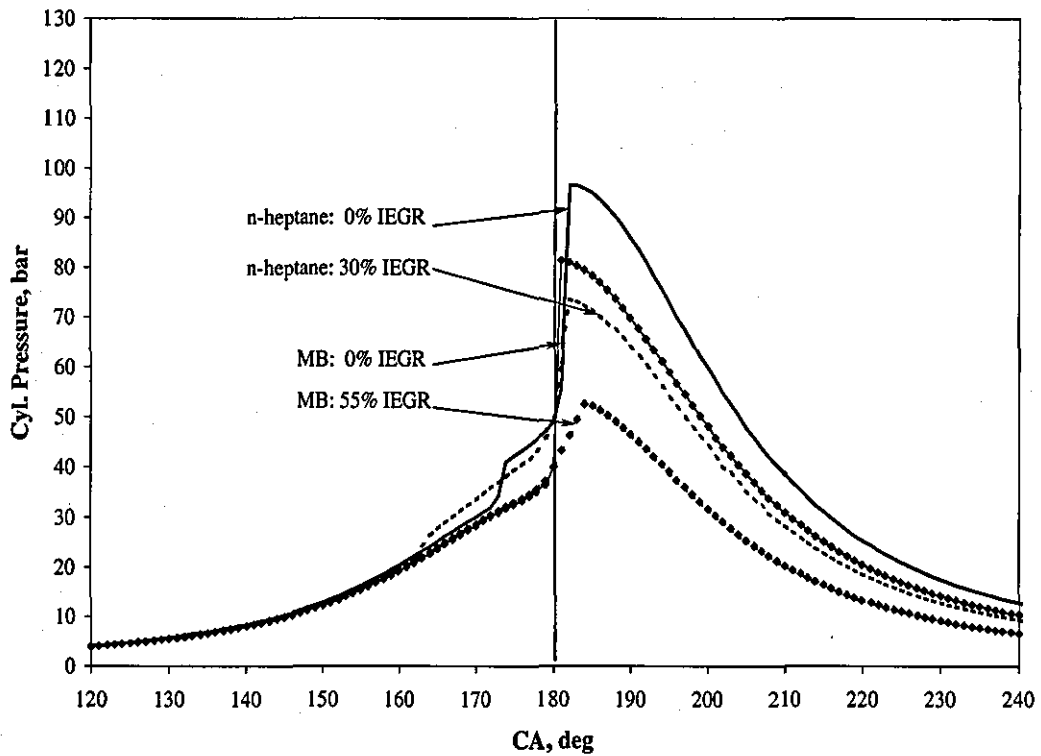
Figure 8.12: Comparison of cylinder pressure traces obtained from ignition initiated with IEGR and without IEGR for *n-heptane* and *MB* fuels in the CI/CAI concept. Symbol (◊) corresponds to *MB* fuel. Solid lines represent the auto-ignition initiated without IEGR , while dashed lines with IEGR.

8.2   Thermal Effect of IEGR

The thermal effect of the IEGR consists of raising the temperature of the fresh air-fuel intake charge in the mixing process and thus influencing the ignition timing and further combustion. A higher temperature boosts kinetic reactivity (chemical reactivity) resulting in the advancing of auto-ignition. The higher chemical reactivity increases the heat release which in turn increases the charge energy level. Increased charge energy level helps to overcome certain activation energy levels for auto-ignition at an earlier stage. Hence, the auto-ignition is advanced.

Therefore, the IEGR thermal effect is similar to the effect of increasing the inlet temperature (pre-inlet heating) since it improves the pre-ignition stage process by boosting kinetic reactivity.

The thermal effect of the IEGR can be seen as being positive for the CAI engine, since it reduces the necessity for the inlet air preheating and eliminates the dependence on the operating conditions.

To investigate the *thermal effect* of trapped hot exhaust gasses (IEGR) another simulation is performed. The model used in this simulation is the same one used previously in Section 8.1. In order to isolate the impact of the IEGR chemical effect from the IEGR thermal effect the quantity of IEGR is fixed at a value of 60%IEGR, while the temperature of IEGR is varied. The temperature of IEGR is varied from 900K to 1200K for SI/CAI concept fuels[5] and from 500K to 800K for CI/CAI concepts. As discussed in Section 8.1, the difference in the values of IEGR temperatures, is due to different operational parameters (CR and ϕ). It is recognized that the range of IEGR temperatures for the SI/CAI concept is higher that it would be normally expected in the real engines (the range should be from 700K to 800K). However, the ranges of IEGR temperatures selected were for the purpose of exploring the thermal effect of IEGR and to see its influence on auto-ignition timing than to analyse its effect on the gas exchange process. Moreover, it is very hard to measure

---

[5]For methane, the IEGR temperature is varied from 1800K to 2000K.

IEGR temperature during the gas exchange process (mixing of fresh air-fuel charge and IEGR between EVC and IVO) since this value is an instantaneous one. On the other hand, as the gas exchange process depends on many factors (such as exhaust and inlet valve opening and closing events, engine load, inlet temperature, fuel type) and because of its importance in the CAI combustion process it will be analysed in Chapter 9.

The other engine operational parameters are those summarised in Table 8.1 for the SI/CAI concept and in Table 8.2 for the CI/CAI concept.

The thermal effect of IEGR on ignition timing for the SI/CAI engine concept's fuels is shown in Figure 8.13 for *n-heptane*, in Figure 8.14 for *iso-octane*, in Figure 8.15 for *ethanol* and in Figure 8.16 for *methane*.

The thermal effect of IEGR on ignition timing for the CI/CAI engine concept's fuels is shown in Figure 8.17 for *n-heptane*, in Figure 8.18 for *DME*, in Figure 8.19 for *MB* and in Figure 8.20 for *MF*.

It can be seen that for all fuels analysed the higher IEGR temperature advances ignition timing and that a minimum temperature exists below which auto-ignition cannot be initiated, under the given operational conditions. This minimum IEGR temperature or minimum level of IEGR thermal energy is a function of the fuel type and its auto-ignition behaviour, as discussed earlier in Chapter 6.

Therefore, it can be concluded that the IEGR thermal effect is similar to the effect of inlet charge pre-heating (presented in Section 7.1-Chapter 7), since it improves the pre-ignition process by boosting kinetic reactivity, which than increases the heat release intensity and therefore advances the start of auto-ignition.

Figure 8.13: Thermal effect of IEGR on the ignition timing of *n-heptane* fuel in the SI/CAI concept.
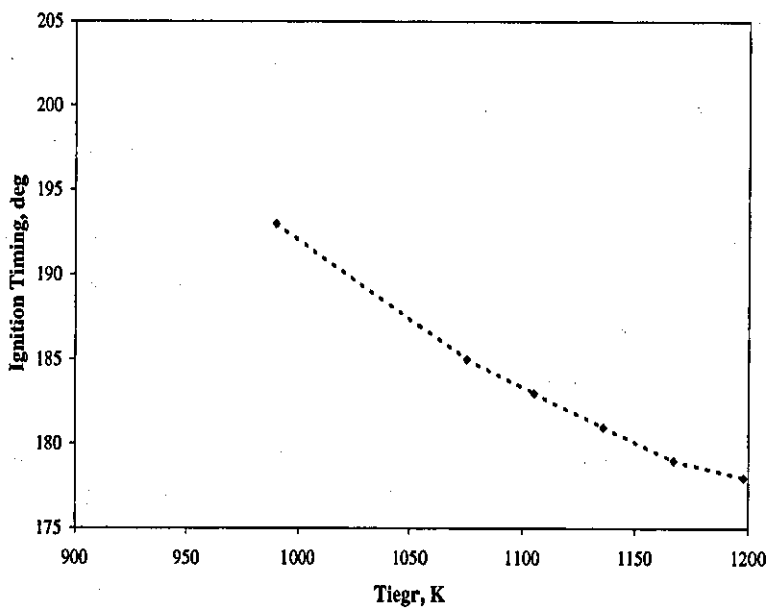
Figure 8.14: Thermal effect of IEGR on the ignition timing of *iso-octane* fuel in the SI/CAI concept.
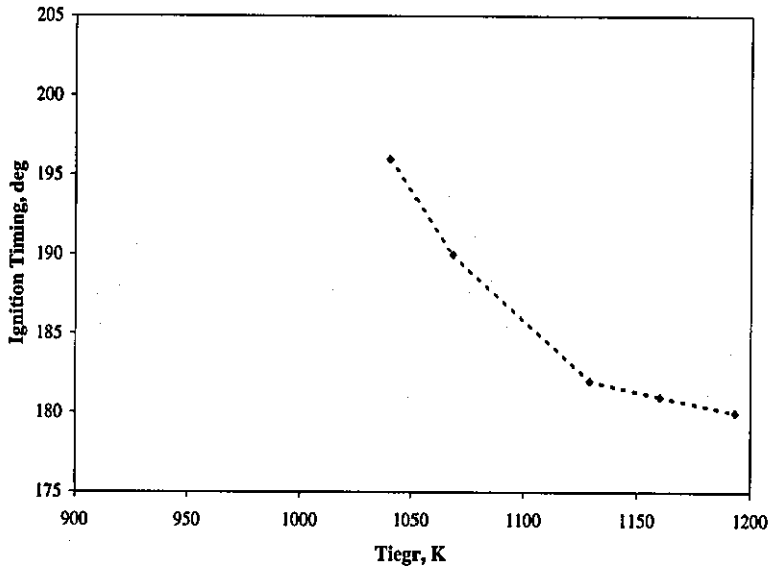
Figure 8.15: Thermal effect of IEGR on the ignition timing of *ethanol* fuel in the SI/CAI concept.
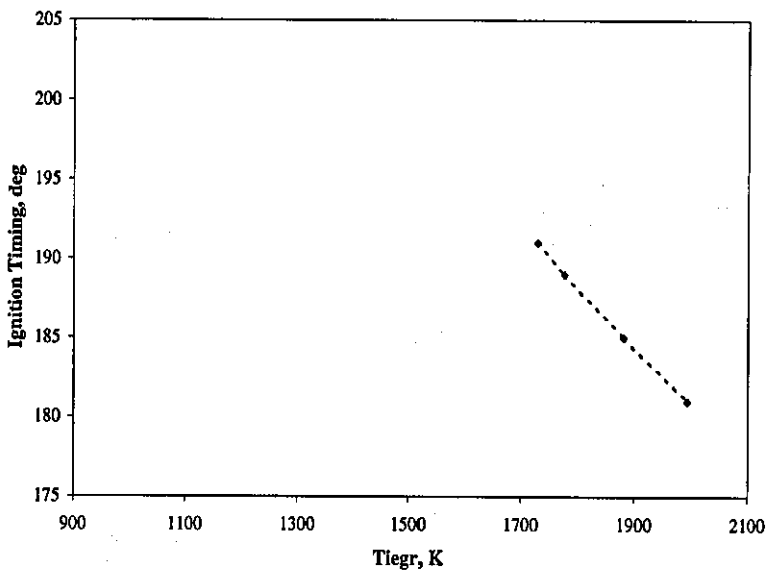
Figure 8.16: Thermal effect of IEGR on the ignition timing of *methane* fuel in the SI/CAI concept.
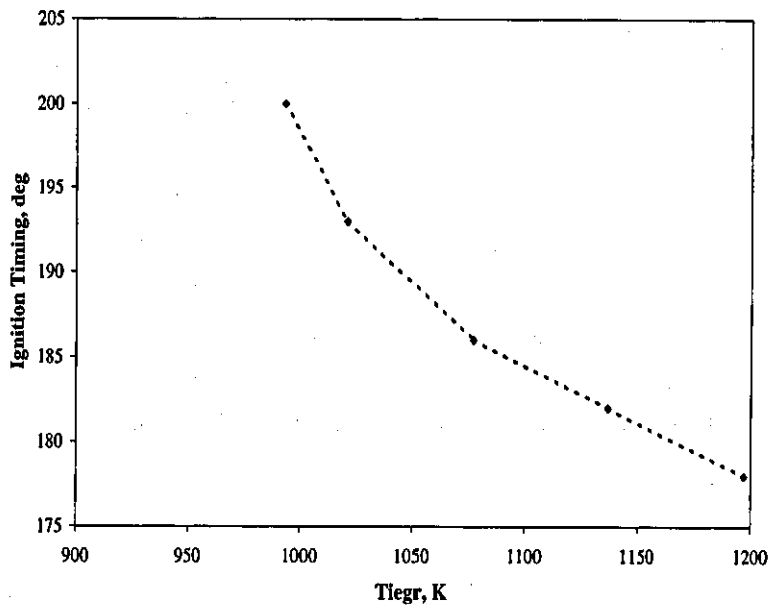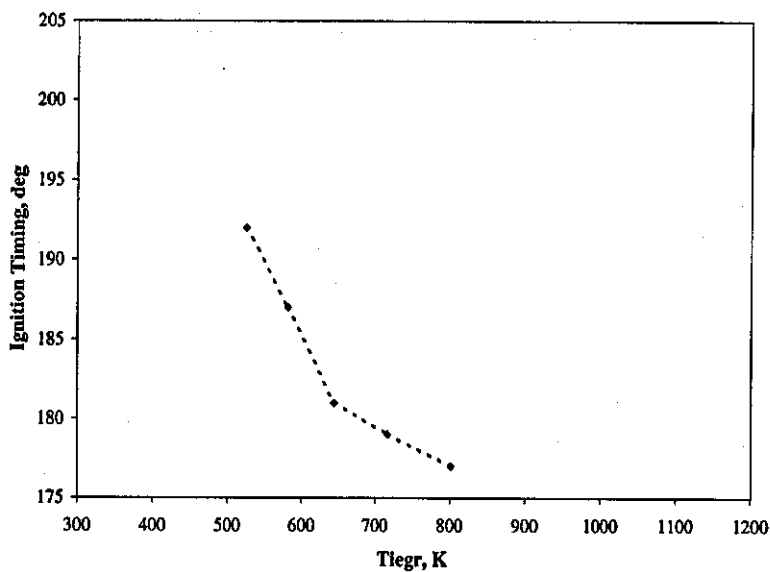
Figure 8.17: Thermal effect of IEGR on the ignition timing of *n-heptane* fuel in the CI/CAI concept.
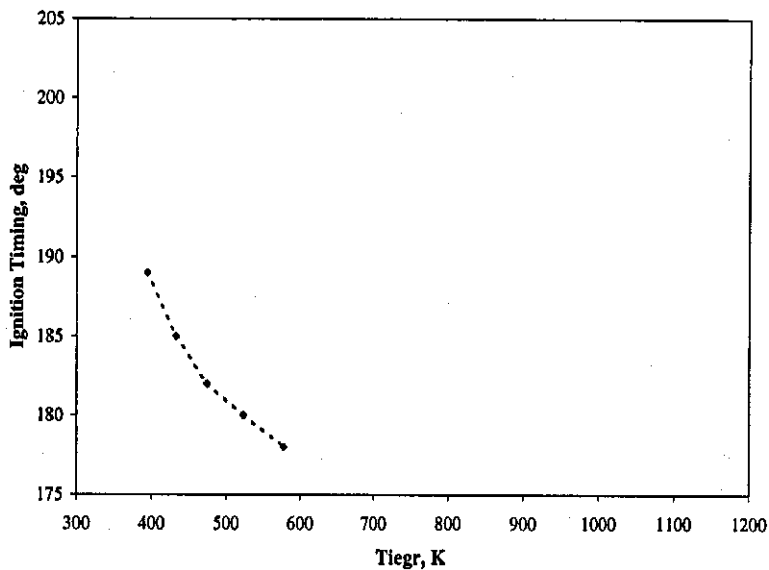
Figure 8.18: Thermal effect of IEGR on the ignition timing of *DME* fuel in the CI/CAI concept.
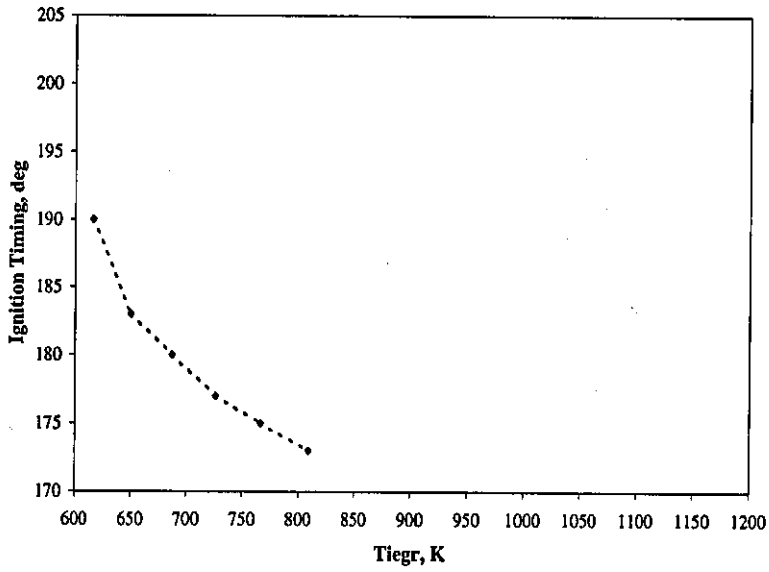
Figure 8.19: Thermal effect of IEGR on the ignition timing of *MB* fuel in the CI/CAI concept.
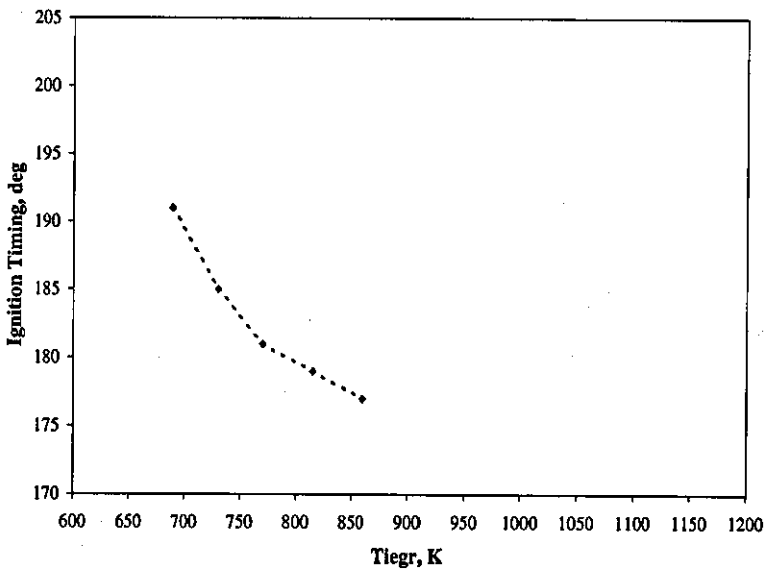
Figure 8.20: Thermal effect of IEGR on the ignition timing of *MF* fuel in the CI/CAI concept.

8.3 Chemical Effect of IEGR

The chemical effect of IEGR actually consists of several different effects which take place simultaneously: changing of the charge mixture heat capacity, dilution of the charge mixture, increasing the concentration of some exhaust gas species and influencing the radicals' production and destruction reactions.

Each gaseous chemical species in the trapped, hot IEGR has a different heat capacity and chemical reactivity towards combustion reaction. Therefore, IEGR will have different effects on the cylinder temperature history and the rate of chemical reactions.

The influence of the IEGR chemical effect on ignition timing is investigated by fixing the temperature of the resulting charge mixture (air/fuel/IEGR), while varying the IEGR percentage. In that way the thermal effect of IEGR is constant and only the chemical effect will be assessed.

In order to have a uniform composition of IEGR for all fuels investigated, the IEGR is considered to consist of the products of complete combustion (N_2, H_2O, and CO_2) and molecular oxygen (O_2) when a lean mixture is used, as explained in Section 8.1.

All other engine operational parameters are kept unchanged and they are summarised in Table 8.1 for the SI/CAI concept and in Table 8.2 for the CI/CAI concept.

Chemical Effect of IEGR on fuels for SI/CAI Concepts Figure 8.21 shows the IEGR chemical effect on the cylinder pressure history and auto-ignition for *n-heptane* fuel, while Figure 8.22 shows details for the cool flame ignition. The influence of the IEGR chemical effect on heat release rate history is presented in Figure 8.23 and details for the cool flame region in Figure 8.24.

The inlet temperature of the resulting charge at the beginning of compression stroke is fixed at 370K. It can be seen that with more IEGR introduction the start of the cool flame ignition is slightly advanced.This is due to fact that the chemical effect

Figure 8.21: Cylinder pressure traces as a function of IEGR chemical effect for *n-heptane* fuel in the SI/CAI concept.

Figure 8.22: Cylinder pressure traces in cool flame region as function of IEGR chemical effect for *n-heptane* fuel in the SI/CAI concept.

Figure 8.23: Heat release rate curves as a function of IEGR chemical effect for *n-heptane* fuel in the SI/CAI concept.
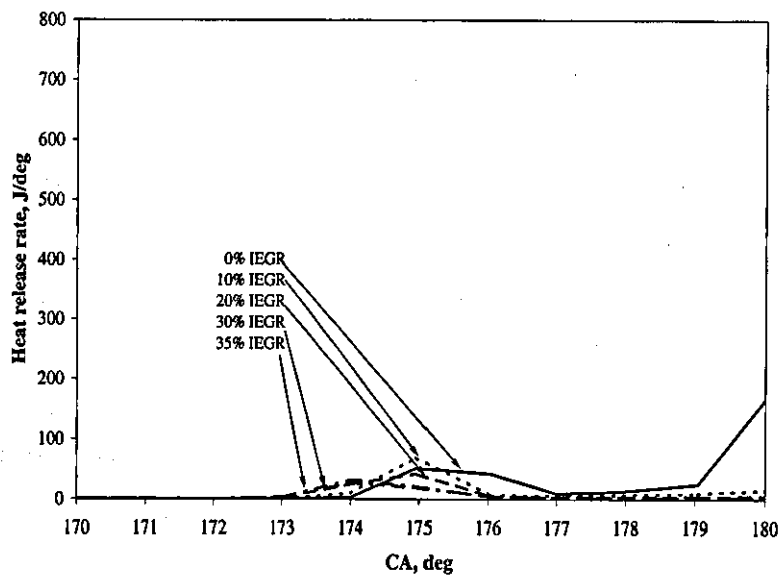
Figure 8.24: Heat release rate curves in cool flame ignition region as function of IEGR chemical effect for *n-heptane* fuel in the SI/CAI concept.

of IEGR has little influence on the low temperature reactions responsible for cool flame ignition in *n-heptane*. As discussed in Section 6.2 (Chapter 6), the cool flame ignition in n-heptane is controlled by the C_7H_{15} radicals, which ultimately leads to a relatively high rate of chain branching from ketohydroperoxide decomposition. This chain branching sequence results in an enhanced yield of OH radicals which start to consume fuel, releasing heat and increasing the temperature of the mixture. The C_7H_{15} radicals and ketohydroperoxide chain branching are very little influenced by the IEGR chemical effect (almost insensitive to the IEGR chemical effect). Therefore, with increasing IEGR quantities, the pressure rise and heat release rate from cool flame ignition remains almost unchanged, as can be seen in Figure 8.22 and Figure 8.24.

On the other hand, it can be seen in Figure 8.21 that with more IEGR introduction, the main ignition timing is significantly delayed. Retarding of the main ignition event is the consequence of the increased induction time, the time between cool flame ignition and of main ignition. Increases in induction time are due to competing influence of three effects:

i) The heat released from from cool flame ignition

ii) The accumulation of a radicals pool

iii) The temperature rise from the compression heating.

When the inlet temperature remains unchanged, more IEGR introduction dilutes the resulting mixture charge and increases its heat capacity. The diluted charge is easier to ignite due to its lower energy level requirement and thus the start of cool flame ignition is slightly advanced. On the other hand, the heat released from cool flame ignition is reduced due to the lower amount of fuel in the resulting charge. This lower amount of the fuel, also, influences the accumulation of radical pools by reducing the base for their formation and therefore increases the duration of the induction period.

Along side these two effects, the higher charge heat capacity due to the higher amount of IEGR in the resulting charge reduces the temperature rise from the compression heating.

Therefore, the induction period becomes longer with higher IEGR amounts due to the lower temperature rise from cool flame ignition, combined with reduced accumulation of radical pools and reduced compression heating. In that way, to reach auto-ignition temperature more heating and thus a longer time is required during the induction period for a diluted mixture.

Thus, the overall ignition timing of *n-heptane* is affected by the IEGR chemical effect through competing dependencies of the strength of cool flame combustion reactions, reduction in the accumulation of radical pools and amount of compression heating[6].

As a result, *n-heptane* exhibits a limited tolerance toward IEGR . The calculated results show that the start of main ignition is very sensitive to the quantity of IEGR introduced. When the IEGR quantity is higher than 30% of the entire charge no main ignition is noticed. However, the cool flame ignition occurs but the associated heat released is not sufficient to lead to the main ignition stage (Refer to Figure 8.23).

In can be seen in Figure 8.21 and Figure 8.23 that the peak cylinder pressure and peak heat release rate become lower with higher IEGR quantities. This is due to the reduced amount of fuel and increased heat capacity of the resulting charge with IEGR introduction, which results in less intense combustion and thus lower peak values of cylinder pressure and heat release rate.

Figure 8.25 shows the IEGR chemical effect on the cylinder pressure history and auto-ignition timing for *iso-octane* fuel. The IEGR chemical effect on heat release rate history is shown in Figure 8.26. The inlet temperature of the entire charge at the beginning of the compression stoke is fixed at 525K.

---

[6]It must be emphasized that if the main ignition occurs after TDC, then the temperature history of the induction period is affected by one more factor, the expansion. Expansion slows down the temperature rise and thus increases the induction period.
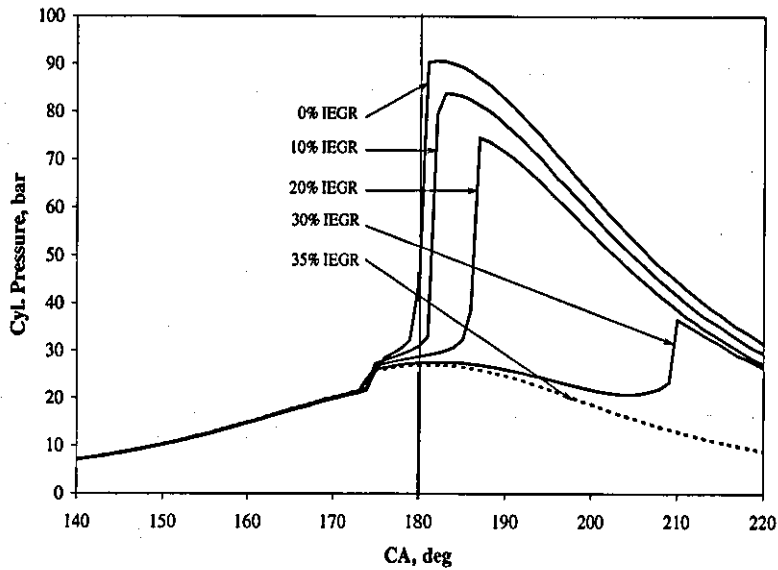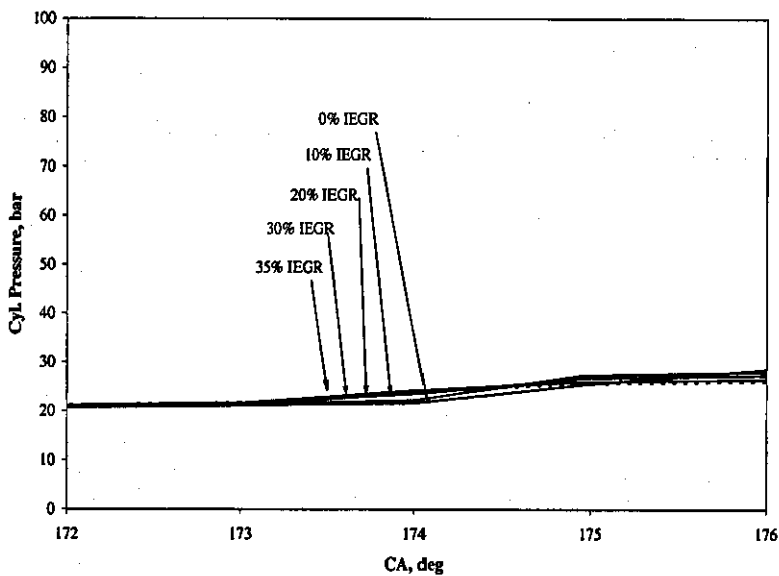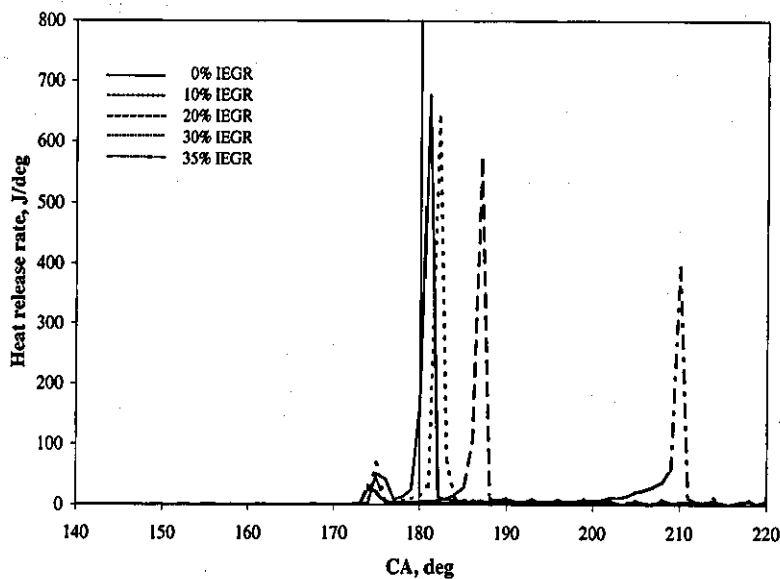
Figure 8.25: Cylinder pressure traces as a function of IEGR chemical effect for *iso-octane* fuel in the SI/CAI concept.

Figure 8.26: Heat release rate curves as a function of IEGR chemical effect for *iso-octane* fuel in the SI/CAI concept.

The effect of IEGR on auto-ignition timing, cylinder pressure and heat release histories for iso-octane fuel is different from that observed for n-heptane fuel. The main ignition timing of *iso-octane* is considerably less affected by IEGR introduction than that of *n-heptane* fuel. With 20% of IEGR, for example, the main ignition for *iso-octane* fuel is delayed 1^0CA, as compared to 6^0CA for n-heptane fuel. Based on this it can be concluded that *iso-octane* has a much higher tolerance of introduced IEGR. It can be seen in Figure 8.25 that initiation of auto-ignition, which leads to complete combustion,is sustained even for very high IEGR quantities up to 70% (for a given set of operational conditions). This quantity of IEGR is about twice as much as that in the case of n-heptane fuel. The different behaviour of iso-octane fuel towards IEGR from that of n-heptane, is due to the fact that iso-octane undergoes single-stage ignition only. In that way the IEGR chemical effect influences only main ignition since no cool flame ignition and corresponding induction phase occurs. The main ignition is governed by the high temperature chemistry which is much faster, once the temperature reaches the 1100K in the system, than low and intermediate temperature chemistry that governs cool flame ignition and the induction phase [20, 34]. The main ignition is affected by IEGR through the amount of compression heating due to changes in charge heat capacity. With the higher IEGR introduction, the resulting charge has higher heat capacity which reduces the temperature rise from the compressing heating. Consequently, the temperature of main ignition is reached later, and therefore the start of auto-ignition is delayed.

The values of peak cylinder pressure and heat release rate, presented in Figure 8.25 and Figure 8.26 respectively, become reduced with increases in IEGR quantity. With IEGR introduction, the amount of fuel in the resulting charge becomes lower and charge heat capacity becomes higher, which results in a less intense rate of energy release (combustion) and therefore in lower values of the peak cylinder pressure and heat release rate.

In Figure 8.27 the IEGR chemical effect on the cylinder pressure history and auto-ignition timing of *ethanol* fuel is shown, while in Figure 8.28 the effect on heat release

rate history is shown. The inlet temperature is fixed at 540K at the beginning of the compression stroke.

The behavior of *ethanol* towards IEGR is quite similar to iso-octane fuel's behaviour. Ethanol tolerates very high quantities of IEGR, hence auto-ignition can be initiated and complete combustion sustained up to 70% IEGR. For the higher IEGR quantities (> 70%), auto-ignition can still be initiated, but it leads to incomplete combustion and thus to unacceptable levels of HC and CO emission and deterioration in engine performance. In contrast to iso-octane fuel, the ignition timing of ethanol fuel is less affected by IEGR introduction. For instance, for *ethanol* even with 30% IEGR introduction, there is no visible ignition delay, while for *iso-octane* 1° CA deegre delay is observed with 20% IEGR introduction. This behaviour is due to the fact that ethanol is an alcohol fuel, which contains oxygen that is required for combustion. On that way the ignition and subsequent oxidation is less sensitive to IEGR .

The changes of the values of peak cylinder pressure and heat release rate with IEGR introduction, presented in Figure 8.27 and Figure 8.28 respectively, show the same trend observed for iso-octane fuel i.e. they become lower with higher IEGR quantities. The values become lower due to reduced energy release rate.

In Figure 8.29 the IEGR chemical effect on cylinder pressure history and auto-ignition timing for *methane* fuel is shown. The IEGR chemical effect on heat release rate history is shown in Figure 8.30. The inlet temperature is fixed at 615K at the beginning of the compression stroke.

It can be seen that the tolerance towards IEGR is higher in comparison to *n-heptane*, but lower than that for *iso-octane* and *ethanol* fuel. The maximum IEGR quantity, which maintains successful ignition and sustains complete combustion is 60% (under the given operational conditions). This behaviour for *methane* towards IEGR chemical effect is mainly due to the characteristics of its chemical structure which influences auto-ignition behaviour. Methane, like iso-octane and ethanol exhibits single stage auto-ignition behaviour. The production of methyl radicals in *methane* slows down its ignition process in comparison to the ignition of *iso-octane*, which
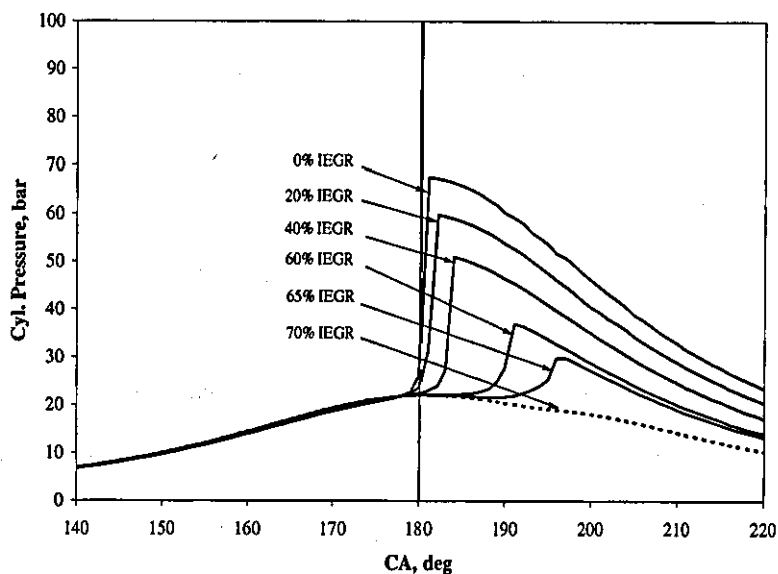
Figure 8.27: Cylinder pressure traces as a function of IEGR chemical effect for *ethanol* fuel in the SI/CA concept.

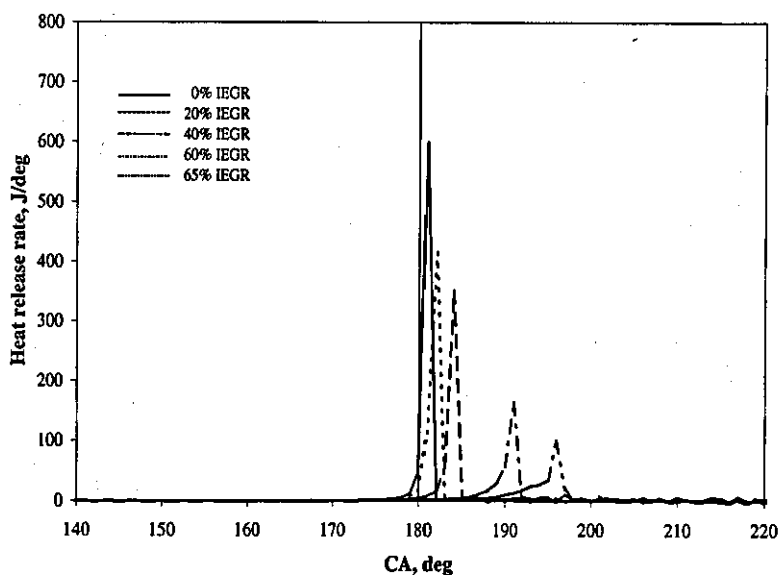Figure 8.28: Heat release rate curves as a function of IEGR chemical effect for *ethanol* fuel in the SI/CAI concept.

Figure 8.29: Cylinder pressure traces as a function of IEGR chemical effect for *methane* fuel in the SI/CAI concept.
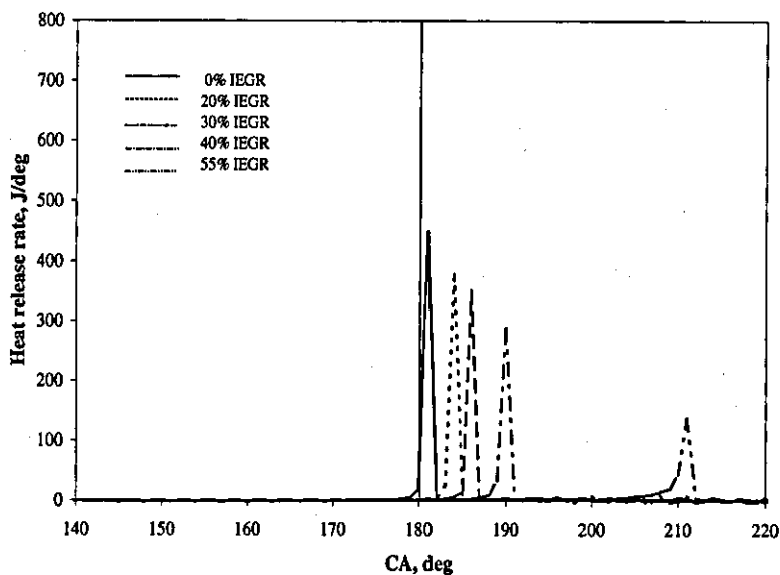
Figure 8.30: Heat release rate curves as a function of IEGR chemical effect for *methane* fuel in the SI/CAI concept.

is governed by alkyl radicals and thus methane exhibits lower IEGR tolerance. In comparison to *ethanol* fuel, *methane* has no oxygen atoms in its structure to compromise the IEGR chemical effect, which again results in lower IEGR tolerance. Consequently, the ignition delay of *methane* is more sensitive to IEGR than that of iso-octane and ethanol, but less in comparison with n-heptane.

With 20% of IEGR, for example, the main ignition for *methane* fuel is delayed 3^0CA, compared with 1^0CA for *iso-octane* and 6^0 CA for *n-heptane* fuel.

The changes of the values of peak cylinder pressure and heat release rate with IEGR introduction, presented in Figure 8.29 and Figure 8.30 respectively, show the same trend observed for iso-octane and ethanol fuels. The values become lower due to reduced rates of energy release.

Figure 8.31 shows the IEGR chemical effect on ignition timing for all four fuels analysed in SI/CAI engine concept conditions. It can be seen that *n-heptane* is the most sensitive fuel to the IEGR chemical effect and thus has the lowest tolerance towards IEGR, *iso-octane* and *ethanol* are considerably less sensitive and thus have much higher tolerance, while *methane* has a medium tolerance (it is less sensitive to the IEGR chemical effect than *n-heptane* but more than *iso-octane* and *ethanol*).

In Figure 8.32 the IEGR chemical effect on combustion duration for all analysed fuels is shown. The combustion duration is defined as the crank angle interval between 5% and 95% fuel burnt[7]. The occurrence of partial burning is assumed when the total mass fraction burnt is less than 95% at the end of simulation cycle.

It can be seen that with higher quantities of IEGR the combustion duration becomes longer as a result of the reduced overall speed of combustion. With IEGR introduction, the amount of fuel in the resulting charge becomes lower and charge heat capacity becomes higher, which results in a less intense rate of energy release and reduced combustion temperature respectively and hence slows down the combustion rate. The combustion duration of *n-heptane* fuel shows the highest sensitivity on

---

[7]Combustion duration may also be defined as the crank angle interval between 10% and 90% fuel burnt or 15% and 85% fuel burnt [21].
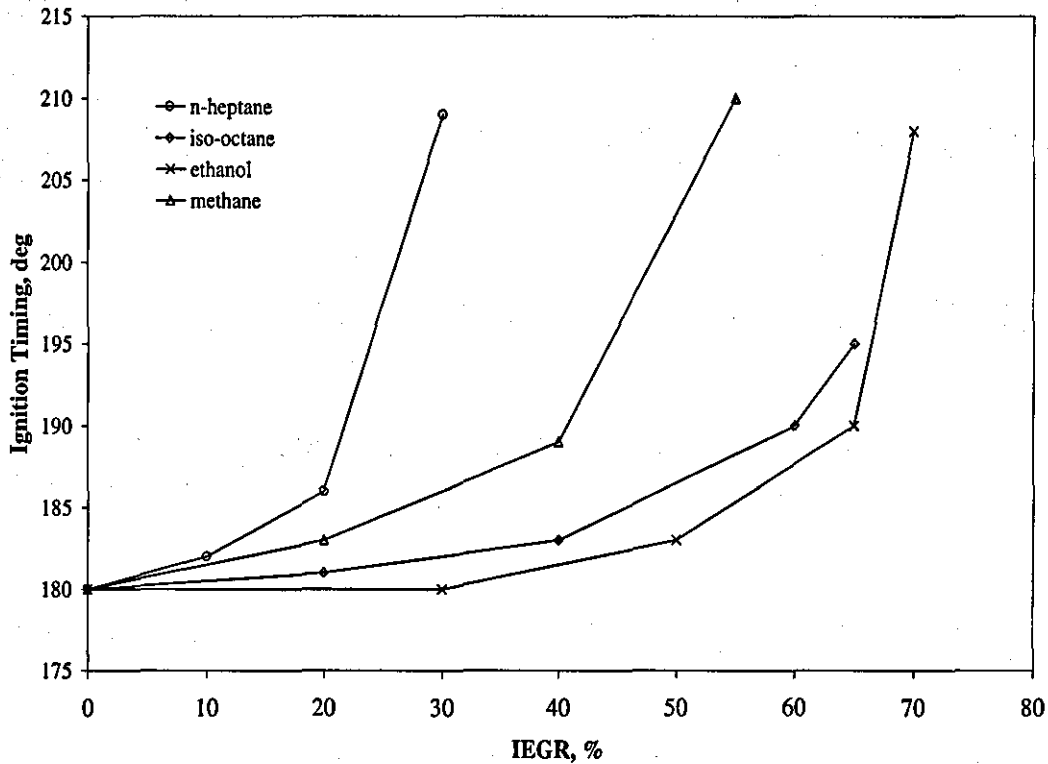
Figure 8.31: Chemical effect of IEGR on ignition timing of *n-heptane, iso-octane, ethanol* and *methane* fuel in the SI/CAI concept. Symbol (o) corresponds to *n-heptane,* (◇) *iso-octane,*(×) *ethanol* and (△) *methane* main ignition timing.

IEGR, combustion duration of *iso-octane* and *ethanol* fuels have the lowest sensitivity, while *methane* fuel has a medium sensitivity (its combustion duration is less sensitive in comparison to that of *n-heptane* but more than those of *iso-octane* and *ethanol*). This trend is similar to that observed for the IEGR chemical effect on ignition timing, which is expected behaviour, since the combustion duration is closely linked with the start of auto-ignition. Longer burn duration conditions are desirable as they provide a smoother and quieter operation.

The results obtained for the IEGR chemical effect on combustion duration of n-heptane, iso-octane, ethanol and methanol fuels are consistent with test results presented in [116, 130] and results from simulation studies presented in [126, 127, 131].
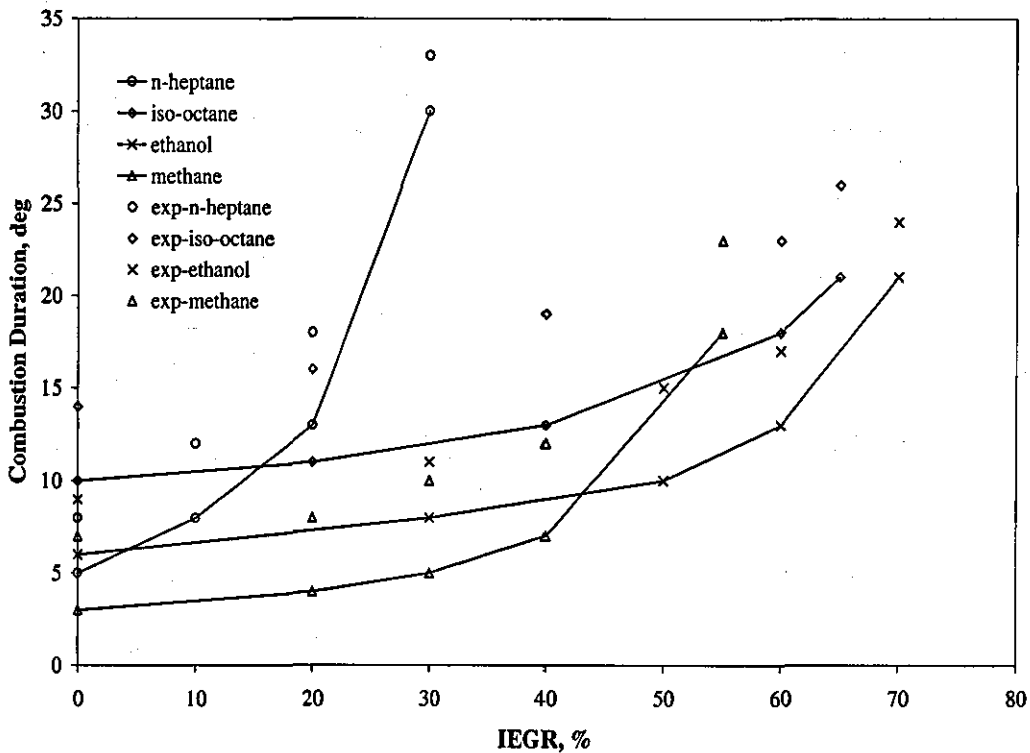
Figure 8.32: Chemical effect of IEGR on combustion duration for *n-heptane, iso-octane, ethanol* and *methane* fuel in the SI/CAI concept. Symbol (o) represents experimental data for *n-heptane,* (◇) *iso-octane,*(×) *ethanol* and (△) *methane* [116, 130].

Chemical Effect of IEGR on fuels for CI/CAI Concepts   Figure 8.33 shows the IEGR chemical effect on the cylinder pressure history and auto-ignition timing for *n-heptane* fuel, Figure 8.34 shows this for *DME* fuel, while Figure 8.35 shows the effect on auto-ignition timing only, for both fuels. The influence of the IEGR chemical effect on the heat release rate history for *n-heptane* fuel is presented in Figure 8.36, and for *DME* fuel in Figure 8.37.

The inlet temperature of the resulting charge at the beginning of the compression stroke is fixed at 320K for *n-heptane* and 298K for *DME* fuel. It can be seen in Figure 8.35 that with more IEGR introduction, for both fuels, the start of cool flame ignition remains almost unchanged, while the main ignition is significantly delayed.
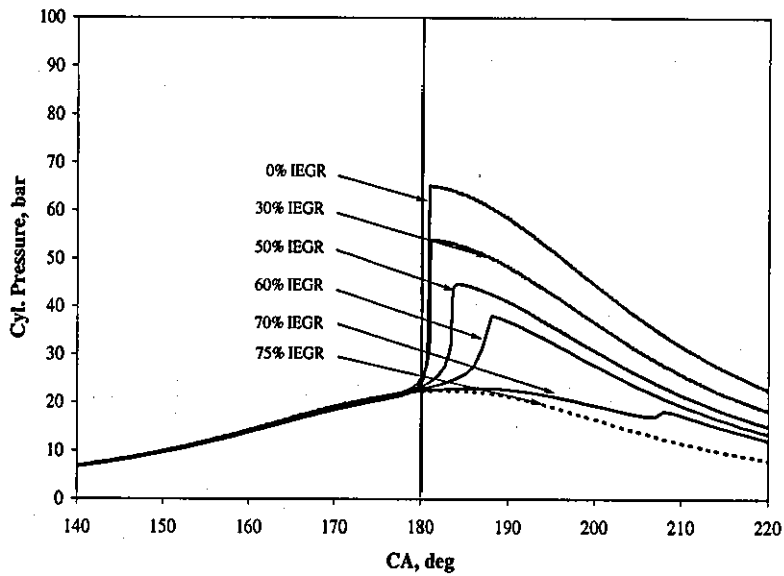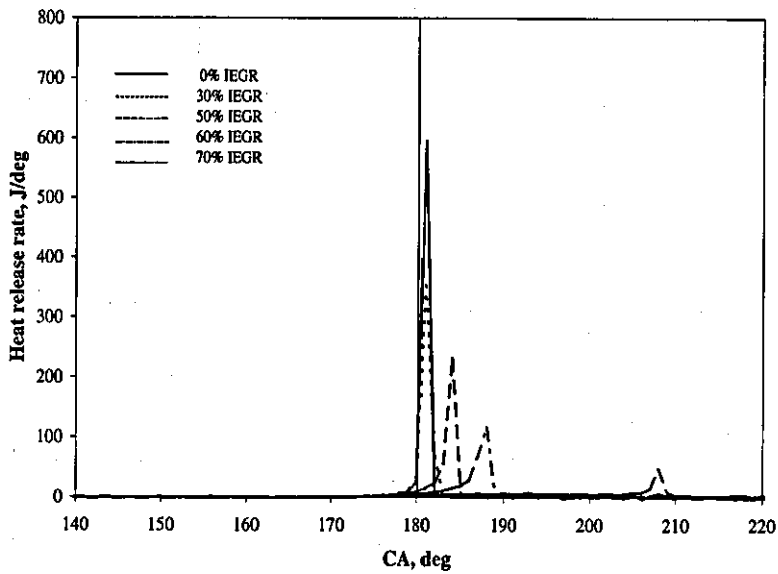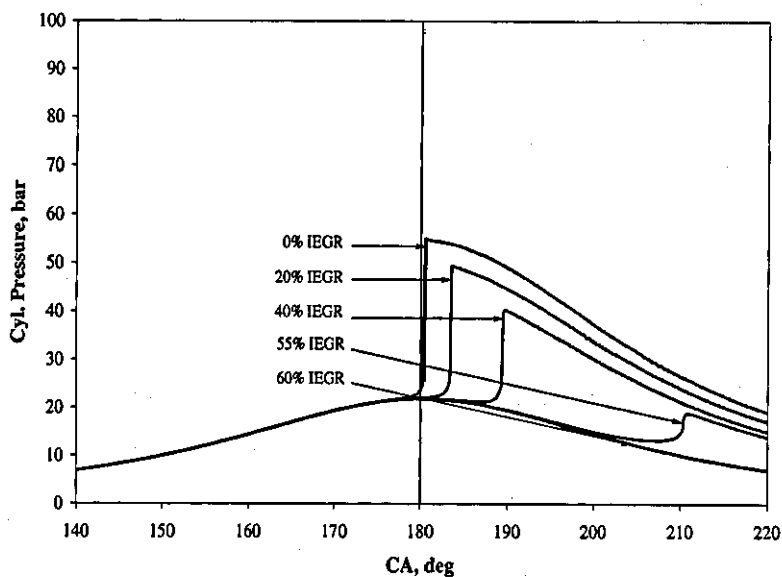
Figure 8.33: Cylinder pressure traces as a function of IEGR chemical effect for *n-heptane* fuel in the CI/CAI concept.

Figure 8.34: Cylinder pressure traces as a function of IEGR chemical effect for *DME* fuel in the CI/CAI concept.

Figure 8.35: Chemical effect IEGR on ignition timing for *n-heptane* and *DME* fuels in the CI/CAI concept. Symbol (o) represents *n-heptane* main ignition, (•) *n-heptane* cool flame ignition, (+) and solid line *DME* main ignition , (+) and dashed line *DME* cool flame ignition. Solid line corresponds to main ignition while dashed line to cool flame ignition.

This is due to the fact that the chemical effect of IEGR has little influence on the low temperature reactions responsible for cool flame ignition in *n-heptane* and *DME*, as explained previously in Paragraph 8.3. On the other hand, IEGR has a very strong influence on the intermediate temperature reactions, by reducing the accumulation of radical pools and temperature rise in the induction period. This results in the temperature for high temperature ignition initiation being reached later in the cycle and therefore the main ignition is delayed.

N-heptane fuel exhibits a higher sensitivity to IEGR than DME fuel and thus the
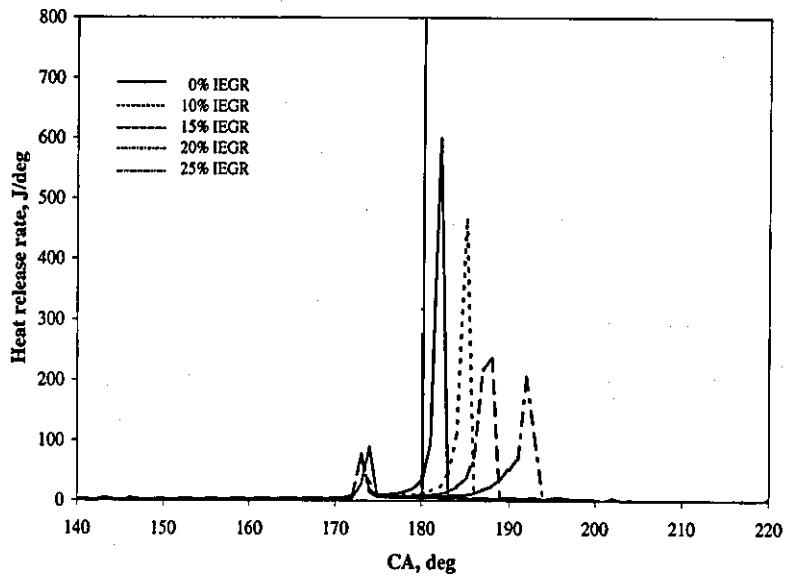
Figure 8.36: Heat release rate curves as a function of IEGR chemical effect for *n-heptane* fuel in the CI/CAI concept.

Figure 8.37: Heat release rate curves as a function of IEGR chemical effect for *DME* fuel in the CI/CAI concept.

lowest tolerance towards IEGR. The ignitability limits, assessed as the quantity of IEGR above which main ignition cannot be initiated, is reached for *n-heptane* at 20%IEGR, while for *DME* at 30%IEGR. Cool-flame ignition for *n-heptane* and *DME* still occurs for higher IEGR amounts, but the strength of cool flame combustion is not sufficient to overcome the influence of the IEGR chemical effect and thus the main ignition is omitted.

Difference in sensitivity to IEGR between *n-heptane* and *DME* is due to the nature of the low and intermediate temperature chain branching processes that are responsible for the cool flame ignition and induction period in these fuels.

The peroxy radicals control the low and intermediate temperature chain branching processes in *DME*, with the C_7H_{15} radicals performing a similar function for *n-heptane*. The chemistry of the former radicals favours chain branching reactions which keep overall fuel reactivity high, and therefore leads to the shorter induction period for DME fuel in comparison to n-heptane fuel. Also, the production of peroxy radicals is less sensitive to IEGR quantity than the production of C_7H_{15} radicals, which results in more heat being released from cool flame ignition for DME fuel than for n-heptane fuel. Therefore, increases in IEGR quantity have a stronger influence on induction period and further main ignition for n-heptane fuel.

A similar trend can be noticed for the changes in the heat release rate history for these two fuels with increasing IEGR quantity. For n-heptane fuel it is presented in Figure 8.36, and in Figure 8.37 for DME fuel. It can be seen that DME fuel has a shorter induction period which is driven by peroxy chemistry and thus higher IEGR tolerance than n-heptane fuel. Therefore, for example, with 10% IEGR the values of the peak cylinder pressure and heat release rate are much higher than that for n-heptane fuel. It is interesting to note that DME fuel exhibits a double peak of the main heat release rate phase for the IEGR quantity on its ignitability limit. This double peak is due to the influence of two competing factors: the expansion and the peroxy chemistry. The expansion tends to reduce the rate of heat release, while the fast peroxy chemistry continues to promote chain branching reactions which

effectively consume fuel and increase the heat release rate. As a result, it is still possible for the main heat release rate to occur well after TDC in the expansion stroke (around 205 CAD).

Consequently, the values of peak cylinder pressure and heat release rate for DME fuel are less affected with the higher IEGR quantities than the values for n-heptane fuel, as can be seen in in Figure 8.33 and Figure 8.34 respectively.

The IEGR chemical effect on the cylinder pressure history and auto-ignition timing for *MB* fuel is shown in Figure 8.38 and for *MF* fuel in Figure 8.39. The effect on ignition timing only, for both fuels, is shown in Figure 8.40. The influence of the IEGR chemical effect on the heat release rate history for *MB* fuel is presented in Figure 8.41 and for *MF* fuel in Figure 8.42.

The inlet temperature of the resulting charge at the beginning of the compression stroke is fixed at 435K for *MB* and 465K for *MF* fuel.

It can be noticed that the ignition timings for *MB* and *MF* are considerably less affected by the IEGR chemical effect in comparison to the ignition timings of *n-heptane* and *DME* fuels.

This behaviour of MB and MF fuel is due to the single stage ignition process and the faster chemistry which leads to the main ignition. As a consequence of this the *MB* and *MF* exhibit higher tolerance to IEGR in comparison to n-heptane and DME. It can be seen in Figure 8.35 and Figure 8.40 that the ignitability limit for *MB* and *MF* is achieved at 50 and 60%IEGR respectively, while for n-heptane at 20%IEGR and for DME at 30%IEGR. Even though the cool-flame ignition for n-heptane and DME fuels still occurs for higher IEGR quantities, but the strength of cool flame combustion is not sufficient to overcome the chemical effect of IEGR and thus the main ignition is omitted.

The values of peak cylinder pressure and heat release rate for MB and MF fuels become reduced with increases in IEGR quantity, as can be seen in Figure 8.38 and Figure 8.41 respectively. With IEGR introduction, the amount of fuel in the
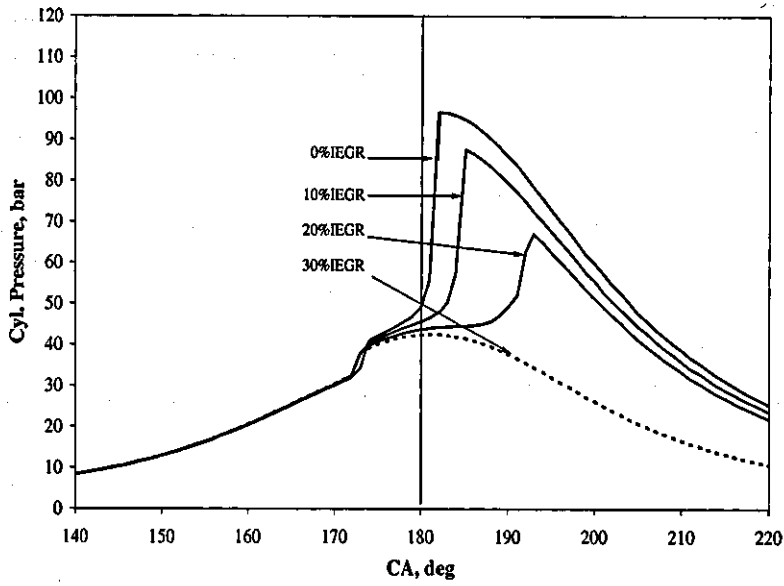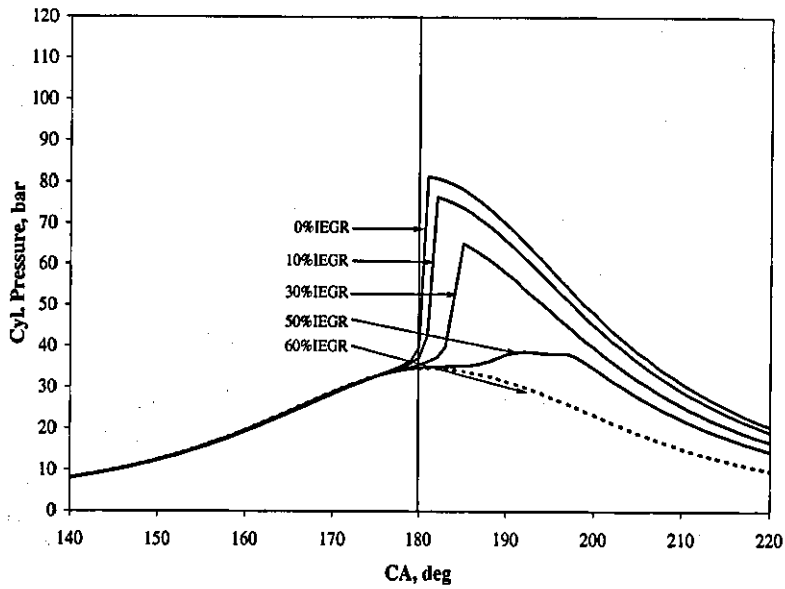
Figure 8.38: Cylinder pressure traces as a function of IEGR chemical effect for *MB* fuel in the CI/CAI concept.
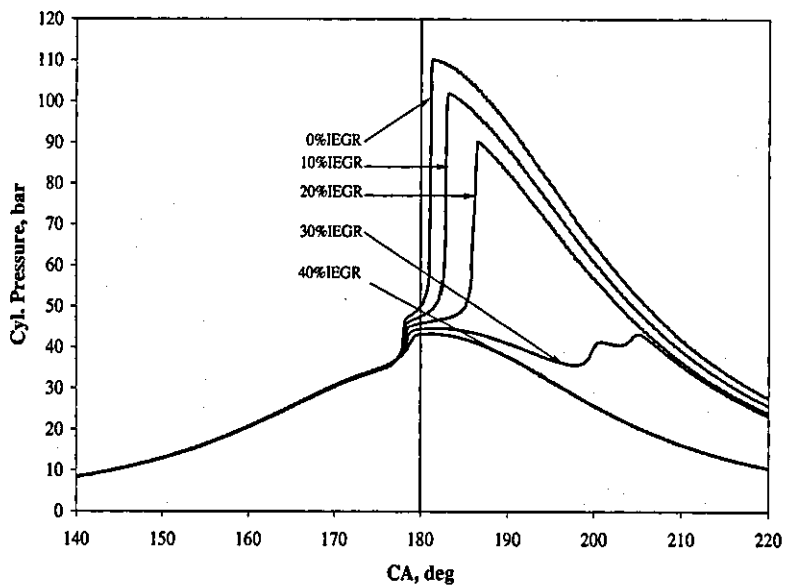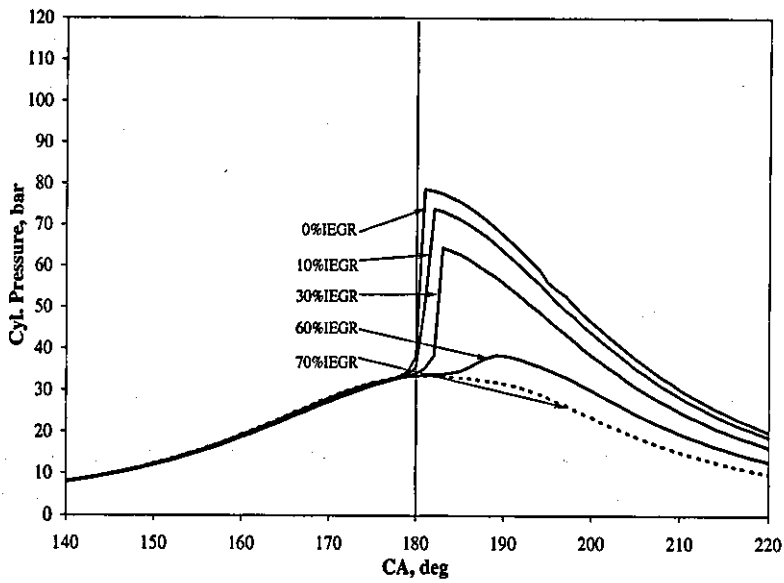

Figure 8.39: Cylinder pressure traces as a function of IEGR chemical effect for *MF* fuel in the CI/CAI concept.
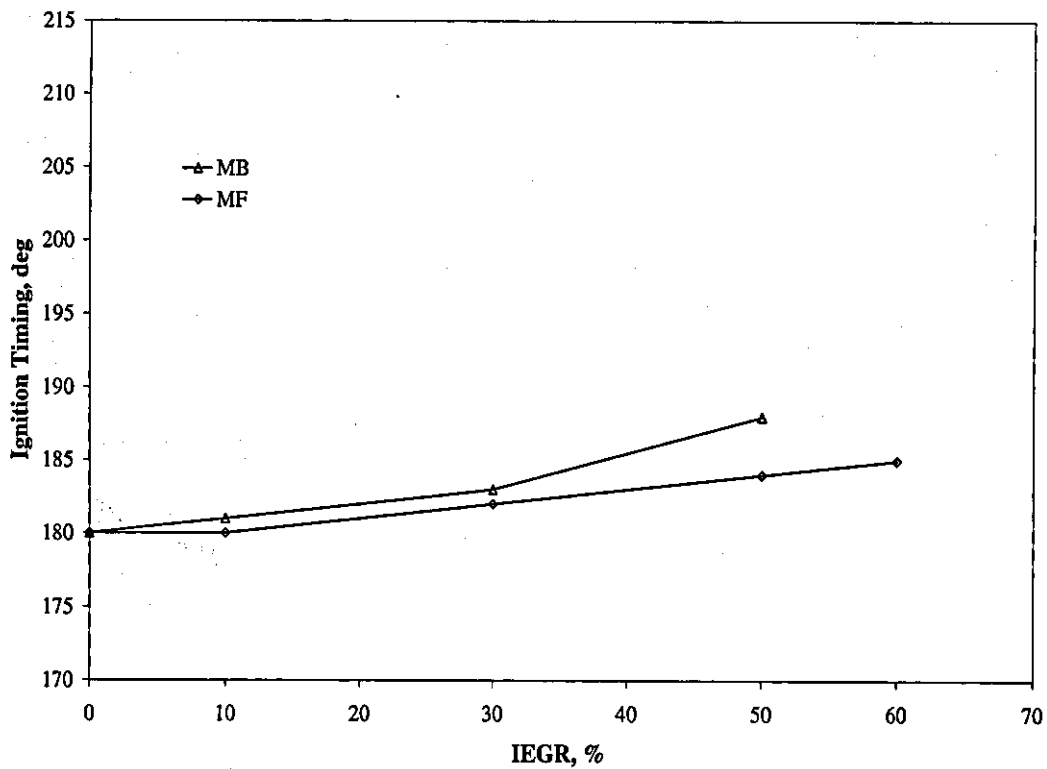
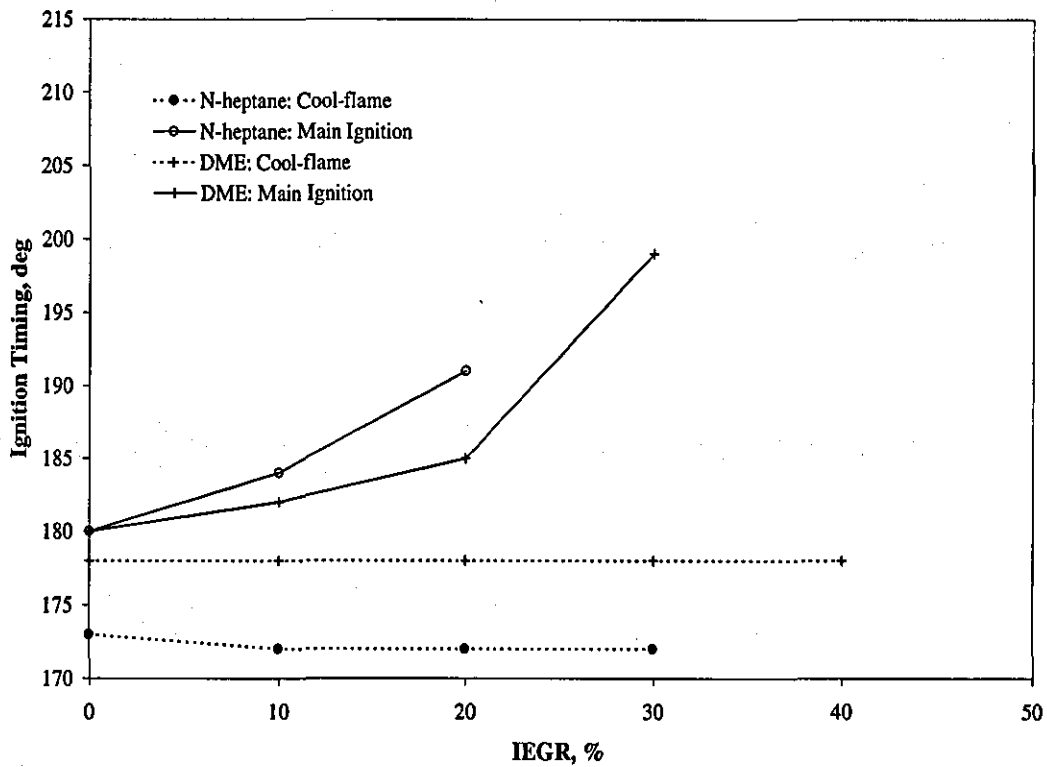Figure 8.40: Chemical effect of IEGR on ignition timing of *MB* and *MF* fuel in the CI/CAI concept. Symbol ($\triangle$) corresponds to *MB* ignition timing, while ($\diamond$) to *MF*ignition timing.

resulting charge becomes lower and the charge heat capacity becomes higher, that result in a less intense rate of energy release and thus in lower values for the peak cylinder pressure and heat release rate.

In Figure 8.43 the IEGR chemical effect on combustion duration for all fuels analysed in the CI/CAI concept is shown. The combustion duration is defined as the crank angle interval between 5% and 95% fuel burnt. The occurrence of partial burning is assumed when the total mass fraction burnt is less than 95% at the end of the simulation cycle.

It can be seen that with higher quantities of IEGR the combustion duration becomes longer as a result of the reduced overall speed of combustion. With IEGR introduction, the amount of fuel in the resulting charge becomes lower and the charge
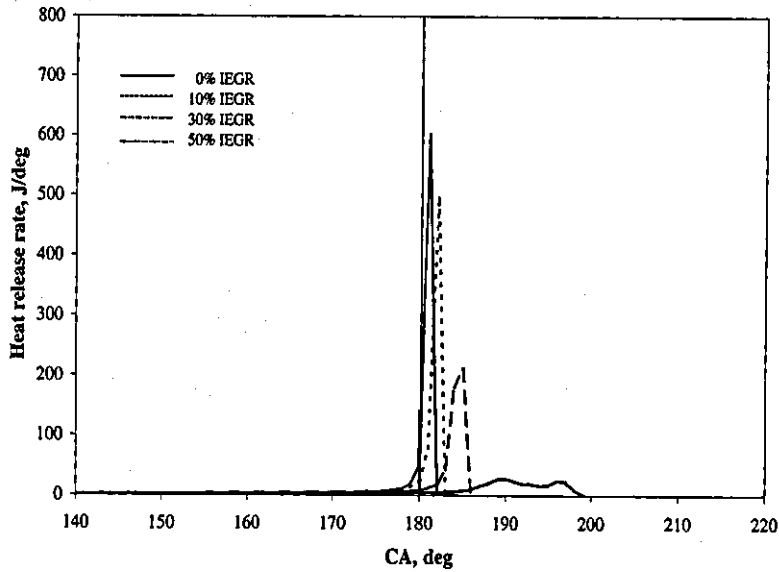
Figure 8.41: Heat release rate curves as a function of IEGR chemical effect for *MB* fuel in the CI/CAI concept.

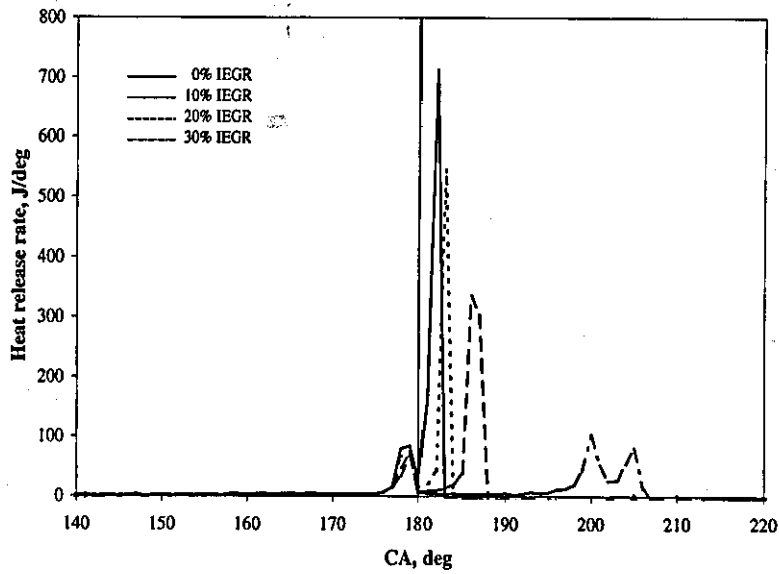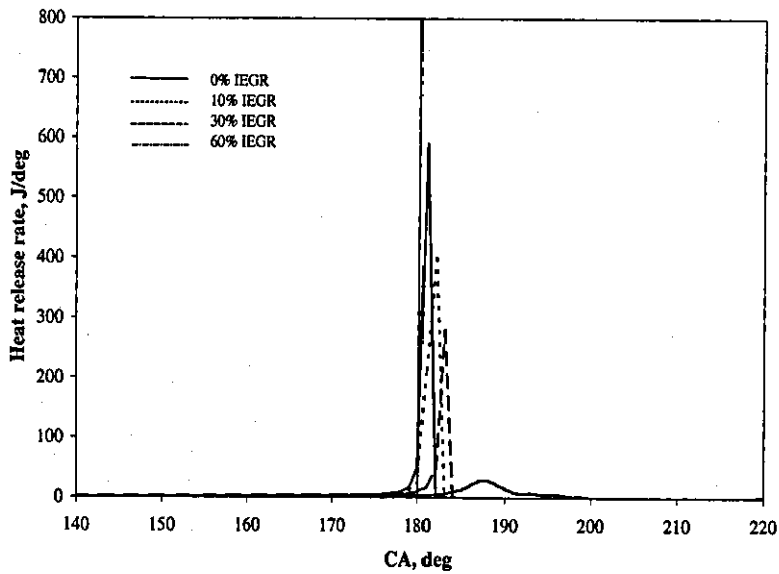Figure 8.42: Heat release rate curves as a function of IEGR chemical effect for *MF* fuel in the CI/CAI concept.
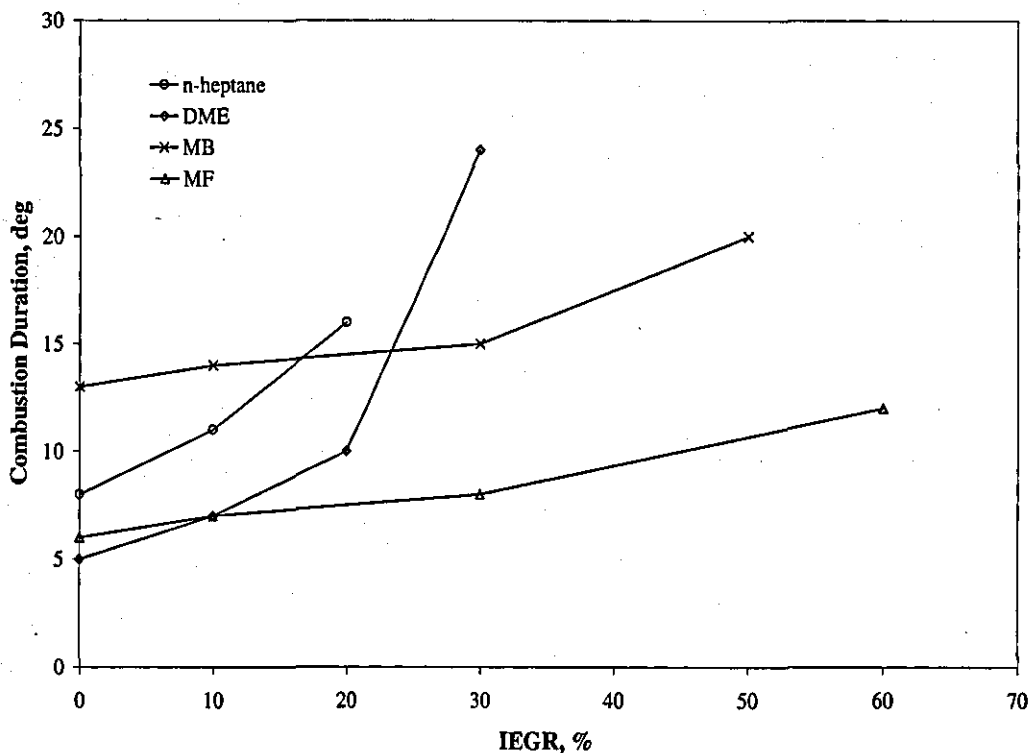
Figure 8.43: Chemical effect of IEGR on combustion duration for *n-heptane*, *DME*, *MB* and *MF* fuel in the CI/CAI concept. Symbol (o) corresponds to *n-heptane*, (◇) *DME*,(×) *MB* and (△) to *MB* combustion duration.

heat capacity becomes higher that result in a less intense rate of energy release and reduced combustion temperature and hence, slows down the combustion rate. The combustion duration shows the highest sensitivity to IEGR for *n-heptane* fuel and the lowest for *MF* fuel. *MB* fuel has a slightly higher sensitivity than that of *MF* fuel, while *DME* has considerably higher sensitivity in comparison to *MF* fuel but lower than that of *n-heptane* fuel. This trend is similar to that observed for the IEGR chemical effect on ignition timing, which is the expected behaviour, since the combustion duration is closely linked with the start of auto-ignition. Longer burn duration conditions are desirable as they provide a smoother and quieter operation.

The results obtained are consistent with test results presented in [58] and results from simulation studies presented in [132].

8.4 Summary of Exhaust Gas Recirculation (IEGR) Effect on CAI Combustion

The exhaust gas recirculation (EGR), obtained by trapping the hot exhaust gases in the cylinder (*internal EGR-IEGR*) or recycling them into the intake manifold (*external EGR-EEGR*) appears to have the potential to control CAI combustion under certain load/speed ranges. IEGR obtained by a fully variable valve train (FVVT) system gives much better results in controlling the CAI combustion process than using EEGR [42, 124, 125].

The engine with AVT allows trapping of a large amount of the IEGR (up to 80% by volume) and quick changes in the trapped percentage of IEGR in comparison to an engine with a camshaft [42].

In the IEGR technique, a fresh air-fuel charge is mixed with hot trapped exhaust gases, increasing the temperature and changing the composition of the newly formed charge mixture (air/fuel/IEGR) and thus influencing the ignition timing and heat release rate. In order to initiate auto-ignition and maintain CAI combustion a certain amount of IEGR has to be captured. This amount depends on engine operating conditions (engine load and speed), and it is accomplished by adjusting the exhaust and inlet valve timings.

IEGR or hot trapped EGR, consists of many species such as the products of complete combustion (CO_2, H_2O, N_2), incomplete combustion (CO), excess oxygen (O_2), particulate matter–PM, unburned hydrocarbons–HC, NO_x and possibly some residual radicals (intermediate products). Different species have different heat capacities and chemical reactivity, and hence different effects on ignition timing and the heat release rate of CAI combustion.

Therefore, it can be said that IEGR shows two effects, a *thermal effect* and a *chemical effect*.

The *thermal effect* of the IEGR consists of raising the temperature of the intake charge (fresh air-fuel charge) in the mixing process with hot exhaust gases and thus

influencing the ignition timing and further combustion. The thermal effect of the IEGR could be seen as an advantage for the CAI engine since it reduces the necessity for intake air preheating and eliminates the dependence on the operating conditions.

The *chemical effect* of IEGR consists of several different effects, which take place simultaneously and influence auto-ignition timing and further combustion process: changing of the charge mixture heat capacity, dilution of the charge mixture, the increasing the concentration of some exhaust species, and influencing the radicals' production and destruction reactions.

The influence of hot trapped exhaust gases (IEGR) and the influence of the IEGR *thermal* and *chemical* effects on the CAI combustion for two engine concepts, SI/CAI and CI/CAI, fuelled with different fuels was simulated. The simulation was carried out by using a single-zone combustion model with detailed chemistry, and the following observations were revealed:

1. *For the SI/CAI engine concept*:

   - The quantity of IEGR that has to be captured to initiate auto-ignition and to sustain complete combustion depends of the type of fuel:
     - For *n-heptane*–30%
     - For *iso-octane*–55%
     - For *ethanol*–60%
     - For *methane*–70%.

   - The thermal effect of IEGR, which is due to its high temperature, increases the resulting charge temperature in the mixing process with fresh air-fuel charge. This effect is similar to the effect of inlet charge preheating .

   - The chemical effect of IEGR shows that *n-heptane* fuel has the highest sensitivity to IEGR, and therefore the lowest tolerance towards IEGR. The *iso-octane* and *ethanol* fuels have a very high tolerance towards

IEGR, while *methane* fuel is somewhere in the middle. Therefore, the auto-ignition timing, heat release rate (combustion duration) and the peak cylinder pressure are the properties most affected by IEGR introduction for *n-heptane* fuel, the least affected for *iso-octane* and *ethanol* fuels and medium affected for *methane* fuel.

2. *For the CI/CAI engine concept*:

- As with the SI/CAI concept, the quantity of IEGR necessary to initiate auto-ignition and to sustain complete combustion depends of the type of fuel:

    - For *DME–0%* [8]

    - For *n-heptane–20%*

    - For *MB–55%*

    - For *MF–60%*.

- The thermal effect of IEGR increases the cylinder temperature during the mixing process with fresh air-fuel charge and it is similar to the effect of inlet charge pre-heating .

- The chemical effect of IEGR on analysed fuels shows that *n-heptane* fuel has the highest sensitivity to IEGR and therefore the lowest tolerance towards IEGR. The tolerance of *DME* is higher than that of *n-heptane* but lower in comparison to the tolerance of *MB* and *MF* fuels. The *MF* fuel has the highest tolerance towards IEGR amongst the fuels analysed.

It can be concluded that fuels with a two-stage ignition process (*n-heptane* and *DME*), need a lower amount of IEGR for initiation of the auto-ignition process and to sustain complete combustion than fuels with a single-stage ignition process (*iso-octane, ethanol, methane, MB* and *MF*). On the other hand, fuels with a single-stage ignition process have a higher tolerance towards IEGR than fuels with a two-stage

---

[8]For DME fuel, no IEGR is necessary to initiate and sustain the CAI combustion under the given engine operational conditions.

ignition process. Therefore, it may be possibly to improve control of both engine concepts, SI/CAI and CI/CAI, by using a mixture of the analysed fuels. The blended fuel should incorporate the benefits of lower ignition temperature from *n-heptane* and high IEGR tolerance from *iso-octane* or *ethanol* fuel for the SI/CAI concept, and from *DME* or *n-heptane* fuel and *methyl butanoate* or *methyl formate* for the CI/CAI concept.

Chapter 9

Effect of Valve Timings on Gas Exchange Process in CAI Engine

It was discussed in Section 2.1 (Chapter 2) that the control of CAI combustion over the entire load/speed range was the problem that limited its practical application and therefore attracted the most attention. The control of CAI combustion consists of two aspects: the control of ignition timing to occur in the vicinity of top dead centre (TDC) compression and the control of heat release rate (combustion speed) at high loads to prevent excessive noise and engine damage. The CAI ignition is determined by the charge mixture temperature and composition and to a smaller extent pressure. In this way, the CAI combustion is achieved by controlling the temperature, composition and pressure of the charge mixture at the beginning of the compression stroke (IVC point). As the CAI combustion is kinetically controlled it means that the rate of heat release depends on correct combustion phasing and is closely linked with the ignition delay. Therefore, the successful control strategy has to be able to control the charge mixture temperature, composition and pressure at the IVC point over the entire load/speed range.

It was demonstrated in Chapter 8 that the use of internal gas recirculation (IEGR) has the potential for controlling CAI combustion. IEGR was accomplished by the

Lotus AVT system, a fully variable valve train (FVVT) system. This system enables quick changes in the amount of trapped hot exhaust gases inside the cylinder and therefore influences the charge mixture temperature, composition and pressure. The AVT system enables individual control of the each of four valve events:

1. The exhaust valve open (EVO) event

2. The exhaust valve closure (EVC) event

3. The inlet valve open (IVO) event

4. The inlet valve closure (IVC) event

The timing of these valve events plays an important role in the *gas exchange process*, the process that takes place between the first valve open event (EVO) and the last valve closure event (IVC). The gas exchange process has a strong influence on engine parameters and charge mixture properties in the engine manifold (IVC point) and therefore on the control of CAI combustion [21].

The aim of this Chapter is to analyse the influence of the variable valve timings on the gas exchange process in a CAI engine fuelled with standard gasoline fuel (95RON). The analysis is performed by the experimental and modelling approaches. The single-cylinder research engine equipped with the Lotus AVT system was used for the experimental study. A combined code consisting of a detailed chemical kinetics code and one-dimensional fluid dynamics code was used for the modelling study.

In this Chapter the experimental set up and results obtained from the test carried out on a hybrid SI/CAI single-cylinder engine, equipped with the AVT system will be presented. The technique for 'switching' from SI to CAI mode will be detailed next followed by a description of the combined simulation code. The simulation code will be calibrated by reproducing the measured pressure histories and several global engine parameters. The effects of the intake and exhaust valve timings on the *engine parameters* (such as IEGR rate, load, pumping losses, volumetric efficiency

and trapped gas temperature) as well as on the *charge mixture properties* (such as composition, temperature and pressure) will be investigated.

The chapter concludes with the summary of the valve timings effects on:

- The gas exchange process.

- The engine performance.

- The charge properties in engine manifolds.

- The control of the CAI combustion.

9.1   Experimental Apparatus and Set-up

Engine   The engine employed in this research is a single cylinder, 4-stroke research engine based on the GM family one-1.8 litre series architecture. A photograph of the engine is shown in Figure 9.1. It consists of a production piston, connecting rod and stroke, with a standard 4-cylinder head on top of a water cooled barrel to join the family one part to the custom made bottom end. Only the front cylinder of the head is operational. The water jacket uses a combination of machined modifications and brackets. Unnecessary water transfer ports are blanked off. The engine has a bespoke single cylinder bottom end designed and developed by Lotus to allow either pure combustion work or optical access versions to be built. The major engine specifications are presented in Table 9.1. The use of conventional parts in the combustion system, wherever possible, ensures that the cost of rebuild is low should a component failure occur (for example, because of an uncontrolled violent detonation, etc). The compression ratio can be easily changed in this engine, due to the separate barrel and, more importantly due to the FVVT system, which rules out the need for modification of the belt runs and other parts. Any change in compression ratio is achieved by means of the deck height being moved up and down by spacers or short liners, or combination of these two. The bottom end can

Figure 9.1: Single-cylinder research engine with Lotus AVT System.

accept various strokes up to and including 100 mm, and is capable of running to 5000 rpm (depending on stroke).

The fitted research FVVT system allows trapping of a pre-defined quantity of IEGR. The open and closure timings of the each of four electro-hydraulically driven valves are independently variable and can be digitally controlled. Valve opening profiles can be selected and entered into the software by the user. The control software uses inputs from a crankcase encoder and valve linear displacement transducers to facilitate a closed-loop control to satisfy a 'desired versus actual' position control until the required profiles are achieved. Fine tuning of valve profiles is accomplished by using valve-specific gain controllers.

The engine is connected to a Fraud AG30, 30KW eddy-current dynamometer. A redline ACAP data acquisition system from DSP Technologies Inc. is used, together

Table 9.1: Single-cylinder engine specifications and test conditions

Bore	80.5 mm
Stroke	88.2 mm
Swept volume	450 cm^3
Compression Ratio	10.5
Speed	up to 5000 rpm
Load Range	2-5 bar (IMEP)
Number of valves per cylinder	4
Valve Control	Electro-hydraulic Lotus AVT-FVVT system
Fuel Injection	Port fuelled
Fuel	Gasoline (95RON)
Equivalence air-fuel ratio	Stoichiometric
Intake Temperature	25^{0}C
Inlet Pressure	Naturally Aspirated
IEGR	up to 80 % (by volume)

with an Horiba MEXA 7100 DEGR emissions analyzer. For the engine management system a conventional Lotus V8 controller is used.

Valve Events for CAI Combustion   The technique used to initiate and to control the CAI combustion relies on the trapping of a pre-determined quantity of exhaust gases by closing the exhaust valves relatively early in the exhaust stroke and by opening the inlet valves relatively late in the induction stroke. The general principle can be seen in Figure 9.2.

The trapped exhaust gases are then compressed during the final stage of the exhaust stroke. As the piston descends on the induction stroke, the inlet valves are opened and a fresh charge is drawn into the cylinder which is partially filled with exhaust gases. At the end of the induction stroke the inlet valves are closed and the mixture of a fresh charge and exhaust gas is then compressed in the next compression stroke. The CAI combustion occurs as the mixture temperature increases in the final stage of the compression stroke.

Once the CAI has occurred, the power stroke drives the piston down and the cycle
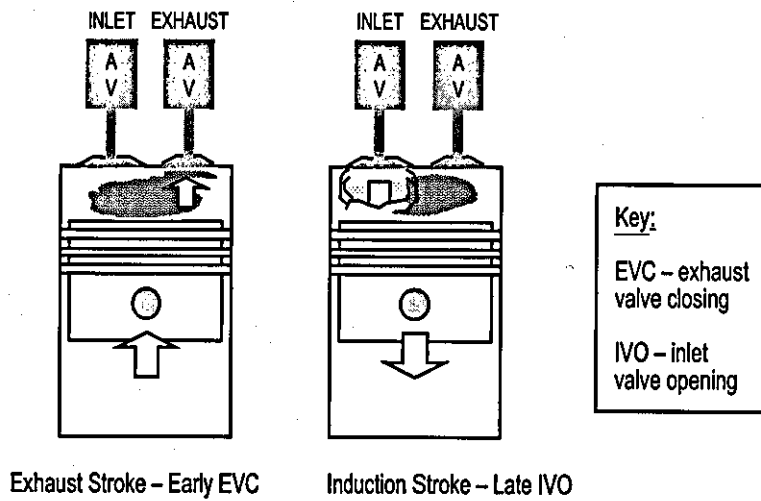
Figure 9.2: The sequential valve event strategy.
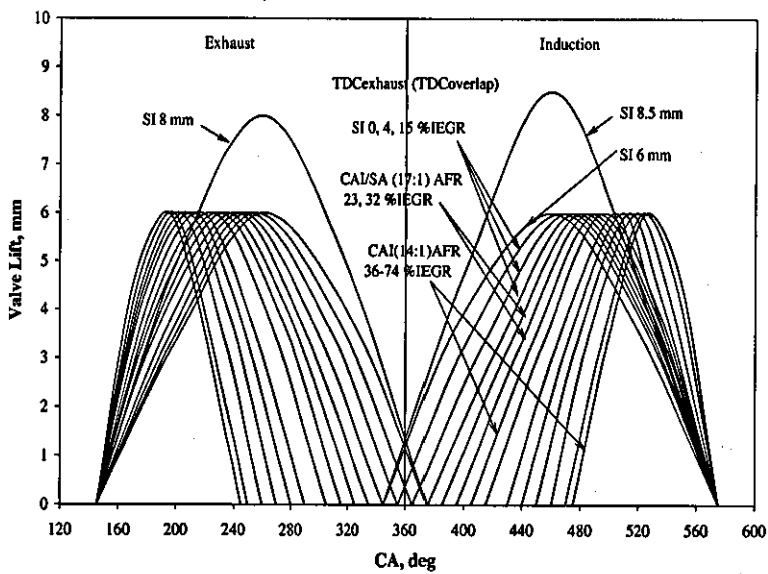
Figure 9.3: Conventional valve profiles for the SI combustion and profiles suitable for the CAI combustion.

is thus repeated. This method is named a *sequential method*. One more method for achieving the CAI combustion, named a *simultaneous method*, has also been derived and detailed explanations can be founded in [42, 43, 133].

In order to trap the various quantities of IEGR and to obtain transition from the conventional SI combustion to CAI combustion, a series of valve timings are used. Figure 9.3 summaries the valve timings and estimated quantities of the trapped IEGR.

Transition from SI to *CAI mode* is achieved by increasing the *negative valve overlap* between the exhaust valve closure event and inlet valve opening event and by reducing the valve lift. The intake and exhaust valve events are varied from a 'normal' valve events with positive valve overlap (as for a typical 4-stroke SI engine), to a very early EVC event coupled to a symmetrically very late inlet IVO event. With the increase of the negative valve overlap, a camless CAI engine goes from the conventional SI operation, through a transient period, and into CAI operation [42, 43, 54]. The valve lift of 8 mm for the exhaust valves and 8.5 mm for the inlet valves is used for the SI mode. When the engine is operated in a transient and the CAI mode, the valve lift is reduced to 6 mm for all valves (exhaust and intake). The reduction in valve lift is applied to reduce the valve dynamic loading to an acceptable level. Although, the valve lift is reduced it can still be used for the conventional SI combustion [103].

The EVC timing is varied from 15 degrees $ATDC_{exh}$ (15 crank angle degrees after TDC of *exhaust stroke*[1]) to -105 $ATDC_{exh}$ (105 crank angle degrees before TDC of *exhaust stroke*), as it is shown in Figure 9.3. The IVO timing is varied symmetrically relative to TDC_{exh}. When the distance from EVC to the TDC_{exh} is equal to the distance from TDC_{exh} to the IVO measured in crank angle degrees, the valve overlap, positive or negative, is symmetrical. When the valve overlap is symmetrical, the cylinder pressure at IVO is approximately the same as that at EVC. This allows

---

[1]Top dead centre gas exchange process-exhaust stroke (TDC_{exh}) is also known as the top dead centre overlap ($TDC_{overlap}$).

maximum recovery of the available compression work with the minimum reverse flow of exhaust gases into the intake manifold [21, 54, 133].

The EVO and IVC timings are kept constant at 35 $BBDC_{exh}$ (35 degrees crank angle before the end of expansion stroke - $BBDC_{exh}$) and 35 $ABDC_{comp}$ (35 degrees after the start of compression stroke) respectively. Other engine parameters, such as compression ratio, engine speed, intake temperature and equivalence air-fuel ratio, are kept constant at values specified in Table 9.1.

9.2   Simulation Model

The simulation of the CAI engine is carried out by combining the Aurora detail chemical kinetics code from the Chemkin III combustion package [67] with the one-dimensional fluid-dynamic Lotus Engine Simulation (LES) code [134].

The Aurora code, as explained in Chapter 5, considers the engine chamber as a single-zone reactor with a variable volume. The volume is varied with time according to the slider-crank relationship. The mixture of fuel, air and exhaust gases is assumed to be homogeneous with even spatial distribution of mixture composition and thermodynamic properties. The heat loss is calculated by using Woschni's heat transfer correlation with a temperature difference between the average gas temperature and the time averaged wall temperature [1]. The other heat losses to the engine chamber walls, blowby and crevices are not considered.

The LES is one-dimensional fluid-dynamic engine simulation code capable of predicting performance of an engine system [134]. The program can be used to calculate:

- The full and part load performance of the engine under steady-state and transient operations.

- The in-cylinder heat transfer data.

- The instantaneous gas property variations within the engine manifolds.

- Turbocharger and supercharger matching conditions.

The LES program allows the user to build a model of the entire engine by selecting engine components from a toolbox and connecting them by pipe elements.

The simulation is started with the Aurora code (the compression and expansion strokes) and continued with LES code (the exhaust and induction strokes), with a time step of 1° crank angle. Aurora is chosen due to its ability to predict accurately auto-ignition of the CAI combustion, whilst the LES code is employed due to its ability to model the instantaneous charge mixture properties in the engine manifolds. *Aurora* calculates the compression (from IVC), auto-ignition, combustion and expansion (until EVO), while the LES carries out the calculation of the *gas exchange process* (from the EVO to IVC point).

9.3   Model Validation

The results obtained by using the simulation model are validated against the experimental results. It was found that at least 30 cycles have to be calculated to reach a satisfactory degree of convergence with the experimental results. The engine specification and conditions used in the simulation are the same as those used in the experiment and summarised in Table 9.1 (*CR 10.5, engine speed 2000 rpm, bore x stroke 80.5 x 88.2, 50% IEGR, gasoline fuel (95RON) and stoichiometric equivalence air-fuel ratio*). The charge mixture pressure, temperature and composition at the IVC point is assumed or estimated. The charge pressure is assumed to be 1 bar (naturally aspirated engine). The charge temperature and composition are estimated from the amount of trapped exhaust gases obtained from the test and by assuming the mixing of the ideal gases. The detailed procedure has been reported in [103, 128, 105] and is given in Appendix B. It is very important to be able to estimate correctly the charge properties at IVC, since it is crucial for the accurate modelling of the ignition of the CAI process. The charge values at IVC are instantaneous ones and therefore difficult to measure accurately. These values greatly

depend on the flow-dynamic and gas exchange processes that take place from the
EVC to IVC points.

For the simulation of gasoline fuel 95RON, a mixture of iso-octane and n-heptane
fuels (95% of iso-octane and 5% of n-heptane by volume) is used. The detailed
chemical kinetic mechanism for a mixture of iso-octane and n-heptane fuel, which
consists of 1087 species and 4392 reactions with complete NOx chemistry, has been
developed in-house and validated successfully against the available test data. The
mechanism is able to predict auto-ignition behaviour for various fuel research octane
numbers (RON) at different temperatures and pressures and it is explained in detail
in Appendix C. The cylinder wall, piston and head are all assumed to be at the
uniform temperature of 500 K.
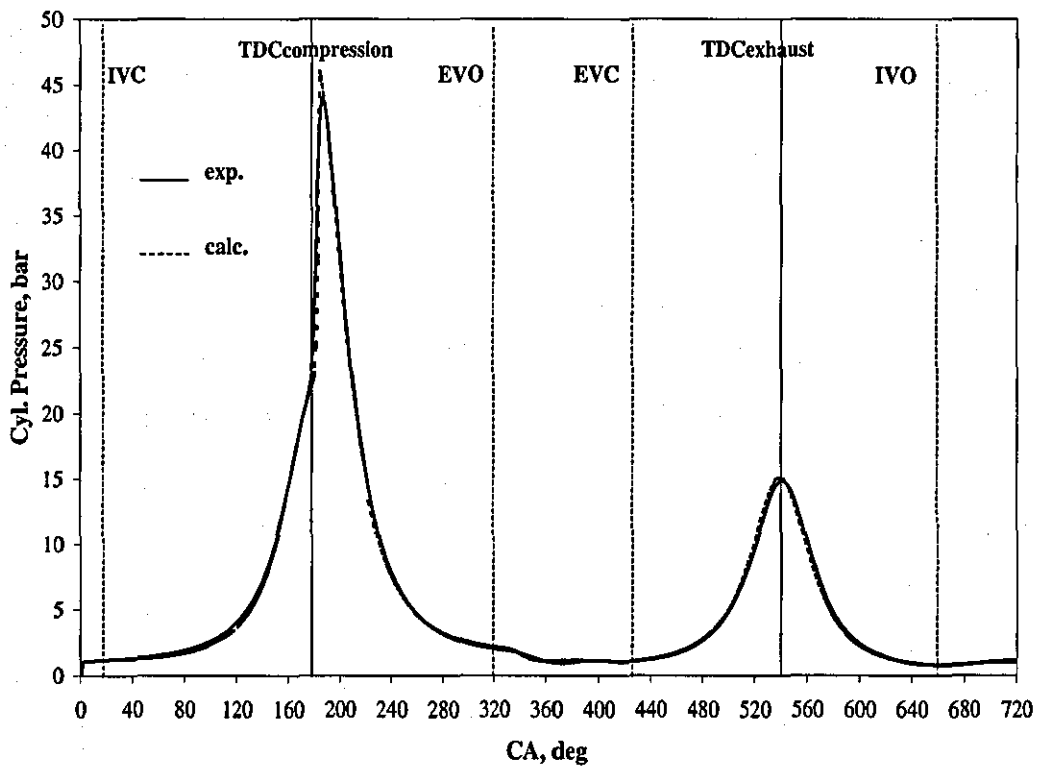
Figure 9.4: Comparison of calculated and experimental cylinder pressure histories
over complete cycle.

The calculated cylinder pressure history over complete cycle is compared to the cylinder pressure history recorded in the test and results are presented in Figure 9.4. For a better clarity the results for compression/expansion strokes and exhaust/induction strokes are zoomed and presented in Figure 9.5 and Figure 9.6 respectively.
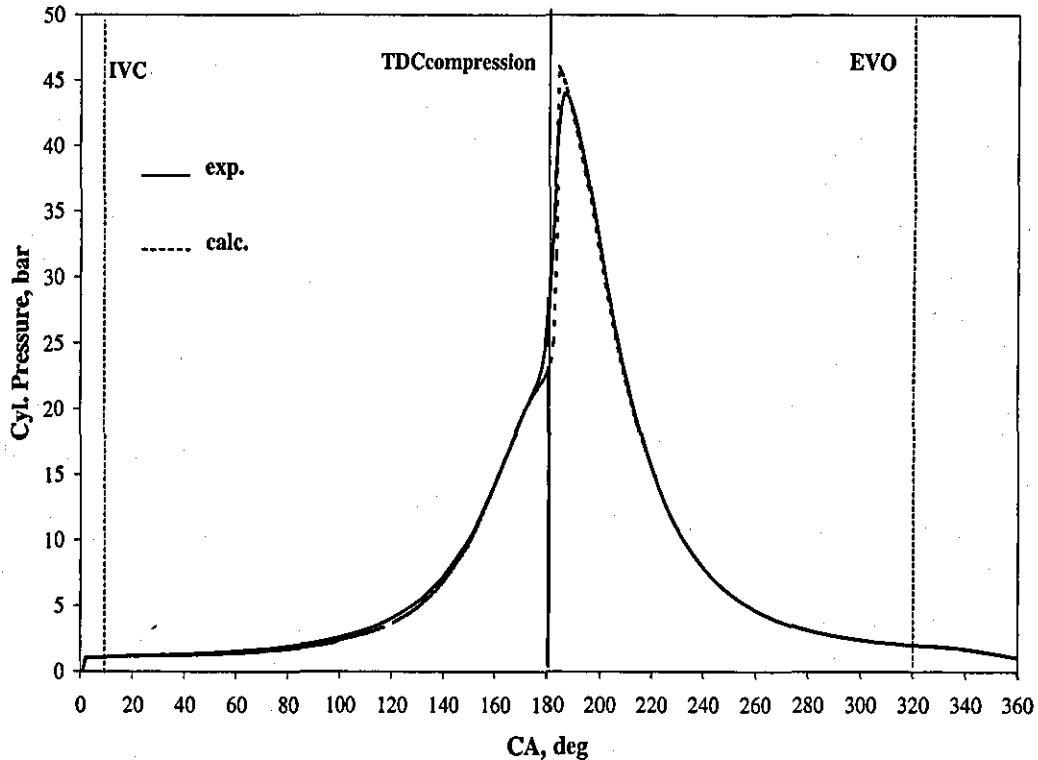
Figure 9.5: Comparison of calculated and experimental cylinder pressure histories over the compression and expansion strokes.

It can be seen that the general shape of the experimental cylinder pressure curve is well reproduced over the complete cycle. The peak cylinder pressure is over predicted due to assumptions that whole cylinder charge burns simultaneously and completely and due to the deficiency of the single-zone assumption to model temperature gradient within the charge mixture. In a real engine, the charge mixture inside the cylinder is not uniform in temperature and composition and a small portion of fuel captured in crevices will not burn. Thus the pressure gradient after ignition will be
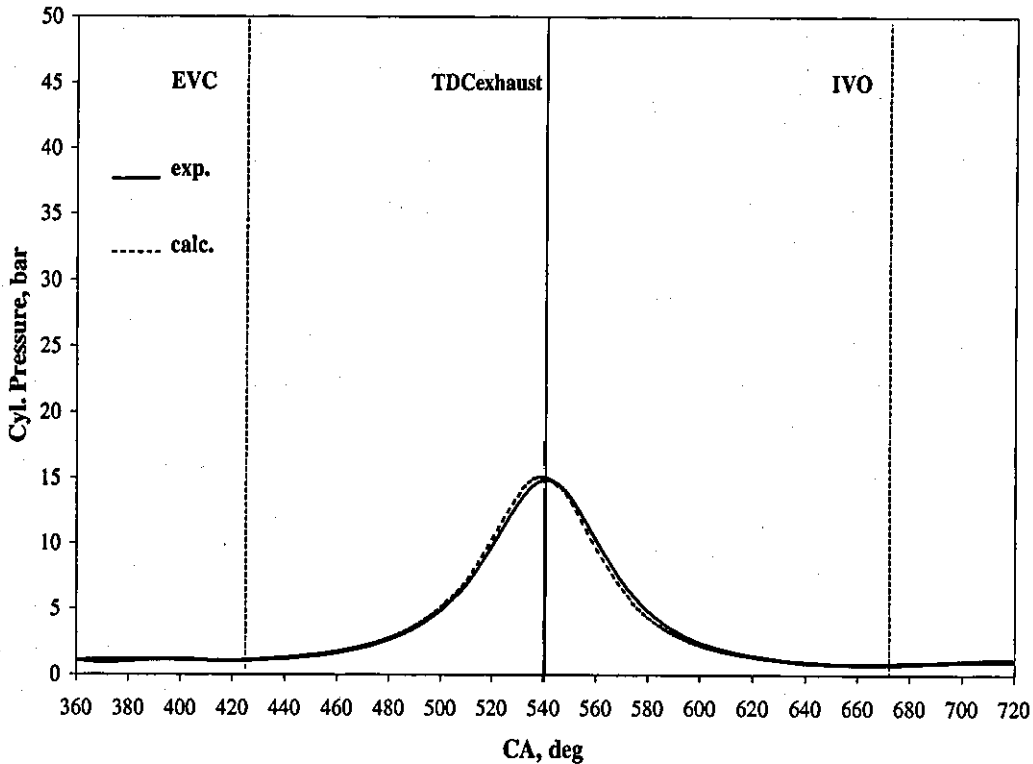
Figure 9.6: Comparison of calculated and experimental cylinder pressure histories over the exhaust and induction strokes.

lower. On the other hand the start of auto-ignition is predicted correctly. The pressure pulses (pressure waves generated by the blow-down and displacement processes) predicted by the LES code, at the start of the gas exchange process (EVO point), are also consistent with the measured ones. The comparison of the calculated and experimental values for several global engine parameters is shown in Table 9.2.

It can be seen that experimental values are generally well matched within a difference of 10%. The values of the engine parameters such as *IMEP*, *Indicated Power* and *Volumetric Efficiency* are over-predicted due to previously commented assumptions that the whole charge burns simultaneously and completely. The temperature in the exhaust manifold is matched within a difference of 1.1% while the difference for the quantity of trapped IEGR is within 4 %. It is worth emphasing that the quantity of trapped IEGR in the experiment was estimated since it could not be measured.

Table 9.2: Comparison of the calculated and experimental values for several engine parameters

Engine Parameter	Calculated	Experimental	Difference (%)
IMEP (bar)	3.78	3.50	+7.4
Indicated power (kW)	2.73	2.63	+3.6
Volumetric efficiency (%)	32.4	30.3	+6.5
Temp. in exhaust manifol. (^0C)	457	452	+1.1
Temp. at IVC point (K)	419	-	-
IEGR (%)	52	50*	+3.8

The range of the differences (errors) for the calculated engine parameters seems acceptable considering that the accuracy of the experimental data is not exactly known. Usually with a pressure transducer suited for a thermodynamic evaluation, IMEP can be determined with less than 3% difference, but sometimes this can be up to 10% [21].

It is worth noting that with the use of LES code for the modelling of the exhaust and induction process, the charge properties at IVC can be automatically calculated and used as an input to the Aurora code. This is very useful because the amount of trapped exhaust gas for a camless CAI engine is not exactly known[2].

An additional validation of the simulation model is carried out for all other points where the CAI operational mode was achieved. These points are for 32, 36, 41, 45, 55 and 59%IEGR. Comparison of the measured values for T_{exh} (exhaust gas temperature measured in the exhaust manifold) with calculated ones is shown in Figure 9.7 and in Figure 9.8 for the IMEP values.

It can be seen that the trends of the experimental results are matched with good agreement and that values of T_{exh} and IMEP are predicted within difference of 10%. The differences are consistent with the results obtain for 50%IEGR.

---

[2]The amount of trapped exhaust gas is an instantaneous value.
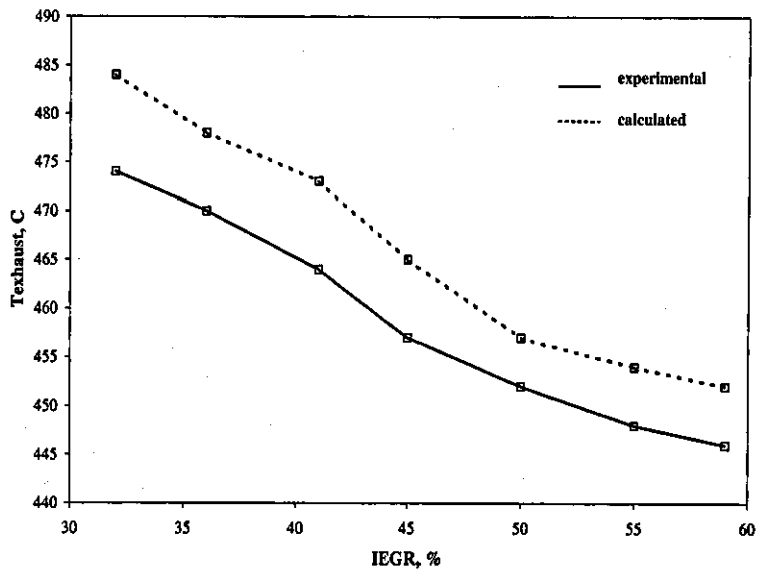
Figure 9.7: Comparison of the experimental and calculated exhaust gas temperature (in the exhaust manifold) for a various amounts of IEGR. Solid line represents experimental results and dotted line calculated results.
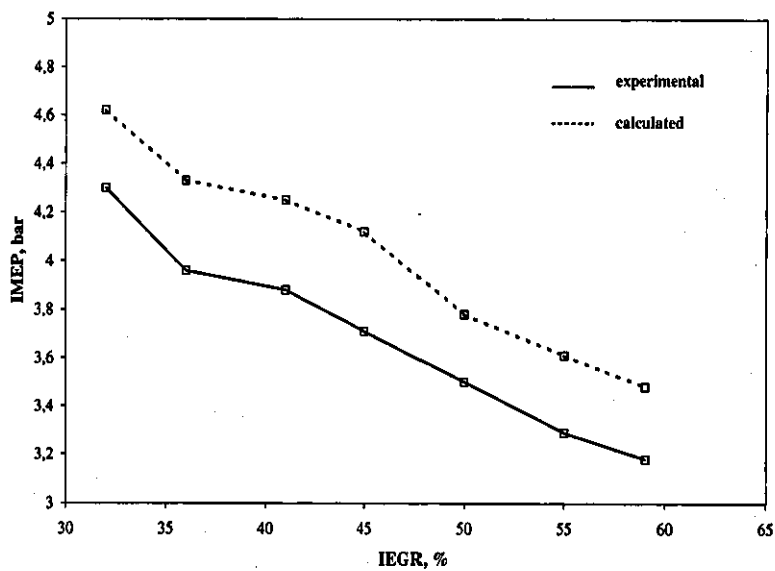
Figure 9.8: Comparison of the experimental and calculated IMEP for a various amounts of IEGR. Solid line represents experimental results and dotted line calculated results.

From above mentioned it appears that the combination of the chemical kinetics code Aurora and 1-D engine simulation code LES has the potential to be used as an engine research and development tool. However, additional calibrations of the code are still needed.

9.4 Experimental Results

Figure 9.9 shows the measured cylinder pressure histories for different quantities of IEGR obtained by increasing the negative valve overlap.
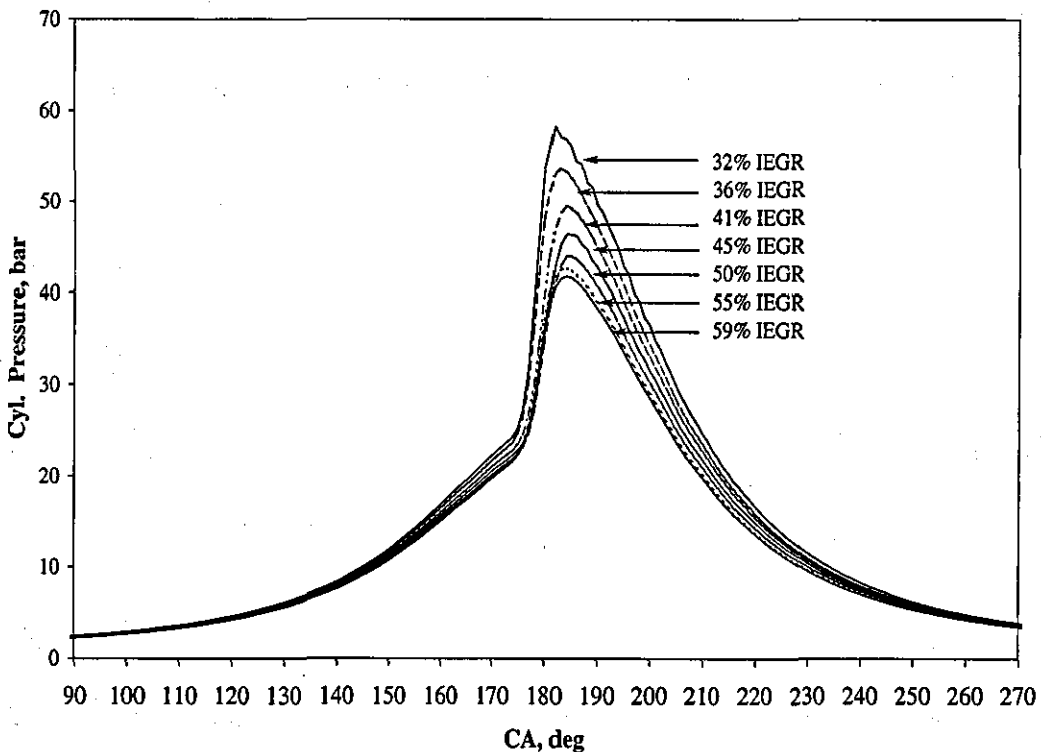
Figure 9.9: Experimental cylinder pressure curves for a various amounts of IEGR obtained by increasing the negative valve overlap.

The engine is first started to work in the SI mode and then transformed to *CAI spark assisted mode* (transient period) and finally to 'pure' *CAI mode*. Transition from the SI to CAI mode is achieved with the increase of IGER amount. This

is obtained by increasing the *negative valve overlap* between the EVC and IVO events. The valves timings are varied from a normal valve timing with positive valve overlap (as for a typical 4-stroke SI engine), to a very early EVC timing coupled to a symmetrically very late IVO timing event. The range of investigated negative valve overlap was explained in Paragraph 9.1. With increasing negative overlap, the camless CAI engine goes from the conventional SI operation, through a transient period, and into CAI operation. The EVO and IVC timings are kept constant. Other engine parameters (such as compression ratio, engine speed, intake temperature and equivalence air-fuel ratio), are also kept constant at values specified in Table 9.1.

It can be seen that the CAI operation mode is achieved at 32%IEGR and it was maintained to 59% of IEGR. For the values higher than 59%IEGR the engine is not operated due to a very low load output, which is inappropriate for the practical application.

For IEGR quantities below 32%, the CAI combustion cannot be generated and self-sustained, and it is necessary to use the spark-plug. The region below 32%IEGR is not the 'pure' CAI operational mode, but neither is it the 'pure' SI mode, since the spark is only used to ignite the charge mixture and turbulent flame propagation in the rest of unburned mixture is not observed. Instead of this, the unburned mixture is auto-ignited and sustained combustion in uniform and simultaneous auto-ignition process, as in the CAI combustion. It is highly likely that this behaviour is achieved because the charge mixture is diluted by the IEGR to such an extent that the temperature rise due to the spark ignited combustion is high enough to trigger auto-ignition in the unburned mixture.

This result indicates that the activation from the spark plug is not used as an essential combustion source as in the SI combustion strategy, but only as an assistance to auto-ignition.

Even though the region below 32%IEGR is not a 'pure' CAI operational mode it is very interesting for an investigation, because it represents the transient mode between the SI and CAI mode. Therefore, it can provide valuable information about

the influence of variable valve timing strategy on the charge properties and thus the potential to obtain control for transient operation. The importance of this region have been discussed in [54, 55, 103, 135].

It can be seen in Figure 9.9 that with a higher amount of IEGR the peak cylinder pressure is reduced which is due to influence of the IEGR chemical effects, as discussed in Section 8.3 (Chapter 8).

Ignition timing is not significantly affected with the increase of the IEGR amount, as can be seen in Figure 9.10. With the highest amount of IEGR (59%IEGR) the ignition timing is advanced only by 2^0 crank angle compared to the 32%IEGR.
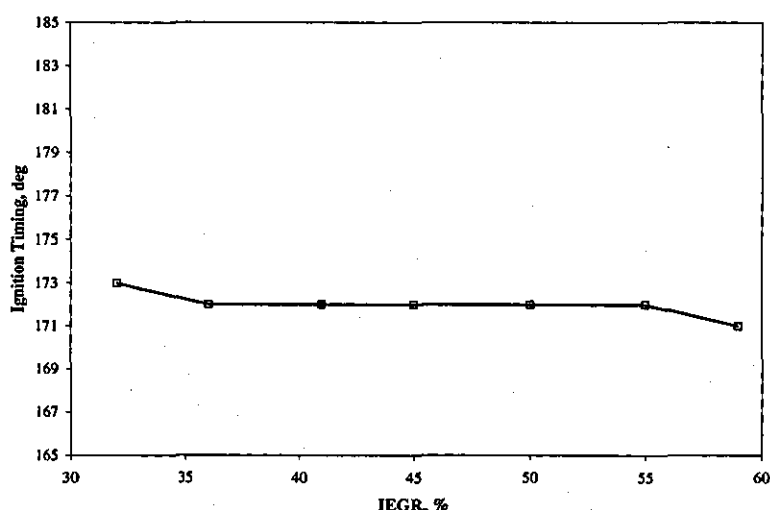
Figure 9.10: Ignition timing as a function of different amounts of IEGR.

On the other hand, Texh and IMEP are appreciable affected by the increase in the amount of trapped IEGR, as can be seen in Figure 9.7 and Figure 9.8 respectively. It can be seen that with the increase in the amount of trapped IEGR, the IMEP and Texh decrease. When a higher value of IEGR is trapped, the amount of fresh air-fuel charge is reduced which results in lower load output–lower IMEP. Consequently, the engine at lower IMEP gives reduced Texh.

9.5 Simulation Results

Analysed Valve Timing Range The analysis of the influence of variable valve timings on the gas exchange process and consequently on the engine parameters (such as trapped gas temperature, IEGR amount, load, pumping losses, volumetric efficiency), and charge mixture properties (composition, temperature and pressure) in engine manifolds is carried out by the LES code. The EVC event from 15 ATDC$_{exh}$ degrees (15 degrees crank angle after TDC of *exhaust stroke*) to -125 ATDC$_{exh}$ (125 degrees crank angle before TDC of *exhaust stroke*) is investigated (Refer to Figure 9.11).
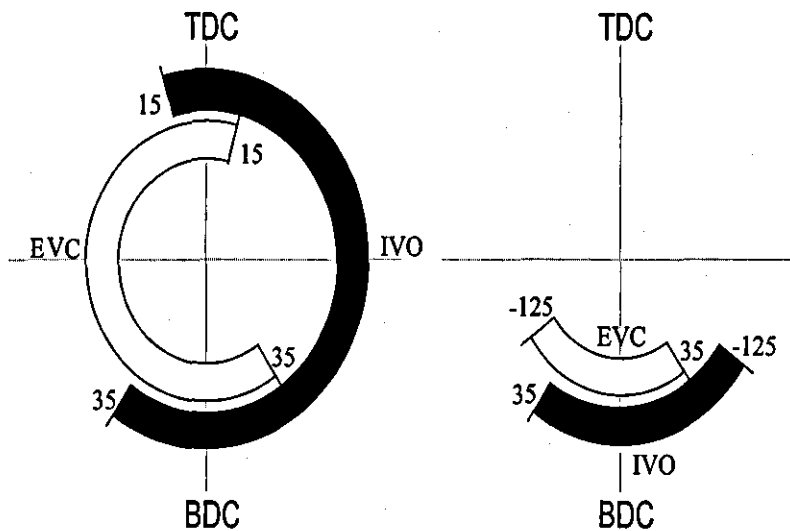
Figure 9.11: Analysed valve timings range from the positive to the negative valve overlap (in crank angle degrees).

The IVO is varied symmetrically relative to TDC$_{exh}$. The benefits of the symmetrical valve overlap were explained in Section 9.1.

The EVO and IVC events are kept constant at 35 BBDC$_{exh}$ (35 degrees crank angle before the end of expansion stroke) and 35 ABDC$_{comp}$ (35 degrees after the start of compression stroke) respectively.

The other engine parameters, such as compression ratio, engine speed, intake temperature and equivalence fuel-air ratio are kept constant at values specified in Table 9.1.

9.5.1 Influence of EVC and IVO Timings on the Engine Parameters

The gas exchange process determines the quantity of IEGR which in turn affects the combustion process and engine performance. The quantity of IEGR influences the charge mixture temperature at the end of the induction stroke (at the beginning of the compression stroke–IVC point) and therefore the ignition timing and heat release rate. Also, the quantity of IEGR determines the amount of the fresh charge and therefore affects the engine's volumetric efficiency and load.

The changes in IEGR quantity with the variations in EVC and IVO timing are shown in Figure 9.12, the changes in IMEP in Figure 9.13, and the changes in volumetric efficiency in Figure 9.14.

It can be seen that the IEGR quantity, IMEP and volumetric efficiency are mainly influenced by the EVC timing. The IEGR decreases with the later EVC because less exhaust gases are trapped. Therefore, the more fresh charge is introduced, resulting in an increase in volumetric efficiency and IMEP. From Figure 9.15 it can be noticed that the correlation between IMEP and IEGR quantities is almost linear.

Overall, the IVO timing has considerably less influence on the IEGR quantity, volumetric efficiency and IMEP, except in the two isolated regions (*'islands'*). These two *'islands'* are for a very late IVO timing (from -125 to -85 $BTDC_{exh}$) and for a relatively early IVO timing (from -20 to -5 $BTDC_{exh}$), while the EVC range is from -110 to -85 $ATDC_{exh}$. A very late IVO causes the trapped exhaust gases to expand to the pressure below the inlet manifold pressure which generates a reverse flow (at the intake valve) and thus affects the IEGR quantity and IMEP. With a relatively early IVO, the cylinder pressure is above the intake manifold pressure which again causes reverse flow and therefore influences the IEGR quantity and IMEP.
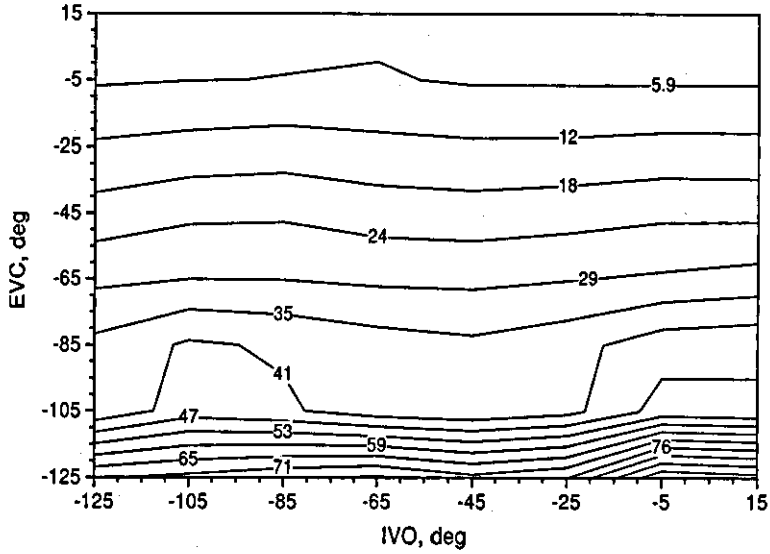
Figure 9.12: IEGR quantity as a function of EVC and IVO timings (in %).
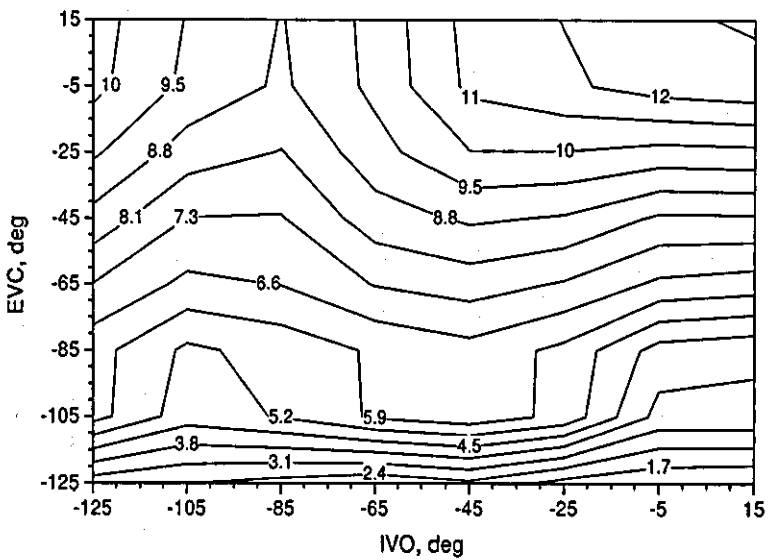
Figure 9.13: IMEP as a function of EVC and IVO timings (in bar).
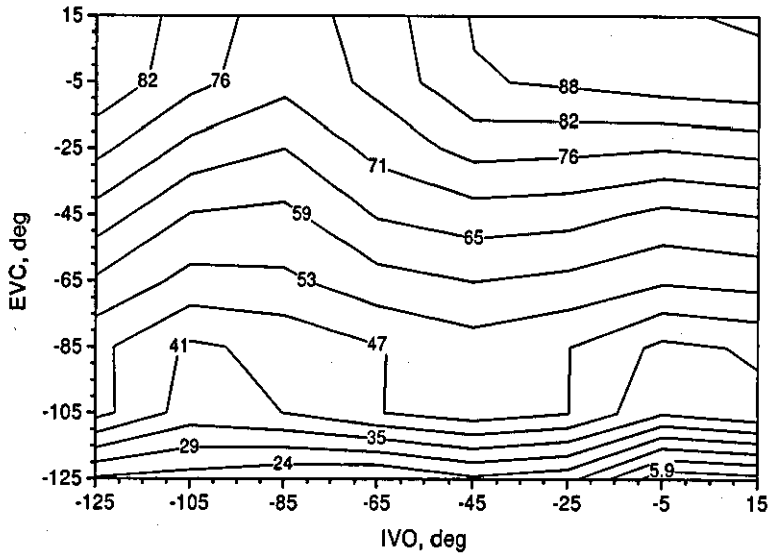
Figure 9.14: Volumetric efficiency as a function of EVC and IVO timings (in %).
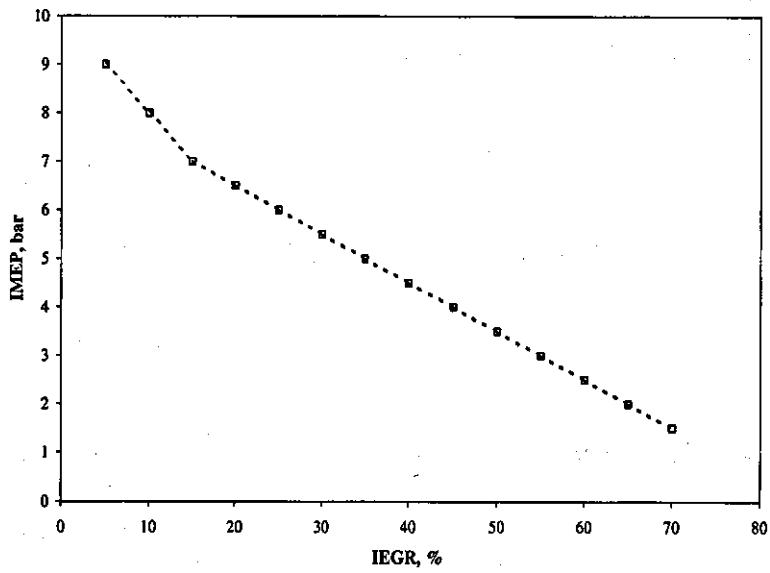
Figure 9.15: Correlation between IMEP and IEGR quantity.
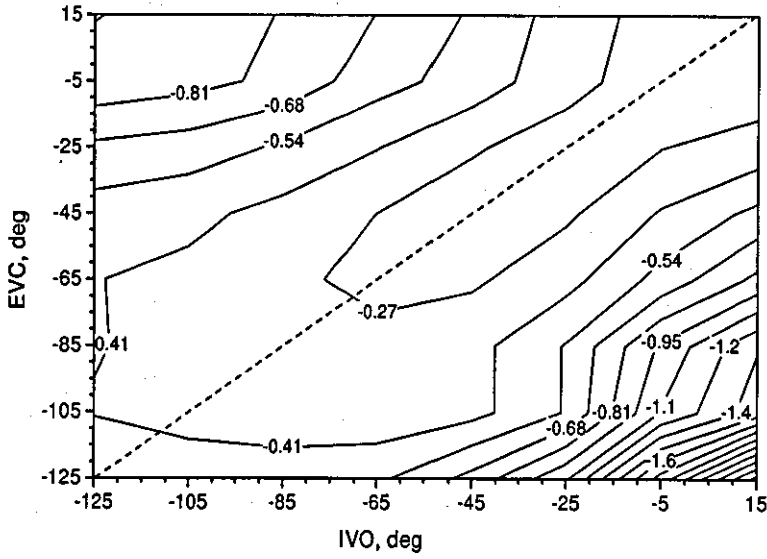
Figure 9.16: Pumping losses as a function of EVC and IVO timings (in bar).
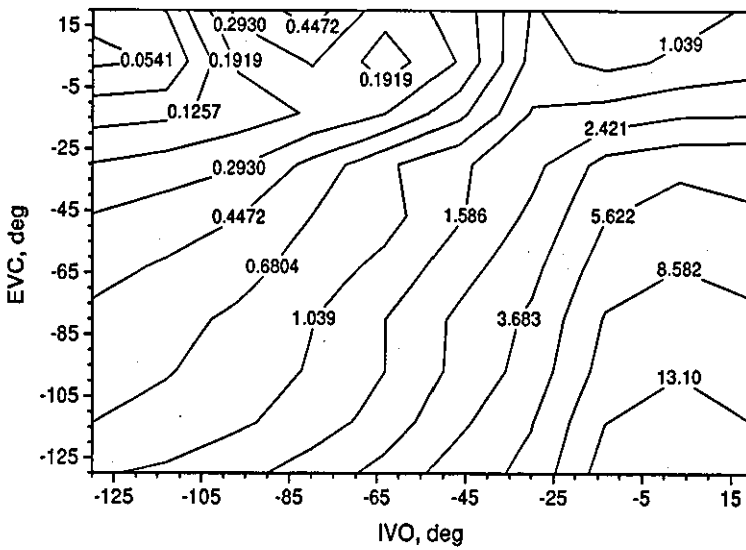
Figure 9.17: Cylinder pressure values at IVO point as a function of EVC and IVC timings (in bar).

Influence of the EVC and IVO timing on the engine pumping losses is shown in Figure 9.16. The pumping losses are evaluated from the IMEP for the exhaust and induction strokes.

It can be seen that the minimum pumping losses take place for the symmetrical EVC and IVO. When the IVO is opened symmetrically, the in-cylinder pressure is near or equal to the intake manifold pressure and the minimum pumping losses occur. For a given EVC, the IVO required for a minimum pumping loss can be found from the dashed line in Figure 9.16.

If the IVO is late it causes the trapped exhaust gas to expand to the pressure below the intake manifold pressure, as can be seen in Figure 9.17 which increases the pumping losses. On the other hand with a relatively early IVO, the cylinder pressure is above the intake manifold pressure which causes reverse flow at the intake valve and thus an increase in the pumping losses.

From the experiments performed on the single-cylinder engine and conditions specified in Table 9.1 it is found that the CAI combustion can be generated and self-sustained only for the quantities of IEGR above 32% (as explained in Section 9.1 and shown in Figure 9.9). For an IEGR quantity below this value the CAI combustion cannot be generated and self-sustained without the use of a spark-plug (transient mode). The transient mode (region) has great importance, since it can provide valuable information about the influence of a variable valve timing strategy on the charge properties and thus the potential to obtain control for this mode.

The maximum quantity of IEGR is constrained by the engine design to the 80%IEGR. Based on these facts it is decided that the region from 23% IEGR (transient mode) to 80% IEGR is interesting for the investigation. It can be seen in Figure 9.12 that this range of IEGR is obtained for the EVC timing from -45 to -125 $ATDC_{exh}$ and the symmetrical IVO timing from -45 to -125 $BTDC_{exh}$. Therefore, the analysis of the influence of EVC and IVO timings on the charge properties in engine manifolds will be performed in this region.

9.5.2 Influence of EVC and IVO Timings on the Charge Mixture Properties

As was explained at the beginning of this Chapter, the *gas exchange process* in the 4-stroke engine takes place between the first valve open event-EVO and the last valve close event-IVC (i.e in the exhaust and induction stroke or in the post and pre combustion periods). Therefore, the gas exchange process comprises the following characteristic points:

- EVO. This usually occurs during the last quarter of the expansion stroke.

- EVC. This takes place in the exhaust stroke.

- TDC_{exh}. This is the point in the exhaust stroke where the piston reaches the top dead centre of the cylinder (before descends in the induction stroke).

- IVO. This occurs in the induction stroke, symmetrically to EVC.

- IVC. This takes place either at the end of the induction stroke (beginning of compression stroke) or in the first quarter of the compression stroke.

The influence of EVC and IVO timings on the charge mixture temperature will be investigated at these characteristic points[3]. The charge mixture temperature is chosen because it is the most influential factor for auto-ignition timing and heat release rate, hence for the control of CAI combustion.

Influence on the temperature at the EVC point The effect of EVC and EVO timings on the IEGR temperature at the EVC point is shown in Figure 9.18.

It can be seen that the temperature at EVC is solely a function of the EVC timing, it decreases with the earlier EVC and thus with the higher IEGR quantity (see Figure 9.12). The reason for this behaviour is the high heat capacity of the IEGR, since it consists mainly of the inert gases. A high heat capacity effectively alters

---

[3]The EVO point is not included in the investigation.
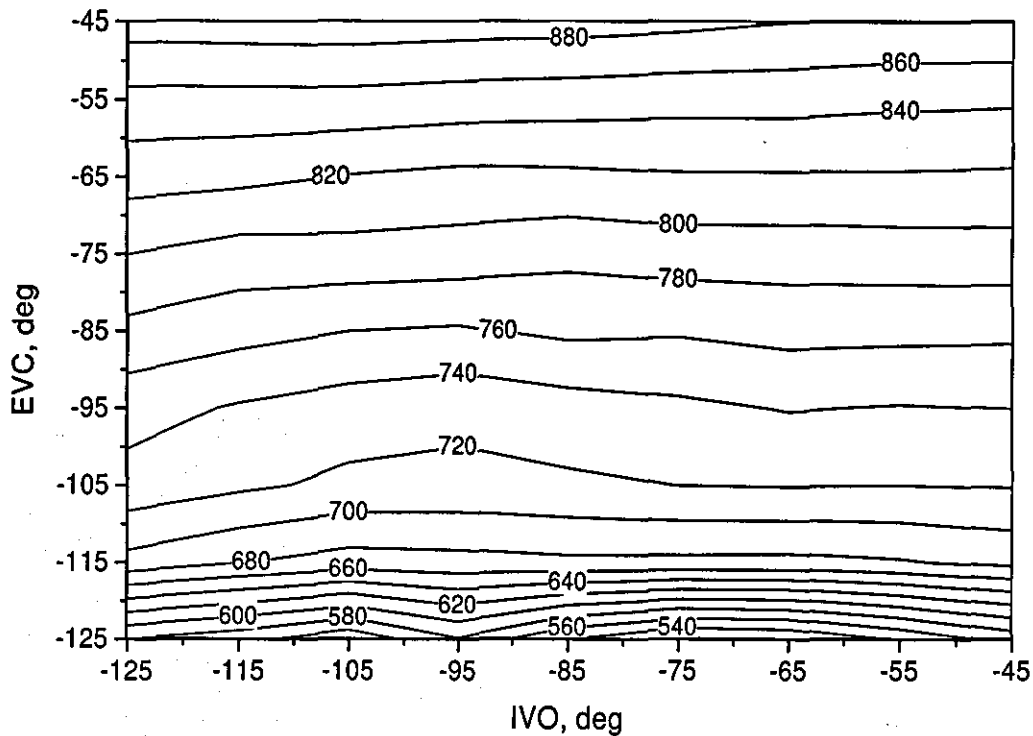
Figure 9.18: IEGR temperature at the EVC point as a function of EVC and IVC timings (in K).

the rate of heat release and thus the temperature rise, as discussed in Chapter 8. Therefore, the higher the IEGR amount is trapped the lower the IEGR temperature at EVC is. This result is consistent with experimental results, i.e. the temperature of the exhaust gas (measured in the exhaust manifold) decreases with the increase in the amount of IEGR (Refer to Figure 9.7). Similar observations have been reported from other experiments [124, 129, 136].

Influence on the temperature at TDC point gas exchange process-TDC$_{exh}$
The changes in the IEGR temperature at TDC$_{exh}$ as the result of EVC and IVO timings are shown in Figure 9.19.

It is clear that the temperature is a primary function of the EVC timing with a negligible influence from the IVO timing. However, the IVO timing has a strong
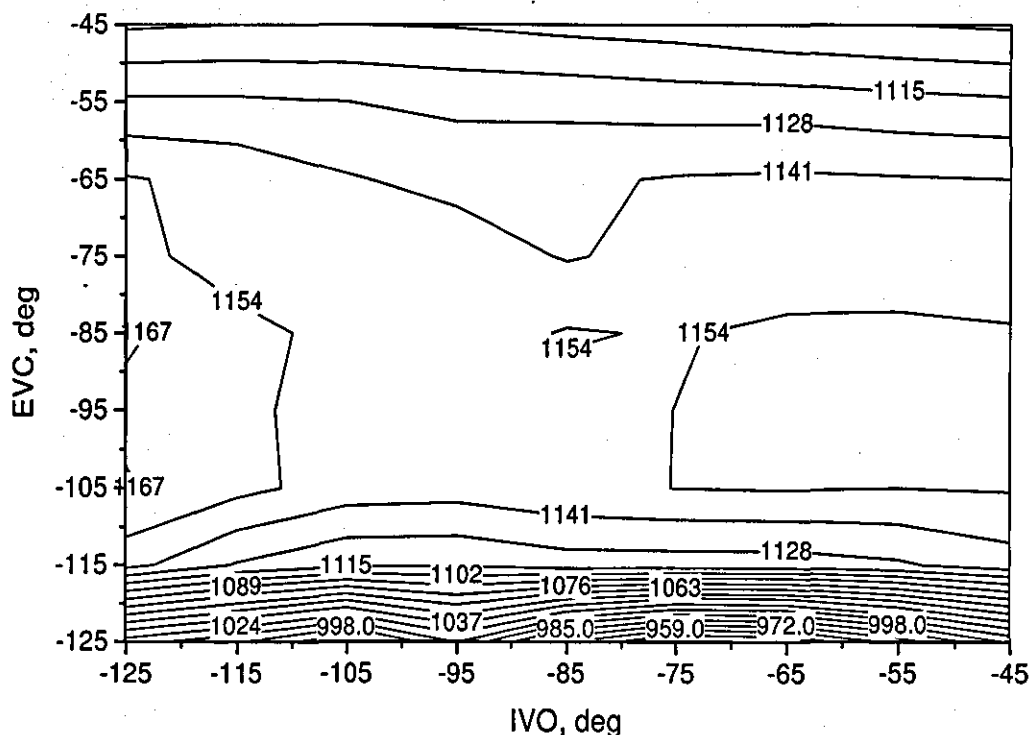
Figure 9.19: IEGR temperature at the TDC_{exh} point as a function of EVC and IVC timings (in K).

influence in two narrow regions, the region of a very late IVO (from -125 to -110 $BTDC_{exh}$, EVC from -110 to -85 $ATDC_{exh}$) and in the region of a relatively early IVO (from -75 to -70 $BTDC_{exh}$, EVC from -110 to -85 $ATDC_{exh}$). In these two regions the IVO influences the IEGR temperature by the existence of a reverse flow, as discussed in Section 9.5.1.

It can be seen that for a very high IEGR quantity and a very early EVC (from -125 to -115 $ATDC_{exh}$), the temperature rise from the compression heating is reduced by the presence of the high amount of inert gases in IEGR . As the IEGR quantity decreases, the charge heat capacity becomes lower and the temperature gain becomes higher resulting in the temperature increase (region from -115 to -75 $ATDC_{exh}$). For a further decrease in IEGR quantity (region -70 to -45 $ATDC_{exh}$), the temperature

starts to decrease again. This is due to a lower charge heating caused by the shorter compression duration (compression of the IEGR in the exhaust stroke). With the later occurrence of EVC, the distance to TDC_{exh} is reduced which leads to the shorter compression duration.

Therefore, the temperature rise during the compression of IEGR in the exhaust stroke is the combined effect of two factors: (i)the IEGR quantity and (ii)the amount of compression heating.

However, there is a region where the IEGR temperature is above 1100K (for EVC between -115 and -45 $ATDC_{exh}$). In this region it is highly likely that a secondary combustion due to IEGR will occur [20, 55, 137]. This combustion might have a strong impact on the unburned hydrocarbons (UHC) in the IEGR and fuel captured in crevices. However, with the LES code, modelling of the UHC and fuel captured in crevices cannot be performed in this stage, but improvements are due in course.

Influence on the temperature at the IVO point   At the IVO point the induction valve is opened and a fresh air-fuel charge is mixed with the hot compressed IEGR. The changes in the IEGR temperature at the IVO point as a function of EVC and IVO timings is presented in Figure 9.20.

It can be seen that the temperature is mainly influenced by the IVO timing, it decreases with the later IVO. With the later IVO, the cylinder volume increases causing a higher heat transfer loss which in turn reduces the IEGR temperature and therefore decreases the charge mixture temperature.

However, there exists two regions where the IEGR temperature is a function of both IVO and EVC timings:

i) The region for a very late IVO timing (from -125 to -105 $BTDC_{exh}$),

ii) The region for a very early EVC timing (from -125 to -115 $ATDC_{exh}$).

In these regions the IEGR temperature is influenced by the reverse IEGR flow
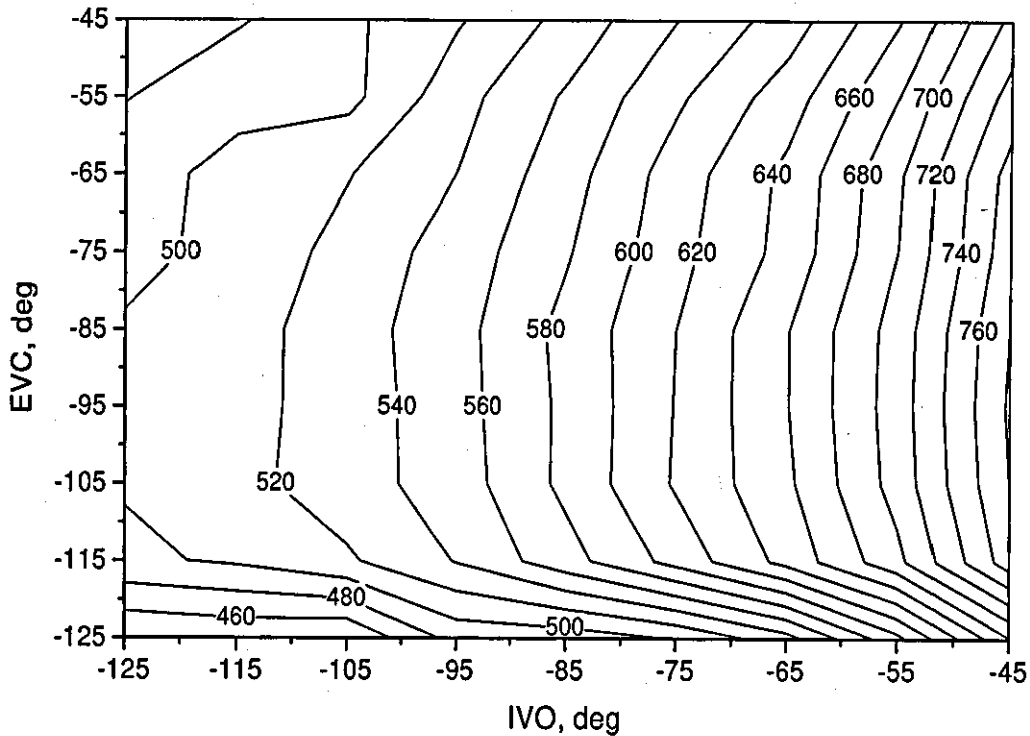
Figure 9.20: IEGR temperature at the IVO point as a function of EVC and IVC timings (in K).

(caused by the IVO) and by a considerable quantity of the IEGR, i.e. its high heat capacity (caused by the EVC).

Influence on temperature at the IVC point   The impact of the valve timing on the charge mixture temperature at IVC is shown in Figure 9.21.

This temperature is closely connected to the IEGR quantity, temperature at TDC_{exh} and intake air temperature. It can be seen that the temperature of the resulting charge mixture varies considerably (from 379 to 424 K) and that three regions exist in which the temperature is determined only by the EVC or only by the IVO timing or by both timings.

In the *first region*, a very early EVC (from -125 to -115 ATDC_{exh}), the temperature is
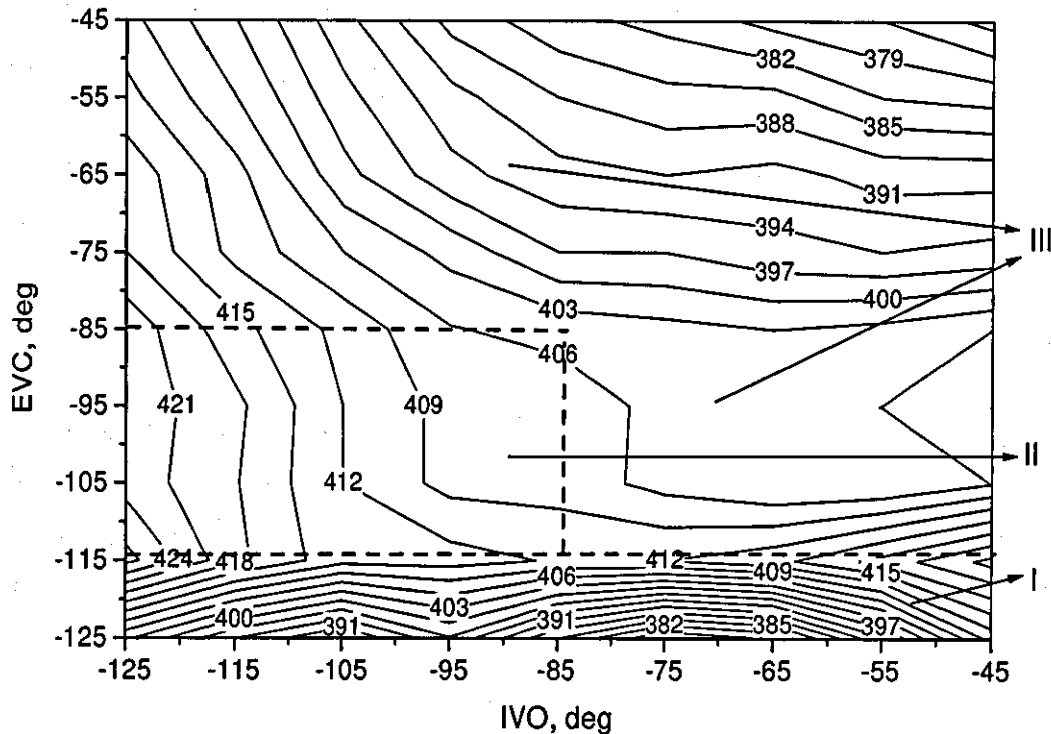
Figure 9.21: Charge mixture temperature at the IVC point as a function of EVC and IVC timings (in K).

determined mainly by the EVC timing. This region is characterised by the highest charge mixture temperature (424K) and the highest temperature gradient (from 424K to 382K).

The highest mixture temperature achieved in this region (424K) is due to the mixing of a large amount of hot IEGR (about 70%) with a small amount of cold fresh air-fuel charge. The charge mixture in this region has a high temperature combined with a high dilution which is very favourable for the CAI combustion as discussed in Chapter 7. It can be expected that this mixture will auto-ignite relatively early in the following cycle, producing a less intense heat release rate (longer combustion duration) and low peak cylinder pressure. This behaviour has been reported in [55, 115].

The highest temperature gradient in this region is the consequence of a significant temperature difference at TDC_{exh} (Refer to Figure 9.19) and the existence of reverse flow at an asymmetrical IVO (Refer to Figure 9.17).

Temperature in the *second region* (EVC from -115 to -85 $ATDC_{exh}$ and IVO from -125 to -85 $BTDC_{exh}$), is primary influenced by the IVO timing. The temperature in this region changes from 421K to 406K which is considerably lower in comparison to the change in the first region. Also, it can be noticed that the temperature gradient in this region is considerably lower than that in the first region.

In the second region the IEGR quantity is nearly constant ($\approx$ 40%) (Refer to Figure 9.12) and therefore the mixing and gas exchange processes are mainly determined by the amount of fresh charge, i.e. by IVO timing. A low variation in charge mixture temperature is due to small differences in temperature at the TDC_{exh} point. The mixture in this region will be expected to auto-ignite later than the mixture in first region and to produce a higher heat release rate and peak cylinder pressure. This observation has been reported in [55, 115].

The rest of the map is the *third region* where the temperature is affected by both EVC and IVO timings. The temperature of resulting mixture in this region varies from 415 K to 379K and it is determined by a relatively low IEGR quantity and the high temperature at the TDC_{exh} point. The existence of a relatively high temperature gradient (from 415K to 379K) for the EVC from -85 to -45 $ATDC_{exh}$ and the IVO from -125 to -45 $BTDC_{exh}$, is mainly due to the influence of temperature variations in IEGR (caused during the compression process of IEGR in the exhaust stroke) and less due to the influence of reverse IEGR flow (at the IVO point). On the other hand a relatively small temperature gradient (from 403K to 379K) for the EVC from -115 to -85 $ATDC_{exh}$ and the IVO from -85 to -45 $BTDC_{exh}$, is due to the larger influence of the reverse flow than that of the temperature variations in IEGR.

A relatively low mixture temperature and small IEGR quantity in the third region, may cause mixture auto-ignition not to occur and require the spark-plug to be used

to initiate the auto-ignition. The dilution of the resulting charge and the temperature rise from the spark-ignited combustion will be high enough to trigger the auto-ignition in the remaining unburned mixture and to sustain the CAI combustion in the way explained in Section 9.4.

9.5.3 Influence of the EVO and IVC Valve Timings on Engine Parameters and Charge Properties

From the test results obtained using the single-cylinder research engine equipped with the FVVT system (explained in Section 9.1) and from the experiments performed by Koopmans, L. and Denbratt [54] it was found that EVO and IVC timings have minor influence on the gas exchange process in a CAI engine. The EVO timing has the major influence on pressure waves generated by the blow down and displacement processes. This result is in agreement with the test results reported in [21]. Nevertheless the pressures waves may have an influence on the IEGR quantity trapped at the EVC point, but this influence is negligible in comparison to the influence of the EVC and IVO timings [55].

The IVC timing has a very low impact on the engine parameters as it mainly influences the effective displacement volume and effective compression ratio. This result is also in agreement with the test results reported in [21].

9.6 Summary of Valve Timing Effect on the Gas Exchange Process in a CAI Engine

The CAI ignition is determined by the charge mixture temperature and composition and, to a smaller extent, pressure. In this way, CAI combustion is achieved by controlling the temperature, composition and pressure of the charge mixture at the beginning of the compression stroke (IVC point). As the CAI combustion is kinetically controlled it means that the rate of heat release depends on correct combustion phasing and is closely linked with the ignition delay. Therefore, the successful control strategy has to be able to control the charge mixture temperature, composition

and pressure at the IVC point over the entire load/speed range.

It was demonstrated that the use of internal exhaust gas recirculation (IEGR) has the potential for controlling the CAI combustion. The IEGR was accomplished by the Lotus AVT system, a fully variable valve train (FVVT) system. This system enables quick changes in an amount of trapped hot exhaust gases inside the cylinder (5-20 cycles in dependence of the engine load and speed) and therefore influences the charge mixture temperature, composition and pressure. The AVT system enables individual control of the each of four valve events: (1) exhaust valve open (EVO), (2) exhaust valve closure (EVC), (3) inlet valve open (IVO) and (4) inlet valve closure (IVC).

The timing of these valve events plays an important role in the *gas exchange process*, the process that takes place between the first valve open event (EVO) and the last valve close event (IVC). The gas exchange process has a strong influence on engine parameters and charge mixture properties in the engine manifold (IVC point) and therefore on the control of CAI combustion [21].

The influence of the variable valve timings on the gas exchange process in a CAI engine fuelled with standard gasoline fuel (95RON) was analysed by the experimental and modelling approaches. The single-cylinder research engine equipped with the Lotus AVT system was used for the experimental study while the combined code consisting of a detailed chemical kinetics code and one-dimensional fluid dynamics code was used for the modelling study.

The results obtained indicate that the variable valve timing strategy has a strong influence on the gas exchange process and therefore on the CAI combustion and engine parameters. This investigation has revealed the following:

1. *Influence of the variable valve timing strategy on the engine parameters*:

   - The quantity of trapped exhaust gases (IEGR) is mainly determined by the EVC timing.

- The IEGR quantity affects other engine parameters such as load, indicated power and volumetric efficiency. In that way it can be concluded that the engine parameters are mainly influenced by the EVC timing.

- The IVO timing has an important influence on the pumping losses and the reverse flow of IEGR.

2. *Influence of the variable valve timing strategy on the charge mixture properties at the characteristic points*:

- A relatively surprising result about the IEGR temperature at the EVC point has been obtained. The more IEGR captured (by the earlier EVC), the lower the IEGR temperature is. This is the result of high charge heat capacity due to the presence of a large amount of inert gases which effectively reduces the temperature rise.

- The IEGR temperature at TDC_{exh} point is determined by two factors:

  i) The IEGR quantity.

  ii) The amount of compression heating.

- The existence of region where the IEGR temperature was above 1100K was observed. Therefore, it is highly likely that the combustion of IEGR will occur in this region.

- The temperature of the charge mixture (air/fuel/IEGR) at the IVO point is mainly the function of the IVO timing. With the later IVO the charge mixture temperature decrease is due to reduced IEGR temperature, caused by the higher cylinder volume and heat transfer losses. However, in two narrow regions of early IVO and early EVC, the charge mixture temperature is influenced by both IVO and EVC timings.

- The temperature of the charge mixture (air/fuel/IEGR) at the IVC point is closely connected to the IEGR quantity, the temperature at the TDC_{exh} point and the intake air temperature. In that way the charge mixture temperature is determined by two factors:

i) The EVC timing.

ii) The IVO timing.

- The existence of three regions (at the IVC point) where the charge mixture temperature is controlled by different factors. In the first region only by the EVC timings, in the second region only by IVO and in the third by both EVC and IVO timings.

- As a consequence of the different control factors considerable temperature variations in these regions were noted. The highest temperature variations were in the first region, the lowest in the second region and a medium variation in the third region. These temperature variations have a strong influence on auto-ignition and further combustion.

- The potential for EVC and IVO timings to control the mixture composition, temperature and pressure at the IVC point was noted.

3. The EVO and IVC timings have minor influence on the gas exchange process in a CAI engine. The EVO has a major influence on the pressure waves generated by the blow down and displacement processes. Nevertheless the pressure waves might influence the IEGR quantity trapped at EVC point, but it was negligible in comparison to the influence of the EVC and IVO timings. The IVC has a very low impact on the engine parameters as it mainly influenced the effective displacement volume and effective compression ratio.

From the results presented it appears that the use of a variable valve timing strategy has the potential to control the charge properties at the IVC point which is the key for successful control of auto-ignition, further combustion and engine parameters in a CAI engine.

Chapter 10

Conclusions

A new combustion principle in internal combustion engines, Controlled Auto Ignition (CAI) combustion, was analysed. In CAI combustion, which combines features of spark ignition (SI) and compression ignition (CI) principles, air/fuel mixture is premixed (in the some way as in SI combustion) and auto-ignited by piston compression (as in CI combustion). Ignition is provided in multiple points, gives the charge a parallel energy release, resulting in uniform and simultaneously auto-ignition and chemical reaction throughout the whole charge without flame propagation. Therefore, CAI combustion is dominated by the chemical kinetics of air/fuel mixture with no influence of turbulence.

The CAI engine offers benefits compared to *spark ignited* engines. These are:

⇒ A higher efficiency due to elimination of throtlling losses at part and idle loads.

⇒ There is a possibility to use high compression ratios since it is not knock limited and

⇒ An appreciable lower NO_x emission ($\approx 90\%$) due to much lower combustion temperature.

The CAI engine offers benefits compared to *compression ignited* engines, also. These are:

⇒ A considerably lower NO_x ($\approx$ 90%) and particle matters (PM) emissions ($\approx$ 50%). Reduced NO_x emission is, same as for SI engines, due to much lower combustion temperature, while reduced PM emission is due to premixed air/fuel mixture and therefore elimination of fuel rich zones.

⇒ A potential benefit of CAI engine might be lower cost than CI engine because it would likely use lower pressure fuel injection equipment

In comparison to both SI and CI engines, there are advantage in fuel-flexibility, since a wide range of fuels can be used as CAI combustion it is not knock constrained.

However, there are several disadvantages of CAI engine that limits its practical application, such as:

- high levels of hydrocarbon and carbon monoxide emissions,

- high peak pressures,

- high rates of heat release,

- reduced power per displacement and

- difficulties in starting and controlling the engine.

Controlling the operation over a wide range of loads and speeds is probably the major difficulty facing CAI engines. Controlling is actually two-components as it consists of auto-ignition phasing and controlling the rates of heat release. As CAI combustion is controlled by the chemical kinetics of air/fuel mixture, the auto-ignition timing and heat release rate are determined by the charge properties such as temperature, composition and pressure. Therefore, changes in engine operational parameters or in types of fuel, result in changing the charge properties, hence, the auto-ignition timing and rate of heat release.

The research aims of this Thesis, were to analyse influences of fuel composition, engine operational parameters, internal exhaust gas recirculation (IEGR) and variable

valve timing strategy on the auto-ignition timing and the rate of heat release in a CAI engine suitable for transport applications. The CAI engine environment was simulated by using single-zone, homogeneous reactor model with in a time varying volume, according to the slider-crank relationship. The model used detailed chemical kinetics and distributed heat transfer losses according to Waschini's heat transfer correlation [1].

The results from the research revealed the following:

1. Auto-ignition starts when the temperature of the reactive air/fuel mixture increases sufficiently (>1100K) that the high temperature chain branching sequence ($H+O_2 \Leftrightarrow OH+O$) takes place and further dominates the remainder of the overall reactions in CAI combustion process. This reaction is essentially independent of the fuel type, and therefore for *all hydrocarbons fuels*, the main ignition occurs at approximately the same temperature (>1100K).

   Even though, the main auto-ignition temperature is the same for all hydrocarbons fuel, *fuel structure and composition* plays an important role in determining the start of auto-ignition and further combustion process. Paraffinic fuels with long straight-chain structure, such as *n-heptane*, characterised by a two stage ignition process (cool flame ignition and main ignition stage) ignite easier than paraffinic fuels with branched-chain structure, such as *iso-octane*, characterised with single stage ignition process, due to heat released at the cool flame stage, which brings reactive air/fuel mixture quicker to the main auto-ignition temperature. The former fuels have low octane numbers, so there is a need for low inlet temperature to start auto-ignition. Later fuels have high octane numbers and request relatively high inlet temperature.

2. **Engine operational parameters** influence CAI combustion in the way that

   ⋆ *Inlet temperature* has the greatest influence, because even small changes (10K) have a significant impact on auto-ignition timing. Higher inlet

temperatures promote chemical reaction rates and thus advances auto-ignition timing and vice versa.

⋆ *Compression ratio* has a similar effect on auto-ignition timing as inlet temperature, higher compression increases the charge temperature and advances the ignition auto-timing, while lower compression ratio retards.

⋆ *Fuel-air ratio* has a prominent influence on auto-ignition timing, in such a way that the leaner mixture is more favourable for auto-ignition independently of the types of fuel. Leaner mixture is more favourable due to lower thermal charge energy (inlet temperature) needed for its initiation as the result of less amount of fuel. However, if the mixture is too lean it ignites later due to higher dilution, which reduces temperature rise from compression heating.

⋆ Changing the *engine speed* changes the amount of time for the auto-ignition chemistry to occur relative to the piston motion. With an increasing in engine speed, auto-ignition timing is retarded and vice versa.

∗ *Fuels with single-stage ignition process* have considerably less variation in auto-ignition timing with changes in fuel loading and engine speed, than fuels with *two-stage ignition process*.

∗ *Fuels with single-stage ignition process* would therefore require less adjustment of engine parameters to maintain optimal ignition timing, over the required engine load/speed ranges.

3. Using of **internal exhaust gas recirculation (IEGR)** by fully variable active valve train (AVT) system shows potentials in controlling CAI combustion. IEGR has a two-fold effect

- *Thermal effect*, which advances the auto-ignition timing by raising the temperature and changing the composition of inlet air/fuel charge in the mixing process with hot trapped exhaust gases. Thermal effect of the IEGR could be accessed as positive since it reduces the necessity for

the inlet air preheating and eliminates the dependence on the operating conditions.

- *Chemical effect*, which retards the auto-ignition timing as well as slowing down the rate of heat release by simultaneous influence of several different effects, such as: dilution of the charge mixture, changing of the charge mixture heat capacity, increasing the concentration of some exhaust species and influencing the radicals' production and destruction reactions.

* *Fuels with two-stage ignition process*, need lower amounts of IEGR for initiation of auto-ignition and sustaining complete combustion in comparison to *fuels with single-stage ignition process*. On the other hand, *fuels with single-stage ignition process*, have higher tolerance towards IEGR than *fuels with two-stage ignition process*.

4. **Variable valve timing strategy** has a strong influence on the gas exchange process, which in turn has a significant effect on engine parameters and charge properties. Hence, on CAI combustion.

- o Quantity of trapped exhaust gases-IEGR is determined solely by the EVC timing. The earlier the EVC, the higher the IEGR quantity and vice versa.

- o *Engine parameters* are mainly affected by IEGR quantity. Hence, by EVC timing.

- o IVO timing influences pumping losses and reverse flow of trapped exhaust gases.

- ▷ IEGR temperature at EVC point is indirectly proportional to IEGR quantity. The more IEGR captured the lower the temperature,(as the result of high charge heat capacity), due to the presence of a large amount of inert gases, which reduces temperature rise from compression heating.

▷ IEGR temperature at TDC_{exh} point is determined by two factors:

i) The IEGR quantity.

ii) The amount of compression heating.

▷ Temperature of charge mixture (air/fuel/IEGR) at IVO point is mainly the function of the IVO timing. With the later IVO charge mixture temperature decrease is due to reduced IEGR temperature, caused by higher cylinder volume and heat transfer losses. In narrow regions of late IVO and early EVC, charge mixture temperature is influenced by both IVO and EVC timings.

▷ The charge mixture temperature at IVC point is closely connected to the IEGR quantity, temperature at TDC_{exh} point and intake air temperature. In that way, the charge mixture temperature at IVC point is determined by two factors:

i) The EVC timing.

ii) The IVO timing.

As a consequence, the existence of three regions with different temperature gradients was observed. In the first region the temperature is determined only by EVC timing, in the second region it is determined only by IVO timing and in the third it is determined by both timings EVC and IVO. It is highly likely that in the real CAI engine, the existence of regions with different temperature and composition gradient will be founded.

▷ EVO and IVC timings have minor influence on gas exchange process, engine parameters and charge properties, hence CAI combustion.

In conclusion, it could be said that CAI has the potential to be highly efficient, with low emissions, and therefore a third combustion strategy in internal combustion engines for use in transport, marine, electric power generation and pipeline pumping applications. Engine controlling over wide load/speed ranges, as the most

demanding problem, is highly likely to be resolved in the near future by using internal exhaust gas recirculation, obtained by independently controlled variable valve timings along side with using mixtures of various fuels and technologies, such as stratification of fuel/air mixtures and the use of fuel additives. In the meantime, it is more realistic it is to use *'hybrid engine concepts'*, SI/CAI or CI/CAI, where the engine will be operated in CAI mode at low power and in SI mode or CI mode at high power. This hybrid concept will take advantage of the all benefits of CAI engine at low power conditions, while eliminating the power limitations and startability problems of CAI engines.

10.1 Further Research

Further research could be implemented in the following areas:

1. **Cold Start.** To develop concepts capable of overcoming the challenge of ignition in cold CAI engines without compromising the warm engine performance. CAI combustion strategy is strongly dependent on the charge temperature. During cold start, the air/fuel charge receives no pre-heating from the intake manifolds and ports, and the heat transfer from the compressed charge to the cold cylinder walls is high. The combination of these effects can significantly reduce the in-cylinder charge temperature and even prevent the CAI engine from firing. Based on previous researches in CI engines few solutions appears to be considered:

   i) The engine could be started as a conventional SI engine, then be switched to CAI mode after a short warm-up. This solution has been performed in several test and provided promising results (Refer to [42, 43, 54, 55]).

   ii) The engine could be started in CAI mode by increasing the compression ratio during the cold start with a variable valve timing system or variable compression ratio system.

iii) A glow plug could be used to assist CAI combustion until the engine warms up.

2. **Emission Control.** To develop emission control systems and control strategies to overcome the challenge of maintaining acceptable levels of emissions. At low loads relatively high emissions of HC and CO appear, whilst at high loads NO_x emission becomes excessive.

   i) *HC and CO emissions* at low loads are the result of incomplete fuel burning near the walls and partial fuel oxidation due to low combustion temperature. A partially stratified fuel strategy may have the potential to mitigate the problem. In addition, the development of a new low temperature oxidation catalyst appropriate for CAI engines at low loads could be another solution.

   ii) *NO_x emission* at high load is the result of increased combustion temperature due to the higher fuel amount in the charge. Using a partially stratified charge (in temperature and composition) which leads to a combustion temperature reduction may be one possible solution.

3. **Multi Cylinder Effect.** To develop inlet and exhaust manifold designs for multi-cylinder CAI engines, (for proper engine operations) the challenge of maintaining strict uniformity of inlet and exhaust flows of each cylinder must be overcome. In multi cylinder engines, manifolds wave dynamics can cause small differences in the amount of hot trapped exhaust gases and the amount of fresh air/fuel charge delivered to the various cylinders. As auto-ignition timing in CAI engines is very sensitive to small changes in charge temperature and composition, these small differences can lead to significant cylinder-to-cylinder variations in combustion phasing.

4. **Fuelling System.** With the rapid advances in technology the author envisages the development of a new fuel delivery system to overcome the challenge of maintaining proper auto-ignition timing, smooth heat release rates and low

emissions over the engine operating range. Various types of fuelling systems may be proposed in dependence of the fuel type

i) *For diesel fuel* the type of injector required will depend on the strategy selected for fuel-air mixing. It is probable that the DI diesel injector will be the most suitable but additional modifications are needed to achieve the very high mixing rates necessary for CAI combustion.

ii) *For gasoline type fuels* DI injectors for SI engines is the most appropriate. However, additional modifications to meet different types of stratification required for various loads, have to be performed.

5. **Control Systems.** To develop methodology for feedback and closed-loop control of the fuel and air systems to keep combustion optimised over wide engine load and speed ranges. Control mechanisms, sensors and appropriate control algorithms are crucial technologies for commercial CAI engines. Closed-loop control has to be able to allow continuous optimisation of engine performances and emissions. Sensors may be needed to monitor auto-ignition timing, the rate of heat release, IEGR levels and HC and NO_x emissions.

6. **Combustion Modelling.** To develop computational fluid dynamics (CFD) and combustion models for CAI engines to overcome the challenge of accurate and computational time, inexpensive evaluation of engine geometry and combustion system designs. Research and development work may need to be focused in a few areas such as:

i) *Chemical kinetics.* To develop detailed skeletal and reduced reaction mechanisms for surrogate fuels that are able to accurately predict auto-ignition characteristics of real fuels, such as gasoline and diesel fuel.

ii) *CFD model improvements.* Understanding and controlling partial charge stratification (mixture and temperature) will probably play an important role in the development of commercial CAI engines. Accurate CFD

models are required to capture the manifold and in-cylinder mixing process used to produce these stratifications. In conjunction, gas exchange and mixing process as between fresh air/fuel charge and trapped hot exhaust gases in a camless engine are required to be modelled in detail. Models must have a sufficient temporal and spatial resolutions to resolve the transient mixing and boundary layer effects. The CFD models must also be compatible with the simultaneous solution of reduced/skeletal-mechanism, chemical kinetics models and sub-models for sprays, and to have incorporated adequate turbulence sub-models.

iii) *Sub-model development.* Both port fuel injection and various direct injection strategies are applicable to CAI engines. Spray and other sub-models are required to reproduce the fuel dispersion, vaporisation and mixing produced by these injectors. Turbulent mixing is the central part to all aspects of mixing and partial charge stratification, and improved turbulence models should be incorporated into CFD models. The application of some advanced turbulence concepts, such as One Dimensional Turbulence (ODT) and Large Eddy Simulation (LES), to in-cylinder processes in CAI engines should be explored further.

Appendix A

Emissions Regulation Standards for Transport Application

The new Emissions Regulation Standards for Transport Application engines imposed worldwide is to take effect in coming years (2005 year). For example EURO 4, Tier II, ULEV, is required to meet very strict norms for levels of carbon oxide, hydro-carbons, NO_x and particulate matter. The emission norms for EURO 4 standard are shown in Table A.1, for Tier II standard in Table A.2 and for ULEV standard in Table A.3.

Table A.1: EURO 4 Emission Standards for Transport Application

Vehicle type	CO, g/km	HC, g/km	HC+NO$_x$, g/km	NO$_x$, g/km	PM, g/km
Passenger Cars					
Diesel	0.50	-	0.30	0.25	0.025
Petrol (Gasoline)	1.0	0.10	-	0.08	-
Light Commercial Vehicles					
Diesel, <1305 kg	0.50	-	0.30	0.25	0.025
Diesel, 1305-1760 kg	0.63	-	0.39	0.33	0.04
Diesel, >1305 kg	0.74	-	0.46	0.39	0.06
Petrol, <1305 kg	1.0	0.1	-	0.08	-
Petrol, 1305-1760 kg	1.81	0.13	-	0.10	-
Petrol, >1760 kg	2.27	0.16	-	0.11	-

Table A.2: Tier II Emission Standards for Transport Application(Given for 50 000 miles/5 years)

Vehicle type	CO, g/mi	THC, g/mi	HC+NO$_x$, g/mi	NO$_x$, g/mi	PM, g/mi
Passenger Cars					
Diesel	3.4	0.21	0.25	0.05	0.08
Petrol (Gasoline)	3.4	0.21	0.25	0.05	0.015
Commercial Vehicles					
Diesel, <3750 lbs	3.4	-	0.25	0.07	0.08
Diesel, >3750 lbs	3.4	-	0.32	0.08	0.08
Diesel, <5750 lbs	3.4	0.32	-	0.11	0.08
Diesel, >5750 lbs	3.4	0.39	-	0.14	0.08
Petrol, <3750 lbs	3.4	-	0.25	0.07	0.08
Petrol, >3750 lbs	3.4	-	0.32	0.08	0.08
Petrol, <5750 lbs	3.4	0.32	-	0.11	0.08
Petrol, >5750 lbs	3.4	0.39	-	0.14	0.08

Table A.3: ULEV Emission Standards for Transport Application (Given for 50 000 miles/5 years)

Vehicle type	CO, g/mi	THC, g/mi	HC+NO$_x$, g/mi	NO$_x$, g/mi	PM, g/mi
Passenger Cars					
Diesel	1.7	0.11	-	0.05	0.05
Petrol (Gasoline)	1.7	0.11	-	0.05	0.05
Commercial Vehicles					
Diesel, <3750 lbs	1.7	-	0.2	0.05	0.08
Diesel, >3750 lbs	2.2	-	0.3	0.08	0.08
Diesel, <5750 lbs	3.2	0.3	-	0.11	0.08
Diesel, >5750 lbs	3.4	0.39	-	0.14	0.08
Petrol, <3750 lbs	1.7	-	0.2	0.05	0.08
Petrol, >3750 lbs	2.2	-	0.3	0.08	0.08
Petrol, <5750 lbs	3.2	0.3	-	0.11	0.08
Petrol, >5750 lbs	3.4	0.39	-	0.14	0.08

Appendix B

Mixing Model of Fresh Air/Fuel Charge and Trapped exhaust gases-IEGR

The IEGR trapped inside the engine cylinder by the AVT system is assumed to consist of burned mixture gases (combustion products). These gases are considered to be in thermodynamic equilibrium and are calculated using the overall combustion equation [105].

$$C_mH_nO_z + (m + \frac{n}{4} - \frac{z}{2})\lambda(O_2 + 3.76N_2) = a_{CO_2}CO_2 + a_{H_2O}H_2O + a_{N_2}N_2 +$$
$$+ a_{O_2}O_2 + a_{CO}CO + a_{H_2}H_2 \quad (B.1)$$
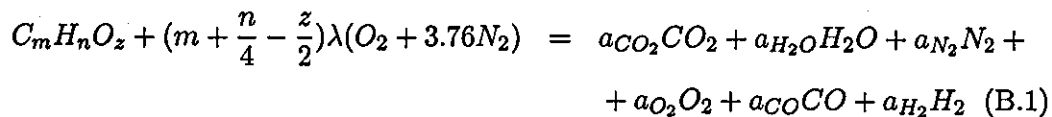
where:

- m is the number of carbon atoms in the fuel

- n is the number of hydrogen atoms in the fuel

- z is the number of oxygen atoms in the fuel

- λ is the equivalence air to fuel ratio

- a_{CO_2} is the number of carbon dioxide molecules in the products

- a_{H_2O} is the number of water vapour molecules in the products

- a_{N_2} is the number of nitrogen molecules in the products

- a_{O_2} is the number of oxygen molecules in the products

- a_{CO} is the number of carbon monoxide molecules in the products

- a_{H_2} is the number of hydrogen molecules in the products.

The composition of the IEGR is determined using the following assumptions:

1. For the lean and stoichiometric mixtures ($\lambda \geq 1$) CO and H₂ can be neglected.

2. For the rich mixtures ($\lambda < 1$) O₂ can be neglected.

3. For the rich mixtures, the water gas reaction

$$CO_2 + H_2 \Leftrightarrow CO + H_2O \qquad (B.2)$$

is assumed to be in equilibrium with the equilibrium constant $K(T)$

$$K(T) = \frac{a_{H_2O} a_{CO}}{a_{CO_2} a_{H_2}} \qquad (B.3)$$

where $K(T)$ is determined from

$$\ln K(T) = 2.743 - \frac{1.761}{t} - \frac{1.611}{t^2} - \frac{0.2803}{t^3} \qquad (B.4)$$

where $t = T/1000$, and T is in degrees K in range (400 < T < 3200 K).

Solutions for both lean and rich cases are given in Table B.1.

In the rich case, the parameter a_{CO} is given by the solution of the quadratic equation, i.e by the use of the equilibrium defined in Equation B.3 :

$$a_{CO} = \frac{-b \pm \sqrt{b^2 - 4ac}}{2a} \qquad (B.5)$$

where

- $a = K_p - 1$

- $b = (-3K_p + 2\lambda K_p - 2\lambda + 2)m + (-K_p + \lambda K_p - \lambda)\frac{n}{2} + (1 - \lambda)(K_p - 1)z$

- $c = mK_p(1 - \lambda)(2m + \frac{n}{2} - z)$

Table B.1: Burned gas composition

Species	a_i	$\lambda \geq 1$	$\lambda < 1$
CO_2	a_{CO_2}	m	m-a_{CO}
H_2O	a_{H_2O}	$\frac{n}{2}$	$z + 2(m + \frac{n}{4} - \frac{z}{2})\lambda - 2m + a_{CO}$
N_2	a_{N_2}	$3.76(m + \frac{n}{4} - \frac{z}{2})\lambda$	$3.76(m + \frac{n}{4} - \frac{z}{2})\lambda$
O_2	a_{O_2}	$(\lambda - 1)(m + \frac{n}{4} - \frac{z}{2})$	0
CO	a_{CO}	0	a_{CO}
H_2	a_{H_2}	0	$\frac{n}{2}$ -z - $2(m + \frac{n}{4} - \frac{z}{2})\lambda$

The engine volumetric efficiency is assumed 100% when no IEGR is introduced. Therefore the initial engine charge volume is that occupied by the inlet air/fuel mixture at the ambient conditions-V_{AF}^0.

When the IEGR is introduced, it occupies a certain fraction of the combustion chamber volume-x. The volume occupied by IEGR is

$$V_{IEGR} = xV_{AF}^0 \tag{B.6}$$

and the rest of the volume is occupied by the fresh air/fuel charge

$$V_{AF} = (1 - x)V_{AF}^0 \tag{B.7}$$

The mole quantity of the fuel, air and IEGR in the resulting charge mixture is obtained from the ideal gas relationship

$$n_i = \frac{p_i V_i}{\tilde{R}T_i} \quad \text{i=air,fuel,IEGR} \tag{B.8}$$

where

- p is pressure. It has value 1atm for both fresh air/fuel mixture and IEGR.

- T is temperature. For air/fuel mixture it is taken from the measured data or assumed to be 25^0C, while the IEGR temperature varies according to the requirement for the auto-ignition (at a given engine load).

- $\tilde{R}$ is the universal gas constant ($\tilde{R}$=8.3143J/molK).

The mixing process between the IEGR and the fresh air-fuel charge is assumed to be mixing of the ideal gases. The resulting charge mixture (air/fuel/IEGR) is assumed to be homogeneous and to have uniform thermodynamic properties. The resulting charge mixture temperature is calculated from the mixed gas components using energy conservation equation

$$H_{mixture} = H_{AF} + H_{IEGR} \tag{B.9}$$

where H_{AF} and H_{IEGR} is the enthalpy of a fresh air/fuel mixture and IEGR, respectively. They are obtained from

$$
\begin{aligned}
H_{AF} &= \sum_{j=1}^{r} y_j H_j \quad \text{j=1,\ldots, r-th reactants} \\
H_{IEGR} &= \sum_{k=1}^{p} y_k H_k \quad \text{k=1,\ldots, p-th IEGR constituents}
\end{aligned}
\tag{B.10}
$$

where y_j and y_k are the molar fraction of each species in fresh air/fuel mixture and in the IEGR respectively, while H_j and H_k represent their enthalpies. The standard state enthalpy of the species i[1] is given in NASA polynomial form[2]

$$\frac{H_i}{\tilde{R}T} = a_{i1} + \frac{a_{i2}}{2}T + \frac{a_{i3}}{3}T^2 + +\frac{a_{i4}}{4}T^3 + \frac{a_{i5}}{5}T^4 + \frac{a_{i6}}{T} \tag{B.11}$$

where $a_{i1}to a_{i6}$ are the numerical coefficients supplied in NASA thermodynamic files [140]. Two temperatures ranges are given, (i) from 300K to 1000K and (ii) from 1000K to 5000K range.

---

[1]Due to simplicity the label i is used of labels j and k.

[2]This is common approach for representing JANAF table thermodynamic data [138] in the NASA equilibrium program [139].

Appendix C

Reaction Mechanism for Mixture of iso-octane and n-heptane Fuels

The real automotive fuels are the complex mixtures of the hydrocarbons, and therefore it is very important to predict the auto-ignition properties of such mixtures in the CAI engine.

In order to obtain more realistic fuel to the standard gasoline fuel (95RON), the mixture of iso-octane and n-heptane fuels is used. The detailed reaction mechanism for this mixture is derived. It consists of 1087 species and 4392 reactions and includes complete NOx chemistry. The mechanism is derived from the detailed n-heptane and iso-octane mechanisms that have been developed by Lawrence Livermore National Laboratory (LLNL). These mechanisms are explained in detail in [89, 90]. The mixture reaction mechanism has ability to predict ignition delays for the fuels with various RON as well as for n-heptane and iso-octane fuels[1]. RON is defined as the percentage of the iso-octane fuel in the mixture (by volume). For example, for the simulation of the gasoline (95RON) the mixture of 95% of iso-octane and 5% of n-heptane is used.

---

[1]The mechanism has also ability to predict ignition delays for hydrogen, methane, acetylene and propane fuels. However, the use of this mechanism for these fuels can be expensive in terms of the computational time. In that case it is wisely to use specific detailed mechanisms derived for each of these fuels, which consists of a significantly less number of species and reactions.

The construction of the mixture reaction mechanism is done by the hierarchial approach, i.e. the mechanism is built systematically from the small parts (mechanisms for the fuels with simple chemical kinetics). The first parts represents the mechanism for the hydrogen oxidation, followed by the mechanism for the oxidation of carbon monoxide. Next, the sub-mechanisms for methane, acetylene, propane, n-heptane and iso-octane oxidation are added step-by-step. After adding the part of reactions for a new sub-mechanism, only the newly included reactions are tuned by comparing the numerical results with the ignition delay times measured in experiments [141, 142]. The reactions tuned on the previous stages of the mechanism construction are left intact. The tuning procedure consists of the sensitivity analysis based on the temperature/reaction rate sensitivities and it is performed by using the Kinalc code [104]. These sensitivities are reaching their maximum values at the moment of the ignition. Based on the results from the sensitivity analysis, the reaction rate coefficients of the most sensitive reactions are modified within the limits that can be found in the literature (in order to obtain better agrement with experimental data). The aim of tuning procedure is to improve mechanism capabilities to predict the combustion of complex fuels, without deteriorating the performances for the sub-mechanisms of more simple fuels developed in the previous steps.

The validation of the mechanism is done by comparison the calculated ignition delay times with the data obtained from the shock tube experiments [141, 142, 143, 144]. To simulate the auto-ignition delay in the shock-tube, Senkin application from Chemkin III package is used [67]. Senkin considers the shock-tube as a homogeneous reactor with the constant volume and with the adiabatic conditions behind the reflected shock waves.

The validation is carried out for the pure iso-octane fuel (100RON), pure n-heptane fuel (0RON) and for various RON, at various concentration, pressures and temperatures.

Figure C.1 shows comparison between the calculated and the experimental ignition delay for the stoichiometric mixture of the pure iso-octane (100RON) at the pressure

range from 10 to 41 bar. It can be seen that a good agreement between calculated and experimental data is obtained at various pressures.

Figure C.1: Comparison of the calculated and the experimental ignition delay times for iso-octane fuel (100RON) in the shock-tube. (At $\lambda = 1$ and a pressure from 10 bar to 41 bar.) Symbols represent experimental data [141, 142, 143, 144, 145], while lines represent calculated data.

Comparison between the calculated and the experimental data for n-heptane fuel (0RON), at the constant pressure of 25 bar and for the various equivalence air/fuel ratios (λ) is shown in Figure C.2. The calculated results show the consistency with the experimental data for all examined equivalence air/fuel ratios. It can be seen that the cool flame ignition behaviour, which is the characteristic of n-heptane, is well reproduced.

In Figure C.3 comparison of the calculated and the experimental ignition delays for the stoichiometric mixture of different RON (100, 80, 60 and 0 RON) at the
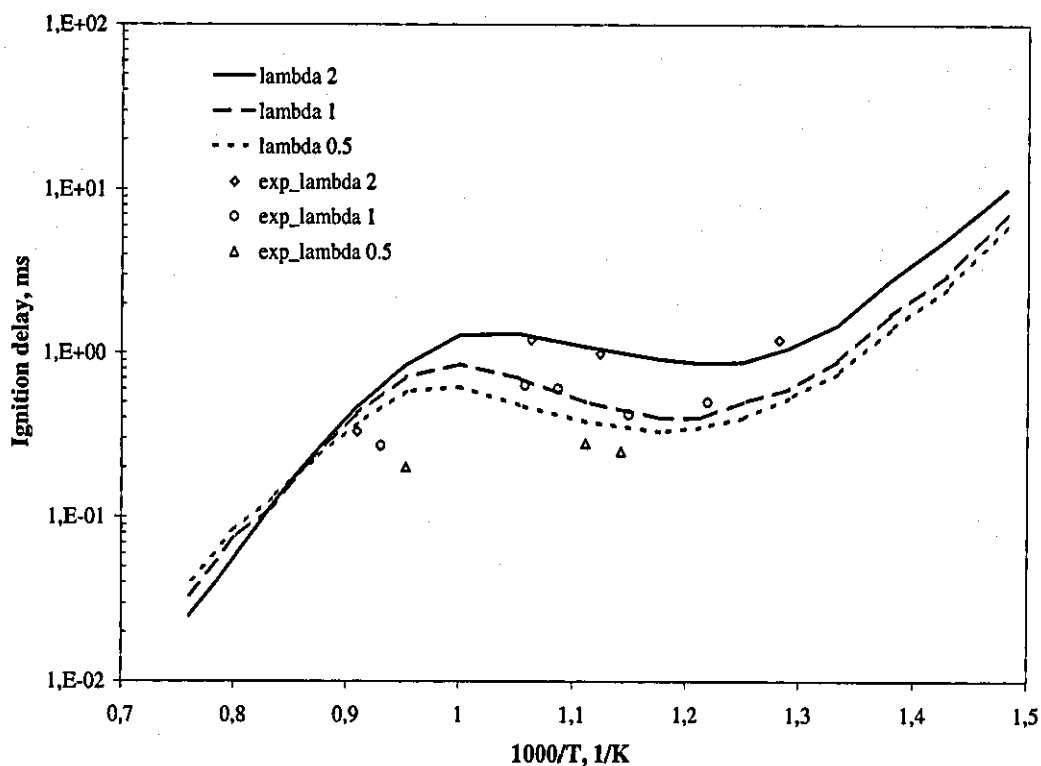
Figure C.2: Comparison of the calculated and the experimental ignition delay times for n-heptane fuel (0RON)in the shock-tube. (For various λ (0.5, 1 and 2) at the constant pressure of 25 bar.) Symbols represent experimental data [142, 143, 145], while lines represent calculated data.

constant pressure of 41 bar is shown. The results show a good agreement between the calculated and the experimental data for different RON's.

The validation in the shock-tubes conditions, shows that developed reaction mechanism for a mixture of iso-octane and n-heptane is capable to predict ignition behaviour for the various fuel research octane number (RON) at the different equivalence air/fuel ratios, pressures and temperatures.

The further validation of the mechanism is carried out by comparison of the calculated ignition delay times with the experimental data [22, 146] in the CAI engine conditions. The results are shown in Figure C.4. For the simulation of the CAI engine environment, the model described in Chapter 5 is used. The model uses
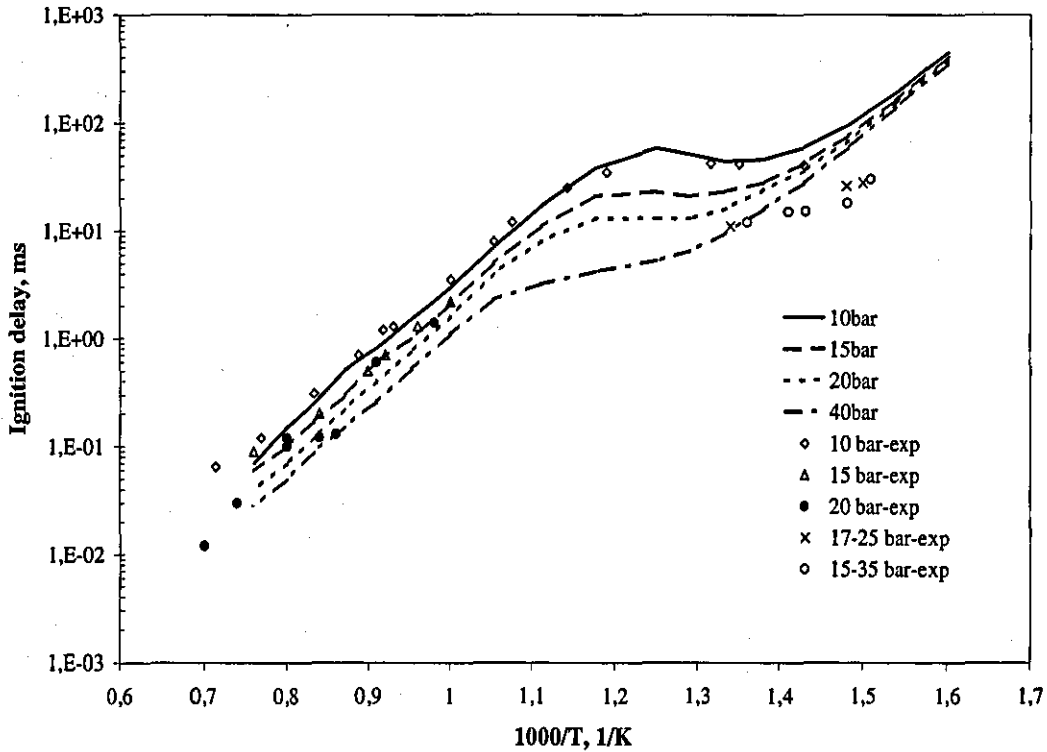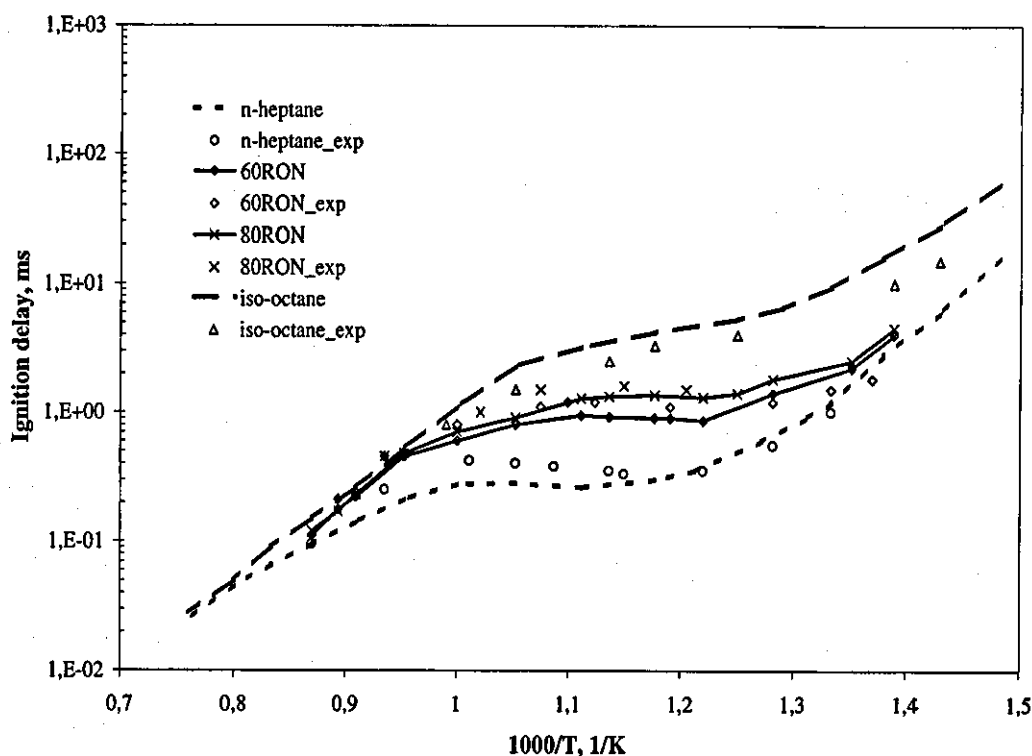
Figure C.3: Comparison of the calculated and the experimental ignition delay times for the fuels with various RON in the shock-tube. (For $\lambda = 1$ at the constant pressure of 41 bar.) Symbols represent experimental data [144], while lines represent calculated data.

detailed chemical kinetics and considers the cylinder as a single-zone, homogeneous reactor with the time variable volume according to the slider-crank relationship [67].

It can be seen that a good agrement between the calculated and experimental data is obtained.

It is worth to note that the auto-ignition timing is a function of the RON. The fuel with a low RON ignites significantly earlier than the fuel with a high RON. However, there is a little difference in the ignition timing in the range of $75 < RON < 95$. This is due to the influence of the cool-flame reactions in the n-heptane fuel[2]. These reactions release heat early in the cycle, and thus increase the temperature in the

---

[2]Although the cool-flame reactions exist in the iso-octane fuel, the heat released from those reactions is negligible.
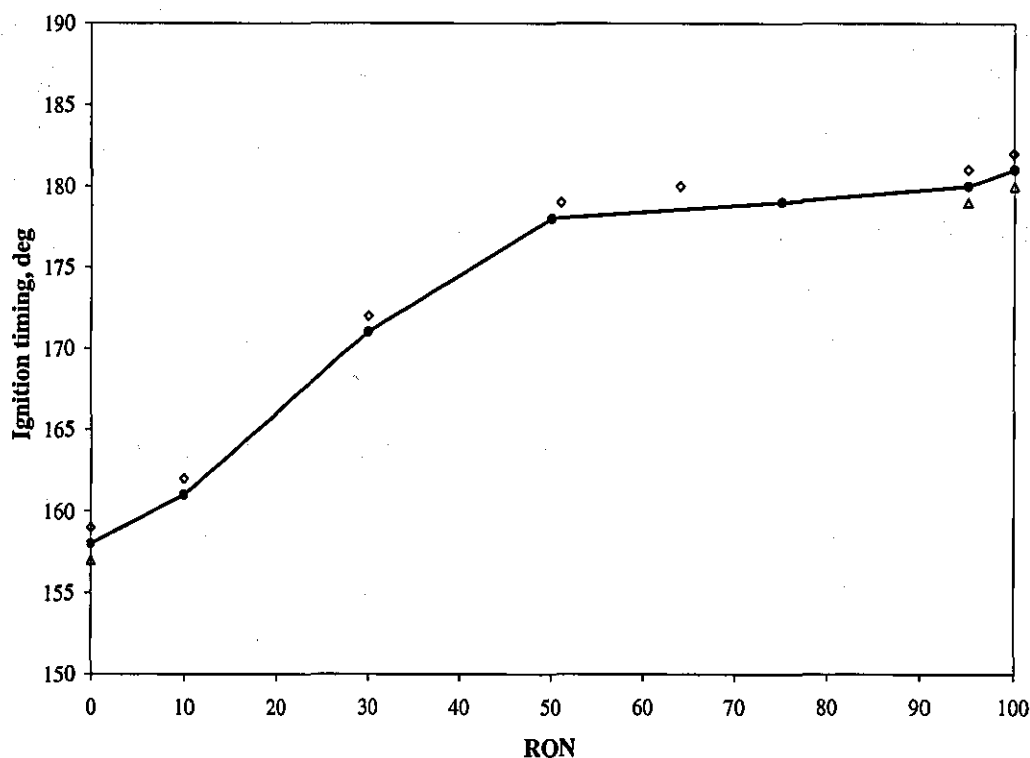
Figure C.4: Comparison of the calculated and experimental auto-ignition timings for the fuels with the various RON in the CAI engine. The open symbols represent experimental data [22, 146], while line represents calculated data.

system, which in turn accelerates the start of the main ignition. This effect is noticeable for the fuels with lower RON as they contain a higher percentage of n-heptane. As the RON increase, iso-octane, which has a single-stage ignition process (without heat releases from cool-flame reactions), begins to dominate in the auto-ignition process and the contribution from the cool-flame process decreases. When RON is higher than 75, the contribution from the cool-flame reactions is virtually override by the single-stage reaction, and therefore no significant differences between ignition timing can be observed. However, there is a clear difference between the pure iso-octane fuel (100RON) and the mixture which contains a small quantity of n-heptane, for example 95RON. This is due to the contribution from n-heptane's cool-flame reactions.

Based on the presented results, it can be concluded that developed reaction mechanism for a mixture of iso-octane and n-heptane is capable to accurately predict the ignition behaviour for the various fuel research octane number (RON) in different environments at various equivalence air/fuel ratios, pressures and temperatures.

Bibliography

[1] Woschini G. Universally Applicable Equation for the Instantaneous Heat Transfer Coefficient in the Internal Combustion Engine. *SAE Paper 670931*, 1967.

[2] Onishi S., Jo S.H., Shoda K., Jo P.D., and S. Kato. Thermo -Atmosphere Combustion (ATAC) - A new Combustion Process for Internal Combustion Engines. *SAE Paper 790501*, 1979.

[3] Oppenheim A.K. The Knock Syndrome-its Cures and its Victims. *SAE Paper 841339*, 1984.

[4] Noguchi M., Y. Tanaka, Tanaka T., and Y. Takeuchi. A Study on Gasoline Engine Combustion by Observation of Intermediate Reactive Products During Combustion. *SAE Paper 790840*, 1979.

[5] Najt P.M. and Foster D.E. Compression-Ignited Homogenous Charge Combustion. *SAE Paper 830264*, 1983.

[6] Thring R.H. Homogenous Charge Compression Ignition (HCCI) Engines. *SAE Paper 892068*, 1989.

[7] Ryan T.W. and J. Erwin. Effects of Fuel Properties and Composition on the Temperature Dependent Autoignition of Diesel Fuel Fractions. *SAE Paper 922229*, 1992.

[8] Sandia National Laboratory (SNL) Lawrence Livermore National Laboratory (LLNL), University of Berkeley (UBC) and Stanford University. Homogeneuos Charge Compression Ignition (HCCI) Technology - A Report to the U.S. Congress. Technical Report CF 106-914, U.S. Department of Energy, Energy Efficiency and Renewable Energy, Office of Transportation Technologies, 2001.

[9] Ogume H., Ichikura T., and Iida N. A Study on Adaptability of Alternative Fuels for Lean Burn Two-Stroke ATAC Engine. *SAE Paper 972097*, 1997.

[10] Iida N. Alternative Fuels and Homogenous Charge Compression Ignition Combustion Technology. *SAE Paper 972098*, 1997.

[11] Esterlingot E., Guilbert P., Lavy J., and Raux S. Thermodynamical and Optical Analyses of Controlled Auto-ignition Combustion in Two Stroke Engines. *SAE Paper 972098*, 1997.

[12] Ishibashi Y., Isomura S., Kudo O., and Tsushima Y. Improving the Exhaust Emissions of Two-Stroke Engines by Applying the Activated Radical Combustion. *SAE Paper 960742*, 1996.

[13] Ishibashi Y., Asai Y., and Nishida K. An Experimental Study of Stratified Scavenging Activated Radical Combustion Engine. *SAE Paper 972077*, 1997.

[14] Duret P. and Venturi S. Automotive Calibration of the IAPAC Fluid Dynamically Controlled Two Stroke Combustion Process. *SAE Paper 960363*, 1996.

[15] Yanagihara H., Sato Y., and Junichi M. A Study of Diesel Combustion under Uniform Higher-Dispersed Mixture Formation. *JSAE 9733675*, 1997.

[16] Aceves S.M., Martinez-Frias J., Flowers D.L., Smith R., Dibble W.R., Wright F.J, and Hessel R. P. A Decoupled Model of Detailed Fluid Mechanics Followed by Detailed Chemical Kinetics for Prediction of Iso-Octane HCCI Combustion. *SAE Paper 2001-01-3612*, 2001.

[17] Marriott D.C. and Reitz D.R. Experimental Investigation of Direct Injection-Gasoline for Premixed Compression Ignited Combution Phasing Control. *SAE Paper 2002-01-0418*, 2002.

[18] Marriott D.C., Kong S.C., and Reitz D.R. Investigation of Hydrocarbon Emissions from a Direct Injection-Gasoline Premixed Charge Compression Ignited Engine. *SAE Paper 2002-01-0419*, 2002.

[19] Sjöberg M., Edling L.O., Eliassen T., Magnusson L., and Ångström H.E. GDI HCCI: Effects of Injection Timing and Air Swirl on Fuel Stratification, Combustion and Emission Formation. *SAE Paper 2002-01-0106*, 2002.

[20] Westbrook C. Chemical Kinetics of Hydrocarbon Ignition in Practical Combustion Systems. In *Proceedings of* 28th *Combustion Symposium, Pleneary Lecture*, Edinburgh, Scotland, UK, July 2000.

[21] Heywood J.B. *Internal Combustion Engine Fundamentals*. McGraw-Hill Book Company, 1988.

[22] Christensen M., Hultqvist A., and Johansson B. Demonstrating the Multi Fuel Capability of a Homogeneous Charge Compression Ignition Engine with Variable Compression Ratio. *SAE Paper 1999-01-3679*, 1999.

[23] Christensen M., Einewall P., and Johansson B. Homogenous Charge Compression Ignition (HCCI) Using Iso-octane, Ethanol and Natural Gas-A Comparison with Spark Ignition Operation. *SAE Paper 972874*, 1997.

[24] Christensen M., Johansson B., Amneus P., and F. Mauss. Supercharged Homogenous Charge Compression Ignition. *SAE Paper 980787*, 1998.

[25] Kimura S., Aoki O., Ogawa H., Muranaka S., and Enomoto Y. New Combustion Concept for Ultra-Clean and High-Efficiency Small DI Diesel Engines. *SAE Paper 1999-01-3681*, 1999.

[26] Hultqvist A., Engdar U., Johansson B., and Klingmann J. Reactiong Boundary Layers in Homogenous Charge Compression Ignition (HCCI) Engine. *SAE Paper 2001-01-1032*, 2001.

[27] Hultqvist A., Christensen M., Johansson B., Franke A., Richter M., and M. Alden. A Study of the Homogenous Charge Compression Ignition Combustion Process by Chemiluminescence Imaging. *SAE Paper 1999-01-3680*, 1999.

[28] Richter M., Franke A., M. Alden, Hultqvist A., and B. Johansson. Optical Diagnostic Applied to a Naturally Aspirated Homogeneous Charge Compression Ignition Engine. *SAE Paper 1999-01-3649*, 1999.

[29] Aceves S.M., Flowers D.L., Westbrook C., Smith R., Pitz W., Dibble W.R., Christensen M., and Johansson R. A Multi-Zone Model for Prediction of HCCI Combustion and Emissions. *SAE Paper 2000-01-0327*, 2000.

[30] Aceves S.M., Flowers D.L.and Martinez-Frias J., Smith R., Westbrook C., Pitz W., Dibble W.R., Wright F.J, Akinyemi W.C., and Hessel R. P. A Sequential Fluid-Mechanic Chemical-Kinetic Model of Propane HCCI Combustion. *SAE Paper 2000-01-1027*, 2000.

[31] Kong S.C., Marriott C.D., Reitz R., and Christensen M. Modelling and Experiments of HCCI Engine Combustion Using Detailed Chemical Kinetics with Multidimensional CFD. *SAE Paper 2001-01-1026*, 2001.

[32] Fiveland S.B. and Assanis D.N. Development of a Two-Zone HCCI Combustion Model Accounting for Boundary Layer Effects. *SAE Paper 2001-01-1028*, 2001.

[33] Christensen M., Johansson B., and Hultqvist. The Effect of Combustion Chamber Geometry on HCCI Operation. *SAE Paper 2002-01-0425*, 2002.

[34] Griffiths J.F. and Barnard J.A. *Flame and Combustion*. Blackie Academic & Professional, 3rd edition, 1995.

[35] Warnatz J., Maas U., and Dibble R.W. *Combustion.* Springer Verlag, 2nd edition, 1999.

[36] Stanglmaier R.H. and Roberts C.E. Homogeneous Charge Compression Ignition (HCCI):Benefits, Compromises, and Future Engine Applications. *SAE Paper 1999-01-3682*, 1999.

[37] Milovanovic N. and Chen R. A Review of Experimental and Simulation Studies on Controlled Auto-Ignition Combustion. *SAE Paper 2001-01-1890*, 2001.

[38] Milovanovic N. Homogeneous Charge Compression Ignition (HCCI) Combustion. PhD Transfer Report, Loughborough University, June 2001.

[39] Gray A.W. and Ryan T.W. III. Homogenous Charge Compression Ignition of Diesel Fuel. *SAE Paper 961160*, 1996.

[40] Flynn P. Premixed Charge Compression Ignition Engine with Optimal Combustion Control. International Patent WO9942718, World Intellectual Property Organization.

[41] Sharke P. Otto or Not, Here it Comes. *Mechanical Engineering*, 122, No. 6, June 2000.

[42] Law D., Kemp D., Allen J., Kirkpartick G., and Copland T. Controlled Combustion in an IC-Engine with a Fully Variable Valve Train. *SAE Paper 2000-01-0251*, 2000.

[43] Allen J. and Law D. Variable Valve Actuated Controlled Auto-Ignition: Speed Loads Maps and Strategic Regimes of Operation. *SAE Paper 2002-01-0422*, 2002.

[44] Lavy J., Dabadie J., Angelberger C., Duret P., Willand J., Juretzka A., Schaflein J., Ma T., Lendresse Y., Satre A., Schulz C., Zhao H., and Damiano L. Innovative Ultra-Low NO_x Controlled Auto-Ignition Combustion Process for Gasoline Engines: the 4-SPACE Project. *SAE Paper 2000-01-1837*, 2000.

[45] Osses M., Andrews G.E., and Greenhough J. Diesel Fumigation Partial Pre-mixing for Reduced Particulate Soot Fraction Emissions. *SAE Paper 980532*, 1998.

[46] Ogawa H., Chenyu L., Tosaka S., Fujiwara Y., and Miyamoto N. Combustion Mechanism Analysis with In-Chamber Gas Composition Measurements in Premixed Lean Compression Ignition Engine. In *Proceedings of the 4th International Symposium, COMODIA 98*, Japan, 1998.

[47] Furutani M., Ohta Y., Kono M., and Hasegawa M. An Ultra-Lean Premixed Compression Ignition Concept and its Characteristics. In *Proceedings of the 4th International Symposium, COMODIA 98*, Japan, 1998.

[48] Iwabuchi Y., Kawai K., Shoji T., and Takeda Y. Trial of New Concept Diesel Combustion System - Premixed Compression Ignited Combustion. *SAE Paper 1999-01-0185*, 1999.

[49] Nagakome K., Shimazaki N., Miimura K, and Kobayashi S. Combustion and Emissions Characteristic of Premixed Lean Diesel Combustion Engine. *SAE Paper 970898*, 1997.

[50] Takeda Y., Keiichi N., and Keiichi M. Emissions Characteristic of Premixed Lean Diesel Combustion with Extremely Early Staged Fuel Injection. *SAE Paper 961163*, 1996.

[51] Mase Y., Kawashima J., Sato T., and Eguchi M. Nissan's New Multi-valve DI Diesel Engine Series. *SAE Paper 981039*, 1998.

[52] Christensen M. and Johansson B. Influence of Mixture Quality on Homogenous Charge Compression Ignition. *SAE Paper 982454*, 1998.

[53] Ishibashi Y. Basic Understanding of Activated Radical Combustion and Its Two-Stroke Engine Application and Benefits. *SAE Paper 2000-01-1836*, 2000.

[54] Koopmans L. and Denbratt I. A Four Stroke Camless Engine, Operated in Homogeneous Charge Compression Ignition Mode with Commercial Gasoline. *SAE Paper 2001-01-3610*, 2001.

[55] Koopmans L., Backlund O., and Denbratt I. Cycle to Cycle Variations: Their Influence on Cycle Resolved Gas Temperature and Unburned Hydrocarbons from a Camless Gasoline Compression Ignition Engine. *SAE Paper 2002-01-0110*, 2002.

[56] Gray A.W. and Ryan T.W. III. Homogenous Charge Compression Ignition (HCCI) of Diesel Fuel. *SAE Paper 971676*, 1997.

[57] Flowers D., Aceves S., Smith R, Torres J., Girard J., and Dibble R. HCCI in a CFR Engine:Experiments and Detailed Kinetic Modeling. *SAE Paper 2000-01-0328*, 2000.

[58] Iida N. and Igarashi T. Auto-ignition and Combustion of n-Butane and DME/Air Mixtures in a Homogeneous Charge Compression Ignition Engine. *SAE Paper 2000-01-1832*, 2000.

[59] Kaimai T., Tsunemoto H., and Ishitani H. Effects of a Hybrid Fuel System With Diesel and Premixed DME/methane Charge on Exaust Emissions in a Small DI Diesel Engine. *SAE Paper 1999-01-1509*, 1999.

[60] Amsden A.A. KIVA-3: A Kiva Program with Block-Structured Mesh for Complex Geometries. Report LA-12503-MS, Los Alamos National Laboratory, USA, 1993.

[61] Akagawa H., Miayamoto T., Harada A., Sasaki S., Shimazaki N., Hashizuma T., and Tsujimura K. Approaches to Solve Problems of the Premixed Lean Diesel Combustion. *SAE Paper 1999-01-0183*, 1999.

[62] Yokota H., Kudo Y., Nakajima H., Kakegawa T., and Suzuki T. A New Concept for Low Emission Diesel Combustion. *SAE Paper 970891*, 1997.

[63] Ishii H., Koike N., Suzuki H., and Odaka M. Exhaust Purification of Diesel Engines by Homogeneous Charge with Compression Ignition Part 2: Analysis of Combustion Phenomena and NO_x Formation by Numerical Simulation with Experiment. *SAE Paper 970315*, 1997.

[64] Hashizume T., Miyamoto T., Akagawa H., and Tsujimura K. Combustion and Emission Characteristic of Multiple Stage Diesel Combustion. *SAE Paper 980505*, 1998.

[65] Miayamoto T., Hayashi A.K., Harada A., Sasaki S., Hisashi A., and Tsujimura K. A Computational Investigation of the Premixed Lean Diesel Combustion. *SAE Paper 1999-01-0229*, 1999.

[66] Lund C.M. HCT - A General Computer Program for Calculating Time Dependent Phenomena Involving One-Dimensional Chemical Kinetics. Report UCRL-52504, Lawrence Livermore National Laboratory, Livermore, CA, USA, 1978.

[67] Kee R.J., Rupley F.M., Meeks E., and Miller J.A. CHEMKIN III: A Fortran Chemical Kinetics Package for the Analysis of Gas-Phase Chemical and Plasma Kinetics. Report SAND96-8216, Sandia National Laboratories, Livermore, CA, USA, 1996.

[68] Hultqvist A., Christensen M., Johansson B., Richter M., Nygren J., Hult J., and M. Alden. The HCCI Combustion Process in a Single Cycle-High Fuel Tracer LIF and Chemiluminescence Imaging. *SAE Paper 2002-01-0424*, 2002.

[69] Aceves S.M., Smith R., Westbrook C.K., and Pitz W.J. Compression Ratio Effect on Methane HCCI Combustion. *Journal of Engineering for Gas Turbines and Power*, 121:569–574, July 1999.

[70] Smith R., Aceves S.M., Westbrook C.K., and Pitz W.J. Modeling of Homogeneous Charge Compression Ignition (HCCI) Of Methane. In *Proceedings of the ASME Internal Combustion Engine 1997 Fall Conference*, Medison, Wisconsin, USA, May 1997.

[71] Kelly-Zion P. and Dec J. A Computational Study of the Effect of Fuel-Type on Ignition Time in HCCI Engines. In *Proceedings of 28th Combustion Symposium*, Edinburgh, Scotland, UK, July 2000.

[72] Easley W.L., Agarwal A., and Lavoie G.A. Modeling of HCCI Combustion and Emissions Using Detailed Chemistry. *SAE Paper 2001-01-1029*, 2001.

[73] Ogink R. and Golovitchev V. Gasolline HCCI Modeling:An Engine Cycle Simulation Code with a Multi-Zone Combustion Model. *SAE Paper 2002-01-1745*, 2002.

[74] Aceves S.M., Martinez-Frias J., Flowers D.L., Smith R., Dibble W.R., and Chen J.Y. A Computer Generated Reduced Iso-Octane Chemical Kinetic Mechanism Applied to Simulation of HCCI Combustion. *SAE Paper 2002-01-2870*, 2002.

[75] Hong S.J., Assanis D.N., and Wooldridge M.S. Modeling of Chemical and Mixing Effects on Autoignition under Direct Injection Stratified Charge Condition. In *Proceedings of 29th Combustion Symposium*, Sapporo, Japan, July 2002.

[76] Kraft M., Maigaard P., Mauss F., Christensen M., and Johansson B. Investigation of Combustion Emissions in a HCCI Engine - Measurements and a New Computational Model. In *Proceedings of 28th Combustion Symposium*, Edinburgh, Scotland, UK, July 2000.

[77] Kraft M., Maigaard P., and Mauss F. Homogeneous Charge Compression Ignition Engine: A Simulation Study on the Effects of Inhomogenities. In *ICE 2000 Spring Techical Conference ASME 2000*, number 2000-ICE-275, pages 63–70. ASME, 2000.

[78] Ogink R. and Golovitchev V. Gasolline HCCI Modeling:Computer Program Combining Detailed Chemistry and Gas Exchange Process. *SAE Paper 2001-01-3614*, 2001.

[79] Cantore G., Montrosi L., Mauss F., and Amneus P. Analysis of a 6-Cylinders Turbocharged HCCI Engine Using a Detailed Kinetics Mechanism. In *Ninth ICNC Symposium*, number MS054, pages 169–170, Sorento, Italy, July 2002. ICNC.

[80] Fiveland S.B. and Assanis D.N. Development and Validation of a Quasi-Dimensional Model for HCCI Engine Performace and Emissions Studies Under Turbocharged Conditions. *SAE Paper 2002-01-1757*, 2002.

[81] Mulcahy M.F.R. *Gas Kinetics*. Springer Verlag, 1st edition, 1973.

[82] Lindemann F.A. Discussion on The Radiation Theory of Chemical Action. *Transaction of Farady Socciety*, 17, 1992.

[83] Robinson P.J. and Holbrook K.A. *Unimolecular Reactions*. Willey-Interscience, New York, 1st edition, 1972.

[84] Atkins P.W. *Physical Chemistry*. Freeman, New York, 5th edition, 1996.

[85] Golden D.M. *Low-temperature Chemistry of the Atmosphere*, chapter Gas Phase Homogeneous Kinetics, pages 69–92. Springer Verlag, Heidelberg, 1994. Moorgat GK editor.

[86] Benson S.W. *The Foundations of Chemical Kinetics*. McGraw Hill, New York, USA, 1960.

[87] Smith P.G. and Golden M.D. and Frenklach M. and Moriarty W.N. and Eiteneer B. and Goldenberg M. and Bowman C.T. and Hanson K.R. and Song S. and Gardiner C.W.Jr. and Lissianski V.V and Qin Z. GRI-Mech 3.0 Mechanism for Natural Gas Combustion. *http : //www.me.berkeley.edu/grimech/*, 1999.

[88] Glassman I. *Combustion*. Academic Press, New York, 1st edition, 1977.

[89] Curran H.J., Gaffuri P., Pitz W.J., and Westbrook C.K. A Comprehesive Modelling Study of n-Heptane Oxidation. *Combustion and Flame*, 114:149–177, 1998.

[90] Curran H.J., Gaffuri P., Pitz W.J., and Westbrook C.K. A Comprehesive Modelling Study of iso-Octane Oxidation. *Combustion and Flame,* 129:253–280, 2002.

[91] Griffiths J.F. Reduced Kinetic Models and their Application to Practical Combustion Systems. *Progress in Energy and Combustion Science,* 21:25–107, 1995.

[92] Griffiths J.F. and Phillips C.H. *Combustion and Flame,* 81:304, 1990.

[93] Gray P. and Scott S.K. *Chemical Oscillation and Instabilities.* Oxford Science Publications, Oxford, UK, 1990.

[94] Dixon-Lewis G. and Williams D.J. *Comprenhensive Chemical Kinetics,* volume 17. 1977. Bamford C.H. and Tipper C.F.H eds.

[95] Gray P. and Scott S.K. *Oscillations and Traveling Waves in Chemical Systems,* page 493. J. Willey and Soons, 1985. Field R.J. and Burger M. eds.

[96] Griffiths J.F. and Scott S.K. *Progress in Energy Combustion and Science,* 13:161, 1987.

[97] Semenov N.N. *Chemical Kinetics and Chain Reactions.* Oxford University Press,UK, 1935.

[98] D.A. Frank-Kamentskii. *Diffusion and Heat Transfer in Chemical Kinetics.* Plenum Press, New York, USA, 2nd edition, 1969.

[99] van't Hoff. *Studies in Chemical Dynamics.* Williams and Northgate, London, UK, 1896.

[100] Lewis B. and von Elbe G. *Combustion, Flames and Explosions of Gases.* Academic Press, New York, USA, 3rd edition, 1987.

[101] Pease R.N. *Journal of American Chemical Society,* 51:1839, 1929.

[102] Pease R.N. *Journal of American Chemical Society,* 60:2244, 1938.

[103] Chen R., Milovanovic N., Turner J., and Blundell D. Thermal Effect of Internal Gas Recirculation on Controlled Auto Ignition. *SAE Paper 2003-01-0750*, 2003.

[104] Turanyi T. and Zsely G.I and Frouzakis C. KINALC, CHEMKIN Based Program for Kinetic Analysis.
http : //www.chem.leeds.ac.uk/Combustion/Combustion.html,
http : //garfield.chem.elte.hu/Combustion/Combustion.html, 2001.

[105] Ferguson C.R. and Kirkpatrick A.T. *Internal Combustion Engines-Applied Thermosciences*. John Willey and Sons. Inc, New York, 2nd edition, 2001.

[106] Curran H.J., Pitz W.J., Westbrook K.C., Callanah C.V., and Dryer F.L. Oxidation of Automotive Primary Reference Fuels at Elevated Pressures. In *Proceedings of 27th Combustion Symposium*, pages 379–387, 1998.

[107] Westbrook K.C., Warnatz J., and Pitz W.J. A Detailed Chemical Kinetic Reaction Mechanism for the Oxidation of iso-Octane and n-Heptane Over an Extended Temperature Range and its Application to Analysis Of Engine Knock. In *Proceedings of 22nd Combustion Symposium*, pages 893–901, 1988.

[108] Nehse M., Warnatz J., and Chevalier C. Kinetic Modelling of the Oxidation of Large Aliphatic Hydrocarbons. In *Proceedings of 26th Combustion Symposium*, pages 773–780, 1996.

[109] Chevalier C., Pitz W.J., Warnatz J., Westbrook K.C., and Melenk H. Hydrocarbon Ignition: Automatic Generation of Reaction Mechanisms and Applications to Modelling of Engine Knock. In *Proceedings of 24th Combustion Symposium*, pages 93–101, 1992.

[110] Curran H.J., Pitz W.J., Westbrook K.C., Hisham M.W.M., and Walker R.W. An Intermediate Temperature Modelling Study of the Combustion of Neopentane. In *Proceedings of 26th Combustion Symposium*, pages 641–649, 1996.
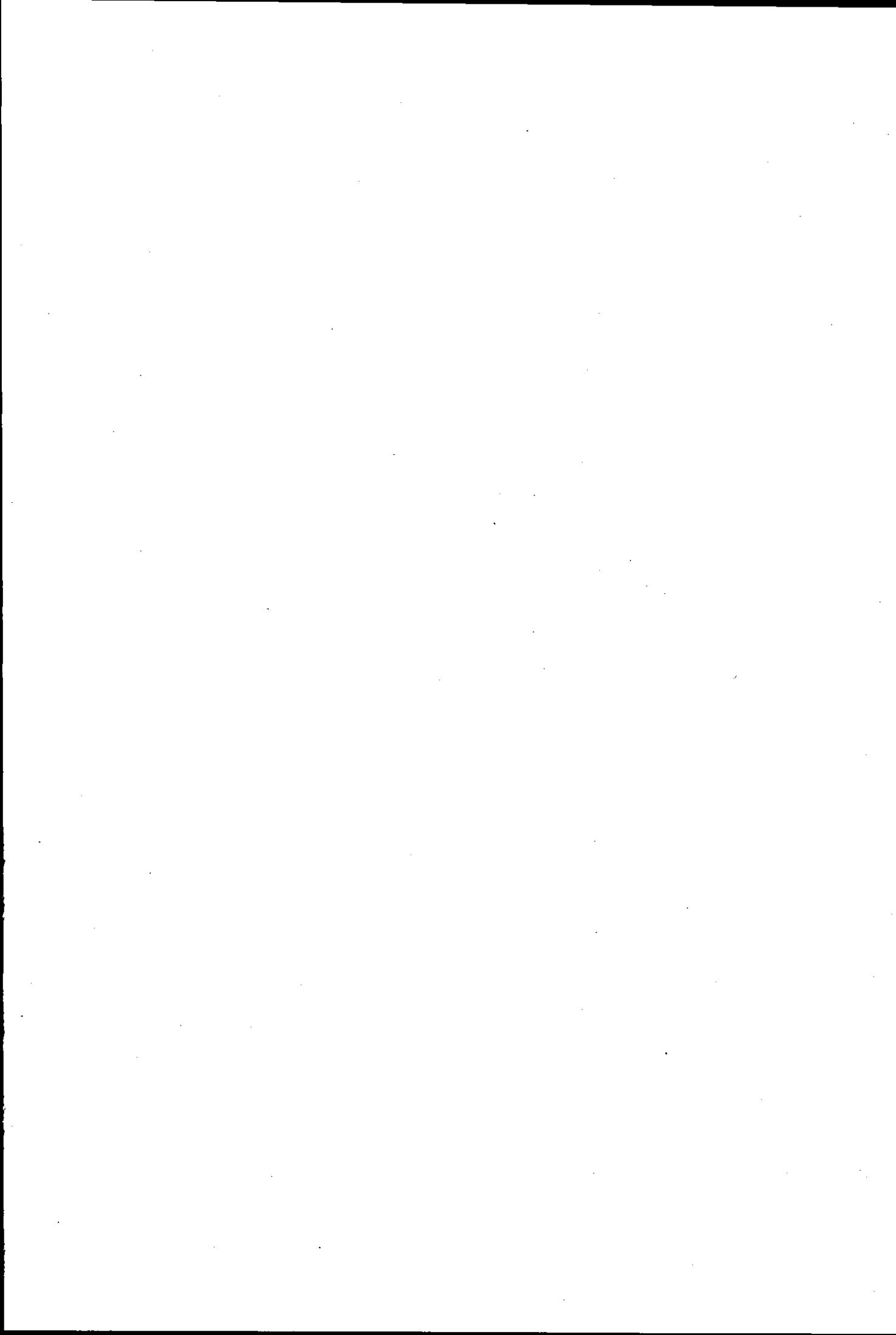
[111] Furutani M., Kono M., Kojima M., Nose M., and Ohta Y. Chemical Species Histories up to Ignition in Premixed-Ignition Natural Gas Engine. In *Proceedings of The Fifth International Symposium on Diagnostic and Modelling of Combustion in Internal Combustion Engines - COMODIA 2001*, pages 461–466, Nagoya, Japan, July 2001.

[112] Yumasaki Y. and Iida N. Numerical Analysis of Auto Ignition and Combustion of n-Butane and Air Mixture in The Homogeneous Charge Compression Ignition Engine by Using Elementary Reactions. In *Proceedings of The Fifth International Symposium on Diagnostic and Modelling of Combustion in Internal Combustion Engines - COMODIA 2001*, pages 417–425, Nagoya, Japan, July 2001.

[113] Milovanovic N. and Chen R. An Ivestigation of Chemical Effect of Exhaust Gas Recirluation on CAI Engine Fulled with Methane: By discussion of all radicals production and destruction reactions. Internal Report, December 2001.

[114] Milovanovic N. and Chen R. Modelling of the Engine Operating Condition Effects on the HCCI Combustion of Methane. In *Current Research in Combustion*, Advantica Research Centre, Loughborough, UK, September 2001. Conference Organised by Institute of Physics - Combustion Physics Group.

[115] Chen R., Milovanovic N., and Law D. A Computational Study on the Ignition Timing of HCCI Combustion in IC Engine Fuelled with Methane. In *Proceeding of 2002 Spring Technical Metting of the Combustion Institute, Canadian Section*, number Paper No. 53, pages 158–163, Windsor, Canada, May 2001. Canadian Section of The Combustion Institute.

[116] Aroonsrisopon T., Sohm V., Werner P., Foster E.D., Morikawa T., and Iida M. An Investigation Into the Effect of Fuel Composition on HCCI Combustion Characteristic. *SAE Paper 2002-01-2830*, 2002.

[117] Cox A., Griffiths J.F., Mohamed C., Curran H.J., Pitz W.J., and Westbrook K.C. Extents of Alkane Combustion During Rapid Compression Leading to a

Single and Two-Stage Ignition. In *Proceedings of 26th Combustion Symposium*, pages 2685–2692, 1996.

[118] Callahan C.V., Held T.J., Dryer F.L., Minetti R., Ribaucour M., Sochet L.R., Faravelli T., Gaffuri P., and Ranzi E. Experimental Data and Kinetic Modeling of Primary Rerefence Fuel Mixtures. In *Proceedings of 26th Combustion Symposium*, pages 739–745, 1996.

[119] Golovitchev V.I., Nordin N., and Chomiak J. Neat Dimethyl Ether: Is It Really Diesel Fuel or Promise. *SAE Paper 982537*, 1998.

[120] Golovitchev V.I., Nordin N., Chomiak J., Nishida K., and Wakai K. Evaluation of Ignition Quality of DME at Diesel Engine Conditions. In *Proceedings of 4th International Conference on Internal Combustion Engines*, Capri, Italy, 1999.

[121] Fisher E.M., Curran H.J., Pittz W., and Westbrook C.K. Detailed Chemical Kinetic Mechanisms for Combustion of Oxygenated Fuels. In *Proceedings of 28th Combustion Symposium*, Edinburgh, UK, July 2000.

[122] Westbrook K.C., Pitz W.J., and Leppard W.R. The Autoignition Chemistry of Paraffinic Fuels and Pro-Knock and Anti-Knock Additives: A Detailed Chemical Kinetic Study. *SAE Paper 912134*, 1991.

[123] Fiveland S.B. and Assanis D.N. A Four-Stroke Homogeneous Charge Compression Ignition Engine Simulation for Combustion and Performace Studies. *SAE Paper 2000-01-0332*, 2000.

[124] Oakley A., Zhao H., Ladommatos N., and Ma T. Experimental Studies on Controlled Auto-ignition (CAI) Combustion of Gasoline in a 4-stroke Engine. *SAE Paper 2001-01-1030*, 2001.

[125] Au Y. M., Girard J., Dibble R., Flowers D., Aceves M.S., Martinez-Frias J., Smith R.J., Seibel C., and Maas U. 1.9-Liter Four-Cylinder HCCI Engine Operation with Exhaust Gas Recirculation. *SAE Paper 2001-01-1894*, 2001.

[126] Zhao H., Peng Z., Williams J., and Ladommatos N. Understanding the Effects of Recycled Burnt Gases on the Controlled Auto-ignition (CAI) Combustion in Four-Stroke Gasoline Engines. *SAE Paper 2001-01-3607*, 2001.

[127] Dec J. A Computational Study of the Effect of Low Fuel Loading and EGR on Heat Release Rates and Combustion Limits in HCCI Engines. *SAE Paper 2002-01-1309*, 2002.

[128] Chen R. and Milovanovic N. A Computational Study Into the Effect of Exhaust Gas Recycling on Homogeneous Charge Compression Ignition Combustion in Internal Combustion Engine Fuelled With Methane. *International Journal of Thermal Sciences*, 41:805–813, 2002.

[129] Zhao H., Li J., Ma T., and Ladommatos N. Performace and Analysis of a 4-Stroke Multi-Cylinder Gasoline Engine with CAI Combustion. *SAE Paper 2002-01-0420*, 2002.

[130] Oakley A., Zhao H., Ladommatos N., and Ma T. Dillution Effect on the Controlled Auto-ignition (CAI) Combustion of Hydrocarbon and Alcohol Fuels. *SAE Paper 2001-01-3606*, 2001.

[131] Milovanovic N., Chen R., Law D., and Turner J. A Computational Study on the Effect on Auto-Ignition Timing of HCCI Engine Fuelled with N-heptane, Iso-octane, Ethanol and Methane. In *Proceeding of 17th Internal Combustion Engine Symposium*, number 20026074, pages 351–354, Tokyo, Japan, October 2002. JSAE.

[132] Chen R., Milovanovic N., Law D., and Turner J. A Theoretical Study on HCCI with Diesel Type Fuels: N-heptane, Dimethyl Ether, Methyl Butanoate and Methyl Formate. In *Proceeding of 17th Internal Combustion Engine Symposium*, number 20026077, pages 365–368, Tokyo, Japan, October 2002. JSAE.

[133] Turner J., Blundell D., Bassett M., Pearson R., and R. Chen. The Impact on Engine Performance of Controlled Auto Ignition Versus Spark Ignition with

Two Methods of Load Control. In *Proceedings of GPC 2002 Global Powertrain Congress*, Michigan, USA, September 2002.

[134] Group of Authors. Lotus Engine Simulation (LES) Code Manual. Published by Lotus Cars Company Ltd., 2001. Hethel, Norfolk, UK.

[135] Koopmans L., Ström H., Lundgren S., Backlund O., and Denbratt I. Demostrating a SI-HCCI-SI Mode Change on a Volvo 5-Cylinder Electronic Valve Control Engine. *SAE Paper 2003-01-0753*, 2003.

[136] Law D., Allen J., and Chen R. On the Mechanism of Controlled Auto Ignition. *SAE Paper 2002-01-0421*, 2002.

[137] Dec J. and Sjöberg M. A Parametric Study of HCCI Combustion- the Sources of Emissions at Low Loads and the Effects of GDI Fuel Injection. *SAE Paper 2003-01-0752*, 2002.

[138] U.S. National Bureau of Standrads. JANAF Thermochemical Tables. NSRDS-NB537, 1971.

[139] Gordon S. and McBride B.J. Computer Program for the Calculation of Complex Chemical Equilibrium Composition, Rocket Performance, Incident and Reflected Shocks, and Champan-Jouguet Detonations. NASA Publications SP-273, 1971. NTIS number N71-37775.

[140] Svehla R.A. and McBride B.J. Fortran IV Computer Program for Calculation of Thermodynamic and Transport Properties of Complex Chemical Systems. NASA technical note TND-7056, 1973. NTIS number N73-15954.

[141] Martinego A. In *Proceedings of 10th Combustion Symposium*, page 323, 1965.

[142] Ciezki H.K. and Adomeit G. Shock-Tube Investigation of Self-Ignition of n-Heptane-Air Mixtures Under Engine Relevant Conditions. *Combustion and Flame*, 93:421–433, 1993.

[143] H. Prehn. *Dissertation Thesis*. PhD thesis, RWTH Aachen, Aachen, Germany, 1996.

[144] Fieweger K., Blumenthal R., and Adomeit G. Self-ignition of S.I. Engine Model Fuels: A Shock Tube Investigation at High Pressure. *Combustion and Flame*, 109:599–619, 1997.

[145] Vermeer D.J., Meyer J.W., and Oppenheim A.K. *Combustion and Flame*, 18:327–336, 1972.

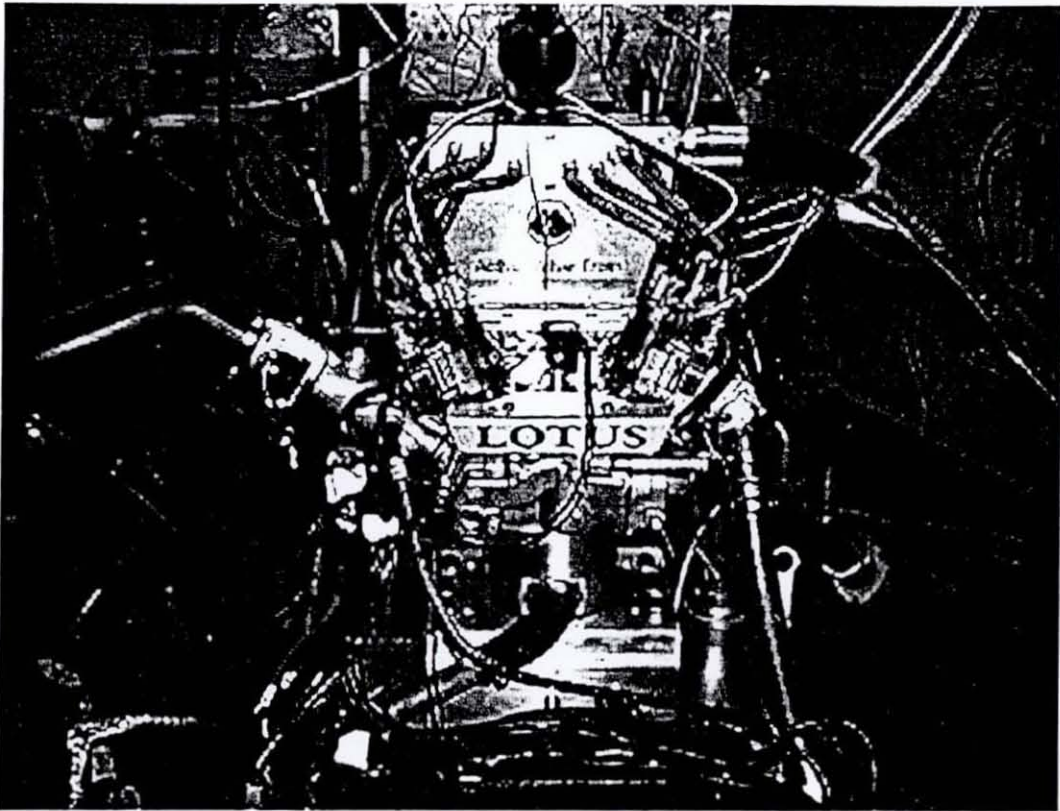[146] Private Communication with Lotus Cars Company Ltd, UK, 2000-2003.

Figure 9.1: Single-cylinder research engine with Lotus AVT System.

accept various strokes up to and including 100 mm, and is capable of running to 5000 rpm (depending on stroke).

The fitted research FVVT system allows trapping of a pre-defined quantity of IEGR. The open and closure timings of the each of four electro-hydraulically driven valves are independently variable and can be digitally controlled. Valve opening profiles can be selected and entered into the software by the user. The control software uses inputs from a crankcase encoder and valve linear displacement transducers to facilitate a closed-loop control to satisfy a 'desired versus actual' position control until the required profiles are achieved. Fine tuning of valve profiles is accomplished by using valve-specific gain controllers.

The engine is connected to a Fraud AG30, 30KW eddy-current dynamometer. A redline ACAP data acquisition system from DSP Technologies Inc. is used, together
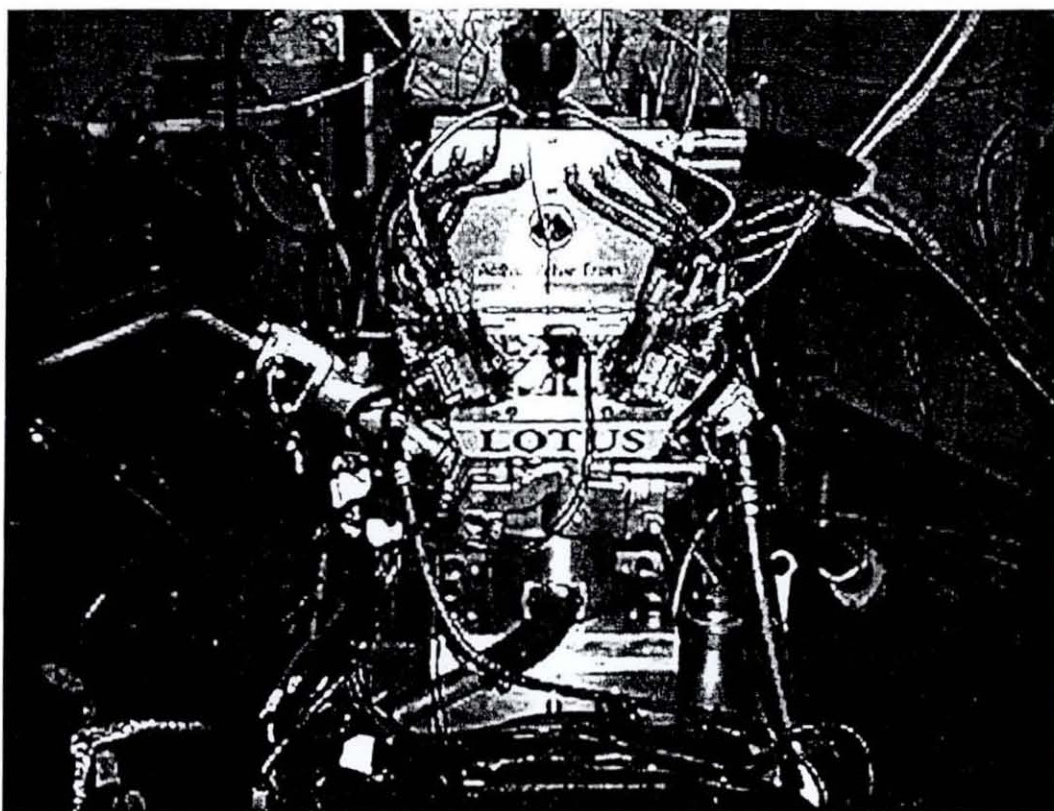
Figure 9.1: Single-cylinder research engine with Lotus AVT System.

accept various strokes up to and including 100 mm, and is capable of running to 5000 rpm (depending on stroke).

The fitted research FVVT system allows trapping of a pre-defined quantity of IEGR. The open and closure timings of the each of four electro-hydraulically driven valves are independently variable and can be digitally controlled. Valve opening profiles can be selected and entered into the software by the user. The control software uses inputs from a crankcase encoder and valve linear displacement transducers to facilitate a closed-loop control to satisfy a 'desired versus actual' position control until the required profiles are achieved. Fine tuning of valve profiles is accomplished by using valve-specific gain controllers.

The engine is connected to a Fraud AG30, 30KW eddy-current dynamometer. A redline ACAP data acquisition system from DSP Technologies Inc. is used, together
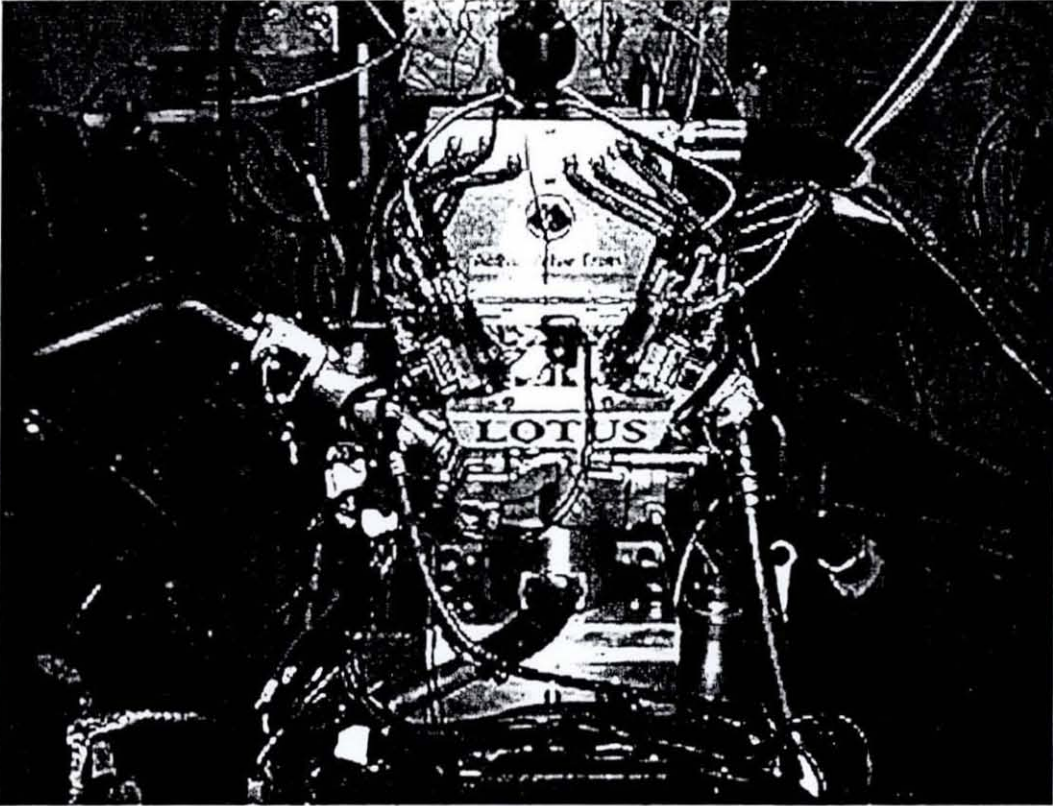
Figure 9.1: Single-cylinder research engine with Lotus AVT System.

accept various strokes up to and including 100 mm, and is capable of running to 5000 rpm (depending on stroke).

The fitted research FVVT system allows trapping of a pre-defined quantity of IEGR. The open and closure timings of the each of four electro-hydraulically driven valves are independently variable and can be digitally controlled. Valve opening profiles can be selected and entered into the software by the user. The control software uses inputs from a crankcase encoder and valve linear displacement transducers to facilitate a closed-loop control to satisfy a 'desired versus actual' position control until the required profiles are achieved. Fine tuning of valve profiles is accomplished by using valve-specific gain controllers.

The engine is connected to a Fraud AG30, 30KW eddy-current dynamometer. A redline ACAP data acquisition system from DSP Technologies Inc. is used, together